

THE UNIVERSITY OF HULL

**SYNTHESIS OF PORPHYRINS AND METALLOPORPHYRINS FOR
BIOLOGICAL APPLICATIONS.**

being a Thesis submitted for the Degree of Doctor of Philosophy in the
University of Hull

by

Sajida Ita, BSc, MSc.

September 2005

Acknowledgements

- All praise and honour to my Sovereign God and Lord Jesus Christ whose strength has seen me through my life.
- To all my family, my husband, David; my son, Immanuel; my mom, Zubeda; my deceased father, Nazir; my sisters, Shahida and Summaiyya; my brothers; Ahmed and Maamun and my grandmother, Mariam, I dedicate this thesis. Thank you all for your love, your trust and confidence.
- Thank you to Drs. Andrew Boa and Ross Boyle for their continuous support throughout this PhD. I could not have done it without my supervisors who were always there to guide me, correct me and motivate me to reach my goal.
- Thank you to Brenda Worthington, Huguette Savoie and Kevin Welham, who are all part of the technical team who have helped me with my work.
- Thank you to Dr. Eric Davoust for his cooperation for the work on sugar porphyrins, truly an excellent colleague and bench mate to work with. Dr. Nela Peša, who was my teacher, friend, colleague and my inspiration to work harder at all times.
- Finally, thank you to all other friends I have in Hull who kept me going, my lab colleagues and EPSRC for funding this PhD.

ABSTRACT

Porphyrins are ideal candidates for PDT (Photodynamic therapy). Their ability to localise preferentially in diseased tissue allows specific targeting of cancerous tissue in certain areas. In recent years, linking photosensitisers to sugar moieties has attracted great interest. Glycosylated porphyrins have increased solubility which enhances their uptake into cells, and also selectivity of the porphyrins. Cationic porphyrins have also been studied due their increased solubility and selective accumulation into mitochondria.

In this project, we have successfully combined these two properties of water-soluble derivatives of porphyrins to enhance their efficacy as potential PDT agents. Thioglycosylated cationic porphyrins have been synthesised, characterised and their photocytotoxicity assays against human colorectal adenocarcinoma cells (HT-29) assessed.

Metalloporphyrins on the other hand were synthesised with the intention of using them as molecular oxygen sensors. Oxygen-dependant changes in phosphorescence lifetime can be used to measure oxygen concentration in biological systems. A versatile method was developed which allowed palladium metal insertion into porphyrin macrocycles. The metalloporphyrins were synthesised, purified and analysed using TLC, MS, ^1H NMR and UV spectroscopy. Further functionalisation of the metalloporphyrins was achieved by the selective substitution of the *para*-fluoro substituent of the pentafluorophenyl group with thiols. In this way, a range of palladium(II) porphyrins were synthesised.

Failure of cells to internalise these porphyrins using conventional methods has prompted further considerations of encapsulating them in nanoparticles.

ABBREVIATIONS

PDT	Photodynamic Therapy
HPLC	High Performance Liquid Chromatography
HpD	Haematoporphyrin Derivative
Pp	Protoporphyrin
ALA	Aminolevulinic Acid
<i>m</i> -THPP	5, 10, 15, 20-Tetra(3-hydroxyphenyl)porphyrin
<i>p</i> -TPPS ₄	5, 10, 15, 20-Tetra(4-sulfonatophenyl)porphyrin
PcS ₂	Chloro(phthalocyaninedisulfonato)-Al(III)
Zn	Phthalocyaninato-Zn(II)
SiNc	Bis(trihexylsiloxo)naphthalocyaninato-Si(IV)
ZnNc	naphthalocyaninato-Zn(II)
<i>m</i> -THPC	5, 10, 15, 20-Tetra(3-hydroxyphenyl)chlorin
<i>m</i> -THPBC	5, 10, 15, 20-Tetra(3-hydroxyphenyl)bacteriochlorin
SnET ₂	Etiopurpurinato-Sn(IV)
Lutex	Texaphyrinato-Lu(III)
BPD	Benzoporphyrin Derivative
BPD-MA	Benzoporphyrin Derivative Monoacid
DMAD	Dimethyl Acetylenedicarboxylate

AMD	Age-related Macular degeneration
Chl <i>a</i>	Chlorophyll <i>a</i>
Chl <i>b</i>	Chlorophyll <i>b</i>
BChl <i>a</i>	Bacteriochlorin <i>a</i>
LDL	Low Density Lipoprotein
HDL	High Density Lipoprotein
BSA	Bovine Serum Albumin
AlPcS ₄	Aluminium Tetrasulfophthalocyanine
Mab	Monoclonal Antibody
PEG-5000	Polyethylene Glycol
AlClPc	Chloroaluminium Phthalocyanine
PVA	Polyvinyl Alcohol
HP	Hematoporphyrin
TPPS	Tetraphenylporphyrin Tetrasulfonic acid
TMPyP	α , β , γ , δ -tetrakis (1-methylpyridinium-4-yl)porphyrin- <i>p</i> -toluenesulfonate
PO ₂	Partial pressure of oxygen
NIR	Near Infra-red
BOLD	Blood-Oxygen Level Dependent
ATP	Adenosine triphosphate
SAM	Self-Assembled Membranes
FQY	Fluorescence Quantum Yield
Rh 123	Rhodamine 123

CMX Ros	Chloromethyl-X-rosamine
DiOC ₆	Dihexyloxacarboyanine iodide
NAO	Nonylacridine Orange
MTG	MitoTracker Green
TMRM	Tetra Methyl Rhodamine Methylester
LCP	Lysyl chlorin p6
PcM	Porphycene Monomer
PcD	Porphycene Dimer
MCP	Monocationic Porphyrin
CPO	Capronyloxyethyl Porphycene
AlPc	Aluminium Phthalocyanine
NPe ₆	<i>N</i> -Aspartyl Chlorin e ₆
SnOPA	Tin Octaethylpurpurin Amidine
LCI	Lysyl Chlorin p6 Imide
TPP	5, 10, 15, 20-Tetraphenylporphyrin
DPP	5, 15-Diphenylporphyrin
DNA	Deoxyribonucleic Acid
RNA	Ribonucleic Acid
TpyP	5, 10, 15, 20-tetrapyridylporphyrin
DMF	<i>N, N</i> -dimethylformamide
TLC	Thin Layer Chromatography
NMR	Nuclear Magnetic Resonance
MS	Mass Spectroscopy

MALDI	Matrix Assisted Laser Desorption Ionisation
FCS	Fetal Calf Serum
MTT	3-(4,5-Dimethylthiazol-2-yl)-2,5-diphenyltetrazolium Bromide
PBS	Phosphate Buffered Saline
HCl	Hydrochloric Acid
IRR	Irradiated
NI	Non-irradiated
HOMO	Highest Occupied Molecular Orbital
LUMO	Lowest unoccupied Molecular Orbital
Ncs	Naphthalocyanines
Pcs	Phthalocyanines

CONTENTS

Chapter one	Introduction	
1.1	General aim	1
1.2	Photodynamic therapy	2
1.2.1	Photochemistry of photodynamic therapy	3
1.2.2	Properties of an ideal photosensitiser	6
1.2.3	First generation photosensitisers: hematoporphyrin and its derivatives	6
1.2.4	Second generation photosensitisers	9
1.2.5	Endogeneous second generation photosensitisers	10
1.2.6	Synthetic second generation photosensitisers	10
1.2.7	Modified naturally occurring second-generation photosensitisers	21
1.2.8	Third generation photosensitisers	26
1.2.9	Further research in photodynamic therapy	37
1.3	Porphyrins as tools for biological analysis	38
1.3.1	Optical sensor systems	38
1.3.2	Measuring oxygen concentrations <i>in vivo</i>	39
1.3.3	Ideal oxygen sensor	39
1.3.4	Methods for measuring oxygen	40

1.3.5	Phosphors-method of choice for measuring O ₂ concentration	44
1.3.6	Molecular oxygen interactions	46
1.3.7	Choice of metal in metalloporphyrins	47
1.3.8	Metalloporphyrins as phosphors	47
1.4	Porphyrins in biological imaging	52
1.4.1	Fluorescence microscopy	54
1.4.2	Basic principles of fluorescence microscopy	54
1.4.3	Fluorescent probes	55
1.4.4	Probes for mitochondria	56
1.4.5	Mitochondrial targeting	59
1.5	Further development	61
Chapter two	Porphyrin synthesis	63
2.1	Synthesis of functionalised porphyrins	63
2.1.1	Adler-Longo method	64
2.1.2	Porphyrin synthesised in this project using Adler-Longo method	65
2.1.3	Lindsey method	69
2.1.4	2+2 Porphyrin synthesis of disubstituted porphyrins	71

2.1.5	Dipyrromethane and disubstituted porphyrin synthesis in project	71
2.2	Development of cationic water-soluble porphyrin synthesis	74
2.2.1	Synthesis of cationic porphyrins	75
2.2.2	Synthetic achievement in cationic porphyrins in project	79
2.3	Development of carbohydrate-porphyrin synthesis	79
2.3.1	Synthesis of thioglycosylated porphyrin	82
2.3.2	General procedure for carbohydrate-conjugation in project	83
2.3.3	General procedure for carbohydrate deprotection in project	86
2.3.4	Achievements in sugar porphyrin synthesis within project	88
2.4	Thioglycosylated cationic porphyrins	88
2.4.1	Route to thioglycosylated cationic porphyrins with direct porphyrin-sugar conjugation in project	89
2.4.2	Cytotoxicity of thioglycosylated cationic porphyrins	94
2.4.3	Cytotoxicity results	95
2.4.4	Discussion	98
2.4.5	Conclusion	99
2.4.6	Further work suggestions	99

Chapter three	Metalloporphyrins	101
3.1	Introduction to metalloporphyrins	101
3.1.1	General considerations for metalation reactions	101
3.1.2	Synthetic approach to palladium metal metalation	102
3.1.3	General synthetic procedure in project	111
3.1.4	Synthetic achievements in project of Pd metalation using benzonitrile method	112
3.1.5	Characterisation of palladium porphyrins	114
3.2	Further modifications of palladium porphyrins	122
3.2.1	Selective substitution of the <i>para</i> -fluorine	123
3.2.2	Palladium metalloporphyin substitution of <i>para</i> -fluorine substituents in project	124
3.2.3	General Method for thiol substitution of <i>para</i> -fluorine substituents on Pd-Metalloporphyrin	127
3.2.4	Synthetic achievement in thiol substitution of <i>para</i> -fluorines in project	127
3.2.5	Conclusions	133
Chapter four	Experimental	134
4.1	Equipment	134
4.2	Methodology	135
	References	221

CHAPTER ONE INTRODUCTION

1.1 GENERAL AIM

The general aims of the project are to synthesise porphyrins which have increased water solubility and functionality to precisely target different cells and organelles. Such porphyrins could be investigated their ability to act as photosensitisers in photodynamic therapy. The project also involves advancement to porphyrin functionality by inserting palladium into the porphyrin core in order to examine their capability as oxygen sensors. Earlier studies conducted by Vanderkooi *et al*¹ involved the synthesis of metal derivative of water-soluble porphyrins for measuring the dioxygen concentration based on quenching of phosphorescence.

This chapter is made up of five subsections, which cover all applications of porphyrins. These are:

1.1 GENERAL AIM

1.2 PHOTODYNAMIC THERAPY

1.3 PORPHYRINS AS TOOLS FOR BIOLOGICAL ANALYSIS

1.4 PORPHYRINS IN BIOLOGICAL IMAGING

1.5 FURTHER DEVELOPMENT

This chapter serves as a literature review, including relevant background reading into the project by reviewing work that has been done by others prior to this project in the areas of interest.

1.2 PHOTODYNAMIC THERAPY

Photodynamic therapy (PDT) is a form of both phototherapy and photochemotherapy.² Phototherapy involves treatments where chemical reactions induced by light are used to treat a disease. This use of "therapeutic light" can be traced to 1900 when Raab reported that the combination of acridine orange and light could destroy paramecium³ (a type of bacteria). Photochemotherapy is a form of phototherapy, in which a chemical substance is used in addition to light. The combination of molecular oxygen, light and a photosensitising drug in photodynamic therapy (PDT) is a promising new approach for treating several diseases, most remarkably cancer. Generally, PDT has been used in the treatment of bladder cancers, breast metastases, brain cancers, skin cancers, thoracic malignancies, gynaecological malignancies, colorectal cancers, and head, oral and neck cancers.⁴ A major advantage of this technique versus conventional chemotherapy is the relatively low inherent toxicity of the photosensitisers in the absence of light.

The selectivity is based on a difference in the photosensitiser concentration between normal and tumour tissues and on the directing of light to the tumour tissue. The observation on the partial accumulation of the photosensitiser in tumour cells was made as early as 1923 by Policard⁵ who found that target tissue was notably more fluorescent than healthy tissue. Between 1940 and 1960, Figge *et al*⁶⁻⁸ and Ramussen-Taxdal *et al*⁹ administered natural porphyrins to patients and tumour bearing animals in order to more accurately detect tumour tissue by fluorescence. Synthetic porphyrins (tetraphenylporphines) were also used as early as 1960 by Winkelman¹⁰⁻¹² to detect

tumour tissue.

1.2.1 Photochemistry of Photodynamic Therapy

The photochemical reactions involved in PDT are illustrated in the diagram below. The ground electronic state of a photosensitiser is a singlet state (S_0). Illuminating the photosensitiser with light of the appropriate wavelength excites it to the short-lived first excited singlet-state (S_1). The photosensitiser can return to its ground state by emitting a fluorescence photon or, alternatively, the S_1 photosensitiser can convert to the first excited triplet state (T_1) via intersystem crossing. The process of intersystem crossing is spin-forbidden as this requires a change of electron spins and hence these transitions occur to a very small extent.¹³

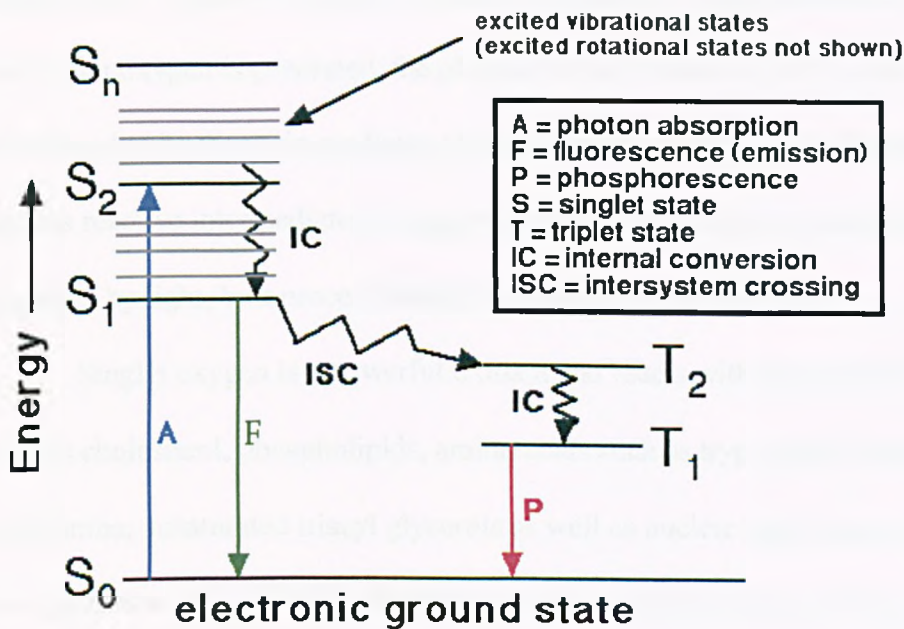


Fig. 1. The Jablonski diagram¹⁴

A good photosensitiser has a high yield of triplet-state which is sufficiently long lived to be involved in further chemical reactions. The T_1 photosensitiser can return to its ground state by emitting phosphorescence or by transferring energy to another molecule via a radiationless transition during collisions with other molecules.¹⁴

The T_1 photosensitiser can undergo further photodynamic reactions in order to return to its ground state (S_0). There are two types of photodynamic reactions¹⁵ which are often denoted Type I and Type II photoprocesses. Type I photoprocesses are electron or hydrogen-transfer reactions between other molecules and the T_1 photosensitisers. These processes involve the production of harmful reactive intermediates such as hydroxyl, hydrogen peroxide, hydroperoxyl and superoxide radicals, thereby returning the photosensitiser to its ground state (S_0). Type II photoprocesses are involved in the formation of singlet oxygen 1O_2 by energy transfer from T_1 photosensitiser to triplet oxygen 3O_2 . This involves spin exchange between the T_1 photosensitiser and 3O_2 and as the singlet oxygen is generated, the photosensitiser returns to the S_0 state. 1O_2 is considered to be the main mediator of phototoxicity in PDT. In both types of reactions, various reactive intermediates are generated and eventually, the photosensitiser is degraded by light, by a process which is known as photobleaching.

Singlet oxygen is a powerful oxidant and reacts with many kinds of biomolecules such as cholesterol, phospholipids, amino acids such as tryptophan, histidine and methionine, unsaturated triacyl glycerols as well as nucleic acid bases such as guanine and guanosine.^{16, 17, 18, 19, 20, 21} Singlet oxygen is very short lived and hence reacts at its site of formation. Areas of photodamage depend on the photosensitiser used as they

differ in distribution and accumulation. Cells die as a result of necrosis or apoptosis after PDT treatment.^{22, 23, 24} Necrosis is defined as degenerative cell death due to extensive cellular damage whereas apoptosis refers to the mechanism of genetically programmed death of old cells in both pathological and physiological conditions of a living organism.^{24, 25} During apoptosis, the contents of a cell are disposed in an organised manner without widespread inflammation.²⁰

The blood-flow hindering vascular damage is also responsible for tissue damage by PDT. The lack of $^3\text{O}_2$ protects cells from photodynamic damage but cells die instead due to $^3\text{O}_2$ shortage.^{23, 24, 26, 27, 28, 29} Inflammation, caused by phagocytic immunity and oxidative damage also plays an important role in cell death. Postnecrotic immunity develops against the target cells, which leads to long term accomplishment of PDT treatment and to obliteration of target cells outside the target area.^{22, 23, 24, 27}

1.2.2 Properties of an ideal Photosensitiser

Early photosensitisers, and the side effects associated with their activity, have been linked with the large number of oligomeric components formed during synthesis and are often inseparable by HPLC. Consequently the ideal photosensitiser should be a pure and single product. It should be relatively easily synthesised and the starting materials readily available. For large-scale synthesis, the reaction should be feasible to make it cost effective with the least number of intermediates to make it high yielding and cost effective.²⁰ The photosensitiser should not be toxic in the absence of light and should not self aggregate much in the body as this would reduce the yield of the excited triplet-state

yield and singlet oxygen yield.

The photosensitiser should be selective in its accumulation in the target tissue and be eliminated from the body fairly quickly to avoid generalised skin photosensitisation. The photosensitiser should also absorb light of adequately long wavelengths ~700nm, the red region of the electromagnetic spectrum. This would allow the penetration of light through tissues to be at a maximum because absorption by endogenous compounds and scattering of light would be minimum.³⁰ Desirably, the photosensitiser should not strongly absorb light of the region 400-600 nm as this would reduce the risk of generalised photosensitivity caused by sunshine.³¹

The excited triplet-state of the photosensitiser should be adequately long lived so as to generate singlet oxygen and should be stable enough to avoid degradation processes such as photobleaching. Finally, the solubility of the photosensitiser should be compatible to the desired method of drug delivery to the target tissue.

1.2.3 First-generation photosensitisers: hematoporphyrin and its derivatives

Amongst the earliest recognised photosensitisers was hematoporphyrin derivative (HpD) which was isolated and studied by Schwartz and Lipson.^{32, 33} Later in 1970s, Dougherty made the discovery that fluorescein diacetate could photodynamically destroy rat and mice tumour cells *in vitro*.³⁴ Dougherty then later began to treat tumour-bearing animals with fluorescein and found that it acted as a photosensitiser.³⁵ Meanwhile, Weishaupt *et al* discovered the cytotoxic product of the photochemical reaction to be

singlet oxygen³⁶ and it was soon realised that fluorescein had a low singlet oxygen quantum yield and absorbed light in the green portion of the electromagnetic spectrum rather than in the red and as a result, did not penetrate deeply into tissue. Efforts were therefore made to test porphyrin photosensitisers for their singlet oxygen generation and also examine their absorption in the red part of the electromagnetic spectrum.

It was then that HpD was "rediscovered" and found to have a high singlet oxygen quantum yield and an absorption maximum in the red. It was also found to be selectively retained in tumour tissue.³⁴ Several years later, Dougherty isolated and identified the active fractions of HpD and produced a purified version named Photofrin®.³⁷

Photofrin® (formerly Photofrin II) became commercially available in 1987 when phase III clinical trials first began.^{38,39} The ability of HpD to act as a photosensitiser *in vivo* is mainly due to its oligomeric components. The fraction enriched with oligomeric components is called "fraction D"⁴⁰ and using HPLC, the monomeric and oligomeric components of this fraction can be partially separated. However, the precise composition of fraction D has not yet been determined. Many commercial versions of HpD such as Photofrin®, Photosan®, Haematodrex®, and Photocarcinorin®² are obtained from this fraction.

Use of HpD is limited due to some major disadvantages. Due to the nature of the complex mixture of monomers, dimers and oligomers, separation is difficult and some of the fractions are not photoactive.^{16,41} The precise composition of the mixture is not known⁴² and has been found to vary from batch to batch.² The components of HpD can also be modified in tissues: ester bonds can be hydrolysed and aggregates broken down.⁴³

These differences in chemical activity complicates studies and particularly dose-response studies and makes the results hard to interpret.^{2, 17, 41, 44} As a result, their distribution and photodynamic properties in tissues differ from one HpD preparation to another and predicting their therapeutic effect is difficult.^{16, 41, 43, 45} Selective targeting of tumour tissue versus healthy tissue is also a problem and consequently, the PDT effect is also experienced in other tissues other than the target tissue.^{2, 42, 46} The only organ which demonstrated high selectivity in the accumulation of HpD was in the treatment of brain tumours. This is due to the blood brain barrier that stops the photosensitiser from accumulating in healthy brain tissue.⁴³

The enrichment factor of HpD in other tumours other than those in the brain is only 3-5¹⁹ and therefore there is a risk of damage to healthy tissues as a result of PDT. Studies have shown that only 0.1-3 % of HpD accumulates in tumour¹⁹ and the rest of the photosensitising components are free to accumulate elsewhere in the body. One organ that has generally shown the effects of the photosensitiser after PDT treatment is the skin. Patients who have had PDT treatment often suffer from photosensitivity for 1-2 months after injection.^{2, 16, 18, 20, 22, 41} The number of treatments a patient can receive is therefore limited due to the long-term photosensitivity associated with the treatment.

However there is one limitation of HpD that exceeds all other, which is due to the electronic absorption spectrum of HpD. The etiochrome spectrum typically contains a Soret band and four Q-bands and is less than ideal for PDT.^{47, 48} The Q-band with the longest wavelength of approximately 630 nm which is used in PDT as light of this wavelength penetrates deepest into tissues and unfortunately this is the weakest absorption of HpD.

As a result, HpD absorbs light of very short wavelength which is insufficient as it does not allow penetration into deep tissues.^{19, 20, 23, 24, 41, 42, 49, 50}

The depth at which a reduction to 37% of the power of radiation is observed is known as the effective penetration depth of light.^{47, 48, 51} The effective penetration depth into soft tissues of light with λ at 630 nm is typically 1-2 mm⁵⁰ and about double for light with λ of 700-850 nm. The effective penetration depth for HpD is about 5-10 mm⁵⁰ which indicates its incapability to be used as a photosensitiser to target tissues which require deep penetration for effective treatment. The intensity of the Q-band with absorption at 630 nm is also very weak; its molar extinction coefficient is only 3500 M⁻¹ cm⁻¹ and as a result large doses of the photosensitiser and light are required to achieve a reasonable therapeutic effect.^{19, 45} The more doses of photosensitiser and light used the more the risk of harmful side effects increases. Hence there still exists a need for research and development to discover the ideal photosensitiser which would have maximum impact with least side effects.

1.2.4 Second-generation photosensitisers

Second-generation photosensitisers have been developed with the intention of improving the efficacy of PDT. Most of these exhibit a strong absorption in the red wavelength region and absorb light of longer wavelengths. These photosensitisers already in clinical trials^{41, 52} can be grouped as porphyrins, texaphyrins, phthalocyanines, chlorins and bacteriochlorins.

1.2.5 Endogenous second-generation photosensitisers

Alternative strategies for triggering photosensitisation is through the use of the endogenous photosensitiser Pp^{2, 16, 49, 51} (protoporphyrin) produced in the biosynthesis of protoheme. In the production of Pp, the rate-limiting step involves the formation of 5-aminolevulinic acid (ALA) from succinyl-coenzyme A and glycine. Administering exogenic ALA as a “prodrug” into the tissue increases the production rate of Pp.

Pp also accumulates in the tumour tissue as well as in healthy tissues and causes generalised photosensitisation.⁵³ However, the advantages of using ALA is the administration as it can be injected, given orally or applied topically on the target tissue.^{2, 16, 24, 54} The tissue can be irradiated 3-6 h later and the skin photosensitisation caused by ALA is mild⁴⁵ and short-lived.^{16, 24} ALA is the first prodrug of a second generation photosensitiser for which marketing clearance was obtained.⁵⁵ As early as 1990, Kennedy was using ALA for the treatment of skin disorders^{23, 38} and at present Pp via ALA as a prodrug is being investigated for the treatments of cutaneous and gastrointestinal cancers, psoriasis, and precancerous lesions.^{16, 29, 45, 55} The relatively simple synthesis of ALA and its accessibility in a pure form has prompted intensive research to be undertaken with this prodrug.

1.2.6 Synthetic second-generation photosensitisers

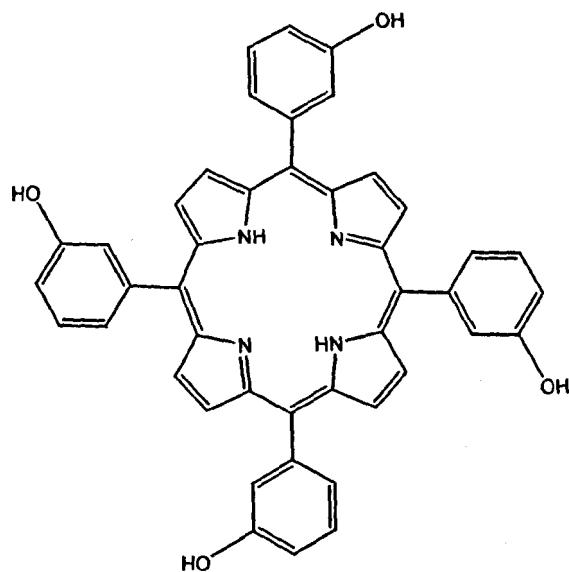
Synthetic second-generation photosensitisers can be placed into four main groups:

- Substituted porphyrins
- Phthalocyanines and naphthalocyanines

- Chlorins and bacteriochlorins
- Porphycenes and texaphyrins

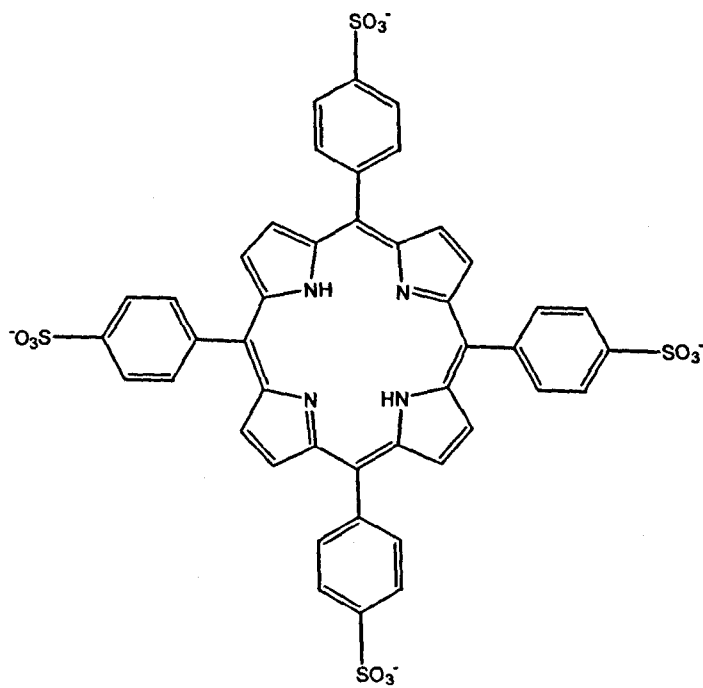
Substituted porphyrins

Advancements in porphyrin synthesis involve preparation of single, well characterised compounds that absorb light of longer wavelengths which have strong absorption in the red region of the electromagnetic spectrum.³⁰ Simple and straightforward chemical modifications have improved the solubility and amphiphilic character of the photosensitisers. 5,10,15,20-Tetra(3-hydroxyphenyl)porphyrin (*m*-THPP) [1] and 5,10,15,20-Tetra(4-sulfonatophenyl)porphyrin (*p*-TPPS₄) [2] are two porphyrins investigated for their use as new potential photosensitisers. *m*-THPP has shown to be 25-30 times as effective at photosensitisation as HpD or Photofrin.⁵⁶ Sulfonation to give *p*-TPPS₄ has the effect of increasing the hydrophilic nature of the porphyrins hence making the delivery of the drug much more effective. This eradicates the use of a carrier, often required to avoid self aggregation of the photosensitiser in the plasma, which ultimately reduces the singlet oxygen yield.



[1]

5,10,15,20-Tetra(3-hydroxyphenyl)porphyrin (*m*-THPP)



[2]

5,10,15,20-Tetra(4-sulfonatophenyl)porphyrin (*p*-TPPS₄)

Fig. 2. Potential photosensitisers for PDT

Phthalocyanines and naphthalocyanines

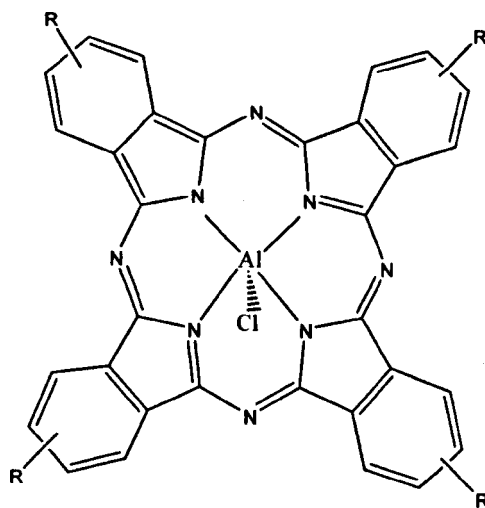
An expansion of the basic porphyrin core and extending its conjugated π -system by joining four benzene or naphthlene rings to the β -pyrrolic positions of the porphyrins, and substituting the methine-bridge carbons with nitrogens, generates phthalocyanines and naphthalocyanines. This modification in ring structure results to strong absorption of phthalocyanines (Pcs) and naphthalocyanines (Ncs) at longer wavelengths, which in turn reduces ¹⁶ the light and drug doses required for their use as PDT agents. Moreover, phthalocyanines and naphthalocyanines absorb light with λ in the range of 400-600 nm less efficiently than porphyrins and consequently the risk of generalised photosensitivity due to sunlight is greatly reduced.^{30, 57} The tumour uptake is at a maximum 1-3 h post injection and Pcs and Ncs are effectively eliminated from the body in 24 hours, therefore cutaneous photosensitivity is only temporary.

The extra conjugation of the π -system in Pcs and the associated increase in hydrophobicity is often counterbalanced by introducing polar substituents to avoid solubility problems.^{2, 43} Sulfonation is an effective way to introduce polarity into these macrocycles. However, a mixture of polysulfonated products are obtained which require intricate separation using chromatography.⁴⁶ An example of a sulfonated phthalocyanines is Chloro(phthalocyaninedisulfonato)-Al(III) (AlPcS₂) [3] which has been extensively investigated as a PDT photosensitiser *in vivo*.^{16, 58}

Coordination of Pcs with diamagnetic metal cations increases their overall triplet state yield and lifetime.^{31, 46} Al(III), Zn(II) and Ga(III) have all previously been inserted into Pcs. Some well known examples include previously mentioned AlPcS₂ and

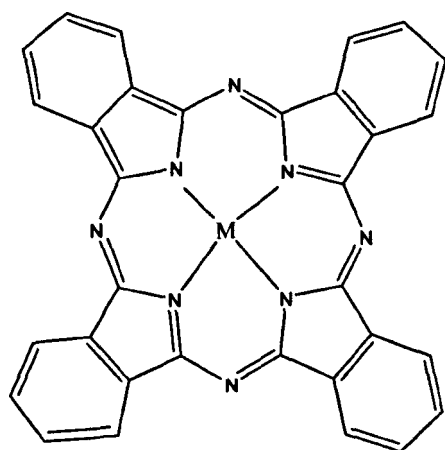
phthalocyaninato-Zn (II) (ZnPc) [4] which is being developed for commercial production.² The hydrophobic nature of ZnPc is overcome by using liposomes as carriers in the body² and they cause only mild generalised photosensitivity.⁴⁵ Further developments include attempts to synthesise sufficiently hydrophilic Pcs, which are isomerically pure in order to obtain an ideal photosensitiser in PDT.^{19,45}

Ncs are hydrophobic and hence insoluble in most bio-compatible solvents.⁴³ They have been found to absorb light at long-wavelengths (~ 700nm) very strongly and are therefore efficient as PDT photosensitisers. Some examples include Bis(trihexylsiloxo) naphthalocyaninato-Si(IV) (SiNc) [5] and naphthalocyaninato-Zn(II) (ZnNc) [6] which have been found to be active *in vivo*⁴¹ and further research continues in the use of Ncs in PDT treatment of strongly pigmented tumours.



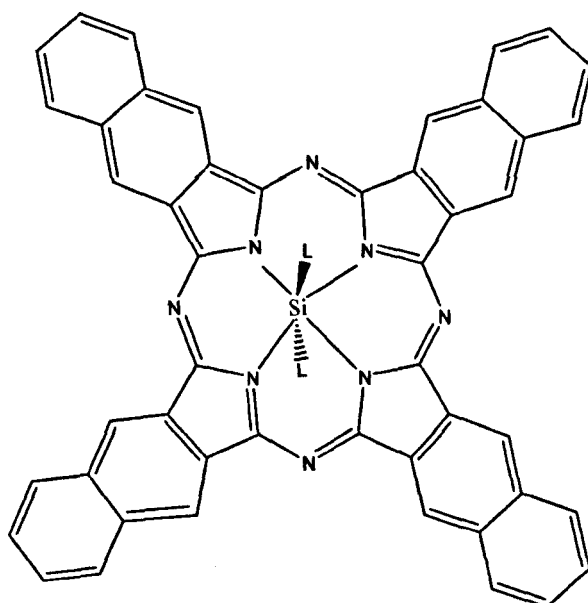
[3]

R = H, H, SO₃⁻, SO₃⁻; AlPcS₂; Chloro(phthalocyaniniedisulfonato)-Al(III)



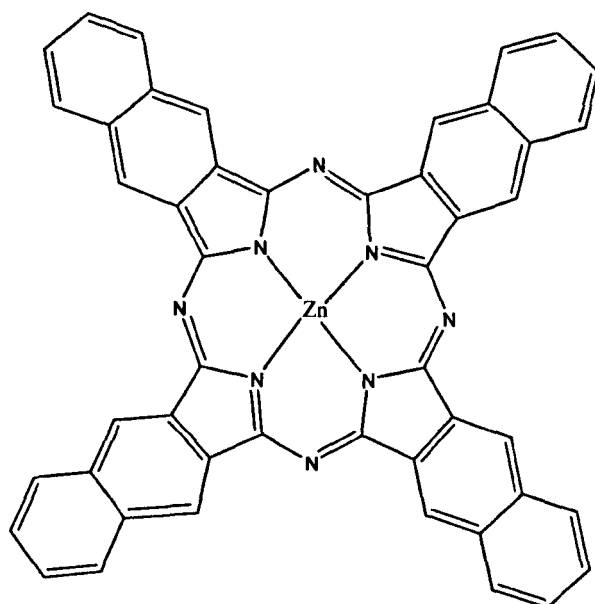
[4]

M = Zn(II), ZnPc; Phthalocyaninato-Zn(II)



[5]

L = OSi(C₆H₁₃)₃;
SiNc; Bis(trihexylsiloxy)naphthalocyaninato-Si(IV)



[6]
Naphthalocyaninato-Zn(II)

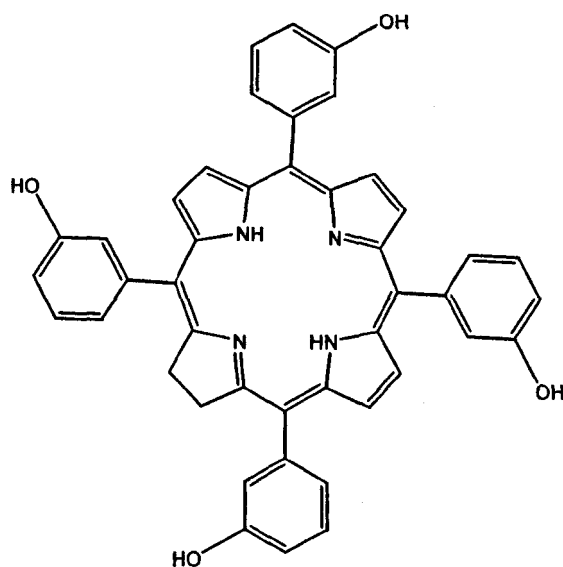
Fig. 3. Phthalocyanine and naphthalocyanine derivatives in PDT

Chlorins and bacteriochlorins

Chlorins are obtained by the reduction of one exocyclic bond of a porphyrin. The resulting dihydroporphyrin obtained has a stronger absorption at longer wavelengths i.e. absorbs further into the red region of the electromagnetic spectrum.¹⁶ In bacteriochlorins, two exocyclic bonds on opposite sides of the porphyrin macrocycle are reduced. This intensifies and moves the absorption even further to the red end of the electromagnetic spectrum. Isobacteriochlorins are produced when two adjacent double bonds on adjacent pyrrole units are reduced. Their absorption is similar to that of chlorins and as synthesis

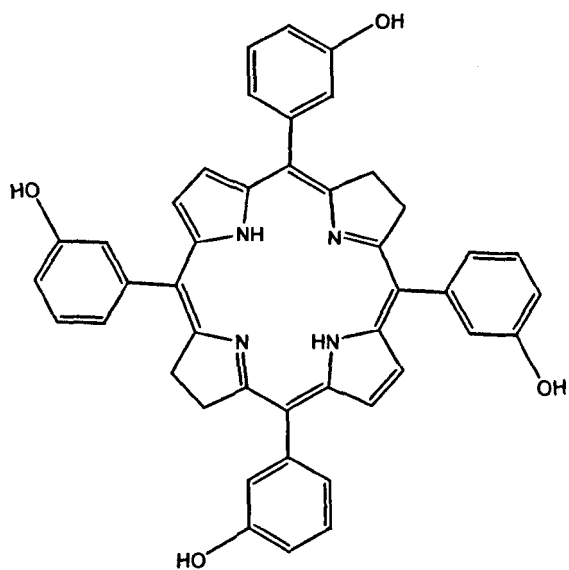
of isobacteriochlorins is more complex than that of chlorins, chlorins are often the preferred choice for PDT photosensitisers.²⁰

Synthetic chlorins that have been investigated as PDT sensitisers are 5,10,15,20-Tetra(3-hydroxyphenyl)chlorin (*m*-THPC) [7], 5,10,15,20-Tetra(3-hydroxyphenyl)bacteriochlorin (*m*-THPBC) [8] and ethiopurpurinato-Sn(IV) (SnET₂) [9].



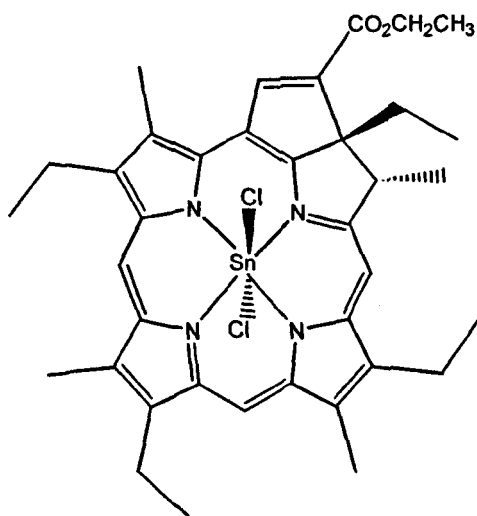
[7]

5,10,15,20-Tetra(3-hydroxyphenyl)chlorin (*m*-THPC)



[8]

5,10,15,20-Tetra(3-hydroxyphenyl)bacteriochlorin (*m*-THPBC).



[9]

Etiopurpurinato-Sn(IV)

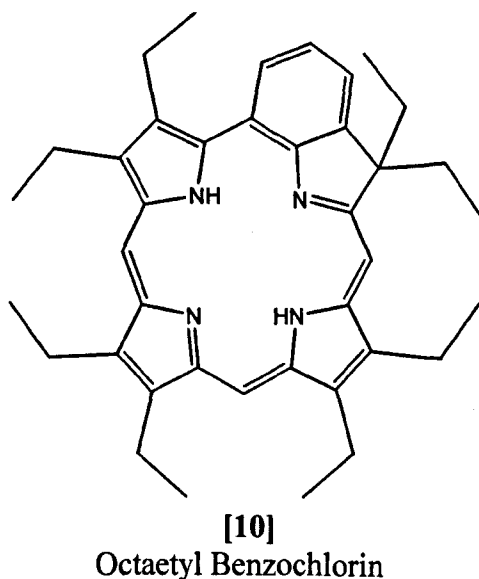
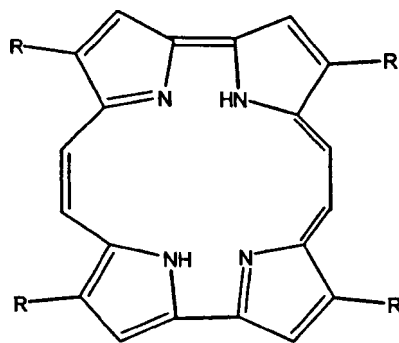


Fig. 4. Synthetic chlorins and bacteriochlorin derivatives in PDT

The reduced forms of the well established 5,10,15,20-Tetra(3-hydroxyphenyl)porphyrin (*m*-THPP) are found to be more active in PDT.¹⁷ Chlorins are often stabilised, to avoid oxidation back to chlorins, by placing large substituents or an exocyclic ring next to the reduced pyrrole ring.^{16, 18, 49} This approach is illustrated in the structures of SnET₂ and benzochlorin [10]. Dimagnetic metal cations are also often coordinated by the macrocycles to intensify the absorption of red light by the photosensitisers and to move their absorption bands to longer wavelegths.²⁰ These improvements have led to the commercialisation of the these chlorins, and continued research to find more chlorins and bacteriochlorins for application in PDT.

Porphycenes and texaphyrins

Structural isomers of porphyrins are known as porphycenes where as texaphyrins are modified porphyrins where a phenyl ring substitutes one pyrrole ring. In 1986, Vogel *et al*²⁰ synthesised the first porphycene [11] via a McMurry rearrangement of bipyrrole dialdehydes. Sessler⁵⁹ synthesised the first texaphyrin by a '3+1' type condensation reaction between a tripyrromethane and 1,2-diamino-3,4-dimethylbenzene. Texaphyrins have good singlet oxygen yield and can also be coordinated to large metal cations to give metal complexes that are photoactive *in vivo*.¹⁶ Ln(II) and Lu(II) are often the metals associated with texaphyrin complexes. The Lu(II)-complex of a texaphyrin (Lu-Tex) [12] is a very stable, hydrophilic PDT photosensitiser. It has the advantage of selectively accumulating into tumours and irradiation can be performed three hours post injection. However, research is still going on to overcome some of the side effects of Lu-Tex, which include cutaneous pain during PDT.^{2, 41, 43, 51} These problems, together with poor yields and separation problems, contribute to more research being needed in this area.



[11]

R = H, Porphycene

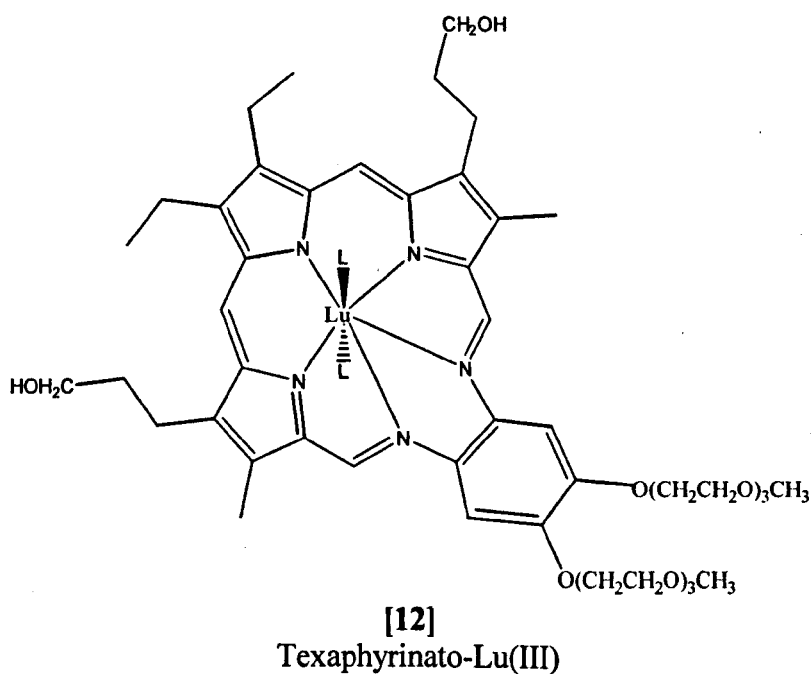


Fig 5. Porphycenes and texaphyrins in PDT

1.2.7 Modified Naturally Occurring second-generation photosensitisers

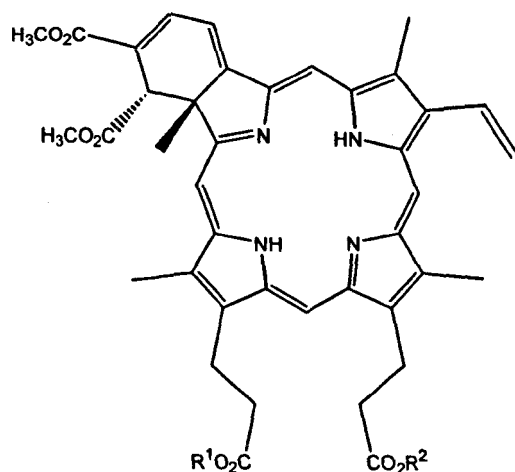
Modified naturally occurring second-generation photosensitisers involve the use of naturally available precursors for their modification for a variety of chlorins. There are two major categories:-

- Chlorins from protohemin or bilirubin
- Chlorophyll derivatives

Chlorins prepared from protohemin or bilirubin

Protohemin [chloro(protochlorophyrinato)-iron(III)] is a vital natural precursor for many partially chlorins. Protohemin was isolated in pure form from bovine blood⁶⁰ as early as 1957. Functional modifications to produce proto-, meso-, deuterio-, carboxylic and hematoporphyrins using simple synthetic methods have been developed.^{61, 62}

Vinyl porphyrins were also investigated for their role in the production of chlorin-like products using Diels-Alder type reactions.⁶³ Benzoporphyrin derivatives (BPD) were later produced by Dolphin and co-workers^{64, 65} as well as Smith and co-workers.⁶⁶ Benzoporphyrin derivative mono acid ring A (BPD-MA) [13] has proven to be a promising photosensitiser, which has recently been clinically approved for the treatment of solid tumours.⁶⁷ Synthesis was achieved by the Diels-Alder reaction of dimethyl ester of protoporphyrin with dimethyl acetylenedicarboxylate (DMAD). BPD-MA is virtually insoluble in water, requiring a liposomal system for its administration. BPD-MA is currently available commercially, as Visudyne® for the treatment of Age-related Macular degeneration (AMD). Long wavelength absorption properties and the ability to clear rapidly from the system have made it an ideal candidate for the treatment of this common eye condition.



[13]

$R^1(R^2) = CH_3$ $R^2(R^1) = H$;

BPD-MA; benzoporphyrin derivative mono acid ring A

Fig 6. Benzoporphyrin derivative mono acid ring A

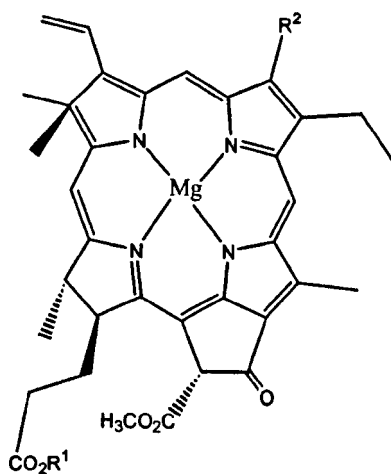
Monforts and co-workers have developed various chlorins, which involve further functional modifications to afford more hydrophilic chlorins.^{68,69} Other compounds derived from naturally occurring bile pigment bilirubin include azachlorins. Azachlorins are cyclic tetrapyrroles that have one to four nitrogen bridges instead of methine bridges. Synthesis involves a route *via* the production of the intermediate 5-oxoniumporphyrinato-Zn(II). Azachlorins exhibit good triplet and singlet oxygen yield. Their photophysical parameters are excellent and hence promising research continues.

Chlorophylls and related chlorins

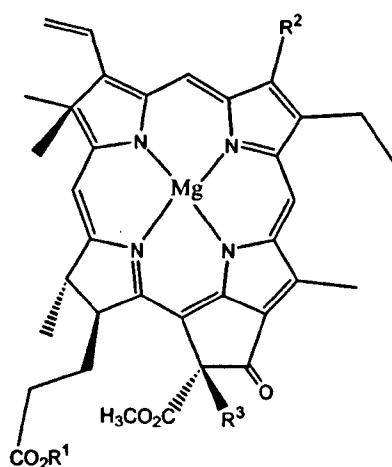
Chlorophyll is a component of the photosynthetic pathway is involved in

acquiring light and transforming it to chemical energy. Chl *a* and Chl *b* are both abundant in all green plants and are the most common of the natural chlorophylls. Natural bacteriochlorophylls, e.g. BChl *a*, are Mg(II)-complexes of bacteriochlorins occurring in certain photosynthetic bacteria. However, bacteriochlorophylls have been found to be unstable under PDT conditions^{27, 41} and hence more stable analogues have been sought.

An advantage of using natural chlorins and bacteriochlorins is their availability and ease of obtaining abundant amounts from plants and algae. Leaves from plants such as spinach, beans, clover can be used to isolate Chl *a* and Chl *b* in sufficient amounts by simple extraction and precipitation methods.⁷⁰ Other methods for separation of stereochemically pure Chl *a* and Chl *b* can be obtained by separation using a sucrose column.⁷¹ Further functional modification by partial synthesis is required to yield a great variety of Chl-related derivatives.⁷²



- [14] $R^1 = \text{phytyl}$, $R^2 = \text{CH}_3 = \text{Chl } a$
 [15] $R^1 = \text{H}$, $R^2 = \text{CH}_3 = \text{Chlid } a$



- [16] $R^1 = \text{phytyl}, R^2 = \text{CH}_3, R^3 = \text{H} = \text{Phe } a$
 [17] $R^1 = \text{phytyl}, R^2 = \text{CHO}, R^3 = \text{H} = \text{Phe } b$

Fig 6. Structure of Chl *a*, Chlid *a*, Phe *a* and Phe *b*.

Chl *a*, containing the lipophilic phytol group, is a hydrophobic photosensitiser and has hydrophilic components such as Mg(II)-atom, the 13¹ and 17³ ester carbonyls (Fig 6). Chl *a* aggregates in aqueous solvents and in non polar organic solvents, which inhibits its ability to generate ¹O₂. The low solubility and high aggregation tendency has consequently led to Chl *a* being only rarely used as a photosensitiser in biological systems.²¹ Derivatives of Chl *a*, such as Chlid *a*, Phe *a*, Phe *b* have all been made in attempt to increase hydrophilicity and minimise aggregation problems. Ongoing research is being conducted to synthesise the ideal photosensitiser from chlorophyll.

1.2.8 Third generation photosensitisers

Second generation photosensitisers have the ability to be taken up by proliferating tumour cells at a faster rate than of normal cells. Consequently, they tend to accumulate more in tumour tissue than in healthy tissue. Photodynamic therapy relies on this preferential, higher uptake of the photosensitiser in order to target tumour tissue and cause minimal damage to healthy tissue.

However, lack of sufficient selectivity of the second generation photosensitisers have led to a large research effort aimed at developing photosensitisers, which have structural characteristics that contribute to more specific localisation. Third generation photosensitisers involve bioconjugates of biological active targeting molecules and photosensitisers. Conjugation with porphyrins, phthalocyanines, chlorins and bacteriochlorins can either occur via covalent or non covalent interactions. Conjugation of various biologically active molecules has been investigated to enhance the localisation properties of PDT sensitisers, some examples are:

- Serum albumin
- Antibodies
- Polymers
- Sugars

The aim would be to attach a biologically active molecule to the photosensitiser via a functional group present on the macromolecule, whilst preserving the

pharmacokinetic properties of the biologically active molecule as well as the photophysical properties of the sensitiser. Also in doing so, improve the systematic introduction of the conjugate by increasing the degree of water solubility.

Serum Albumin conjugates

Covalent conjugation of a photosensitiser to a ligand that is specifically recognised and internalised by a cell-surface receptor may be a way of improving the selectivity of photodynamic therapy (PDT). Serum albumin is a highly abundant blood protein that is produced in the hepatocytes of the liver. It has a molecular mass of 66500Da and is well characterised in the literature. It has been shown to be a general purpose carrier of metabolites and drugs around the body, providing a high capacity reservoir to stabilise the concentrations of many free ligands. It is also a carrier for nutrients such as vitamins, amino acids, metal ions [Cu(II) and Zn(II)] and steroids.

Tumour cells which are rapidly dividing require an elevated supply of nutrients. Hence the procedures by which such nutrients are delivered to the cells are enhanced and as albumin itself is a nutrient which is digested in cells, an increased uptake of albumin would allow a higher accumulation of the attached photosensitiser in the tumour tissue. Therefore albumin is a good candidate for bioconjugation with photosensitisers to enhance their localisation.

The earliest investigation carried out on photosensitisers covalently attached to serum proteins was reported by Hamblin and Newman.^{73, 74} The investigation involved

the study of covalently attached hematoporphyrin with bovine serum albumin, transferrin, low density lipoprotein (LDL), high density lipoprotein (HDL). They investigated the uptake and phototoxicity of the conjugates in three different cell lines: human adenocarcinoma cells (HT29) and mouse fibroblasts (3T3) in J774 which is derived from Balb/c mice that *in vitro* behaves as macrophages. Noticeably the phagocytic cell line J774 displayed the higher uptake of BSA and lipoprotein conjugates compared to the other cell lines. In non-phagocytic cell lines, HT29 and 3T3, the BSA-hematoporphyrin conjugates were found to accumulate predominantly at the cell surface whereas transferrin and LDL conjugates showed receptor mediated internalisation. Comparison studies indicated that these conjugates displayed an elevated level of toxicity to all cell lines compared to the unconjugated hematoporphyrin.

Phthalocyanine conjugation with serum albumin was investigated by Brasseur *et al*⁷⁵ who targeted the delivery of aluminium tetrasulfophthalocyanine (AlPcS₄) to the scavenger receptor of macrophages, via coupling to maleylated bovine serum albumin (mal-BSA). AlPcS₄ was covalently coupled to BSA *via* one or two sulfonamide-hexanoic-amide spacer chains to yield the BSA-phthalocyanine conjugates. The study investigated the uptake and phototoxicity of the conjugates in two cell lines: J774, which is derived from Balb/c mice that *in vitro* behaves as macrophages and non-phagocytic EMT-6 cells.

Both conjugates were shown to be non-specifically taken up by EMT-6 cells. But majority of both conjugates remained accumulated with the cell surface, an observation

explained by the inherent low phototoxicity exhibited by both AlPcS₄-mal-BSA as well as AlPcS₄-BSA. On the other hand J774 cells displayed specific and receptor mediated uptake of the conjugate. Comparative studies indicated that the conjugates were recognised by the scavenger receptor. The coupling with mal-BSA also improved the binding affinity. Phototoxicity of the conjugates towards J774 cells corresponded to their relative affinity, with mal-BSA-AlPcS₄ coupled via two spacer chains exhibiting the highest activity. In conclusion, conjugates displayed less phototoxicity toward the EMT-6 cell line than J774 cell line but in both cases, conjugated AlPcS₄ was found to have lower activity than that of free disulfonated AlPcS₂.

Further research was conducted by conjugating Chlorin (e₆) covalently to bovine serum albumin to give conjugates with BSA and mal-BSA. Photosensitiser uptake was measured by target J774 murine macrophage like cells and non-target OVCAR-5 human ovarian cancer cells. The conjugates were found to be abundant in the J774 cells and overall a high degree of photoinduced cytotoxicity was observed whereas the OVCAR-5 cells showed a very small uptake and no phototoxicity towards the conjugates. The uptake and phototoxicity decreased after incubation of the J774 cells at 4 °C suggesting the internalisation of the photosensitiser which was confirmed using confocal microscopy indicating lysosomal localisation. Addition of the mal-BSA conjugates indicated competitive uptake and phototoxicity. The study concluded the higher degree of specificity towards macrophages upon conjugation and therefore an overall improvement in the photoactivity and localisation of the photosensitiser.

Antibody conjugates

Antibody conjugates target antigens expressed by tumour cells hence allowing selective accumulation of the photosensitiser in these cells. Selective administration to the tumour would avoid the use of high drug doses and consequently minimum photosensitivity side effects would be experienced. Natural immunisation of animals gives rise to various antibodies which differ in important properties such as specificity, subclass and affinity. These antibodies are known as polyclonal as they arise from many different lymphocytes coming into contact with the antigen when the animal is exposed. Monoclonal antibodies (Mab) vary from polyclonal antibodies as they have homogenous properties. To obtain monoclonal antibodies, plasma β cells are obtained from the spleen of an animal and are all subsequently fused with malignant myeloma cells. This gives rise to heterogeneous populations of hybrid cells which are separated into homogenous populations and grown *in vitro* to generate a high yield of monoclonal antibodies.

The earliest studies of Mab-conjugates was reported in 1983⁷⁶ where hematoporphyrin derivative was conjugated to a Mab directed against DBA/2J myosarcoma M-1. The study found that the time interval between injection and light activation was an important factor in tumour suppression. The study also showed that the conjugated photosensitiser inhibited tumour growth compared to the controls used. The same research group investigated benzoporphyrin derivative mono acid ring A (BPD)-Mab conjugation with a polyvinyl alcohol linker.⁷⁷ However no therapeutic applications have been reported so far. Further work was conducted by Goff *et al*⁷⁸ who used

polyglutamic acid as a linker in conjugation of chlorin (e₆) with Mab. Overall results from the study concluded improved survival where the conjugates were used as compared to the unconjugated chlorin e₆.

Oseroff *et al*⁷⁹ also reported the use of chlorin e₆-Mab conjugates in studying the selective photolysis of human T-cell leukemia cells *in vitro*. Cytotoxicity assays were performed using HPB-ALLT-leukemia cells and two Leu-1 antigen negative cell lines. Control conjugates and free chlorins were also administered as controls but showed no significant toxicity to the HPP-ALL cell line. In contrast, the anti -Leu-1-dex-chlorin e₆ showed significant photolysis of these cells in a high dose dependant manner.

More recent antibody conjugation studies involve one of the most promising second generation photosensitisers, *meta*-tetra hydroxyphenyl chlorin (*m*THPC).⁸⁰ *m*-THPC is a well characterised and highly efficient photosensitiser used in the treatment of head and neck cancers, as well as in the treatment of early second primary squamous cell carcinoma of the oesophagus, bronchi and mouth.⁸¹ However, *m*-THPC based PDT lacks tumour selectivity which can result in severe normal tissue damage after PDT of large surface areas. Recent developments have allowed conjugation of *m*-THPC with Mabs directed against tumour associated antigens. This enables the photosensitiser to be targeted selectively at the tumour. The *m*-THPC-Mab conjugates have been found to be suitable for the treatment of multiple tumour foci in large areas. This advancement has minimised the problem of phototoxicity as the Mabs have limited access to the skin.

The *m*-THPC-Mab conjugate synthesis has not been fully exploited and a serious

problem encountered is the poor water solubility of *m*-THPC. Other problems include cross linking during conjugation, change in the pharmacokinetic activity of the antibody as well as the photochemical activity of the photosensitiser. In the study, aggregation and solubility problems were overcome by attaching four *m*-THPC molecules to a monoclonal antibody and after 48 hours post injection, there was a higher concentration of the conjugate in the blood in respect to the unconjugated *m*-THPC. Tumour selectivity of Mab-conjugated *m*-THPC increased in comparison to the unmodified *m*-THPC and after 48 hours, the level of Mab-conjugated *m*-THPC in the skin was much lower than that of the unconjugated *m*-THPC. This minimised the photosensitivity experienced during PDT and improved its efficacy as a targeting photosensitiser.

Polymer conjugates

A limiting factor for second generation PDT photosensitisers in their use against intracavity tumours, such as disseminated ovarian cancer, is its selectivity of the photosensitiser for tumour tissue compared with normal tissue. Covalent attachment of water-soluble polymer allows the delivery of hydrophobic photosensitisers⁸² and conjugation with a polymer may also increase selectivity of the photosensitiser.

Westermann *et al*⁸³ investigated the use of polyethylene glycol (PEG-5000) to improve the selectivity and biodistribution of *meta*-tetra hydroxyphenyl chlorin (*m*-THPC). The study involved attaching PEG to the four hydroxyl groups of *m*-THPC covalently and conducting comparative studies using conjugated and unconjugated *m*-THPC in nude mice bearing human colon carcinoma LS174T xenografts. Results

indicated that pegylation of *m*-THPC resulted in a higher tumour uptake and higher tumour to normal tissue ratio at all times. These results indicate that pegylation had improved the selectivity of the conjugate for tumour cells over healthy tissue.

Other studies include work carried out by Brasseur *et al*⁸² who used water-soluble polymers (PEG-2000 and polyvinyl alcohol) for the delivery of the hydrophobic photosensitiser chloroaluminium phthalocyanine (AlClPc) to Balb/c mice bearing interdermal EMT-6, or colon carcinoma colo-26 tumours. Results indicated that the AlPc-PVA conjugate had prolonged plasma half life, lower retention by the liver and spleen and a considerably higher tumour to normal cell ratio in comparison to unconjugated AlClPc.

Further work was carried out by Hamblin *et al*⁸⁴ and involved the attachment of polyethylene glycol (pegylation) to a polyacetylated conjugate of poly-1-lysine and chlorin e₆. Conjugates were investigated *in vitro* using an ovarian cancer line (OVCAR-5) and the macrophage cell line (J774). Comparative studies with the unconjugated chlorin indicated that the conjugate increased the relative phototoxicity towards the ovarian cancer line (OVCAR-5) whilst reducing it towards the macrophage cell line (J774). Notably, this was not the case with the unconjugated chlorin, and interestingly the increase in phototoxicity observed was reflected by the reduced oxygen consumption and aggregation. Confocal fluorescence microscopy revealed greater mitochondrial localisation in the OVCAR-5 than J774 and, on illumination switching of the cell death mechanism from necrosis to apoptosis was observed only in the OVCAR-5 cell line. Upon injection of the conjugates into nude mice bearing OVCAR-5 tumours, pegylated

conjugates gave higher amounts of photosensitiser in the tumour as well as a high tumour to normal tissue ratio and also increased the physical depth to which chlorin e_6 would penetrate unconjugated. All factors pointed out to an increase in efficacy of photodynamic therapy for ovarian cancer using pegylated PDT agents.

Sugar (carbohydrate) conjugates

Second generation photosensitisers and the problems encountered during PDT, such as low selectivity and slow clearance leading to long lasting photosensitivity, have led to research on new photosensitisers that have well defined structure, exhibit higher selectivity for tumour tissue as well as being quickly eliminated from healthy tissue. As previously described, compounds showing strong absorption of light in the red region of the visible spectrum are also preferred.

The mechanism for photosensitiser uptake by tumour cells has been well studied, but many factors are still uncertain. However, there is evidence that hydrophobic or amphiphilic sensitisers are carried by low density proteins and this route of delivery is efficient due to the high level of LDL receptors found on cancer cells.^{85,86} Furthermore, many amphiphilic porphyrins linked to sugar moieties have been synthesised and results show porphyrins bearing one or two carbohydrate substituents gave encouraging results.⁸⁷ Porphyrins with sugar moieties have been found to have good solubility in aqueous solutions and possibly acquire specific membrane interactions.^{88,89}

Synthesis of glycoconjugated porphyrins are found mostly by using sugar

derivatised pyrroles, dipyrromethanes and aldehydes. Early work includes that of Maruyama and co-workers⁹⁰ who synthesised tetra-glycosylated porphyrins via aldehydes derived from ribose, fructose and galactose which were converted to their corresponding nitroalkenes by condensation with nitroethane. The studies found that the tetra-glycosylated porphyrin was not as effective as hematoporphyrin and Rose bengal in generating singlet oxygen and prompted more work to be carried out to obtain more efficient photosensitisers. Many porphyrins linked to sugar moieties have been synthesised since then and some derivatives have proved to possess activity in PDT.⁹¹⁻⁹⁸

Sol *et al*⁹⁹ investigated the synthesis and characterisation of amino acid glycosylporphyrin derivatives and compared their *in vitro* photocytotoxic activity with hematoporphyrin (HP). Synthesis involved the condensation in different ratios of two benzaldehydes with pyrrole using Lindsey's conditions.¹⁰⁰ In order to improve cell membrane recognition, glucose and other sugar molecules were substituted at the *meso* positions of the tetra pyrrolic macrocycles. The phototoxicity of these synthetic porphyrins was tested against K562 human chronic myelogenous leukemia cells and found that the intermediate dead cell counts were always higher for the modified porphyrins than those observed with HP. Furthermore, the sensitising abilities of these compounds are of considerable interest for photodynamic therapy.

Other glycoconjugated porphyrin studies include work done by Mikata *et al.*¹⁰¹ The study concentrated on finding the correlation between the hydrophilicity of the compound and the phototherapeutic activity. New tetraphenylporphyrin derivatives

having eight glucose molecules were synthesised and their activity compared to tetraglucosylated tetraphenylporphyrins. The photosensitising ability of the compounds was evaluated ¹⁰² and so was the calculation of the singlet oxygen yield (¹O₂). The results indicated that the sugar-linked porphyrins were as effective as hematoporphyrin (HP) and tetraphenylporphyrin tetrasulfonic acid (TPPS), both well established PDT photosensitisers and ¹O₂ generators. The phototoxic properties of the octa-glucosylated sensitisers were measured against the HeLa cell line. Comparative studies were conducted using TPPS and $\alpha, \beta, \gamma, \delta$ -tetrakis(1-methylpyridinium-4-yl)porphyrin-*p*-toluenesulfonate (TMPyP). The glucosylated compounds indicated minimal cytotoxicity in the dark at low drug concentrations. Results also showed porphyrins having four protected sugar groups (tetraacetylglucose) were most photoactive suggesting that the glucose moiety protected with acetyl groups increased the uptake of the drug into the cell. However it is worth noting that porphyrins having eight glucose moieties (octa-glucosylated derivative) did not exhibit any marked effect, possibly due to the increased steric bulk associated with the eight acetyl groups.

More recent developments involve conjugation of glucose with chlorins. Due to the enhanced activity of chlorins over TPP ³³, chlorins were considered better candidates for derivatisation with sugars in order to improve their solubility, targeting and localisation ability. Laville *et al* ¹⁰³ studied the synthesis of tri and tetra (meta-hydroxyphenyl)chlorins and the effect of the glycoconjugation on the photoactivity of the molecule. Comparative studies were performed in HT29 human adenocarcinoma cells of the glycoconjugated chlorins and *m*-THPC, Foscan®. Results indicated that *m*-THPC

was poorly internalised and weakly photoactive. In contrast, the amphiphilic tri(meta-hydroxyphenyl)chlorin demonstrated much higher phototoxicity compared to *m*-THPC. Studies concluded that internalisation proceeded *via* an active receptor-mediated endocytosis mechanism and the higher phototoxicity was linked to higher mitochondrial uptake by the amphiphilic tri(meta-hydroxyphenyl)chlorin. Overall, studies confirmed that in most cases, glycoconjugation improved photoactivity and targeting. Further work in sugar derivatives of PDT agents still continues as results are proving to be promising.

1.2.9 Further research in photodynamic therapy

Currently, many developments based on new porphyrin photosensitisers are being investigated. However, there is still a lot of research required into the third generation of photosensitisers. The use of biological substrates for conjugation and as carriers for the photosensitiser has included some exotic and unique applications. The use of third generation photosensitisers has placed emphasis on the study of their pharmacokinetics, biochemistry, immunology, catalysis and drug metabolism.

Many synthetic pathways that have been developed but still are low yielding and often involving many steps and giving a mixture of by-products. Hence more work is needed to develop efficient, high yielding and synthesis of pure photosensitisers. Furthermore, the most important emphasis for this research is the focus on targeting, delivery and mode of activity of the photosensitisers in the cells. *In vitro* and *in vivo* work needs to be done to establish the mechanism of action of the photosensitisers in

tumour cells in order to improve selectivity and subcellular localisation of the photosensitisers.

1.3 PORPHYRINS AS TOOLS FOR BIOLOGICAL ANALYSIS

The aim of this section is to discuss the underlying principles for porphyrins being suitable for biological analysis. Emphasis is placed on their use as optical oxygen sensors for the measurement of oxygen concentration.

1.3.1 Optical sensor systems

Molecular oxygen has various applications in cells which are often highly dependant on the amount of oxygen present. Basic physiological and biochemical processes are highly dependant on local oxygen pressure to maintain cellular homeostasis.¹⁰⁴ Many methods have been established to measure oxygen and each method has its advantages and disadvantages. A particular method or a combination of methods may be used to determine the oxygen concentration at the site in question. Direct oxygen measurements can be taken in the circulatory system but this approach has many limitations. Such measurements of blood gases are invasive, time consuming and provide discontinuous data.¹⁰⁵ Moreover, the largest limitation of measurements in the circulatory system is that they do not give oxygen levels within the tissues where most interactions take place. Therefore, more methods of determining the partial pressure of oxygen (PO_2) are being sought.

1.3.2 Measuring oxygen concentrations *in vivo*

Several methods exist for the measurement of oxygen levels *in vivo*. The most appropriate method will depend on several factors and those that should be considered include:

- The site under investigation.
- The oxygen levels likely to exist and the accuracy required for the measurements.
- The time resolution required.
- The overall number of measurements required, i.e. single or multiple.
- Other physiological information to be considered to obtain the oxygen measurements i.e. membrane barriers etc.
- The extent of invasiveness that can be experienced without affecting the measurements.

1.3.3 Ideal oxygen sensor

Most molecular oxygen sensors have limited applications, low sensitivity and are difficult to synthesise or set up. Some qualities that are required for optimum results are:

- Non-invasiveness - Measurements should be preferably taken with causing minimal disruption of the system.
- Repeatability - Measurements should be ideally made frequently over a long amount of time within a system.
- Accuracy - Repeated measurements should display marginal variability and the data obtained should be accurate and correlate closely to measurements taken by other

reference methods.

- Sensitivity - Sensors should enable measurements to be made at a range of PO₂ and especially at low PO₂ levels.
- Little or no toxicity - The sensors should not exhibit any form of toxicity or cause any adverse side effects in the system.
- Multiple measurements - More than one measurement should be taken so as to improve the viability and accuracy of the results.
- Synthesis - Synthesis of molecular sensors should involve single, pure compounds with minimum synthetic steps and purification procedures so as to obtain the sensors in adequate yields.

1.3.4 Methods of measuring oxygen

The approach to our research is based on metalloporphyrins as oxygen sensors. However, before discussing this approach in detail, it is necessary to review some other related and complementary techniques for measuring oxygen concentrations.

Luminescence quenching

Luminescence based optical sensors have been widely investigated.¹⁰⁶ Heavy transition metals such as Ru(II) complexes have been used for their high yield of luminescence.¹⁰⁷ Some sensors involve the absorption of the dye in a polymer layer such as the absorption of ionic insoluble dyes on the surface of carrier particles (e.g. silica) entrapped within a silicone rubber matrix allowing the immobilisation of the dye.¹⁰⁸

Other Ru(II) complexes have been directly dissolved in glassy polystyrene layers.¹⁰⁹

Luminescence quenching of tris(4, 7'-diphenyl-1, 10'-phenanthroline)Ru(II) perchlorate, dissolved in a polystyrene layer has been investigated for its use as an oxygen sensor.¹¹⁰ This method has been found to be effected by temperature, concentration and aggregation qualities. Other dyes that have also been studied include tris(2, 2'-bipyridyl)Ru(II)dichloride in poly(vinyl alcohol) and poly(vinyl pyrrolidone) matrices¹¹¹ as well as RuPh₂PhenCl₂ in plasticised cellulose acetate.¹¹²

However, as these oxygen sensors are invasive, insensitive and often require calibration to stabilise the systems, this method is often used in conjunction with other methods.

Polarography

This is the most commonly used method for measuring oxygen concentrations and the technique is best for obtaining spatially resolved, accurate and multiple measurements of PO₂ *in vivo*. It provides measurements of PO₂ and in forms such as the Eppendorf histogram, displaying partial oxygen against time in order to provide a profile measurement of PO₂ values along a track. Disadvantages of this method include possible tissue damage during insertion of the electrodes, fragility of the system, unsuitability for repeated measurements and the variation in results in the electrode region due to the consumption of O₂. However, it is still considered as the “golden standard” for measurements of PO₂ and hence often used as a reference method in many systems.¹⁰⁴

Near Infra-red spectroscopy

Near Infra-red (NIR) spectroscopy can be used to measure the concentration of certain organic species and can be applied to even challenging media. Bonds in biologically important molecules such as aliphatic, alkene and aromatic C-H, amine N-H, hydroxyl O-H as well as C-O absorb in the NIR range. As each chemical structure is related to a specific position, shape and size of the analyte's absorption band, the concentration can be calculated from the data obtained. However, often advanced data-analysis algorithms are required to obtain accurate data.

This technique has potential advantages, especially when combined with other methods that measure PO_2 directly in tissues, such as polarography. NIR measurements of haemoglobin provide quantifiable data on intravascular haemoglobin content and saturation, hence producing additional data on the supply of oxygen to the tissue from the vascular system and the total oxygen capacity. Recent developments allow time-resolved or frequency-domain light measurements, which improve the accuracy of the results obtained. The system has been studied to quantify the exact haemoglobin concentration and oxygen saturation within bulk tissue¹¹³ as well as providing data from relatively deep tissue sites and the opportunity for imaging haemoglobin with modest spatial resolution.¹¹⁴ The method allows data acquisition for haemoglobin and PO_2 , hence facilitating the investigation of the demand and supply of oxygen within a tissue. The information obtained can be vital for determining the response of a tissue to damage or the viability of a tissue.

NMR methods

The wide availability of NMR instruments and the advantage of being non-invasive makes this method of measuring O_2 concentration very favourable. NMR has been used to make direct measurements of local PO_2 , by measuring the oxygen sensitive T_1 relaxation rate of perfluorocarbons.¹¹⁵ Previous studies involved the introduction of perfluorocarbons into the area under investigation by direct injection¹¹⁶ or vascular infusion.¹¹⁷ The injection method was shown to allow the direct placement of the perfluorocarbons where as vascular infusion limited the distribution and localisation of the perfluorocarbons. In the later case, the localisation of the perfluorocarbons was based on the cellular uptake and as a consequence deposition was restricted to perfused regions only.¹¹⁸ Simple washings would allow the manipulation of the incubation times and hence measurements could be made hours after direct injection or several days after being taken up by the cells. The sensitivity of the technique was investigated and shown to have improved chemical composition by increasing more fluorine atoms of identical chemical shifts to improve the signal and T_1 measurements. The method provided enhanced sensitive PO_2 data which was very similar to that obtained with the Eppendorf microelectrode without causing any disturbance to the cells. Recent developments include blood-oxygen level dependent imaging (BOLD) which has been used to investigate deviations in local oxygenation. This area is still being studied and is seen as a challenging area of research in NMR studies.

NMR studies of myoglobin has proved to be a useful technique for measuring O_2 concentrations in tissues that are enriched with myoglobin.¹¹⁹ The method again was

non-invasive but indicated limited sensitivity. The method has been applied to study low oxygen level conditions such as radiobiological oxygen effect and ischaemia/reperfusion injury.

NMR methods have the advantage of being sensitive over the observed range of haemoglobin saturation and are potentially useful to measure oxygen levels in all tissues. However, the methods also have limitations as measurements only reflect changes in haemoglobin saturation and hence additional information is required to obtain PO_2 values.^{120, 121}

1.3.5 Phosphors - method of choice for measuring O_2 concentration

During the past few years, the use of oxygen-dependant quenching of phosphorescence has proved to be a reliable and reproducible technique in measuring the oxygen levels at subcellular regions.¹⁰⁶ The choice of phosphors for investigation in this project is metalloporphyrins and will be discussed in detail later.

The use of phosphors as a method of oxygen measurement has many advantages over the conventional methods and one of them is the response time. The response time associated with this method allows accurate measurement of the oxygen pressure throughout the physiological important range of 760 torr down to 10^{-2} torr and can be applied to all living cells without invasion of the tissue. The most desirable and useful aspect of this technique is that simple optical measurements can be used to calculate the oxygen pressure in the area under investigation.

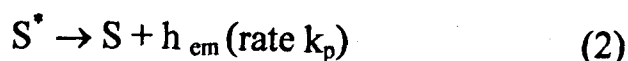
The Stern-Volmer relationship can be applied to convert the phosphorescence into

quantitative measurements. The equation below shows the Stern-Volmer relationship:-

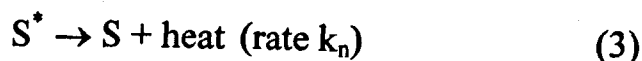
$$I_0 / I = \tau_0 / \tau = K_q \tau_0 [\text{O}_2] \quad (1)$$

Where I_0 and I are phosphorescence intensities in the absence and presence of oxygen concentration $[\text{O}_2]$ respectively, τ_0 and τ are the singlet lifetimes in the absence and the presence of oxygen respectively and K_q is the bimolecular quenching constant. The bimolecular quenching constant is related to the rate of diffusion of oxygen of the particular metalloporphyrin / luminophore (a molecule that gives out light).

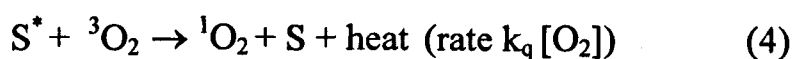
The detailed discussion of the photochemistry of porphyrins involved has been covered previously. In summary, upon illumination of the luminophore, photoexcitation allows the molecule to be raised to an excited state S^* which has a lifetime τ . From the excited state, the luminophore has several ways of returning to the ground state. The first possibility is by emitting a photon:



Another route is for S^* to return to its excited state non-radiatively:



Yet another common route involves the return to the ground state by energy transfer to other molecules (quenching). In biological systems, the most abundant quenching agent is oxygen.



The higher the concentration of oxygen available, the more this third pathway is preferred. Consequently, as the concentration of oxygen increases, the phosphorescence emission intensity decreases. This is the basis of using phosphors for measuring oxygen concentration.

1.3.6 Molecular oxygen interactions

Knowledge of the different energy states is important in order to understand the interaction of the luminophore with oxygen. It can be concluded that photoexcitation of a luminophore allows it to be raised to a higher energy state S^* and the luminophore returns to the ground state via many mechanisms including phosphorescence. Oxygen is an abundant quenching agent, available in most biological systems, and therefore the energy released during phosphorescence may be quenched by oxygen in its ground state 3O_2 producing the higher in energy 1O_2 state.

1.3.7 Choice of metal in metalloporphyrins

The choice of metal coordinated to the central nitrogen atoms of the porphyrin macrocycle determines the types of reaction the porphyrin undergoes. The introduction of divalent central metals forms highly electronegative porphyrin complexes in the order $\text{MgP} > \text{ZnP} > \text{CuP} > \text{NiP} > \text{PdP}$.¹²² The high electron density around the centre, makes the centre of the porphyrin macrocycle quite stable and hence any reactions would involve the substitution at the *meso*-carbons other than the β positions.

Pt (II) and Pd (II) are particularly important metals for their use as optical sensors to detect low oxygen concentrations. These metals have the electronic configurations $6d^8$ and $5d^8$ respectively. These electrons are involved in the backbonding between the d orbitals of the metal and the π^* orbitals of the porphyrin and allow rapid intersystem crossing. This results into little or no fluorescence during the conversion of the luminophore from its singlet state to its triplet state. Consequently, this leads to their phosphorescence quantum efficiency to be higher than that of other metalloporphyrins.

1.3.8 Metalloporphyrins as phosphors

In most oxygen quenched phosphorescence sensors, palladium and platinum complexes are employed. A range of studies have taken place to establish this desirable property of metalloporphyrins without the associated tissue damage obtained by porphyrins acting as PDT agents. This is achieved by using minimal amounts of the metalloporphyrin. These include studies where the porphyrin is embedded in an appropriate polymer matrix such as polystyrene to produce a solid-state phosphorescent

coating.^{123,124,125} Molecular oxygen penetrates the coating and quenches the phosphorescence intensity and consequently shortens the lifetime via phosphorescence quenching. In most studies, the phosphorescence lifetime of the oxygen probe which has been found to be independent of the concentration, geometrical as well as instrumental factors is used for quantification of oxygen. Singlet lifetime can be monitored on a real time-scale using phase-modulation techniques.¹²⁶ In early studies, experiments provided time-resolved data that were analysed to give “apparent” oxygen concentrations. Recently, frequency domain time-resolved phosphorometry has provided a more practical, technical and significant system for measuring oxygen distribution.^{127,128}

Early studies conducted by Vanderkooi *et al*¹ involved water-soluble derivatives of porphines and fluoresceins as triplet state probes of oxygen. The probes include fluoresceins derivatives, 4' 5'-diiodofluorescein, eosin Y, 5-(and 6)-carboxyeosin, erythrosin and 5-(and 6)-carboxyerythrosin as well as Zn(II), Y(III), Sn(IV), Lu(III) and Pd(II) derivatives of meso-tetra-(4 - sulfonatophenyl)-porphine, meso-tetra-(*N*-methyl-4-pyridyl)-porphine and coproporphyrin. Using the Stern-Volmer relationship, the phosphorescence lifetimes of the probes were found to be dependent on the concentration. Binding of the probes to bovine serum albumin (BSA) prolonged the half-life of the probes by inhibiting self quenching and protection from collision with quenchers. The study indicated the possibility of measuring oxygen from ~ 250 μM (air saturation) down to nanomolar range. Hence a simple, reliable, stable and sensitive method of measuring oxygen was described.

A further study investigated the involvement of oxygen in the production of

adenosine triphosphate (ATP) which is required for energy release in bioprocesses such as biosynthesis, transport and mechanical work.¹²⁹ This study concentrated on the effects of oxygen deficiency using an understanding of the dependence of the oxygen concentration on mitochondrial oxidative phosphorylation. The method involved the phosphor palladium corpoporphyrin as an oxygen indicator. The phosphorescence-lifetime method allowed rapid (< 100 ms) measurement of oxygen concentration. Using isolated rat liver mitochondria, the results indicated that overall, in the absence of oxygen, cytochrome c reduction was observed. Also, pH dependence of the suspending medium on the reduction of cytochrome c was established, where reduction was notably observed at even higher oxygen concentrations when the pH was made more alkaline. This investigation confirmed that the method was able to measure oxygen concentrations from greater than 10^{-3} M to less than 10^{-8} M. The technique was fast and the measurements were repeatable. Overall an efficient method of measuring oxygen concentration *in vitro* was obtained.

In 1988 Rumsey *et al*¹³⁰ investigated the possibility that phosphorescence measurements could be used to obtain images of oxygen distribution in tissue without invasion of that tissue. The choice of phosphor used in the study was palladium (Pd) corpoporphyrin because it remained in the perfusate and was not taken up by the tissue. This was shown by the complete disappearance of the image within 2 mins, after the tissue had been returned to the perfusion medium without the probe. Isolated rat livers were perfused through the portal vein with media containing palladium corpoporphyrin. As the tissue was illuminated and the Pd corpoporphyrin excited to its triplet state, the

liver was imaged at various perfusion rates. As oxygen is a powerful quenching agent for phosphors, a large increase in phosphorescence was observed from well-perfused liver to anoxia (no flow of oxygen).

More *in vivo* studies were made with two new phosphors called Oxyphor R2 and Oxyphor G2.¹³¹ One was based on Pd-meso-tetra-(4-carboxyphenyl)porphyrin and the other on Pd-meso-tetra-(4-carboxyphenyl)-tetra-benzoporphyrin. In the study, the phosphors used were second generation polyglutamic Pd-porphyrin-dendrimers bearing 16 carboxylate groups on the outer layer. Both were found to be highly soluble in biological fluids such as blood plasma and their ability to penetrate biological membranes was found to be low. *In vivo* applications demonstrated the use of Oxyphor G2 to non-invasive determination of oxygen distribution in a subcutaneous tumour growing in rats. The calibration constants of the phosphors were found to be independent of pH in the physiological range (6.4 to 7.8) hence making them good probes for measuring oxygen concentration.

Furthermore, oxygen pressure distribution in R3230 AC mammary tumours growing in dorsal flap window chambers in rats was also investigated.¹³² The study involved the use of oxygen dependent quenching of phosphorescence after the injection of Oxyphor R2 into the tail vein. Oxygen pressure maps were obtained, which detailed that the oxygen pressure in the growing edge of the tumours was lower than those in the central core of the tumour and much lower than those of the host tissue. In conclusion the studies showed that using the phosphor Oxyphor R2 allowed the oxygen distribution in the tumour to be studied without invasion of the tissue.

Pd-meso-tetra-(4-carboxyphenyl)porphyrin has been widely used as a phosphor to measure oxygen concentrations in tumour cells ¹³³ and also in self-assembled membranes on alumina (SAM).¹³⁴ SAM techniques have been exploited as effective methods to design a solid surface with a well defined composition, structure and thickness for interfacial optical studies.¹³⁵ Compounds enriched with the carboxyl functional group are the most effective in preparing a SAM of an organic compound on a metal oxide surface. Pd porphyrins in general exhibit strong room temperature phosphorescence with high quantum yield and a long natural lifetime.¹³⁶ Pd TCPP was found to be a suitable optical oxygen sensitising device using SAM due to the stable membrane formation on alumina and its carboxyl group.

Recently more “exotic” palladium complexes have been adopted for their use in oxygen concentration measurements. In the study, Pd (and Pt) porphyrins which were previously used as basic phosphors were encapsulated inside dendrimers. A series of polyglutamic Pd-porphyrins-dendrimers,¹³⁷ Pd-tetra-benzoporphyrin-dendrimers ¹³⁸ and phthalocyanine-dendrimers ¹³⁹ have been synthesised and investigated for their ability to measure oxygen concentrations. Studies have indicated that dendrimers regulated that access of oxygen to the phosphors cores, and adjusting the dendrimers size allowed tuning of the phosphorescence oxygen quenching properties. Further studies indicated that hydrophobic dendrimers allowed folding of the lipophilic dendritic matrix in water and diminished the mobility of the protecting shell and hence were found to enhance oxygen diffusion barriers.¹⁴⁰ At the same time the study observed that multiple peripheral functionalities served as anchor points for linking hydrophilic modifiers

(PEGs, polyalcohols etc) and resulted in minimum interactions with proteins and other macromolecules *in vivo*, making the phosphorescence quenching specific only to oxygen.

Overall, Pd porphyrins have been studied for their role as oxygen sensors and have indicated a wide variety of methods, applications and outcomes which all designate their ability as sufficient oxygen measuring phosphors.

1.4 PORPHYRINS IN BIOLOGICAL IMAGING

Biological imaging has been developed on a tissue, cell and intercellular level where porphyrin molecules are introduced and due to their fluorescent nature, can be traced upon elimination of light, a process which can assist in displaying the structure and the properties associated with the specific cell or organelle. Fluorescence has been introduced previously and is the basis of the way in which these imaging agents work.

The basic principle of fluorescence involves a fluorophore which is in the ground state. Upon illumination with light and at the correct wavelength, the fluorophore absorbs energy in the form of a photon, which increases its energy state placing it in an excited energy state. Some of the energy from the light may be lost internally within the fluorophore but in order to return back to its ground state, energy must be released in the form of emitted light (fluorescence). As the energy released from the fluorophore is via a photon of lower energy, the emitted light is a different colour. The exact magnitude of the excitation and emission light are both dependent upon the fluorophore involved. Hence, a fluorophore in the form of a fluorescent dye / porphyrin can be attached to a specific molecule in a sample / cell/ system and selectively only those molecules of

interest in the sample would be seen.

An ideal fluorophore used for imaging would have a high fluorescence quantum yield (FQY). FQY is the ratio of the number of photons emitted to the number of photons absorbed and is given as a value between zero and one. Fluorophores are often designed so as to allow minimal depopulation of the S_1 state by incorporating rigid functionalities into the porphyrin macrocycle. This inhibits thermal relaxation and has an overall influence of prolonging the lifetime of S_1 and consequently increasing fluorescence emission. An ideal fluorophore would also display a large Stokes shift and hence allow greater sensitivity in the measurement of the phosphorescence. Stokes shift is defined as the difference in wavelength between the excitation and emission λ_{max} of a fluorophore. A large Stokes shift value enhances the sensitivity as it allows the emission photons to be detected against a low background level isolated from excitation photons.

Undesirable qualities in a fluorophore include photobleaching and fluorescence quenching. Photobleaching refers to the eventual degradation of a fluorophore by light, which is an irreversible process and an inevitable destiny of fluorophores. Fluorescence quenching is also an undesirable effect that reduces FQY and may arise due to self quenching, collisional quenching or from the formation of non-fluorescent ground state species. Fluorescence in porphyrin macrocycles is susceptible to rigid quenching due to their propensity to be involved in π - π stacking. Other quenching agents include proteins and water.¹⁴¹

1.4.1 Fluorescence Microscopy

Microscopy is used to detect structures, molecules or proteins within the cell through visualisation of fluorescence. Basic forms of microscopy, such as optical microscopy, are based on macroscopic specimen features, such as phase gradients, light absorption, and birefringence. Fluorescence microscopy on the other hand allows the imaging of a fluorophore via the distribution of a specific molecular species based solely on the properties of fluorescence emission. Fluorescence microscopy can hence be used easily to investigate the precise location of intracellular components labelled with specific fluorophores. Other information such as the associated diffusion coefficients, transport characteristics, and interactions with other biomolecules can also be easily determined. Additionally, the dramatic response in fluorescence to localised environmental variables enables the investigation of refractive index, viscosity ionic concentrations, membrane potential, pH and solvent polarity in living cells and tissues.

1.4.2 Basic principles of fluorescence microscopy

The underlying principle of fluorescence microscopy involves the use of a dye which is often used to stain cells. The dye is illuminated with filtered light at the absorbing wavelength, specific to the dye being used. The emitted light from the dye is then filtered through another filter that allows only the emitted wavelength to reach the eyepiece or camera port of the microscope and the dye is seen to glow brightly against a dark background.

Sometimes, the fluorescent molecule itself can be used as a direct stain or probe

for precise structures. Alternatively, the fluorescent dye can be bound to another non-fluorescent probe that recognises specific structures. Some examples include the fluorescent molecule, rhodamine which may be conjugated to phalloidin, which binds the filamentous actin. Yet another important method to identify specific proteins is to couple fluorescent dyes to antibodies that bind very specifically to macromolecules in the cell.

1.4.3 Fluorescent probes

As mentioned earlier, a desirable property of fluorophores is to have a large FQY value. Many of the currently available commercial fluorophores have been designed to have a high FQY value. The majority of the fluorophores have an aromatic ring substituent¹⁴² which increases their degree of conjugation hence allowing the wavelength to shift into the red region of the spectrum. FQY values may also be increased by the introduction of ring activators and electron-donating groups.

Incorporation of different substituents has different effects on the FQY values. A decrease in FQY values is prompted by the depopulation of the excited state and may be achieved by adding electron withdrawing groups as well as heavy atoms to the aromatic ring systems. Heavy atoms encourage the depopulation of the excited state by allowing intersystem crossing to occur more rapidly to the triplet excited state. This allows other processes such as phosphorescence to dominate and minimises fluorescence activity of the fluorophore. Halogen substituents also have a marked effect on their FQY values. They behave as fluorescence quenchers and hence reduce the overall fluorescence obtained in the order $I > Br > Cl$.

Commercial fluorescence probes are designed to be extremely efficient and are manufactured to be compatible with most imaging instruments. This allows investigations into processes such as mitosis, apoptosis, substrate degradation and respiration. Recent advances include incorporation of fluorophores with antibodies, especially monoclonal antibodies, allowing investigations into organelle structure and activity in live cells with minimum interruption of the cellular function.¹⁴³ Fluorophores display a range of absorption characteristics, solubilities and bioconjugate functionality so that they may target specific organelles within the cells. Organelles which attract a great deal of interest are mitochondria, lysosomes, endoplasmic reticulum and the Golgi apparatus.

In this project, the main interest is with mitochondrial probes which are discussed in detail below.

1.4.4 Probes for mitochondria

Mitochondria are often referred to as the “energy stations” of the cells. This is where ATP (Adenosine Triphosphate) molecules which release energy are produced. The energy is stored in high energy phosphate bonds in the ATP molecule. ATP is converted from adenosine diphosphate by adding the phosphate group with the high-energy bond. Various reactions in the cell can either use energy (whereby the ATP is converted back to ADP, releasing the high energy bond) or produce it (whereby the ATP is produced from ADP).

ATP is synthesised in two different pathways, the first pathway requires no

oxygen and is called anaerobic metabolism. This pathway is called glycolysis and it occurs in the cytoplasm outside the mitochondria. During glycolysis, glucose is broken down into pyruvate. However, only 4 ATP molecules can be made by one molecule of glucose run through this pathway. The other process is aerobic and involves mitochondria and oxygen which are involved in the Krebs's cycle to produce many hydrogen ions. The enzyme ATP synthase uses the energy of the hydrogen ion gradient to form ATP from ADP and Phosphate. It also produces water from the hydrogen and the oxygen. The Krebs's cycle generates 24-28 ATP molecules out of one molecule of glucose in addition to the 4 molecules that glycolysis yields.

Found in eukaryotic cells, they make up about 10 % of the total cell volume. They are pleomorphic (many physical forms) and exhibit structural variations depending on the cell type, cell cycle stage and intercellular metabolic state. Mitochondria are involved in energy production through oxidative phosphorylation and lipid oxidation. They have shown to play a significant role in apoptosis,¹⁴⁴ a mode of cell death that is programmed into normal cell types.¹⁴⁵

Mitochondrial selective fluorophores allow studies involving mitochondrial activity, localisation and abundance. Different types of commercially available fluorophores exist, conventional fluorescent probes include Rhodamine 123 which is often used as a reference stain in most experiments. The diagram below shows the structure of Rhodamine 123.

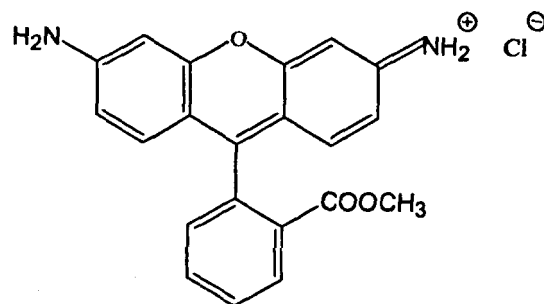


Fig 7 Chemical structure of Rhodamine 123

Rhodamine 123 is a cationic, lipophilic dye which has been used as a mitochondrial fluorophore. Rhodamine 123 (Rh 123) has been shown to be retained in human carcinoma cells for more than 24 hours hence making it a potential anticancer agent for photodynamic therapy.¹⁴⁶ Rh 123 has been used as a mitochondrial-selective fluorophore in many studies including apoptosis,¹⁴⁷ bacterial viability and vitality,¹⁴⁸ multidrug resistance,¹⁴⁹ and mitochondrial enzymatic activities.¹⁵⁰

New commercial mitochondrial probes have been developed that are specifically concentrated by active bacteria and are well retained during cell fixation. The series of fluorophores designed by molecular probes include; Chloromethyl-X-rosamine [CMX Ros],^{151, 152} 3, 3'-Dihexyloxycarbocyanine iodide [DiOC₆(3)],^{153, 154} Nonylacridine orange [NAO],¹⁵⁵ MitoTracker green™ [MTG],¹⁵⁶ Tetramethylrhodaminemethylester [TMRM],¹⁵⁷ and many more. Many studies have involved the use of these commercially available fluorophores to examine mitochondrial activity.^{158, 159}

Numerous fluorophores are now available for visualisation of mitochondria in

cells and tissues. These differ in their oxidation states, fixability, solubility, bioconjugate functionality as well as spectral characteristics and can be chosen to suit special requirements of the studies.

1.4.5 Mitochondrial targeting

Porphyryns have been known for their success as photodynamic therapy photosensitisers. This in itself is a limitation of porphyryns as fluorophores. Their role as PDT agents involves depopulation of the S_1 state and the consequent population of the triplet excited state hence reducing the overall fluorescence emitted by the fluorophore . Therefore, there have been no examples of non toxic porphyryn fluorophores which do not express photosensitising action.

However, the ability of porphyryns to fluoresce allows them to be visualised within living tissues without the need for auxiliary labelling. Therefore, by incorporating certain functionalities would allow selective accumulation of the porphyryn sensitiser in specific organelles and facilitate further investigations of the photosensitiser activity in the cell.

Sanberg *et al*^{160, 161} have established that the intracellular distribution of porphyryns is determined by the different functional groups present. Later, Woodburn *et al*¹⁶² studied the *in vitro* subcellular distribution patterns of ten porphyryns, varying in charge and hydrophobicity. Two cell lines were investigated, V79 and C₆ glioma and the distribution of porphyryns were studied using confocal laser scanning microscopy, with Rh-123 used as a control fluorescent probe. The results indicated that all the porphyryns

were taken up by both cell lines, however distinct differences were observed in the porphyrin distribution patterns. Porphyrins with cationic side chains were identified to localise in the mitochondria whereas those with anionic character predominantly localised in lysosomes.

Dummin *et al*¹⁶³ investigated the effect of photosensitiser lipophilicity on the photodynamic efficacy *in vitro*. The study involved the use of HeLa cells and their photosensitisation by a series of cationic Zn(II)phthalocyanines bearing lipophilic side chains. The results indicated that the most lipophilic photosensitiser of the series, ZnPcA₆ was also the most photodynamically active, and was found to accumulate selectively in the inner mitochondrial membrane.

Several studies have implicated the mitochondria as a sensitive target for photodynamic therapy. This is based on the findings that apoptotic cell death was initiated by PDT.^{164, 165} Further studies have indicated a link between cell death and mitochondrial photodamage.^{144, 166} Mitochondrial based apoptosis of cells can be indicated by disruption of the transmembrane potential during apoptosis^{153, 154} as well as the release of intermembrane proteins such as AIF and cytochrome *c* which trigger apoptogenic caspases and nucleases.^{167, 168}

Studies conducted by Kessel *et al*¹⁴⁴ involved the use of P388 and L1210 murine leukemia cell lines and their treatment with Lysyl chlorin p6 (LCP), porphycene monomer (PcM) and porphycene dimer (PcD) and the cationic porphyrin MCP. The results indicated that PDT induced an apoptotic response after mitochondrial damage, but not after selective damage to lysosomes or to the cell membrane. The results also

indicated that the release of mitochondrial contents triggered an apoptotic response and further studies indicated the specific release of cytochrome *c* to have an impact on apoptosis.¹⁶⁹

Further studies were conducted by Kessel *et al* investigated the effect of Lu-Tex, an agent that was known to localise in lysosomes, which was found to initiate apoptotic response in animal tumour models.^{170, 171} The study involved the use of a series of photosensitising agents with known sub-cellular targets in L1210 cells. These include the capronylxyethyl porphycene (CPO),¹⁶⁹ a monocationic porphyrin (MCP),¹⁷² tin etiopurpurin (SnET₂),¹⁷³ aluminium phthalocyanine (AlPc),¹⁷⁴ LuTex; *N*-aspartyl chlorin e₆ (NPe₆),¹⁷⁵ lysyl chlorin p6 (LCP),¹⁷⁶ tin octaethylpurpurin amidine (SnOPA),¹⁷⁶ and lysyl chlorin p6 imide (LCI).¹⁶⁶ The study suggested that mitochondrial and combined (mitochondrial with lysosomal) damage led to a rapid apoptotic response, related to the release of cytochrome *c* from mitochondria into the cytosol. Lysosomal damage led to the immediate release of cathepsins and other proteolytic enzymes, the apoptotic response to lysosomal photodamage being slow and incomplete where many non-viable cells were shown to exhibit no apoptotic morphology. The study therefore indicated a clear distinction between mitochondrial targeted and lysosomal targeted photosensitisers and their ability to induce apoptosis in cells.

1.5 Further development

Apart from the use of porphyrins for photodynamic therapy, the use of porphyrins as tools for biological analysis covers a large number of applications. The two main areas of

interest for this project are in their use as phosphorescence quenching oxygen sensors and fluorescence imaging fluorophores.

Ideally, a multifunctional porphyrin design would be where the porphyrin could act as an oxygen sensor and also as a fluorophore. However, oxygen sensors are often palladium based and this allows rapid intersystem crossing and maximum phosphorescence yield. The opposite effect is needed for an efficient fluorophore, where minimal intersystem crossing should occur hence maximising the fluorescence quantum yield (FQY).

Current developments in fluorescence imaging, such as monoclonal antibody conjugation allow specific organelle targeting and therefore minimises the doses needed and light required for visualisation of the dyes. Further work would involve discovery of more organelle-specific fluorophores that would allow investigations into distribution and subcellular localisation of the fluorophores to be determined.

Oxygen sensors have been investigated in more detail recently and, as it is a fairly new concept, more work requires to be done in terms of developing simple and less trivial synthesis as well as purification with high yields. Solubility, aggregation problems as well as selective targeting of specific organelles within a cell are areas that require attention for the identification of more efficient metalloporphyrin oxygen sensors.

2.1 SYNTHESIS OF FUNCTIONALISED PORPHYRINS

As mentioned in the previous chapter, porphyrins and other photosensitisers have been investigated since the early 1900s.¹⁷⁷ Since then, significant advancements have been made especially in their synthesis. Discoveries in the last century for porphyrin synthesis have led to two Nobel prizes: Hans Fischer (1930) for synthesis of Iron protoporphyrin IX¹⁷⁷ and R.B Woodward (1965) for synthesis of chlorophyll a.¹⁷⁸

All porphyrins include a macrocyclic framework composed of carbon-hydrogen and nitrogen (porphine) which make up the core of this class of molecules. The diagram below shows the structure of porphine indicating different positions for substituent attachment. Interestingly, all naturally occurring porphyrins are substituted at the β -positions and bear meso-substituents, only when part of an exocyclic fused ring.

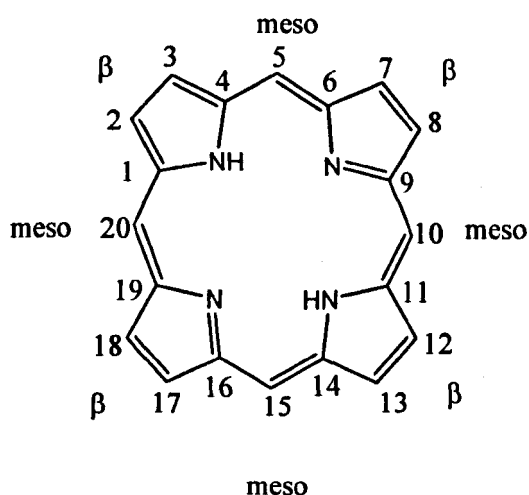
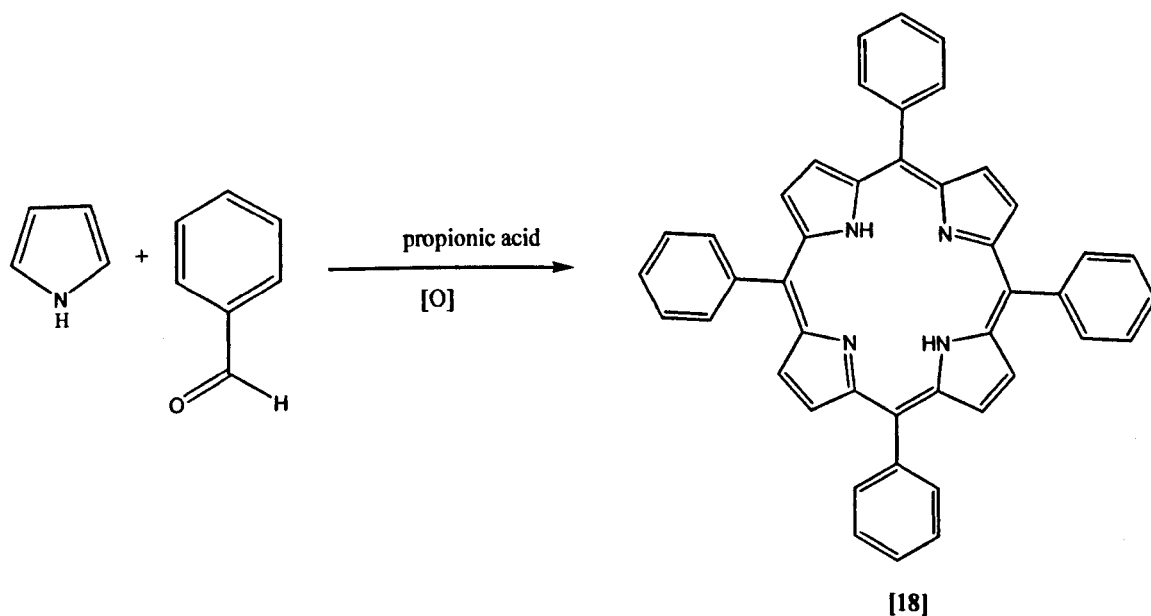


Fig 8: Structure of porphine

Porphyrin synthesis is not at all trivial; processes are lengthy and involve tedious purification steps which are often uneconomical and impractical. Generally, the more symmetric the distribution of substituents around the macrocyclic core the simpler the synthesis becomes, and for the most extreme examples, such as 5, 10, 15, 20-tetraphenyl- or 2, 3, 7, 8, 12, 13, 17, 18-octaethylporphyrin, multigram preparations are possible. Any variation to give unsymmetrical porphyrins however complicates synthesis considerably. Separation of the different products also becomes more difficult and the yields obtained are often very low due to the number of different isomers formed.

2.1.1 Adler-Longo method

In 1936 Rothmund¹⁷⁹ synthesised the first tetraphenylporphyrin (TPP) [18]. The reaction, performed in a sealed bomb, involved heating the starting material at 150 °C. The reaction was very low yielding and hence an improvement to the method was suggested by Adler and Longo¹⁸⁰ in 1967.

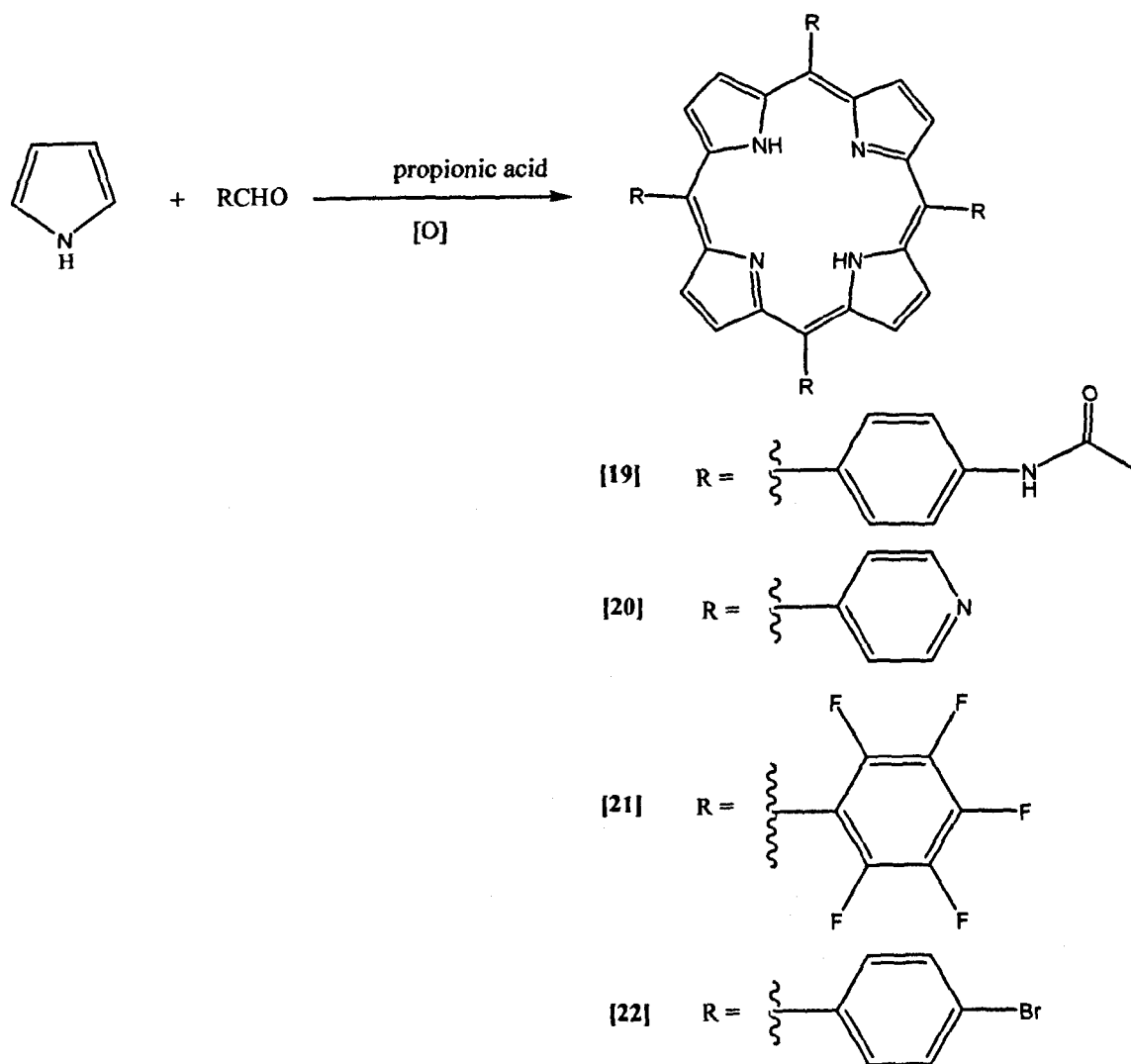


Scheme 9: Adler-Longo method for formation of tetraphenylporphyrin¹⁸⁰

Their method involved reacting pyrrole and benzaldehyde in refluxing propionic acid open to air for 30 minutes. These conditions also allowed the condensation of other substituted benzaldehydes to give multigram yields of up to 20% of the desired product.

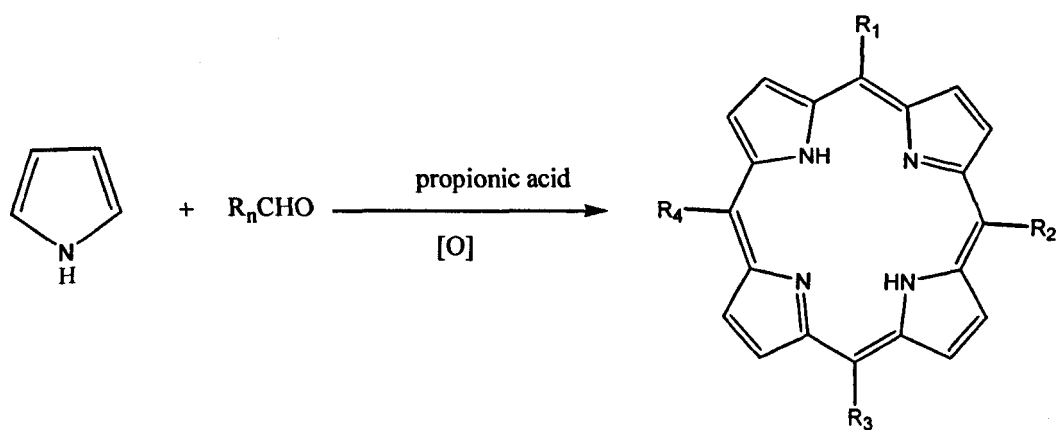
2.1.2 Porphyrins synthesised in this project using Adler-Longo method.

In this project, using the Adler-Longo method, symmetrical and unsymmetrical porphyrins were synthesised. Symmetrical substituted porphyrins were synthesised by using pyrrole and the appropriate substituted benzaldehyde in propionic acid. Using this method, 5,10,15,20-tetra-(4-acetamidophenyl)porphyrin [19], 5,10,15,20-tetra-(4-pyridyl)porphyrin [20], 5,10,15,20-tetra-(pentafluorophenyl)porphyrin[21] and 5,10,15,20-tetra-(4-bromophenyl)porphyrin [22], were synthesised. The full experimental procedures are outlined in chapter four but the scheme below shows the experimental outline.



Scheme 10: Symmetrical tetrasubstituted porphyrins synthesised in project.

The Adler-Longo method can also be used to obtain unsymmetrical tetrasubstituted porphyrins by using more than one type of aldehyde under the same conditions.¹⁸⁰ By varying the stoichiometry of the reagents, yields of the desired product can be maximised. In such circumstances, chromatographic separation of the products can be complicated involving many different solvent systems to obtain the desired pure product.



The table below indicates the products achieved by using the Adler-Longo conditions.

Porphyrin	R1	R2	R3	R4
[23]				
[24]				
[25]				
[26]				
[27]				
[28]				

Scheme 11: Unsymmetrical tetrasubstituted porphyrins synthesised in project.

In this project, the synthesis of 5-(4-acetamidophenyl)-10,15,20-tris-(3, 5-dimethoxyphenyl)porphyrin [23] and 5-(4-pyridyl)-10,15,20-tri-(pentafluorophenyl)porphyrin [24] are examples where the aldehydes used were varied stoichiometrically to obtain the asymmetric porphyrins. Other syntheses that involved lengthy separation and characterisation were of porphyrins [25], [26], [27], [28] which were obtained as a result of the reaction using pentafluorobenzaldehyde and 4-methoxybenzaldehyde together in a 1:1 ratio. These products are 5-(4-methoxyphenyl)-10,15,20-tris-(pentafluorophenyl)porphyrin [25] and 5,15-di-(4-methoxyphenyl)-10,20-di-(pentafluorophenyl)porphyrin [26] and 5-(pentafluorophenyl)-10,15,20-tris-(4-methoxyphenyl)porphyrin [27] and 5,10,15,20-tetrakis-(4-methoxyphenyl)porphyrin [28]. Such complicated separations of unsymmetrical porphyrins give low yields as seen in the synthesis procedure.

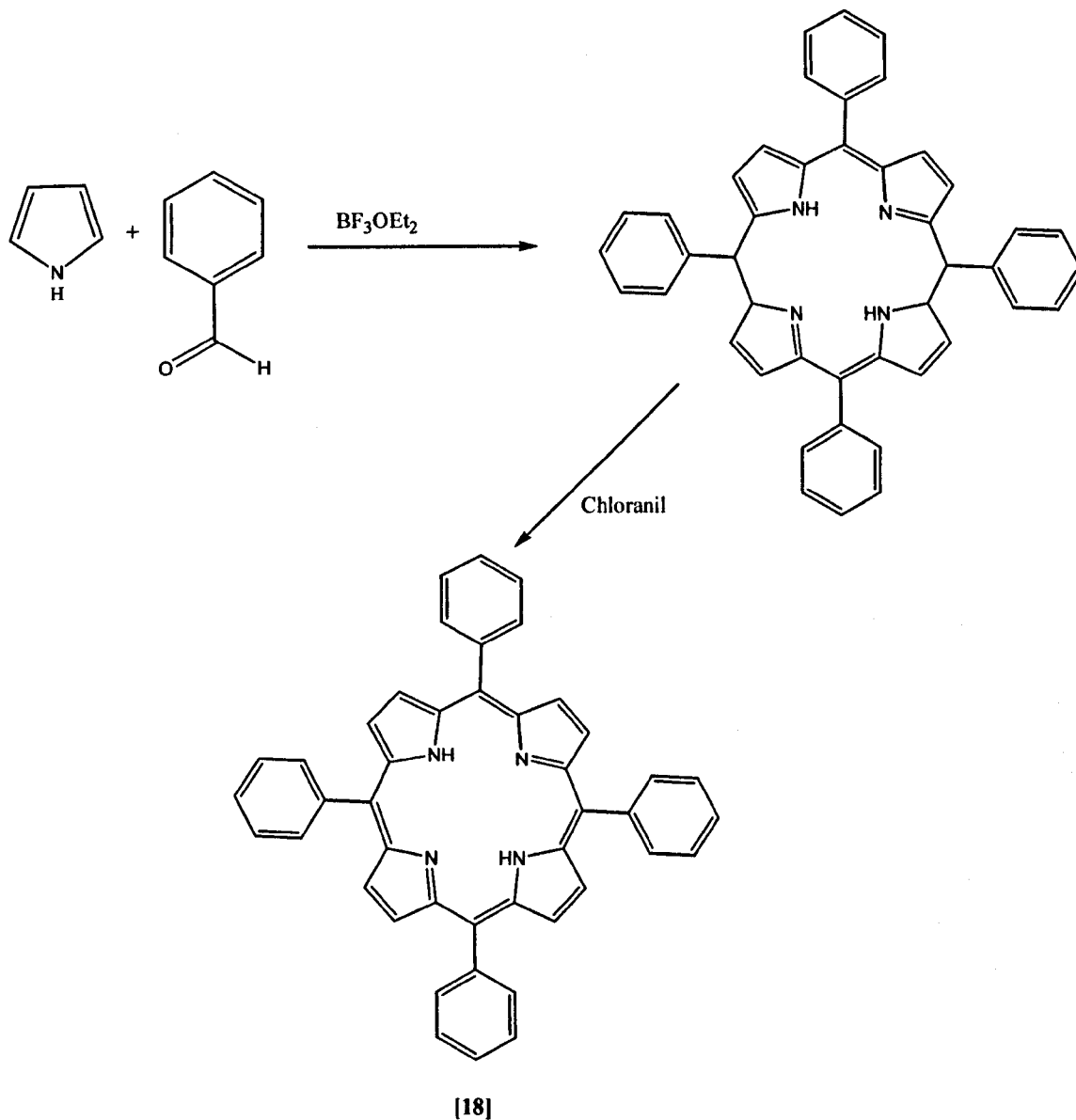
The Adler-Longo method however has limitations as it does not allow benzaldehydes bearing acid sensitive groups to be condensed, therefore limiting the synthesis of TPP analogues to those bearing less acid sensitive functionality. An example would be 5-(4-aminophenyl)-10,15,20-tris-(3,5-dimethoxyphenyl)porphyrin [29], where the amino group on the phenyl is acid sensitive and hence could not be directly synthesised using the Adler-Longo conditions. The porphyrin was alternatively derived from the treatment of 5-(4-acetamidophenyl)-10,15,20-tris-(3,5-dimethoxyphenyl)porphyrin [19] with acid. Other major drawbacks involve the production of chlorins and other pyrrole polymers which contaminate the final product and require lengthy and non-trivial chromatographic purification to obtain the pure product.

2.1.3 Lindsey method

In 1987, Lindsey *et al*¹⁸¹ proposed a different method for the synthesis of TPP. The Lindsey method involved a milder set of conditions which included using a catalytic amount of Lewis acid and gentle heating. This method relies on the formation of porphyrinogen as an intermediate in porphyrin synthesis. Equilibrium is established between the porphyrinogen and the benzaldehyde/pyrrole starting materials, a quinone based oxidant is then added which irreversibly converts the porphyrinogen to porphyrin.

Lindsey's synthesis of porphyrins involved using pyrrole, benzaldehyde, triethylorthoacetate as a water scavenger with boron trifluoride at room temperature. These conditions enabled the synthesis of porphyrins from sensitive aldehydes in higher yields and with easier purification. However, the requirement of high dilution conditions means that the reaction cannot be easily scaled up indefinitely and hence this method was not used in this research.

The scheme below outlines the Lindsey conditions for porphyrin synthesis.



Scheme 12: Formation of tetraphenylporphyrin using Lindsey conditions ¹⁸¹

Apart from tetra-substituted porphyrins, the synthesis of disubstituted porphyrins has been widely used in this project. Simple disubstituted porphyrins offer the possibility of performing reactions at the vacant 10,20-*meso* positions as well as the β positions, which are less sterically hindered compared to TPP. Disubstituted porphyrins are

synthesised using the “2+2 porphyrin synthesis method” discussed below.

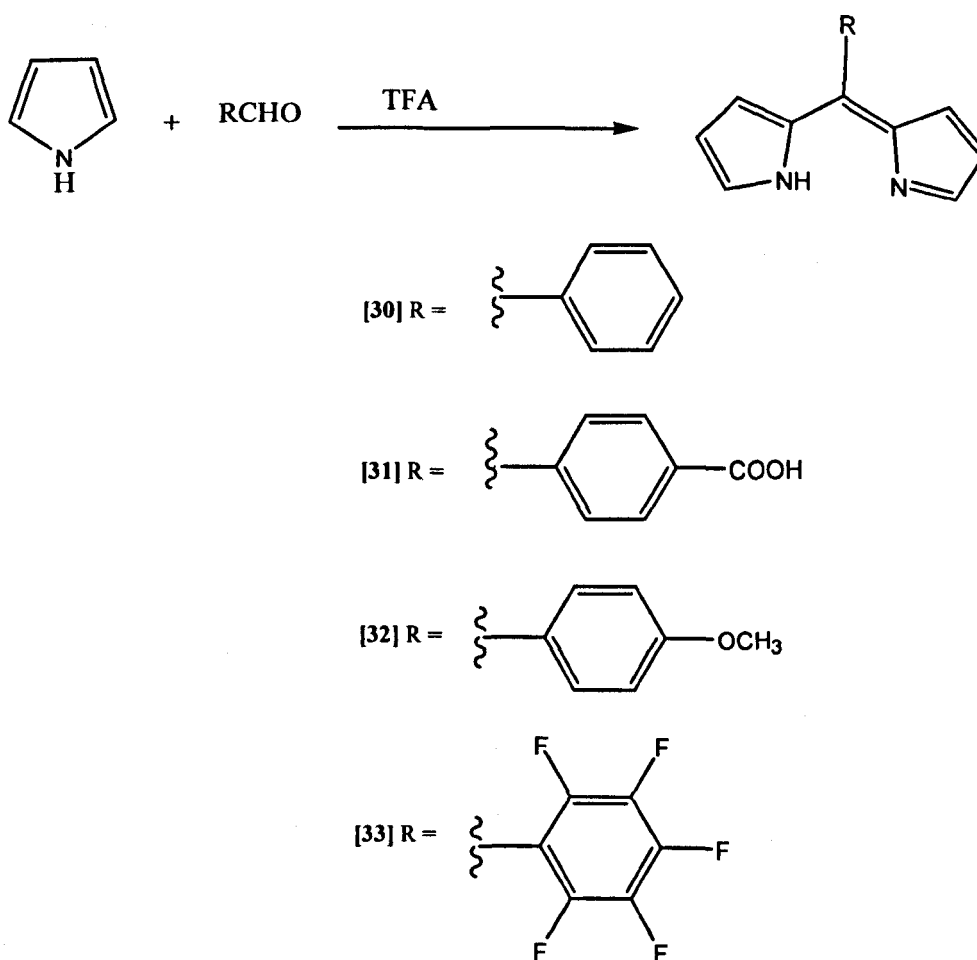
2.1.4 2+2 Porphyrin synthesis of disubstituted porphyrins

2+2 Porphyrin synthesis involves the formation of disubstituted porphyrins by the condensation of two dipyrromethanes (fragments containing two pyrrole units). The process relies on the formation of the porphyrin from two dipyrromethane units, each containing two pyrrole units. The synthesis of dipyrromethane involve reacting pyrrole, the appropriate benzaldehyde and trifluoroacetic acid. Early work in this area was conducted by Mac Donald ¹⁸² who proposed the synthesis involving the use of one dipyrromethane with no α - substitution and another dipyrromethane bearing two formyl groups alpha (α) to the pyrrolic nitrogens.

Honeybourne *et al* ¹⁸³ used a modified Mac Donald method to synthesise dipyrromethanes containing different substituted positions and formyl groups at the terminal α positions. The use of 5-phenyldipyrromethane for the synthesis of diphenylporphyrin (DPP) was reported by Bruckner and co-workers in 1998.¹⁸⁴

2.1.5 Dipyrromethane and disubstituted porphyrin synthesis in project.

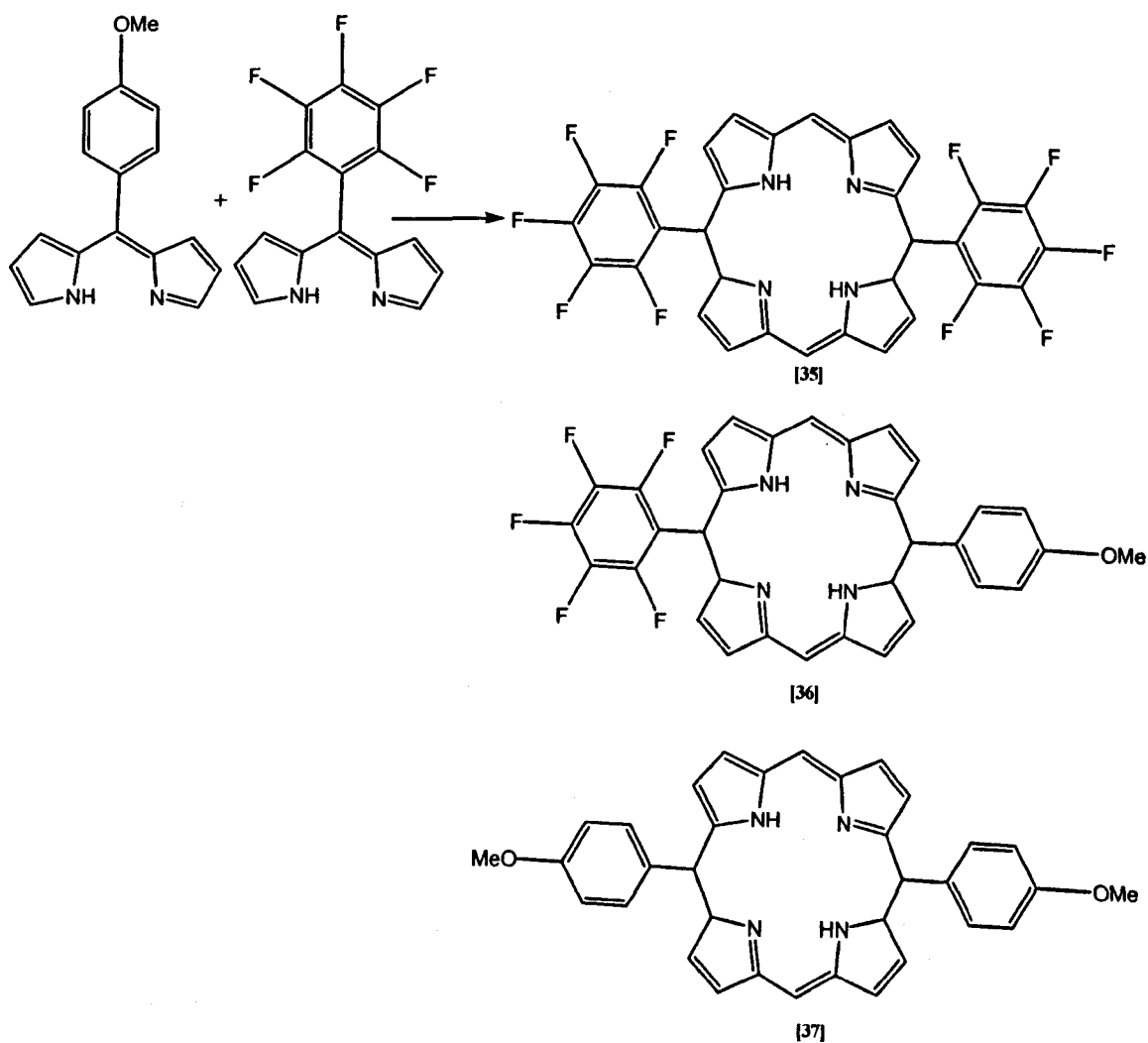
In our research, different dipyrromethanes were synthesised using the Mac Donald ¹⁸² method. The scheme below outlines the synthetic procedures involved.



Scheme 13: Dipyrromethanes synthesised in project.

Our work involving the condensation of 5-phenyldipyrromethane [30] with triethylorthoformate, in dichloromethane at room temperature followed by air oxidation of the intermediate porphyrinogen gave DPP [34]. The full details of the experiment is found in chapter four. Unsymmetrical disubstituted porphyrins were also synthesised using similar conditions. Equivalent amounts of (4-methoxyphenyl)-dipyrromethane [32] and pentafluorophenyl dipyrromethane [33] were condensed together with triethylorthoformate to give a mixture of three products, 5,15-dipentafluorophenyl

porphyrin [35], 5-pentafluorophenyl-15-(4-methoxyphenyl) porphyrin [36] and 5,15-di-(4-methoxyphenyl) porphyrin [37]. This synthesis involved the complex purification of the three products which can usually be problematic where R_f values for the porphyrins are similar. Secondly, the yield for the desired product was very low due to the 1:2:1 statistical mixture of products. The reaction is outlined in the scheme below. However, the full method is detailed in chapter four.



Scheme 14: Unsymmetric disubstituted porphyrins synthesised in project.

2.2 DEVELOPMENT OF CATIONIC WATER-SOLUBLE PORPHYRIN SYNTHESIS

A series of water-soluble porphyrins have been derived from porphyrin precursors insoluble in water, such as phenyl or pyridyl porphyrins, by the introduction of ionic groups such as $-\text{SO}_3^-$, $=\text{N}^+-\text{CH}_3$, COO^- or $\text{N}^+(\text{CH}_2\text{CH}_3)_3$. These peripheral, charged groups influence the chemical, spectral and redox properties of the porphyrins and their metal complexes.¹⁸⁴ Pasternack *et al*¹⁸⁵ reported in 1972, the three most common water-soluble porphyrins as seen below.

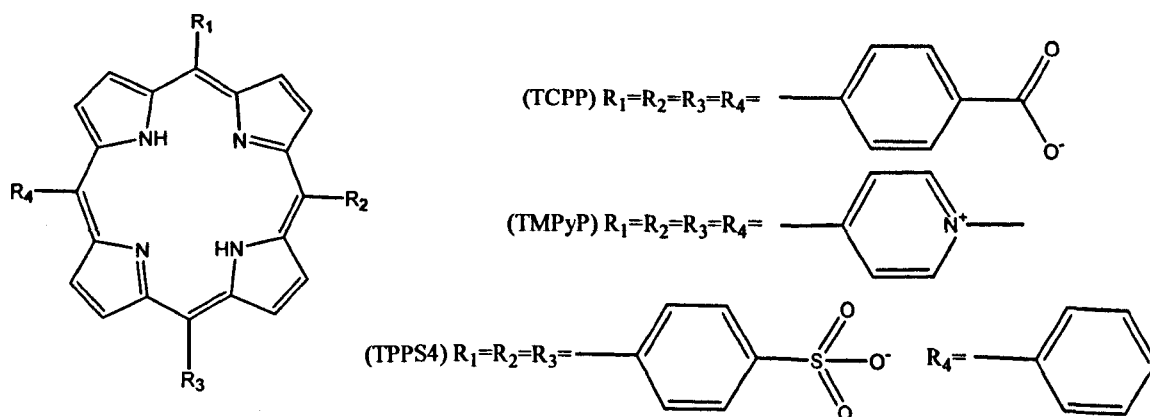


Figure 15 : The most common water-soluble porphyrins¹⁸⁵

The synthesis and characterisation of the porphyrins was demonstrated and these have been used since as basic templates for the development of more complex water-soluble porphyrins. The study of these water-soluble porphyrins in neutral aqueous medium indicated that the cationic group on the molecule allowed π electron density to be drawn away from the macrocycle core and hence reducing the potential for dimerisation.

Further studies conducted by Pasternack *et al*¹⁸⁶ involved tetrakis(4-*N*-methylpyridyl)porphyrin and a number of its metal derivatives. Cationic porphyrins derived from the alkylation of the tetrapyridylporphyrin (TPyP) system have a wide variety of uses including that as antiviral agents,¹⁸⁷ DNA binding,¹⁸⁸ RNA binding,¹⁸⁹ antibacterial agents.¹⁹⁰ Studies have shown that the metal derivatives of TPyP interact differently with the GC regions on the DNA than with the AT regions.¹⁹¹

Georgiou *et al*¹⁹² reported the distribution of porphyrins within the cell as being dependant upon the structure of the pendant side chains. In summary it was suggested that the predominantly cationic side chains have a clear tendency to localise in the mitochondria, whereas those with anionic character tend to localise in lysosomes.

2.2.1 Synthesis of cationic porphyrins in project

In order to demonstrate the alkylation of the nitrogen proton, a basic reaction was conducted. This involved reacting 4-mercaptopyridine with excess iodomethane, in anhydrous DMF. The product obtained indicated the preferential methylation of the nitrogen on the pyridyl group which had a ¹H NMR peak at approximately 4.4 ppm. The reaction is outlined in the scheme below.

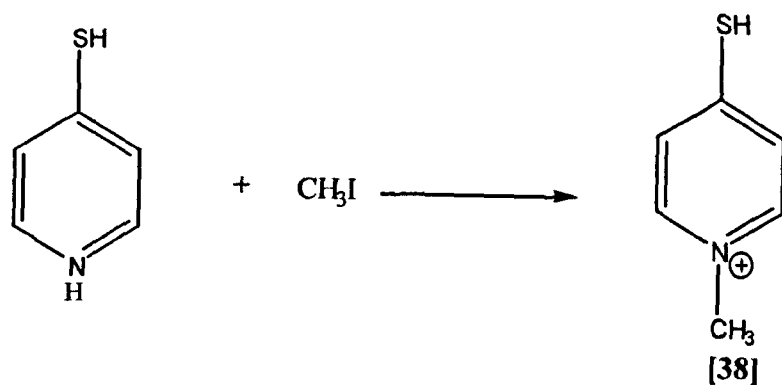
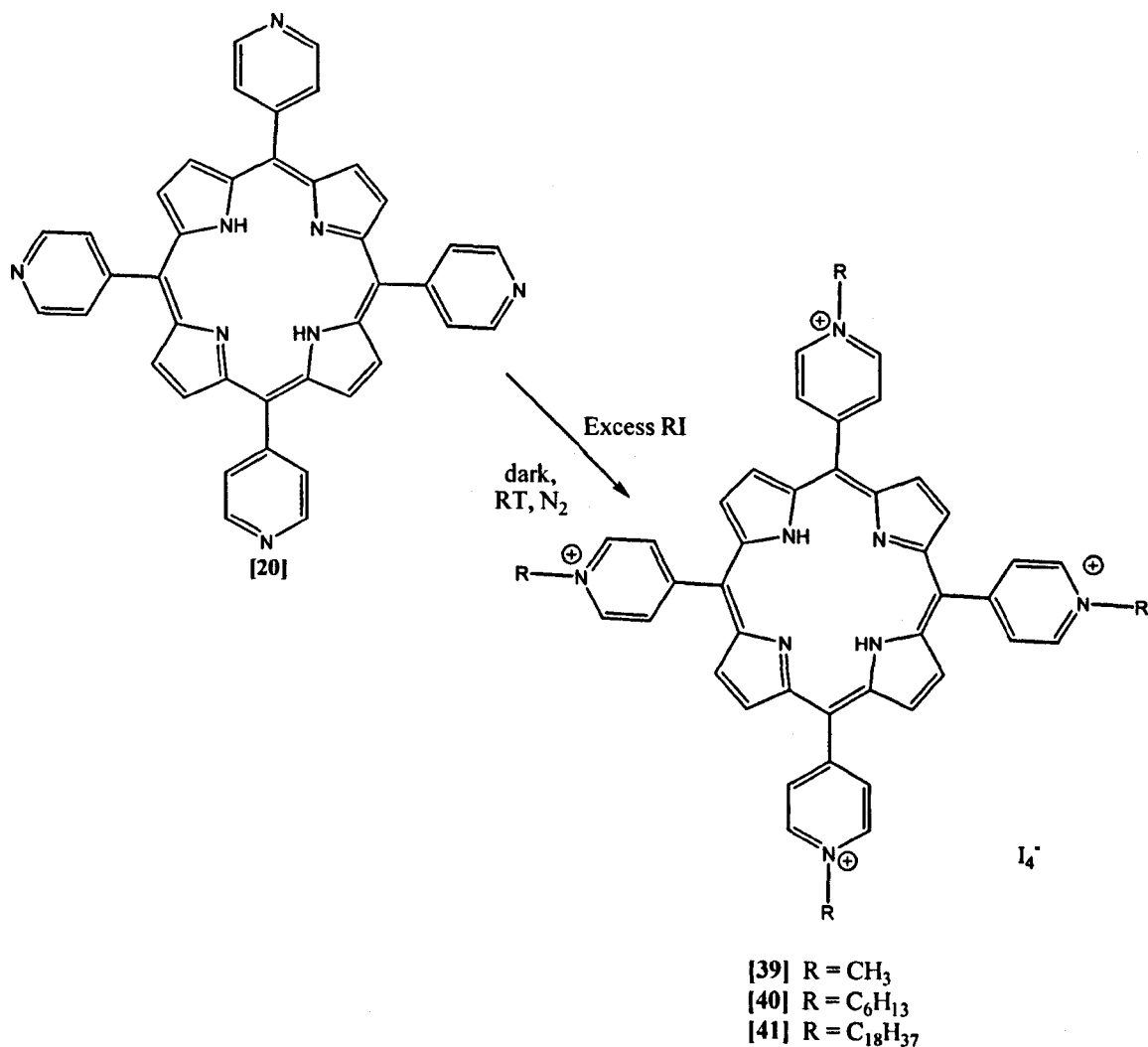


Figure 16 : Reaction of 4-mercaptopyridine and iodomethane

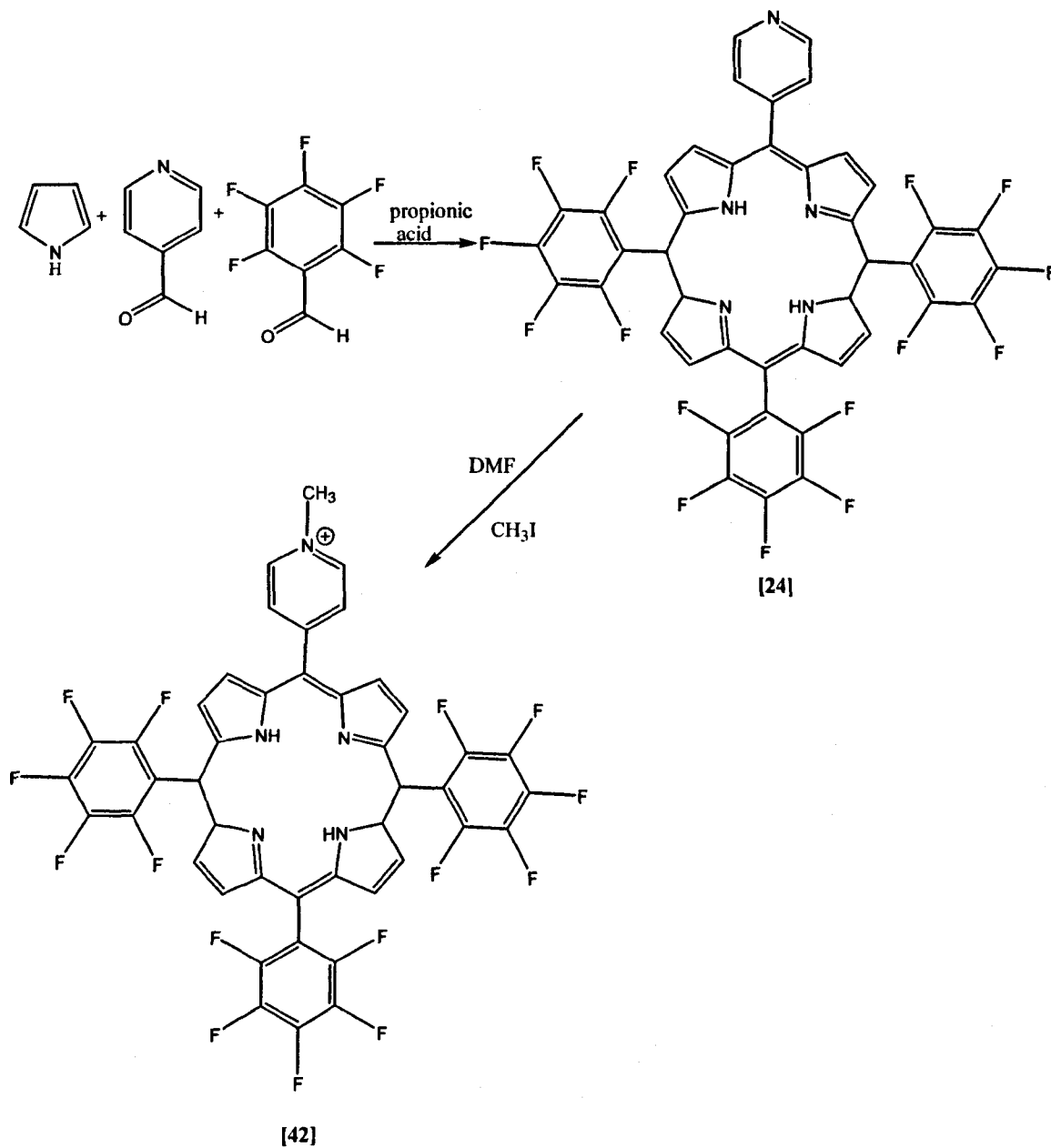
Cationic porphyrins synthesised in this project were synthesised by alkylation of the parent tetrapyrrolylporphyrin (TPyP) to give various pyridiniumyl porphyrins. Initial TPyP synthesis was obtained using Adler Longo methodology.¹⁸⁰ 4-Pyridine carboxybenzaldehyde, pyrrole and propionic acid were reacted together and the mixture separated to obtain the parent TPyP [20]. The yield of the reaction was 5%, considerably low due to the chromatographic separation of the product. Alkylation of the pyridyl nitrogen was performed by reaction with an excess of the alkylating agent. Different alkylating agents were considered but the most effective alkylating agents were found to be alkyl iodides. By reaction of the parent TPyP with excess alkylating agent the reaction could be driven to completion. This avoided the use of chromatographic separation and hence allowed the reaction to proceed in high yield >50%. Porphyrins [39], [40] and [41] are all straight forward alkylation reactions.



Scheme 17: Synthesis of tetracationic porphyrins varying in lipophilicity.

An unsymmetrical substituted cationic porphyrin, 5-(*N*-methyl-4-pyridyl)-10,15,20-tris-(pentafluorophenyl)porphyrin was also synthesised. Preparation of the unsymmetrical parent porphyrin, 5-(4-pyridyl)-10,15,20-tris-(pentafluorophenyl) porphyrin [24] involved the of Adler Longo mixed condensation reaction of pyrrole, together with pentafluorobenzaldehyde and pyridine-4-carboxybenzaldehyde in a 1:3 molar ratio, in propionic acid. After chromatographic purification and characterisation,

the product was treated with a large excess of methyl iodide at room temperature to obtain the 5-(*N*-methyl-4-pyridyl)-10,15,20-tris-(pentafluorophenyl)porphyrin [42] in 38% yield. The scheme below outlines the reactions involved.



Scheme 18: Synthesis of 5-(*N*-methyl-4-pyridyl)-10,15,20-tris-(pentafluorophenyl) porphyrin

2.2.2 Synthetic achievements in cationic porphyrins in project

In conclusion, porphyrins bearing cationic side chains have been synthesised successfully. Both symmetrical and unsymmetrical parent porphyrins were synthesised using the Adler Longo method and purified using flash column chromatography. After characterisation, the parent porphyrins were treated with excess alkyl iodides to obtain the cationic porphyrins.

Previously, work had already been done on the localisation and PDT activity of the symmetrical porphyrins.¹⁹² However, the advancement in this project was to design unsymmetrical porphyrin [42] which was used as a control porphyrin in further PDT studies. This aspect of cationic porphyrins will be discussed later on in section 2.4.

2.3 DEVELOPMENT OF CARBOHYDRATE- PORPHYRIN SYNTHESIS

As discussed in chapter one, sugar-porphyrin conjugates have been an area of considerable interest in the past few years. Their potential as second generation photosensitisers in PDT arises from the solubility of such molecules in water⁶⁶, which allows them to be compatible with biological media. Porphyrins bearing sugar moieties have also been found to improve specific cancer targeting.¹⁹³ Also, carbohydrates have been found to be specifically recognised by carbohydrates found on cell surfaces.¹⁹⁴ These carbohydrates on the cell surface play critical roles in cell-cell recognition, adhesion, signalling between cells, and as markers for disease progression. Sugar-specific receptors (lectins) are present on cells, and interact with sugars on other cells.

This results to adhesion of the two cells via carbohydrates and specific cell-surface receptors. Such carbohydrate-directed cell adhesion appears to be important in many intercellular activities including infection by bacteria and viruses, communication among cells of lower eukaryotes, specific binding of sperm to egg; and recirculation of lymphocytes, among others. Neural cells for instance use carbohydrates to facilitate development and regeneration and viruses recognise carbohydrates to gain entry into host cells. Each lectin has specificity toward a particular carbohydrate structure, some lectins will bind only to structures with mannose or glucose residues, while others may recognise only galactose residues. Some lectins require that the particular sugar be in a terminal non-reducing position in the oligosaccharide, while others can bind to sugars within the oligosaccharide chain. Some lectins do not discriminate between α and β anomers, while others require not only the correct anomeric structure but a specific sequence of sugars for binding. The porphyrin glycoconjugates with sugar moieties would mimic the receptor-sugar interaction and as a result attach to the cell surface and hence allow the porphyrin to express its therapeutic effect.

Syntheses of glycosylated porphyrins has previously utilised Lindsey's method¹⁸¹ involving condensation of pyrrole with different sugar based benzaldehydes.⁹⁹ Such synthetic routes are not ideal as they require attachment of the sensitive sugar residue before porphyrin formation, followed by extensive chromatographic separation of the porphyrin-sugar conjugates. Early studies have involved symmetrically substituted porphyrin-sugar conjugates that have been screened for photodynamic activity and compared to photosensitisers currently in the clinic.¹⁹⁵ The compounds were found to be active but the results were disappointing and, as a result, porphyrins bearing both sugar

substituents and also other functional groups, such as quaternised pyridyl moieties⁹⁶ and amino acid residues⁹⁹ were synthesised and screened.

Krausz *et al*⁹⁶ introduced the idea of glycosylated cationic porphyrins as potential agents in cancer phototherapy. Their approach to the synthesis involved initially acetylating salicylaldehyde β -D-glucoside with acetic acid in pyridine at 0 °C to obtain the protected sugar benzaldehyde. The porphyrins were then synthesised by condensation of 4-pyridine carboxyaldehyde, the protected sugar benzaldehyde and pyrrole according to the Adler-Longo method.¹⁸⁰ After chromatographic purification, only 7% yield was obtained of the desired 5-(2-tetraacetyl- β -D-glucopyranosylphenyl)-10,15,20-tris-(4-pyridyl)porphyrin. Finally, the porphyrins were quaternised using different alkyl halides and then deprotected to yield the final products. This approach to synthesise glycosylated cationic porphyrins was tedious as it involved finding a suitable sugar benzaldehyde and also protecting it before synthesis. This limits the types of functional groups that can be used as the harsh conditions of porphyrin synthesis may not be well suited for sensitive functional groups.

Another modification which has been suggested are porphyrin-sugar conjugates linked by a thioether bond, as this has been reported to reduce sensitivity of the conjugates to enzymic hydrolysis.¹⁹⁶ *S*-Glycosides are preferred conjugates because they are considered to be good mimics of *O*-glycosides with improved stability towards enzymatic hydrolysis. The research found that glycoconjugates with a *S*-glycoside link were more stable during the formation, during subsequent reactions, and in the presence of different functional groups. Therefore, they allowed successful synthesis of glycoconjugated porphyrins in high yield and with increased hydrolytic stability towards

enzymes. The glycoconjugates formed however exhibited poor photoactivity due to the amphiphatic character of the macrocycles and hence improvement was required so as to make these glycoconjugated porphyrins more photoactive.

Our aim in this project was to bring together the synthesis involving *S*-glycoconjugation¹⁹⁶ and apply it to produce glycosylated cationic porphyrins⁹⁶ in high yields and good hydrolytic stability.

2.3.1 Synthesis of thioglycosylated porphyrins in project.

Previously our research group had developed a number of synthetic methods to displace the fluorine at the *para* position of a pentafluorinated phenyl ring with thiolate nucleophiles.¹⁹⁷ Further work was also done by reacting thiophenolate intermediate formed by treatment of pentafluorophenyl bearing porphyrins with sodium sulphide, to attack electrophiles.¹⁹⁸ Both substitution reactions involved mild conditions and the synthesis was efficient. These conditions allowed a wide range of functional groups such as hydroxy, amido and nitro substituents including sensitive groups such as amino groups to be incorporated.

It was envisaged that this method could potentially be adapted to allow the facile introduction of sugar residues onto pre-formed porphyrins, and that their conjugation would link sugar to porphyrin via the more hydrolytically stable thioether bond. To investigate the viability of this reaction a range of precursor porphyrins were prepared, including symmetrical and unsymmetrical porphyrins. Conditions were then sought which could be adapted to the wide range of porphyrins with good yields.

The type of sugar thiol used was 2,3,4,6-tetra-*O*-acetyl- β -D-thioglucopyranose. This was

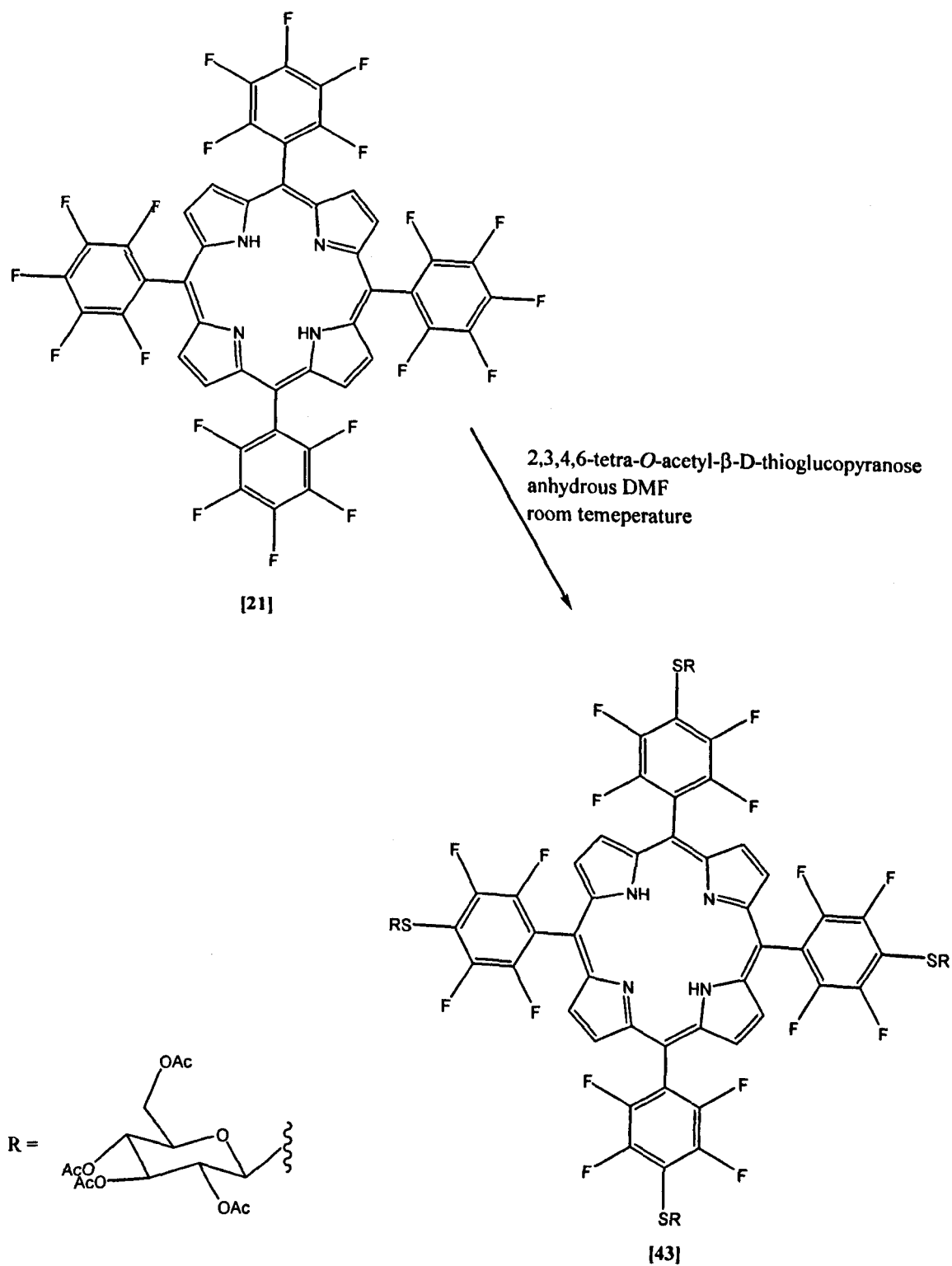
the preferred glycoconjugate as it bears the glucose residue which is recognised by the carbohydrate cell receptors found on the cell surface. Along with its structural stability in the pyranose form and ease of solubility, was presumed to be the best candidate for porphyrin-sugar conjugation.

2.3.2 General procedure for carbohydrate conjugation in project

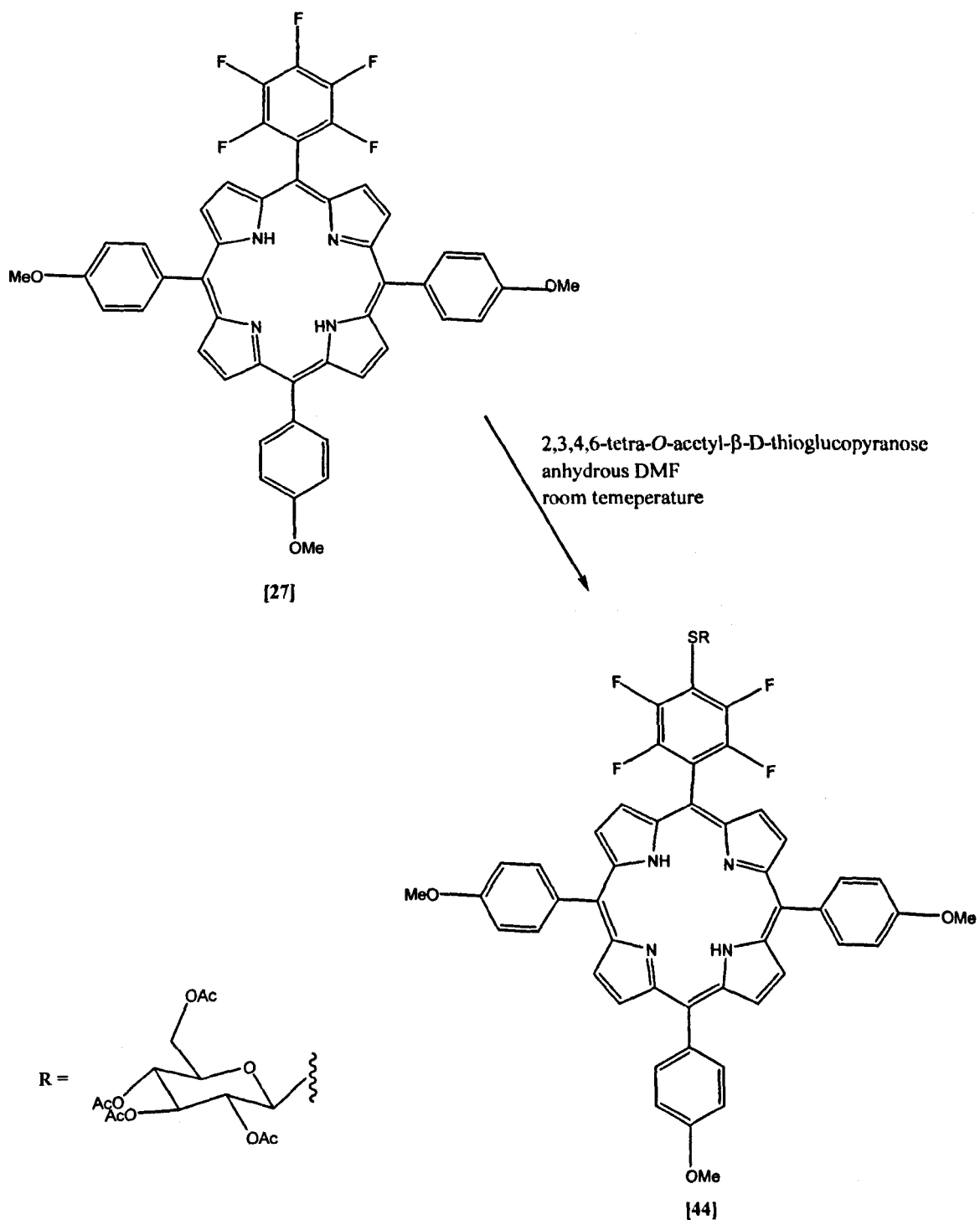
Initially, the symmetrical 5,10,15,20-tetra(pentafluorophenyl)porphyrin [21] was treated with 2,3,4,6-tetra-*O*-acetyl- β -D-thioglucopyranose in anhydrous DMF at room temperature. TLC analysis of the reaction showed the initial development of a series of well separated spots, which were separated by chromatographic purification (SiO₂: toluene/acetone 80/20) as detailed in the experimental section. The product, 5,10,15,20-[4-(2',3',4',6'-tetra-*O*-acetyl- β -D-glucopyranosylthio)-2,3,5,6-(tetrafluorophenyl)]porphyrin [43] was obtained. This reaction is outlined in the scheme 19 below.

Due to the recent interest shown in porphyrins substituted with sugar residues and other functional groups, the versatility and generality of the reaction for the synthesis of such unsymmetrically substituted macrocycles was investigated. Porphyrins substituted with one pentafluorophenyl group and bearing 4-methoxyphenyl groups at the remaining *meso*-positions, 5-(pentafluorophenyl)-10,15,20-tris-(4-methoxyphenyl)porphyrin [27] was synthesised and reacted with 2,3,4,6-tetra-*O*-acetyl- β -D-thioglucopyranose in anhydrous DMF at room temperature. The reaction gave the expected product 5-[4-(2',3',4',6',-tetra-*O*-acetyl- β -D-glucopyranosylthio)-2,3,5,6-(tetrafluorophenyl)]-10,15,20-tris-(4-methoxyphenyl)porphyrin [44] in which, the 4-fluoro atom of the pentafluorophenyl group was substituted by a thioglycosyl residue. The full procedure is

detailed in the experimental section. The scheme 20 below outlines the procedure.



Scheme 19: Synthesis of 5,10,15,20-[4-(2',3',4',6'-tetra-*O*-acetyl- β -D-glucopyranosylthio)-2,3,5,6-(tetrafluorophenyl)] porphyrin [43]



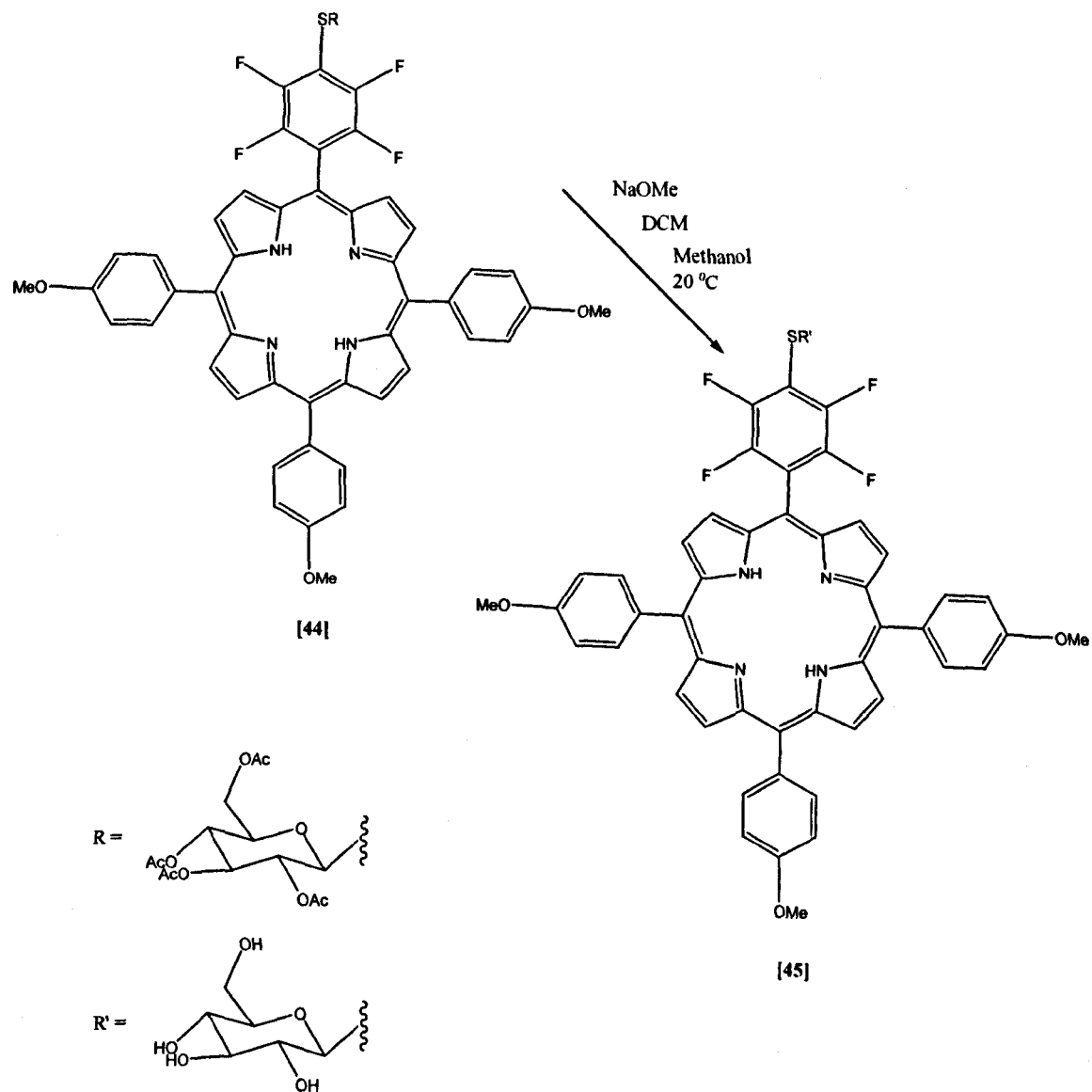
Scheme 20: Synthesis of 5-[4-(2',3',4',6',-tetra-*O*-acetyl- β -D-glucopyranosylthio)-2,3,5,6-(tetrafluorophenyl)]-10,15,20-tris-(4-methoxyphenyl)porphyrin [44]

2.3.3 General procedure for carbohydrate deprotection in project

Removal of the protecting acetyl group on the sugar residues proceeded via the treatment of the porphyrin with excess sodium methoxide in dichloromethane/methanol for 16 hours at room temperature. However, the analysis of the product indicated that, while all the sugar residues had been efficiently deacetylated, a mixture of products were obtained corresponding to substitution of one to four fluorines by methoxy groups. Rationalising that kinetics for acetyl deprotection should be significantly faster than for S_NAr displacement of fluorine by methoxide ion, a series of parallel reactions were run varying both the time and temperature of the reaction. Optimised conditions involved a strictly controlled temperature of 20 °C for one hour, which resulted in efficient deprotection of the acetyl group, with no other fluorine displacements in yield > 90% for compound 5-[4-(β -D-glucopyranosylthio)-2,3,5,6-(tetrafluorophenyl)]-10,15,20-tris-(4-methoxyphenyl)porphyrin [45]. Scheme 21 below summarises the reactions involved.

Although the synthesis may sound trivial, this was absolutely not the case. Many failed attempts were made earlier due to different conditions such as lack of temperature control which resulted into the decomposition of the porphyrin at high temperature. Exact timing was required as prolonged exposure of the 2,3,4,6-tetra-*O*-acetyl- β -D-thioglucopyranose with the porphyrin resulted to displacement of fluorine atoms at positions other than the *para*-position of the pentafluorophenyl ring. Different solvent systems were tested for the chromatographic separation of the glycoconjugated porphyrins which involved changing solvents, solvent ratios and eventually the type of silica used in the chromatography was sought, which would be able to separate porphyrins that have polar sugar substituents. Many experiments were done on a small

scale to determine the reaction conditions, and they were all put together, fine tuned and applied to synthesise the glycoconjugated porphyrins obtained.



Scheme 21: Deprotection of acetyl groups on sugar residue.

2.3.4 Achievements in sugar porphyrin synthesis within project

In conclusion, the synthetic method described allows easy access to a diverse range of symmetrical and unsymmetrical porphyrins bearing sugar residues with hydrolytically stable thioether bonds. Level of sugar substitution was easily varied and the reaction was found to be tolerant of a range of secondary functional groups attached to the porphyrin. The acetyl protecting groups on the sugar groups were selectively removed in high yield by careful control of reaction conditions.

It was next decided to attempt to incorporate the water-solubility and selectivity properties of cationic and sugar porphyrins to give “hybrid” sugar-cationic porphyrins. This brings together concepts and synthetic achievements discussed in sections 2.2 and 2.3 to create a novel class of compound with potential as sensitisers for use in photodynamic therapy.¹⁹⁸

2.4 THIOGLYCOSYLATED CATIONIC PORPHYRINS

It is desirable, for ease of systematic administration, that photodynamic sensitisers have full water solubility, thus avoiding the need for complex and expensive delivery vehicles. It has also been shown that porphyrins bearing one positive charge tend to localise around the mitochondria of the cell.¹⁶² Photodynamic damage to the mitochondria has been implicated in rapid induction of apoptosis, and this subcellular site is therefore a major target for PDT. Cationic water soluble porphyrins, such as the commercially available 5,10,15,20-tetrakis(*N*-methyl-4-pyridyl)porphyrin and 5,10,15,20-tetrakis[4-(trimethylammonio)phenyl]porphyrin are powerful photosensitisers; however they have also demonstrated significant toxicity in the absence of light, often referred to

as "dark" toxicity.

Recently, interest has been shown in porphyrins bearing both sugar residues and positively charged groups as PDT sensitisers, this combination of functionalities allow water solubility, but also greater membrane permeability, compared with porphyrins solubilised solely by multiple charged groups.⁹⁶ Previously, glycosyl cationic porphyrins have been synthesised by condensing mixtures of sugar substituted benzaldehydes with 4-pyridinecarboxyaldehyde and pyrrole in propionic acid at reflux, followed by chromatographic purification of the required porphyrins from the resulting statistical mixture.⁹⁶ Subsequent quaternisation of the porphyrin gave the required compounds. Although this method was successful, it requires sensitive and sterically bulky sugar residues to be introduced prior to porphyrin formation. Hence a method of synthesis was sought that would allow the synthesis of such sensitive porphyrins without much complications.

2.4.1 Route to thioglycosylated cationic porphyrins with direct porphyrin-sugar conjugation in project.

After establishing optimum conditions for the synthesis of glycoconjugated porphyrins, the same reaction conditions were applied to the conjugation of the sugar moieties in the formation of the cationic thioglycosylated porphyrins

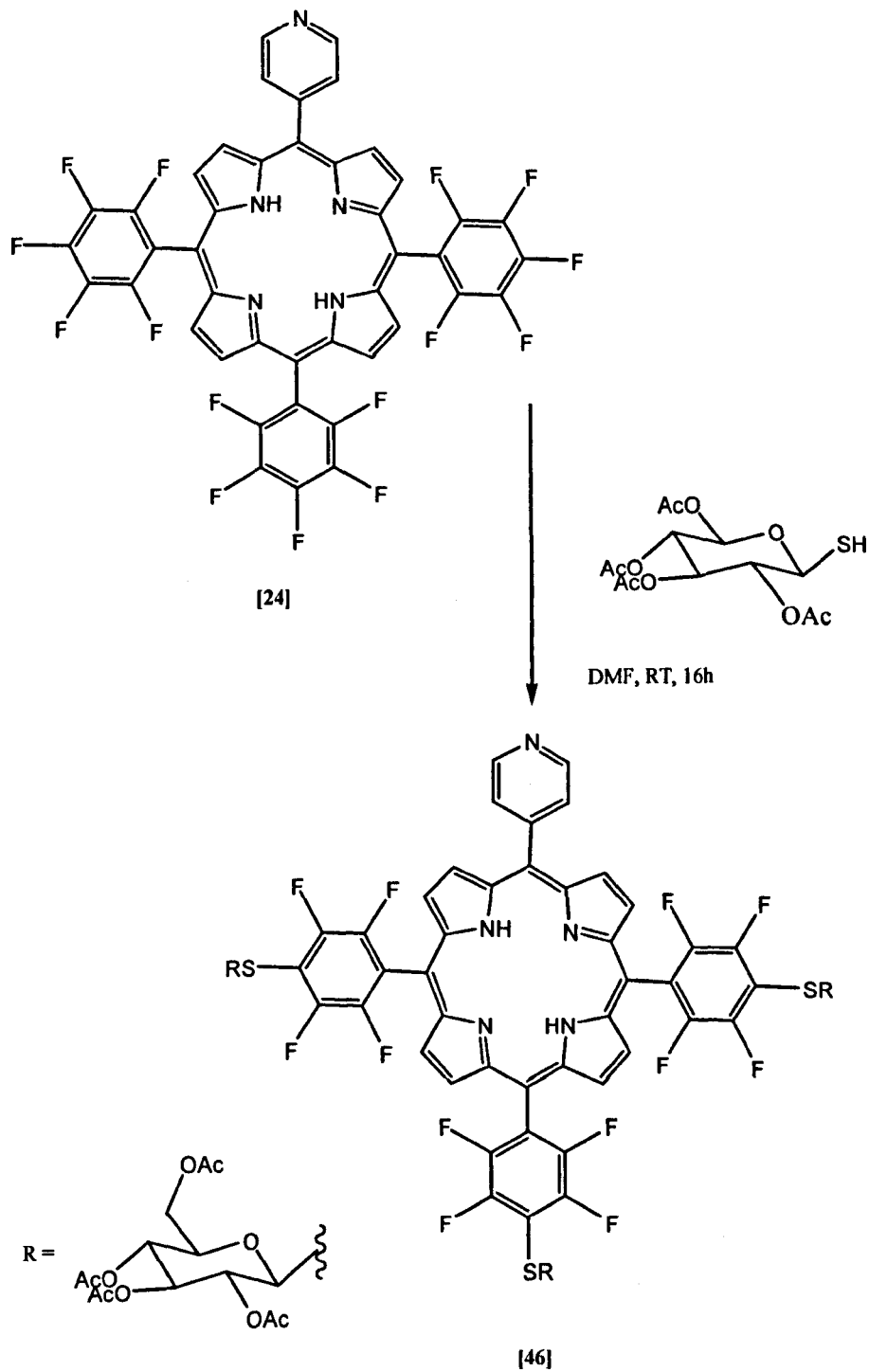
We have developed a method to generate a small series of 5-(*N*-alkyl-4-pyridyl)-10,15,20-tris(4-thioglycosyl-2,3,5,6-tetrafluorophenyl)porphyrins.¹⁹⁹ The precursor porphyrin in the synthesis was 5-(4-pyridyl)-10,15,20-tris(pentafluorophenyl)porphyrin [24]. This was synthesised by Adler-Longo conditions¹⁸⁰ in propionic acid using a 1:3

molar ratio of pentafluorobenzaldehyde and pyridine-4-carboxyaldehyde respectively.

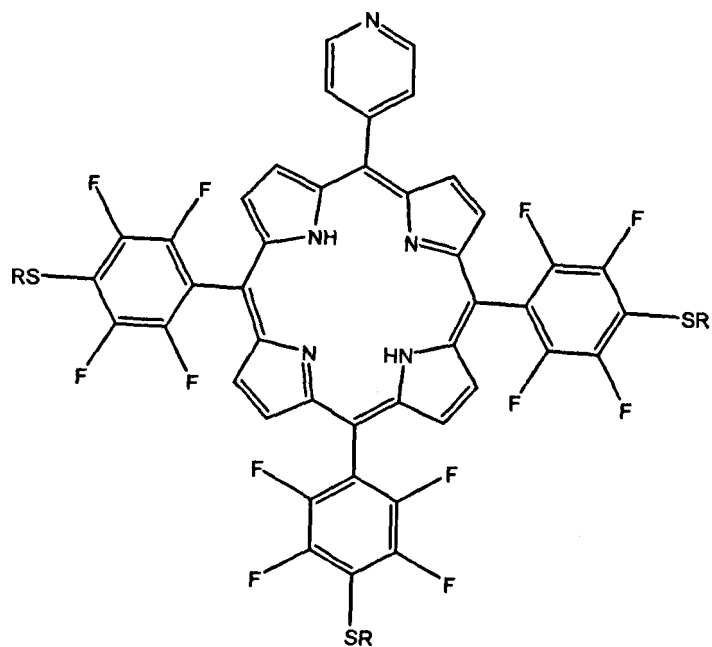
Once the porphyrin had been synthesised, the next step was glycoconjugation via the displacement of *para* fluorine atoms by the *S*-glycosides. 5-(Pyridyl)-10,15,20-tris(pentafluorophenyl)porphyrin was dissolved in dry anhydrous DMF (3 ml). 2,3,4,6-Tetra-*O*-acetyl- β -D-thioglucopyranose (4.5 eq) in DMF (4 ml) was added. The mixture was stirred at room temperature and the reaction monitored by TLC. After 16 hours, the solvent was evaporated *in vacuo*, followed by chromatographic separation to obtain the product in high yield (77 %). The full synthesis of thioglycosylated cationic porphyrins is discussed in chapter four, but a general overview of the synthesis is given in scheme 22.

Quaternisation using the alkyl iodides was fairly straight forward due the excess use of the alkylating agent ensuring completion of the reaction. Treatment of 5-(4-pyridyl)-10,15,20-tris[4-(2',3',4',6'-tetra-*O*-acetyl- β -D-glucopyranosylthio)-2,3,5,6-tetrafluorophenyl] porphyrin [46] with a small range of alkyl iodides gave the cationic 5-(*N*-alkyl-4-pyridyl)-10,15,20-tris-4-(2',3',4',6'-tetra-*O*-acetyl- β -D-glucopyranosylthio)-2,3,5,6-tetrafluorophenyl] porphyrins. This reaction is schematically shown in scheme 23.

Finally the sugar residues were deprotected by stirring with sodium methoxide in methanol at room temperature for one hour, to give 5-(*N*-alkyl-4-pyridyl)-10, 15, 20-tris-[4-(β -D-glucopyranosylthio)-2,3,5,6-tetrafluorophenyl] porphyrins. All compounds were shown to be single compounds by TLC and were characterised by $^1\text{H NMR}$, MS (MALDI-TOF) and UV spectroscopy. This reaction is summarised in scheme 24 and the full details can be found in chapter four.

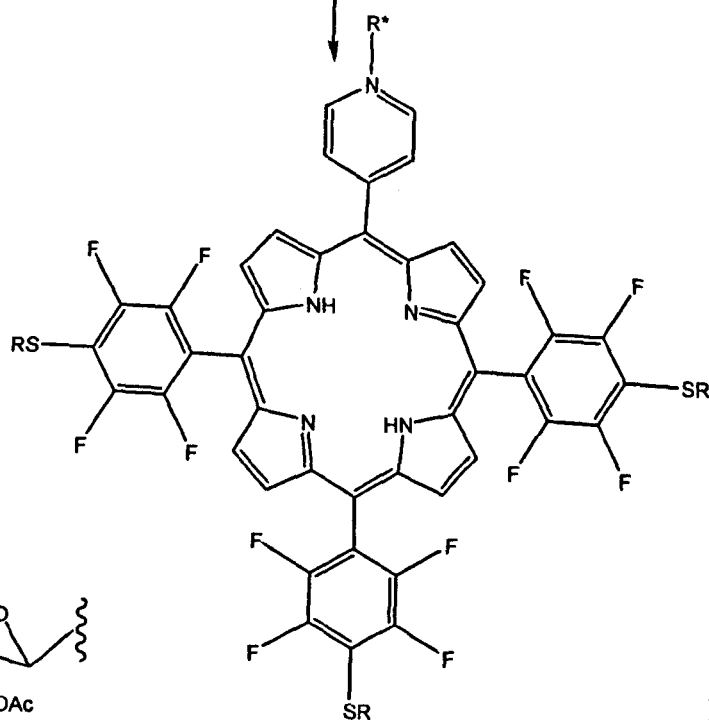


Scheme 22: Initial S-glycosylation

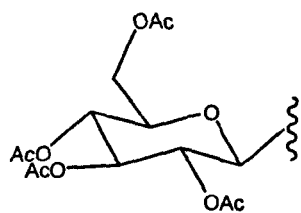


[46]

excess RI, DMF, RT, 16h

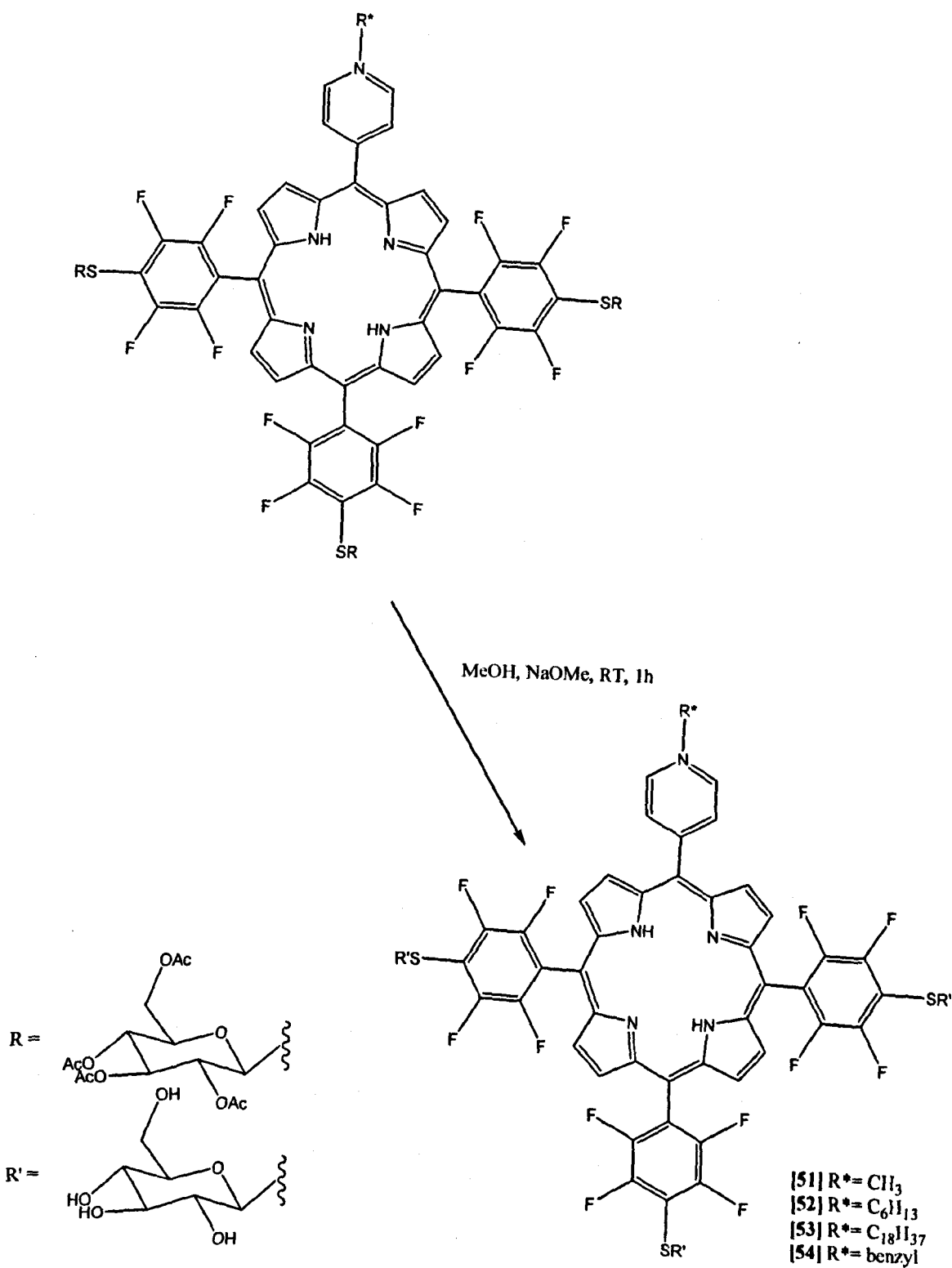


R =



- [47] R* = CH₃
- [48] R* = C₆H₁₃
- [49] R* = C₁₈H₃₇
- [50] R* = benzyl

Scheme 23: Quaternisation of sugar conjugated porphyrins



Scheme 24: Deprotection of sugar residues

Once synthesised and characterised, the compounds [51–54] were then investigated for their photodynamic activity *in vitro*.

2.4.2 Cytotoxicity of thioglycosylated cationic porphyrins

Four of the thioglycosylated cationic porphyrins [51], [52], [53] and [54] as well as (5-methyl-4-pyridyl)-10,15,20-(pentafluorophenyl)porphyrin [42] were all used for cytotoxicity evaluations as PDT agents. HT-29 (Human colorectal adenocarcinoma cells) were incubated in the dark for 1 hour at different concentrations of the compounds for control purposes and also to evaluate "dark toxicity" associated with the PDT agents.

Briefly, the assays consisted of incubating HT-29 cells with the porphyrins for one hour followed by washing to remove the photosensitiser, which had failed to associate with the cells. Cells were plated in 96 well plates in quadruplicate and irradiated with cooled filtered red light (630nm; 3.6 J cm^{-2}). After irradiation, 5 μL FCS (Fetal Calf Serum) was added to each well and the cells were incubated overnight. Finally, cell survival was determined by MTT (3-(4,5-dimethylthiazol-2-yl)-2, 5-diphenyltetrazolium bromide) assay.

MTT assay as described by Mossman²⁰⁰ involved the addition of 10 μL of MTT at 5mg/mL PBS (phosphate buffered saline) at 24 hours post irradiation, to each well. The plates were placed back into the incubator for 1 hour to allow the colour to develop. Afterwards, 150 μL of isopropanol containing HCL (0.04 *N*) was added to stop the reaction. The cells were lysed, and the blue formazan crystals produced by the mitochondria of living cells were dissolved by vigorous pipetting. The plates were then read at 570 nm using a Bio-Tek Elx 800 plate reader. The percentage of cell survival was

calculated in proportion to the number of cells incubated without photosensitiser.

2.4.3 Cytotoxicity results

In order to access the efficiency of the compounds as PDT agents and any trends that can be deduced, graphs are plotted for each compound displaying % cell survival versus concentration (M). Two sets of data are presented for each compound; irradiated (IRR) and non-irradiated (NI). The final figure (Fig 30) indicates a combined graph which displays all the results obtained for both irradiated and non irradiated.

5- (N-Methyl-4-pyridyl)10,15,20- tris[4-(β -D-glucopyranosylthio)-2,3,5,6-tetrafluorophenyl] porphyrin [51]

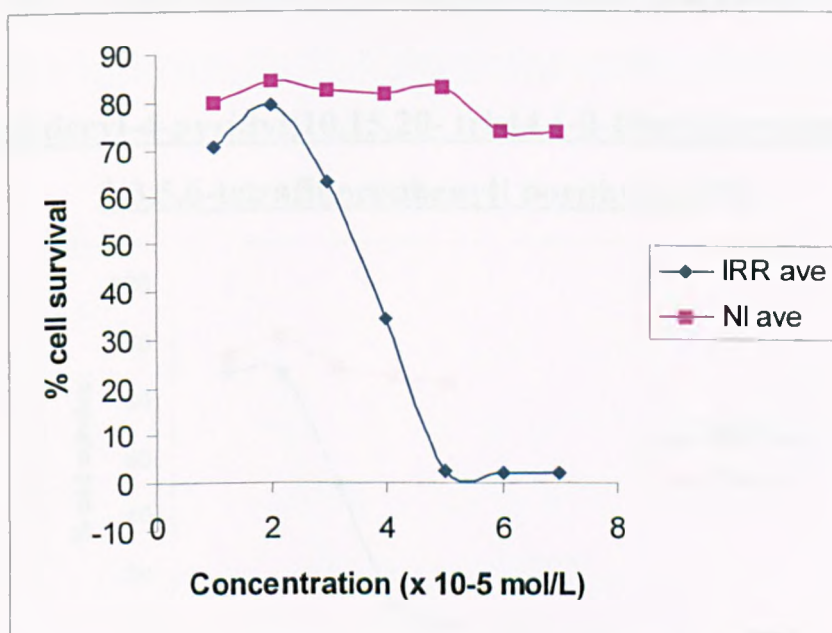


Fig 25 : Cytotoxicity data for 5- (N-methyl-4-pyridyl)-10,15,20- tris[4-(β -D-glucopyranosylthio)-2,3,5,6-tetrafluorophenyl] porphyrin[51]

5- (N-Hexyl-4-pyridyl)10,15,20- tris[4-(β -D-glucoopyranosylthio)-2,3,5,6-tetrafluorophenyl] porphyrin [52]

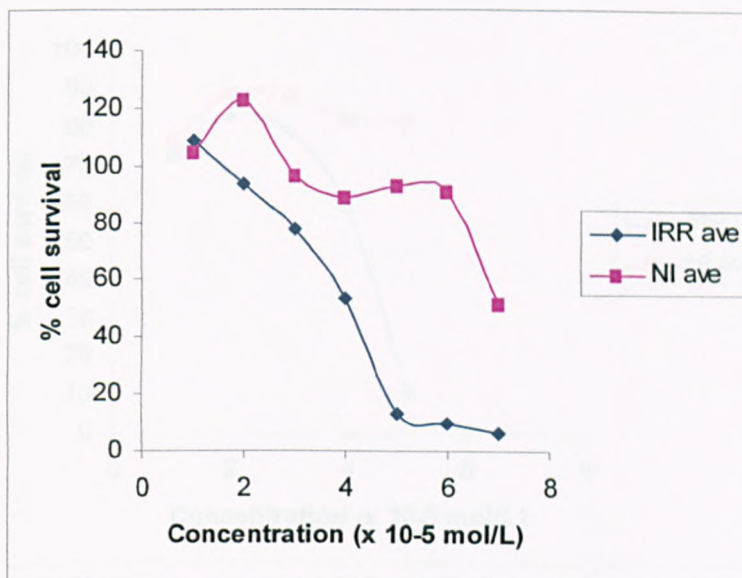


Fig 26 : Cytotoxicity data for 5- (N-hexyl-4-pyridyl)-10,15,20- tris[4-(β -D-glucoopyranosylthio)-2,3,5,6-tetrafluorophenyl] porphyrin[52]

5- (N-Octadecyl-4-pyridyl)10,15,20- tris[4-(β -D-glucoopyranosylthio)-2,3,5,6-tetrafluorophenyl] porphyrin [53]

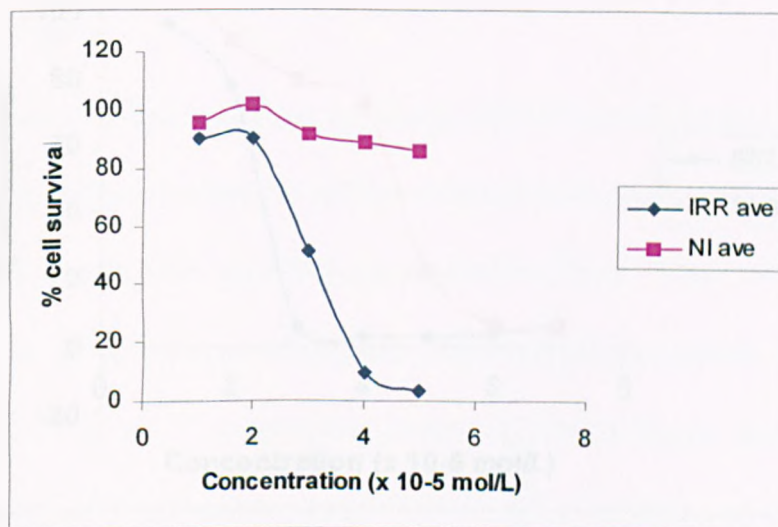


Fig 27 : Cytotoxicity data for 5- (N-octadecyl-4-pyridyl)-10,15,20- tris[4-(β -D-glucoopyranosylthio)-2,3,5,6-tetrafluorophenyl] porphyrin[53]

5- (N-Benzyl-4-pyridyl)10,15,20- tris[4-(β -D-gluconopyranosylthio)-2,3,5,6-tetrafluorophenyl] porphyrin [54]

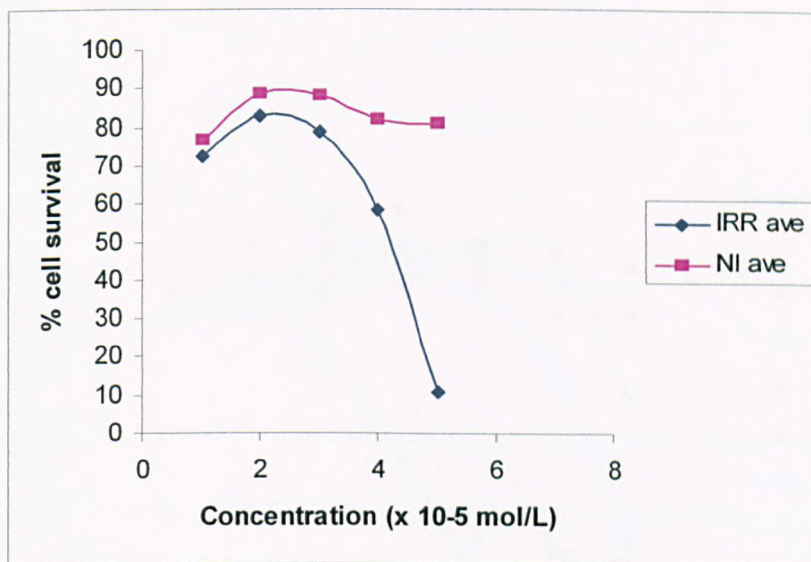


Fig 28 : Cytotoxicity data for 5- (N-benzyl-4-pyridyl)-10,15,20- tris[4-(β -D-gluconopyranosylthio)-2,3,5,6-tetrafluorophenyl] porphyrin[54]

5- (methyl-4-pyridyl)-10, 15, 20-(pentafluorophenyl)porphyrin [42]

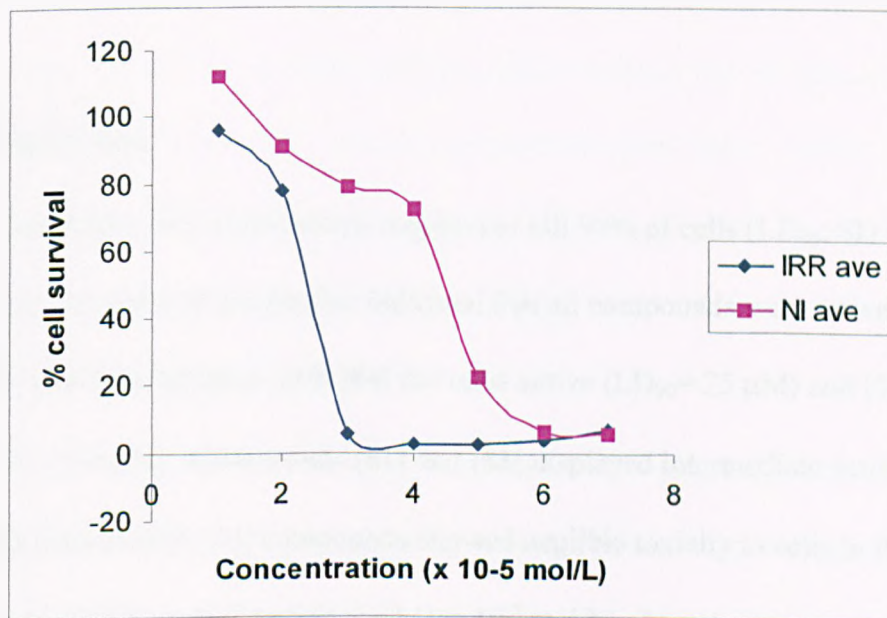


Fig 29 : Cytotoxicity data for 5- (methyl-4-pyridyl)-10,15,20- (pentafluorophenyl)porphyrin[69]

Graph showing all thioglycosylated cationic porphyrins with irradiated and non-irradiated cytotoxicity results.

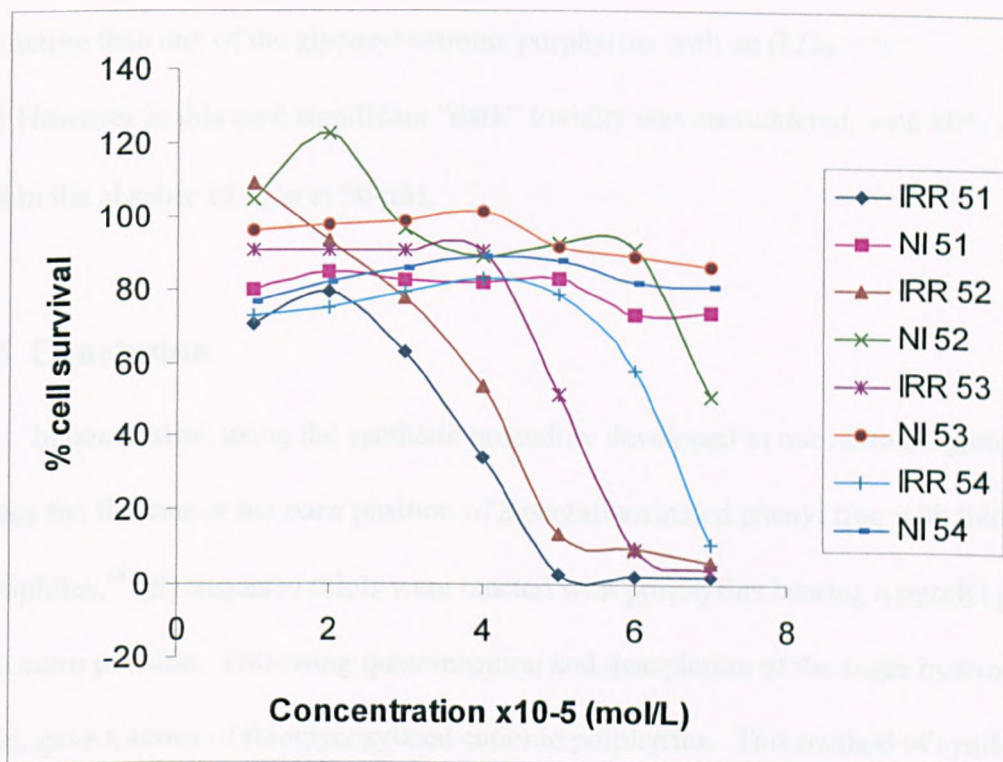


Fig 30 : Cytotoxicity data for all thioglycosylated cationic porphyrins synthesis

2.4.4 Discussion

Comparison of concentrations required to kill 90% of cells (LD_{90} ; $SD < 0.05$) for the four glycosyl cationic porphyrins indicated that all compounds were active to this level in the micromolar range with [54] the most active ($LD_{90} = 25 \mu M$) and [54] the least active ($LD_{90} = 50 \mu M$). Compounds [51] and [52] displayed intermediate activity of 35 and 45 μM respectively. All compounds showed negligible toxicity to cells in the absence of light at the highest concentration used ($5 \times 10^{-5} \text{ mol/L}$). In order to investigate the effect of the cationic porphyrin in the absence of sugar residues, (5-methyl-4-pyridyl)-

10,15,20-(pentafluorophenyl)porphyrin iodide salt [42] was synthesised and its photodynamic potential was also determined. Interestingly, porphyrin [42] was even more active than any of the glycosyl cationic porphyrins with an ($LD_{90} = 5 \mu\text{M}$). However in this case significant “dark” toxicity was encountered, with 80% of cells killed in the absence of light at $50 \mu\text{M}$.

2.4.5 Conclusion

In conclusion, using the synthetic procedure developed in our research group to displace the fluorine at the *para* position of a pentafluorinated phenyl ring with thiol nucleophiles,¹⁹⁷ glycosylated thiols were reacted with porphyrins bearing a pyridyl group at one *meso* position. Following quaternisation and deacylation of the sugar hydroxyl groups, gave a series of thioglycosylated cationic porphyrins. This method of synthesis was flexible, moderate and good yield were obtained of the photosensitisers. PDT results on HT-29 (Human colorectal adenocarcinoma cells) indicated that the glycosyl substituents played an important role in the moderation of the “dark” toxicity associated with many cationic PDT agents.

2.4.6 Further work suggestions

An extension of this work would be the systematic investigation of the effect of the *N*-alkyl group on PDT activity. Alkyl sidechains on the pyridyl nitrogen ranging from methyl to octadecyl sidechains could be made with an increment of one carbon atom at a time. This would enable any trends to be seen more clearly between the values of LD_{90}

and carbon chain length.

Also, perhaps further insight into the localisation of the glycosylated porphyrins in the cells using confocal microscopy would give a clearer picture with regards to the mechanism of cell death during PDT. At this moment, without further proof one can only speculate as to whether necrosis or apoptosis is responsible for the cell death during PDT.

3.1 INTRODUCTION TO METALLOPORPHYRINS

Metalloporphyrins were previously introduced in chapter one. In this chapter, the development of a synthetic procedure is described that allows the insertion of palladium (II) into the different porphyrin macrocycles synthesised. Many factors had to be taken into consideration prior to the achievement of this aim and progress was slow in obtaining a sensible synthetic route that could be adapted for a wide range of porphyrins.

Our aim in this project was to use a range of porphyrins which could be coordinated with palladium and thereafter under go further modifications to yield hopefully suitable oxygen sensors. The different categories of porphyrins used include symmetrical, unsymmetrical tetraarylporphyrins as well as symmetrical and unsymmetrical diarylporphyrins. Hence a method was sought that would allow the metal insertion to the different types of porphyrins with high yields.

3.1.1 General considerations for metalation reactions

The metalation of porphyrin free bases can be divided into five stages:-

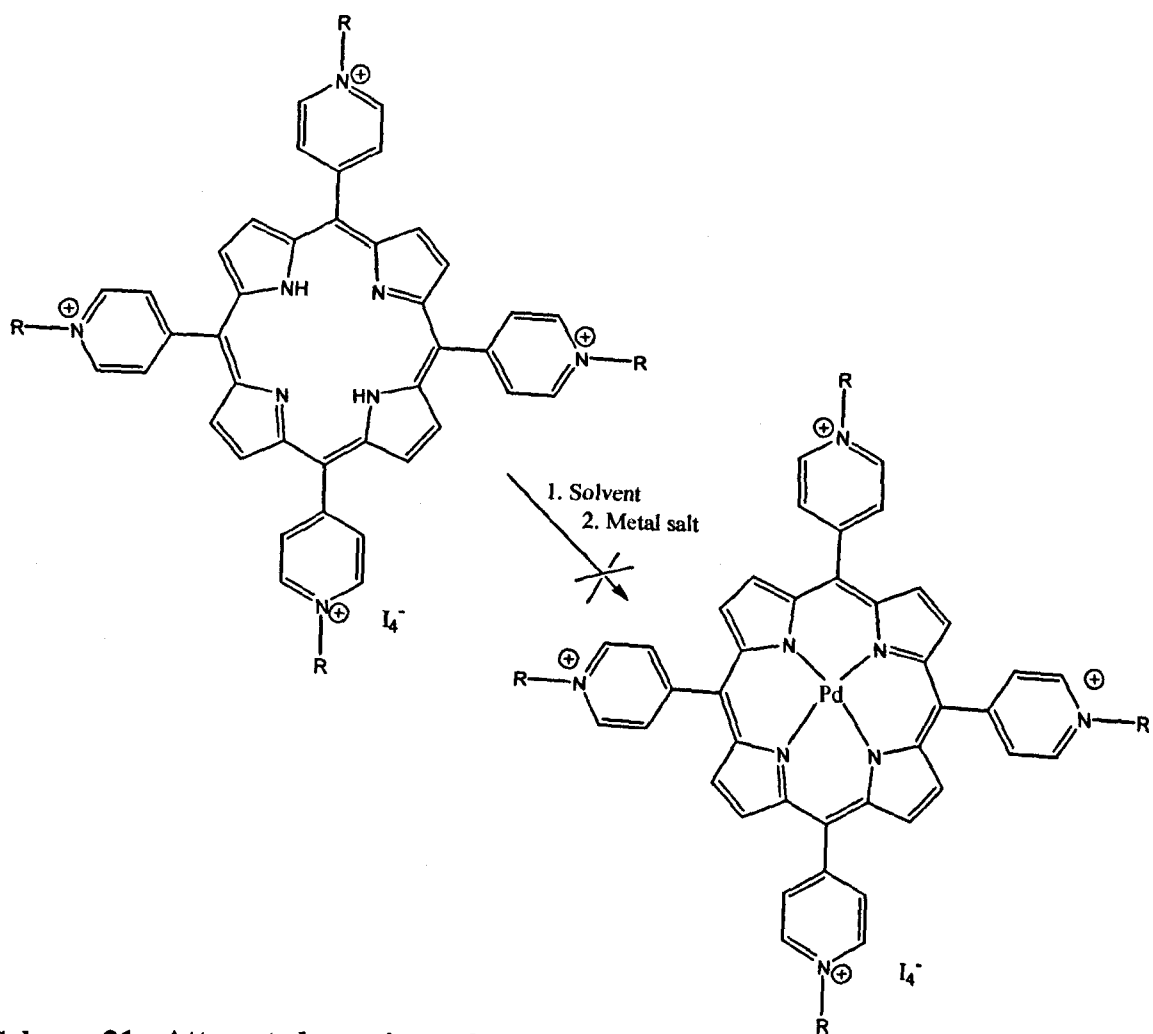
1. Deprotonation of the free base
2. Dissociation of the metal salt/complex
3. Coordination of the ligand to the metal ion
4. Adjustment of the charge balance
5. Completion of the most stable coordination sphere for the metal complex.

Steps one and two required a solvent in which the metal salt and porphyrin were soluble. Since step one was an equilibrium step, the solvent could not be too acidic as this would protonate the porphyrin competitively. Unfortunately, most organic solvents do not dissolve common metal salts, but refluxing N, N-dimethylformamide and benzonitrile were investigated in our project.

3.1.2 Synthetic approach to palladium metal metalation.

The aim was to synthesise palladium porphyrins that have some water solubility for use in biological systems. As mentioned in chapter one, cationic porphyrins with positively charged side chains were the obvious initial choice. The basic porphyrin skeleton used was 5,10,15,20-tetrakis-(4-pyridyl)-porphyrin [20] which was synthesised using the Adler Longo conditions.¹⁸⁰ 4-Pyridine carboxybenzaldehyde, pyrrole and propionic acid were reacted together and the product separated from linear polypyrroles. The yield of the reaction was 5%, of analytically pure product. Alkylation of the pyridyl nitrogen was performed by reaction with excess alkylating agent.

As mentioned earlier, insertion of palladium into porphyrin macrocycles is not at all trivial. Many attempts were made where different conditions were used in order to obtain a general method which was applicable to all the porphyrins being considered. Intensive research was carried out with both quaternised and unquaternised pyridiniumyl porphyrins on metal insertion reactions. A general summary of the reactions carried out is described below:-



Scheme 31: Attempted reactions of palladium metalation.

Where R = CH₃, or C₆H₁₃, Metal salt = palladium acetate or palladium chloride
(+K₂CO₃)

Solvent = DMF, DCM, MeCN, CHCl₃, benzonitrile or methanol.

Unfortunately, all attempts to obtain the desired products using the general reactions outlined in scheme 31 were unsuccessful. Attempts were made to insert the metal both before and after quaternisation with the R group (methyl or hexyl) but to no avail. On a number of occasions, only the starting material was obtained or alternatively,

a black solid resulted that was insoluble in both polar and non-polar solvents. It was thought that the poor solubility was due to the formation of supramolecular polymeric species of limited solubility. The π - π interaction would allow the porphyrin to form a metal-porphyrin aggregate. This suggestion would be similar to the illustration below.

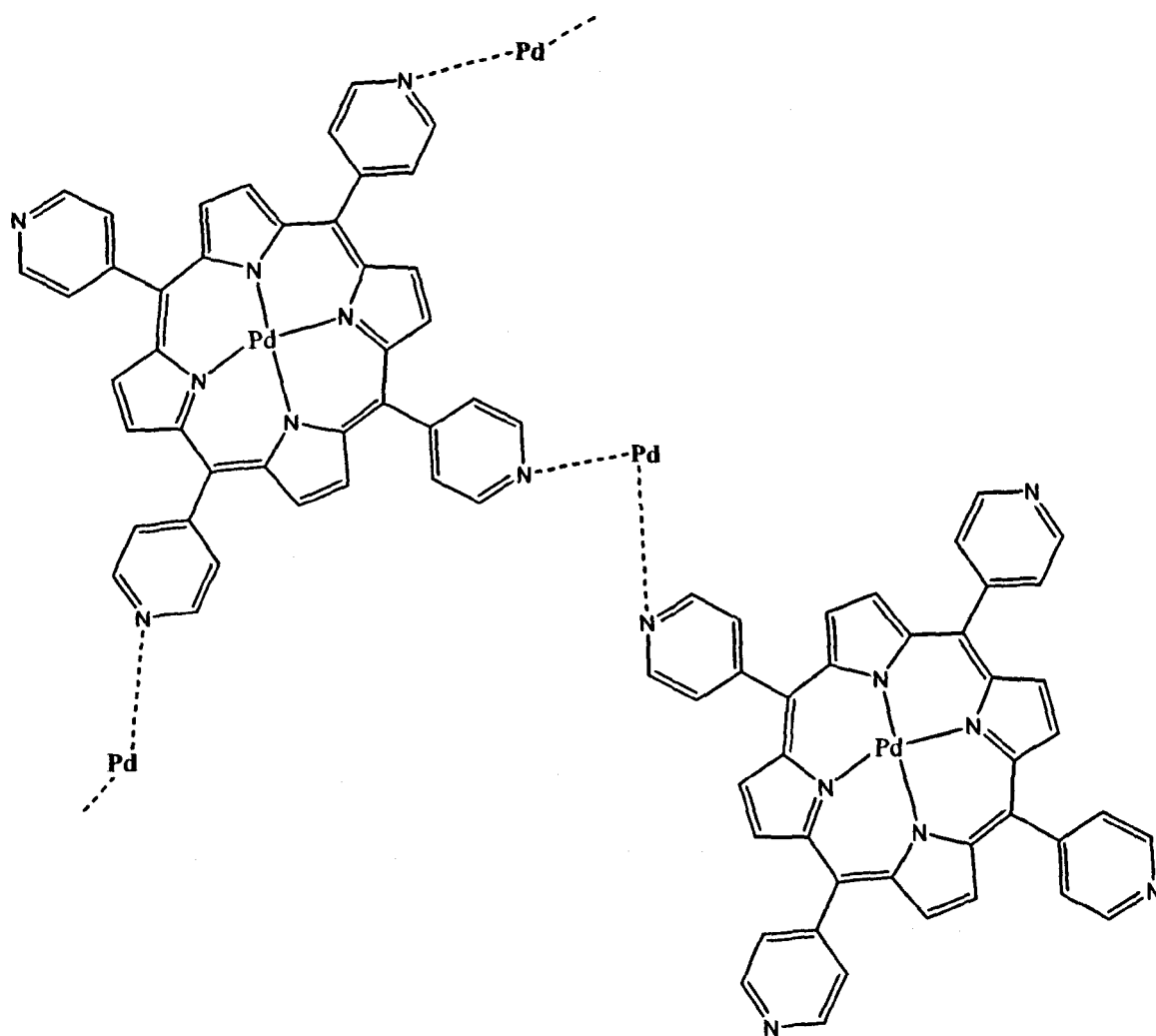


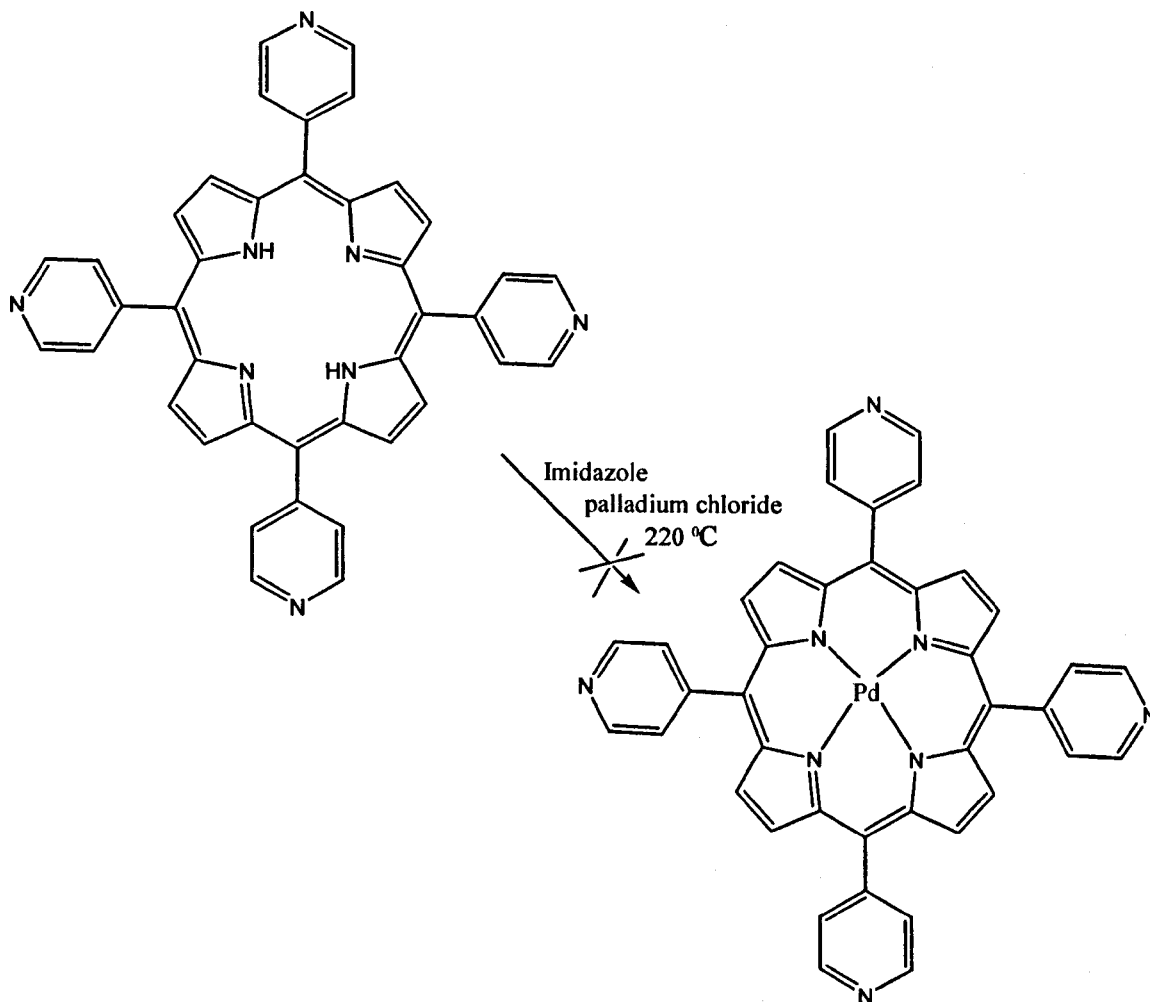
Fig 32: Proposed structure of supramolecular complex formed

The exact nature of any putative supramolecular complex was, however, impossible to ascertain, due to the insoluble nature of the product obtained. Only speculation can therefore be made on the products from these synthetic approaches, however there are several reports in the literature of supramolecular complex formation between pyridyl porphyrins and metals.

Due to the failure to obtain any positive results from the synthetic procedures demonstrated above, a different approach was adapted from a study conducted by Vanderkooi *et al.*¹ The study involved the synthesis of metal derivatives from water-soluble porphyrins for measuring the dioxygen concentration based on the quenching of phosphorescence. Their work involved the "imidazole melt method" for the preparation of the palladium metal complexes where the imadazole, porphyrin and palladium chloride were all reacted together in a reaction vessel. Unfortunately, in our hands the product of this reaction was identified as the starting material and even after altering factors such as the concentration of palladium chloride, the reaction time, the temperature and the amount of imidazole used, no product was obtained other than the starting material.

In the work conducted by Vanderkooi *et al.*¹ the palladium porphyrins used were; coproporphyrin 1, meso-tetra-(*N*-methyl-4-pyridyl)porphyrin (TMPP) and meso-tetra-(4-sulfonatophenyl)porphyrin (TSPP). Careful consideration showed that the reaction did not work in the project as the porphyrin TMPP was unquartenised and hence the lone pair of electrons on the nitrogen of the pyridyl group may have interfered in the reaction pathway yielding an unsuccessful reaction. Therefore, this reaction pathway was also found to be inappropriate for synthesising palladium metal complexes. The scheme below outlines the "imidazole melt method" adapted from work conducted by Vanderkooi

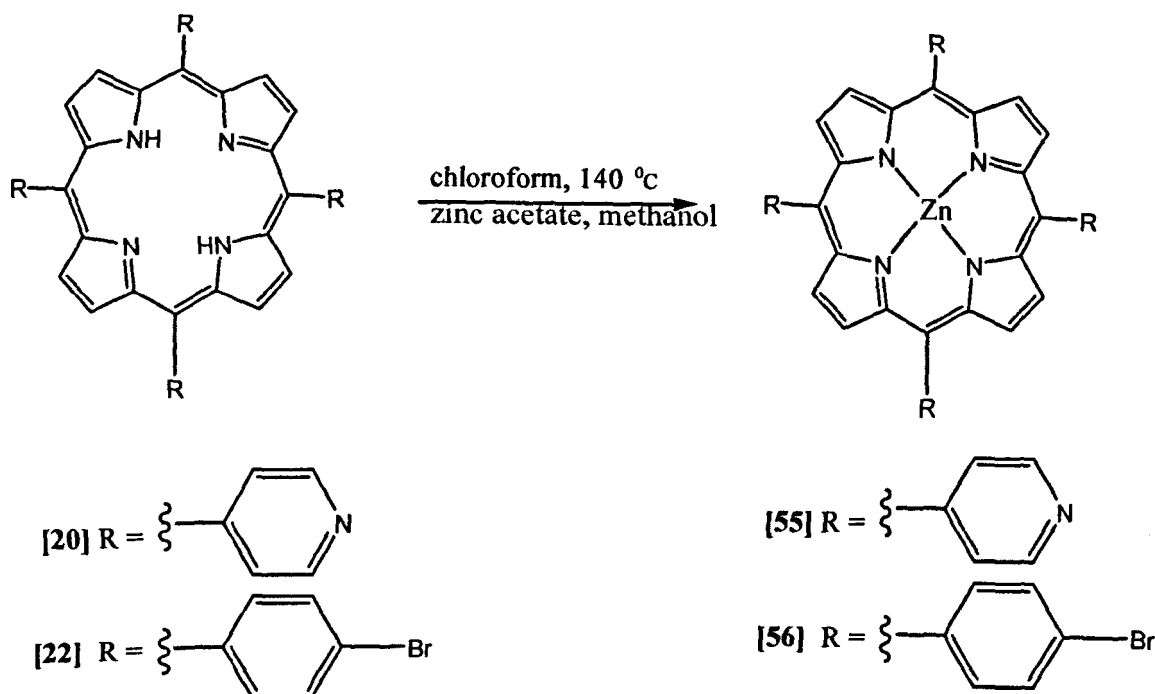
*et al*¹ to obtain metalloporphyrins.



Scheme 33: Imidazole melt synthetic route for metalation.

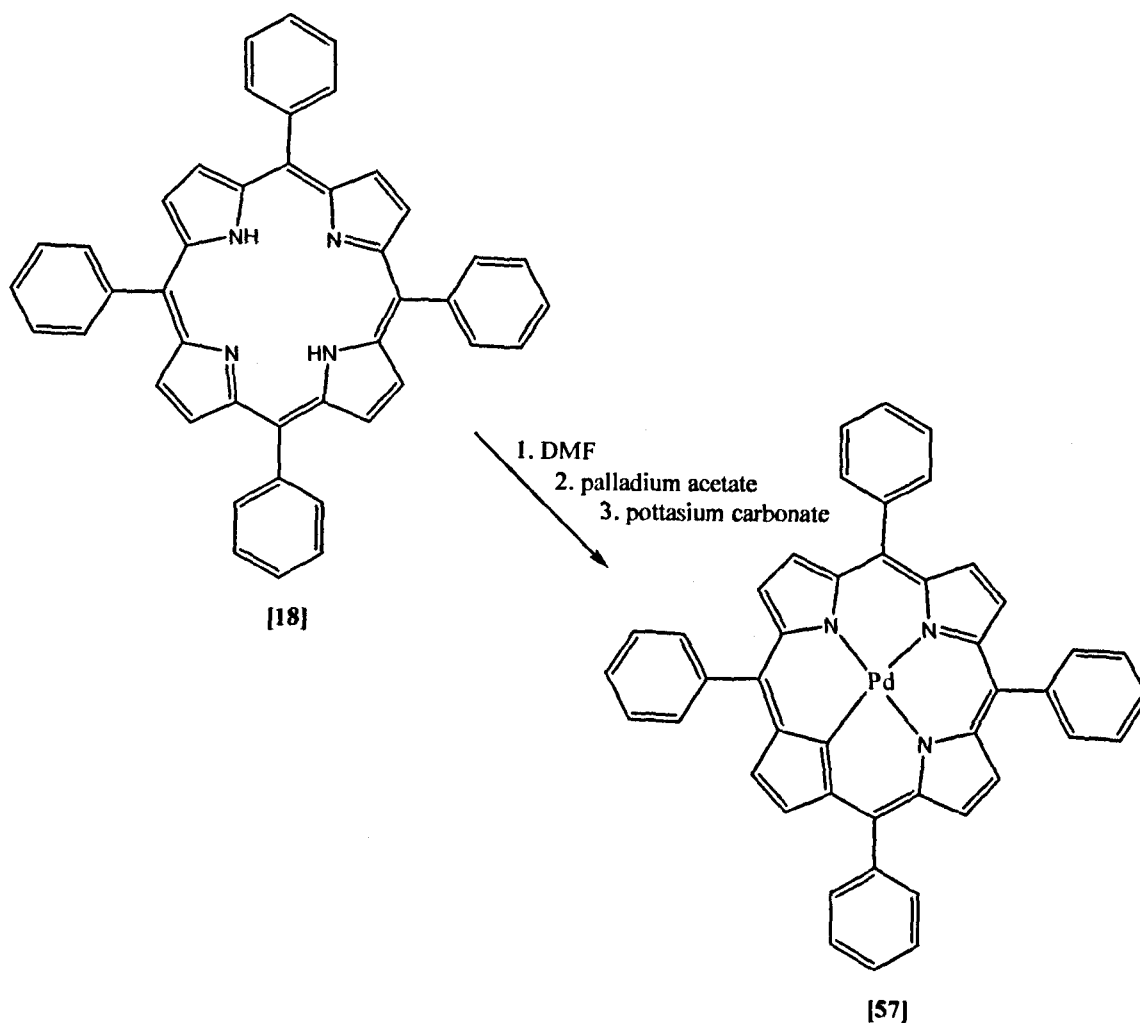
The next approach attempted was to incorporate metals other than palladium into the 5,10,15,20-tetra(4-pyridyl)porphyrin centre. This approach yielded zinc(II)-5,10,15,20-tetra(4-pyridyl)porphyrin [55] with 93% yield. Successful metalation with zinc metal was also observed to yield yet another symmetric tetraarylporphyrin, zinc(II)-5,10,15,20-tetra-(4-bromophenyl)porphyrin [56]. The synthesis involved using chloroform as a solvent and adding a saturated solution of zinc acetate in methanol and heating the reaction mixture under reflux for 30 minutes before purification. The scheme

below outlines the reaction procedure followed.



Scheme 34: Successful metalation of tetraarylporphyrins with zinc in project.

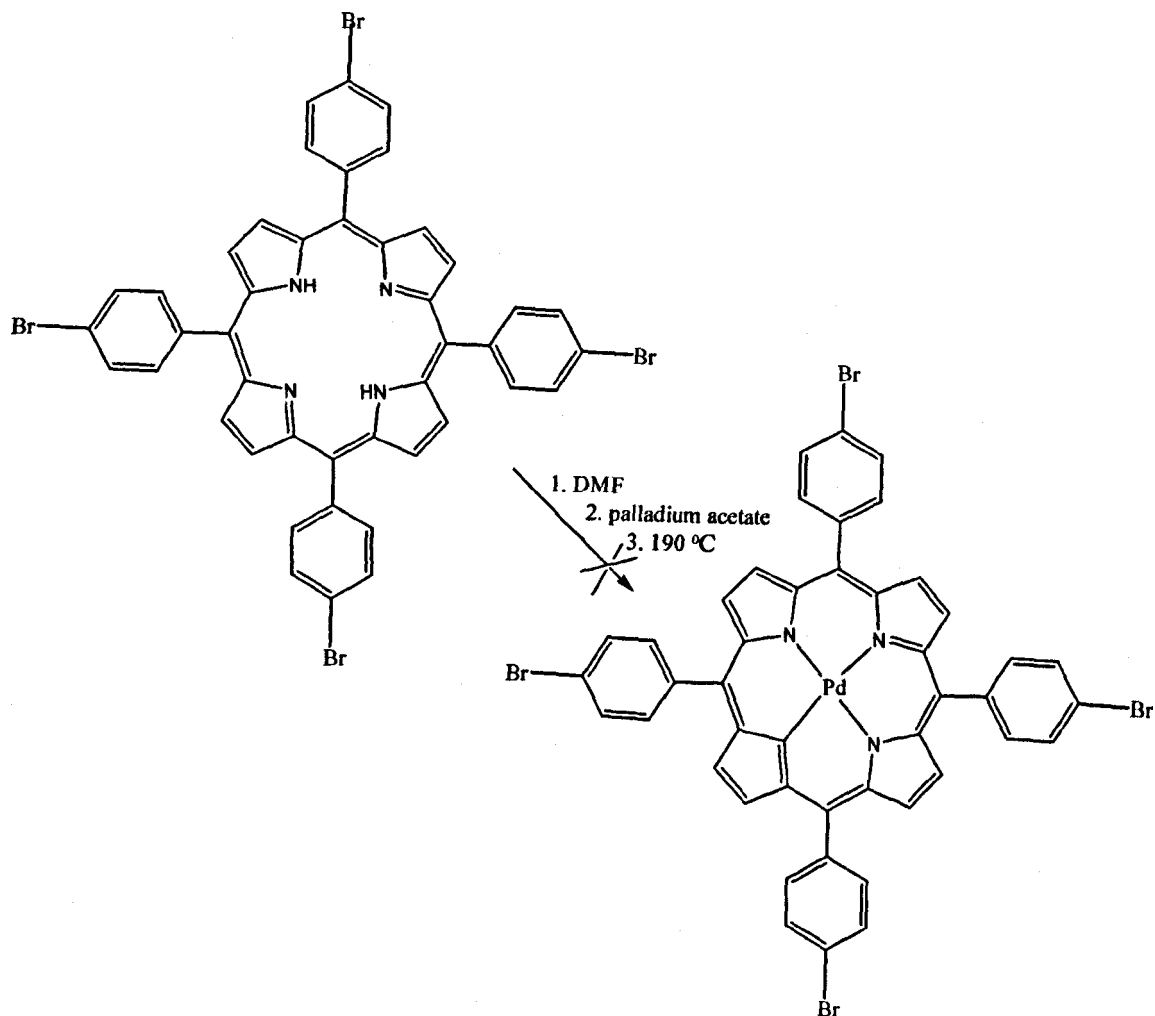
Having obtained evidence of a successful metal insertion into the tetrapyrrolyl complex, the next step was to obtain evidence of palladium insertion into a simple porphyrin, and tetraphenylporphyrin (TPP) was the porphyrin of choice. Using purified palladium acetate, potassium carbonate and DMF, the palladium tetraphenylporphyrin complex was obtained in 73% yield. The scheme below outlines the procedure followed for successful metalation into TPP.



Scheme 35: Initial metalation of tetraphenylporphyrin with Palladium in project.

These experiments revealed that tetrapyrrolyl porphyrin could undergo metal insertion reactions and also that palladium metal could be inserted into other porphyrin macrocycles. It was therefore deduced that the size of the metal, its electron density as well as that of the porphyrin macrocycle had an effect upon metal insertion into the porphyrin macrocycle. Other reactions that were attempted, but did not give any positive results, were reactions involving the insertion of the palladium into porphyrin macrocycles with halogenated phenyl substituents. The scheme below is an example of

the reactions attempted.



Scheme 36: Attempted palladium metal insertion into halogenated porphyrin.

The ^1H NMR obtained indicated the absence of the signal for the N-H bonds in the centre of the porphyrin macrocycle, which suggested that the metal had been incorporated as desired. However, it also indicated the signal for the β hydrogens to be a multiplet suggesting that they were non-equivalent. It was thought that the palladium metal may have inserted into the bromine-carbon bond just as it does during the initial stages of the Suzuki coupling reactions and hence this would make the β hydrogens non-equivalent.

This behaviour has recently been confirmed by Arnold *et al*²⁰¹ who found it was possible to isolate the product of such palladium insertion reactions.

Unsatisfactory results were also obtained for reactions attempted using palladium 5,10,15,20-tetra-(pentafluorophenyl)porphyrin using DMF. The findings were explained using results obtained from a study conducted by Kadish *et al*.²⁰² They suggested that where the solvent used was DMF, the final product produced was not simply a metal centred derivative. DMF can break down at reflux to give dimethylamine, which can also substitute the halogen at the *para*-positions of the phenyl rings. This explained why the data obtained was not easily interpretable. The material produced was a mixture of partially or fully substituted products with one, two, three or all four fluorines at the *para*-positions substituted with N(CH₃)₂ groups. The mixture also contained the starting material and the metal inserted, but unsubstituted, porphyrin which could not be separated easily. This evidence explained why the signal for the β hydrogens was no longer a broad singlet, but a multiplet. A strategy that was suggested in order to overcome this side reaction was to use other solvents such as acetonitrile and benzonitrile.

Previous work done by Tyulyaeva *et al*²⁰³ indicated the use of boiling benzonitrile to produce stable platinum complexes. Benzonitrile was also used by Soini *et al*²⁰³ to give platinum metal porphyrins and hence, a method was designed using benzonitrile as the solvent in our research. Many other factors contributed to the successful insertion of palladium metal into the porphyrin macrocycles. In our research, it was found that reactions were successful when the metal acetate was used as opposed to the corresponding metal chlorides, which failed to insert cleanly. This was explained simply by the fact that the metal acetates were more soluble than the metal chlorides in

the solvent systems used. Also, during the reactions, metal acetate was required in an excess of almost ten times relative to the porphyrin used for the reaction to take place. Other factors that were found to be important were purity of the metal salt, purity of the solvent, dryness of the solvent, amount of light entering the reaction flask and having an inert gas atmosphere during the reaction. Once all the above mentioned factors were discovered and the reaction conditions optimised, it was possible to design a synthetic procedure that allowed palladium metal insertion into porphyrin macrocycles.

In conclusion it was observed that the best reaction conditions for palladium insertion into porphyrins were; benzonitrile, excess palladium acetate, 240 °C, inert gas atmosphere and lack of light during the reaction.

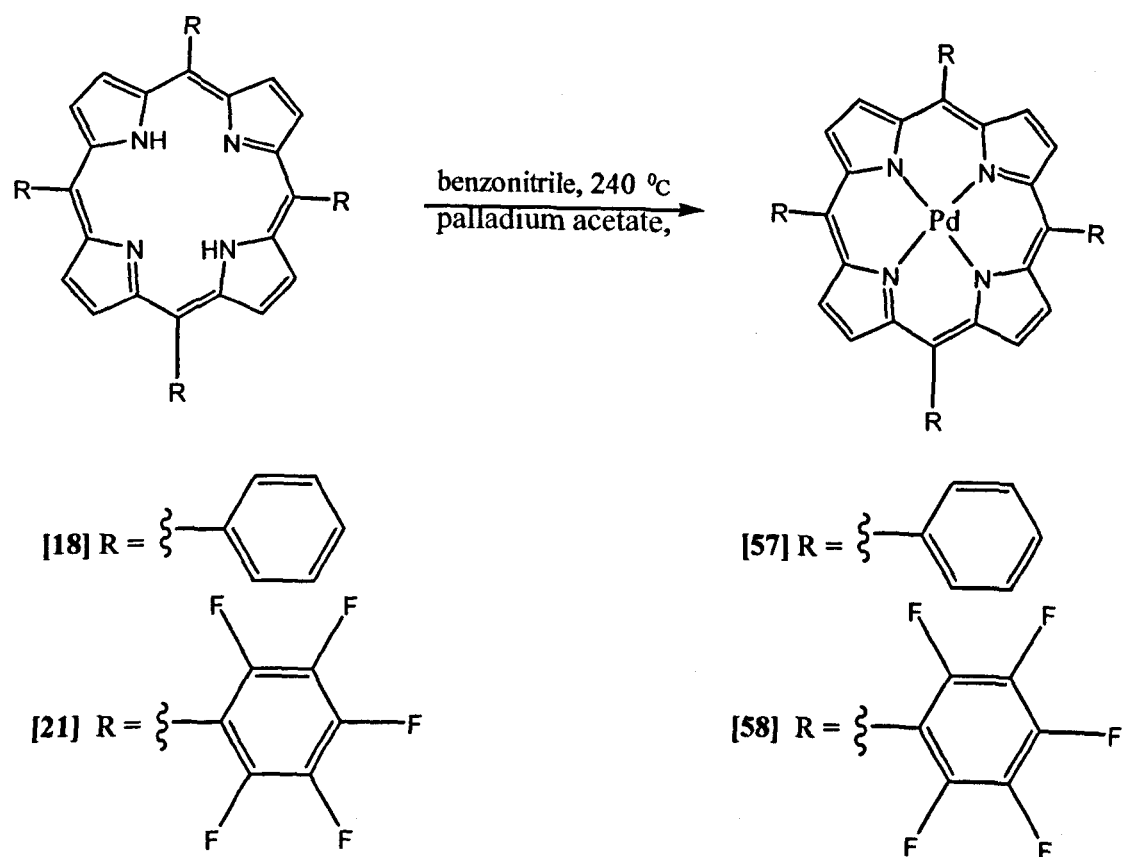
3.1.3 General synthetic procedure in project

With the aim of developing a versatile method, a range of basic porphyrins were subjected to metal insertion. The general method given involved using a ten times molar excess of Pd(OAc)₂ dissolved in a minimum amount of benzonitrile (~5 ml). The reaction mixture was heated under reflux at 240 °C, for 30 minutes under argon and protected from light. The porphyrin was then added whilst heating and the mixture stirred under reflux for 72 hours. Upon cooling, the solvent was removed *in vacuo* and the resulting solid redissolved into a minimum amount of benzene. The mixture was filtered through a neutral alumina column and the filtrate collected, dried and the solvent removed *in vacuo* to obtain the product. The product was recrystallised using chloroform and dried to give the final product. The full details of each experiment is discussed in the

experimental chapter four.

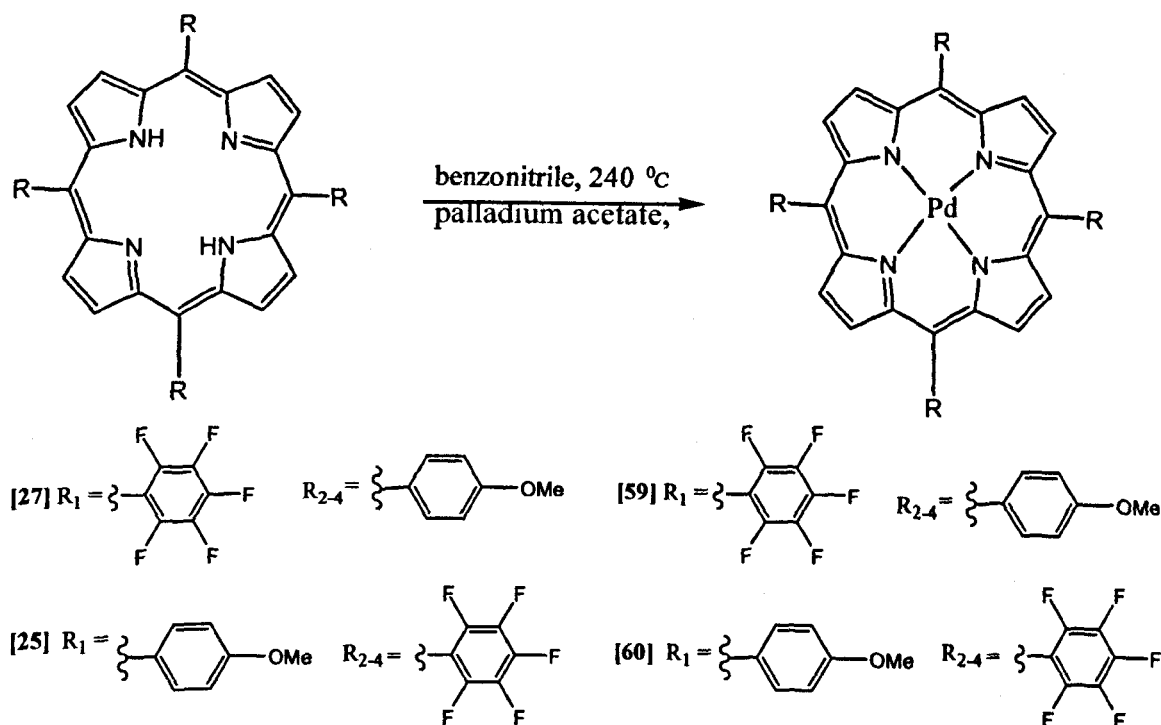
3.1.4 Synthetic achievements in project of Pd metalation using benzonitrile method.

Different types of porphyrins were metalated which were symmetrical and unsymmetrical, tetraarylporphyrins and diarylporphyrins. Symmetrical tetraarylporphyrins which were successfully metalated using Pd, included 5,10,15,20-(tetraphenyl)porphyrin [57] and 5,10,15,20-tetra(pentafluorophenyl)porphyrin [58]. The scheme below outlines the reaction procedure.



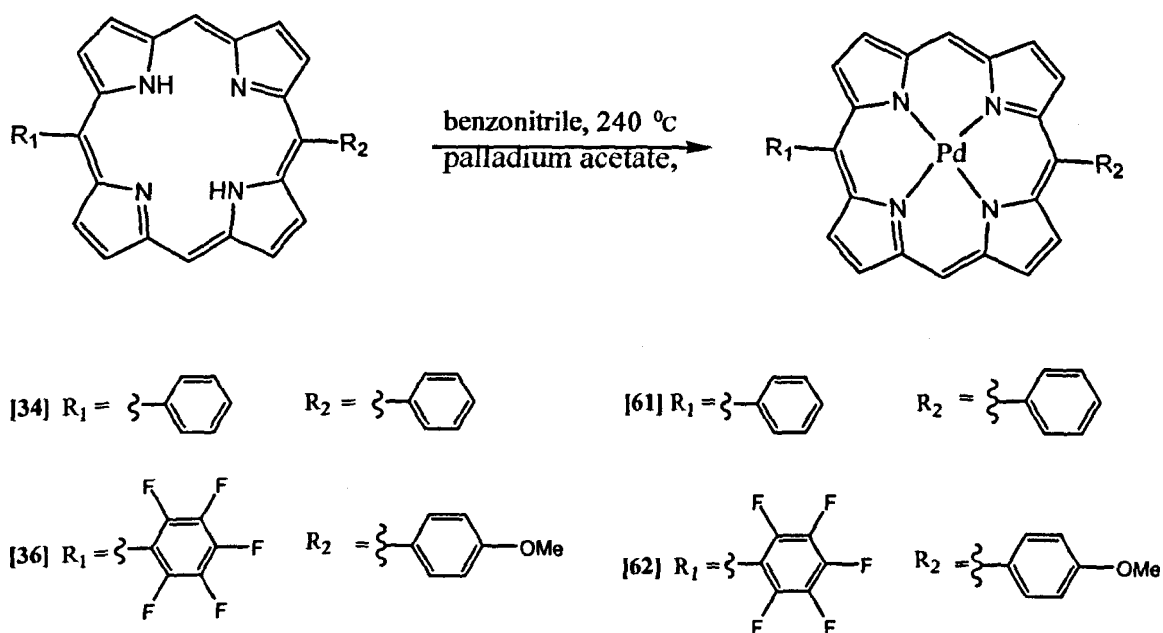
Scheme 37: Palladium metal insertion into symmetric tetraarylporphyrins.

Unsymmetric tetraarylporphyrins were also metalated successfully to give Pd(II)-5-(pentafluorophenyl)-10,15,20-tris-(4-methoxyphenyl)porphyrin [59] and Pd(II)-5-(4-methoxyphenyl)-10,15,20-tris-(pentafluorophenyl)porphyrin [60].



Scheme 38: Successful palladium metal insertion into unsymmetric tetraarylporphyrins.

Diarylporphyrins were also successfully metalated using identical conditions to give both symmetrical and unsymmetrical diarylporphyrins. In both cases, Pd(II)-diphenylporphyrin [61] and Pd(II)-5-(pentafluorophenyl)-15-(4-methoxyphenyl)porphyrin [62] were synthesised respectively. The scheme below outlines the reaction summary.



Scheme 39: Successful palladium metal insertion into diarylporphyrins.

Following this general procedure, palladium metal porphyrins were obtained in good yields (37-85%) and were fully characterised by ¹H NMR, ¹³C NMR, MS, UV and TLC.

3.1.5 Characterisation of palladium porphyrins

This section is aimed at describing the methods used to investigate the molecular structure of compounds. Basic organic analytical procedures such as ¹H NMR, ¹³C NMR, MS, UV and TLC were all used in this project. The underlying principles of the analytical methods will not be discussed but rather emphasis placed on the use of these analytical methods to determine important molecular information.

Notable features of ^1H NMR spectra.

The most recognised feature of a free base ^1H NMR is the presence of a signal with a negative chemical shift relative to TMS $\sim -2\text{ppm}$. The signal represents two highly shielded central pyrrolic NH protons. The negative signal is due to the efficient shielding by the powerful aromatic ring current caused by the conjugated macrocycle. The other signal that is unusually low field (9 ppm), representing the protons at the β positions. These protons lie outside the macrocyclic ring current and as a result experience a deshielding effect, which in turn has an effect of increasing the chemical shift values to be higher than is normally expected for aromatic protons.

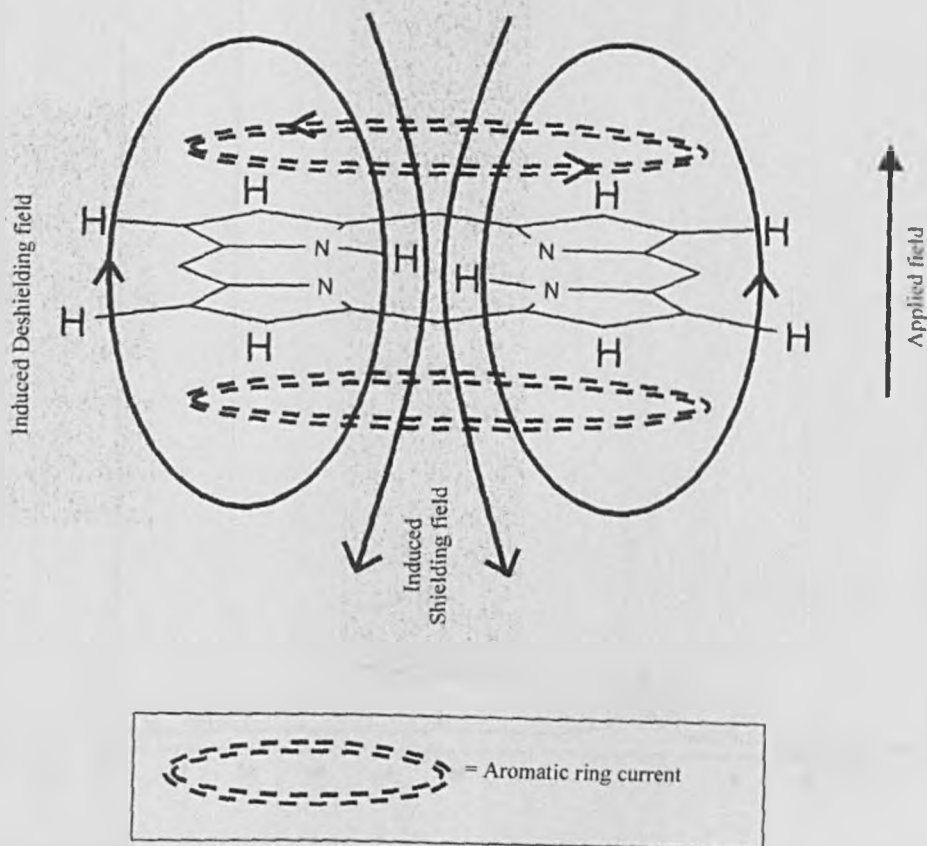


Fig 40: Shielding effect of aromatic ring on porphyrin.

Metalloporphyrins on the other hand do not have a negative signal associated with the central pyrrolic NH protons. This is due to the metal coordination to the pyrrolic nitrogens and the loss of the protons previously found on the nitrogens. The lack of the signal at ~ 2 ppm is often an indicator used alongside other analytical methods including UV-vis spectroscopy, to ensure metal insertion.

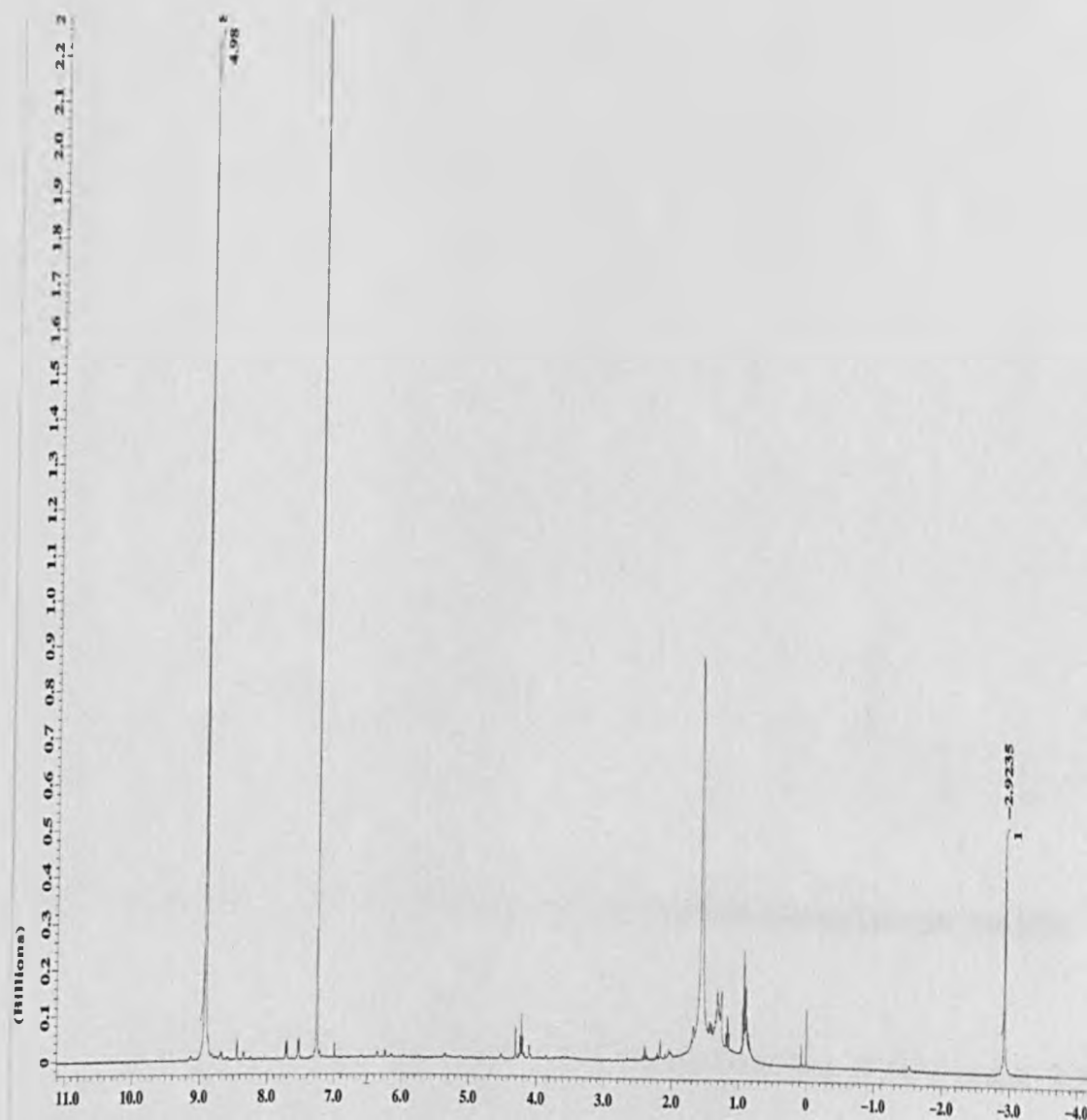


Fig 41: ^1H NMR for free base 5,10,15,20-tetra(pentafluorophenyl)porphyrin [21]

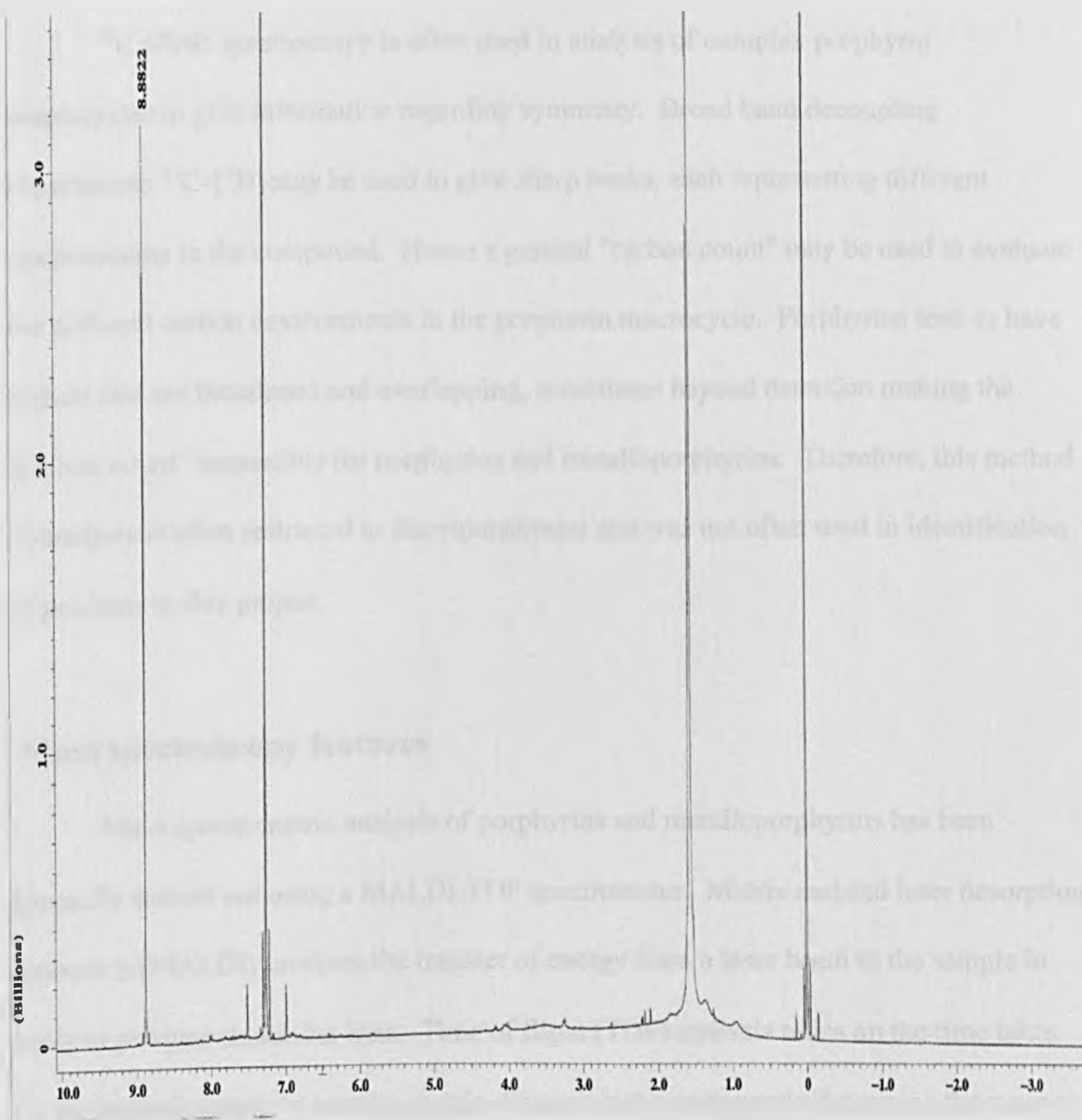


Fig 42: ^1H NMR for Pd(II) 5,10,15,20-tetra(pentafluorophenyl)porphyrin [58]

Noticeable difference in both ^1H NMR spectra is the lack of the signal at -2.9 ppm for the palladium porphyrin.

¹³C NMR spectra features

¹³C NMR spectroscopy is often used in analysis of complex porphyrin macrocycles to give information regarding symmetry. Broad band decoupling experiments ¹³C-¹H may be used to give sharp peaks, each representing different environments in the compound. Hence a general "carbon count" may be used to evaluate the different carbon environments in the porphyrin macrocycle. Porphyrins tend to have signals that are broadened and overlapping, sometimes beyond detection making the "carbon count" impossible for porphyrins and metalloporphyrins. Therefore, this method of analysis is often restricted to diarylporphyrins and was not often used in identification of products in this project.

Mass spectroscopy features

Mass spectrometric analysis of porphyrins and metalloporphyrins has been generally carried out using a MALDI-TOF spectrometer. Matrix assisted laser desorption ionisation (MALDI) involves the transfer of energy from a laser beam to the sample in order to produce molecular ions. Time of flight (TOF) analysis relies on the time taken for an ionised sample to travel a certain distance and consequently determine the mass to charge ratio, which varies inversely with the speed of the particles.

This method was found to be well adapted to porphyrins and metalloporphyrins for determining molecular weights, it was also effective, sensitive and reliable for such large molecules such as free base porphyrins as well as metal inserted porphyrins. MALDI is a non-fragmenting mild ionisation method, and when used in this project, produced protonated molecular ions for both free base and metal inserted porphyrins, for

palladium porphyrins, a specific isotope pattern was observed, which was due to the several natural stable isotopes of palladium. This specific characteristic isotope pattern was a clear indication of the presence of the metal ion.

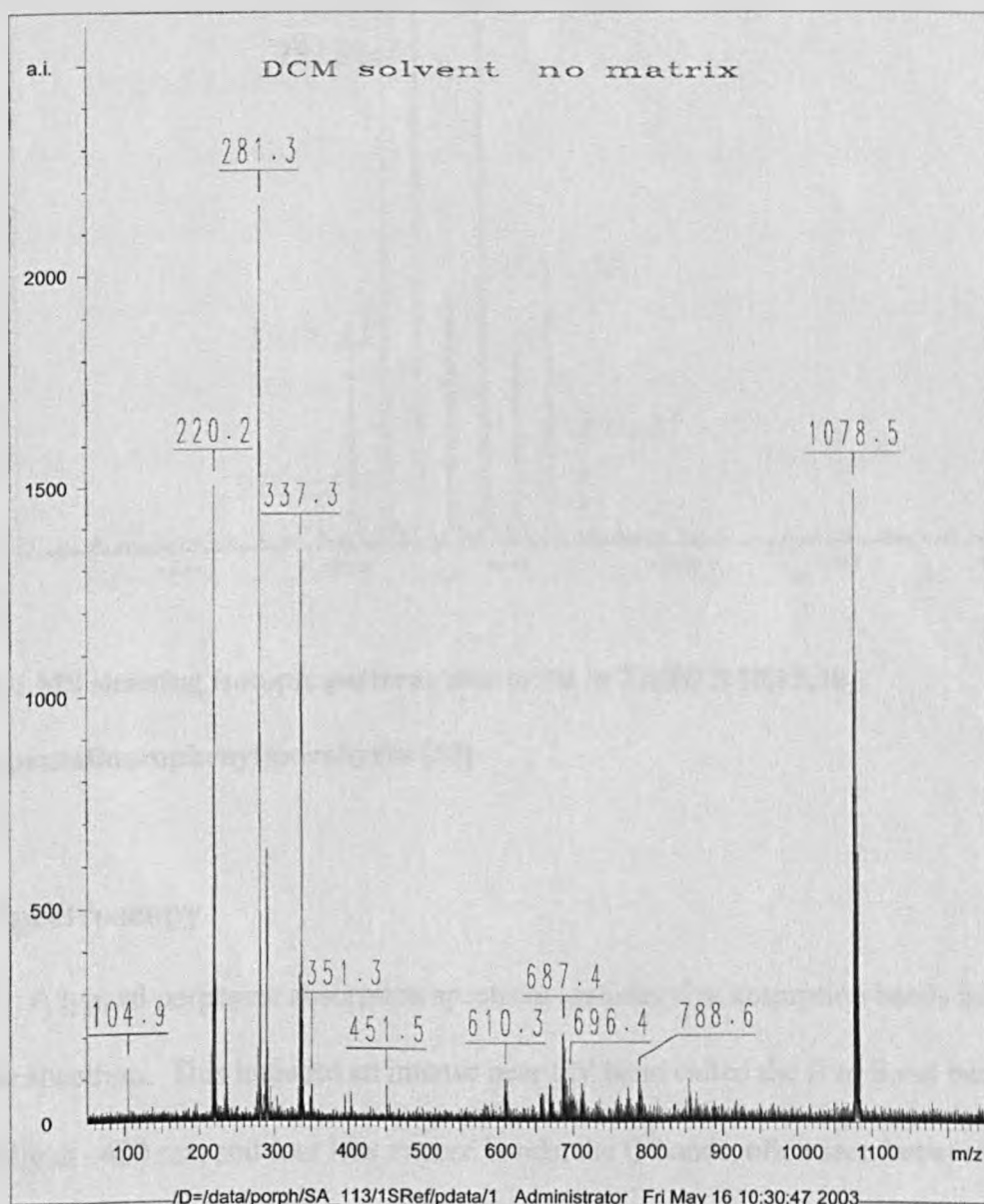


Fig 43: MS for Pd(II) 5,10,15,20-tetra(pentafluorophenyl)porphyrin [58]

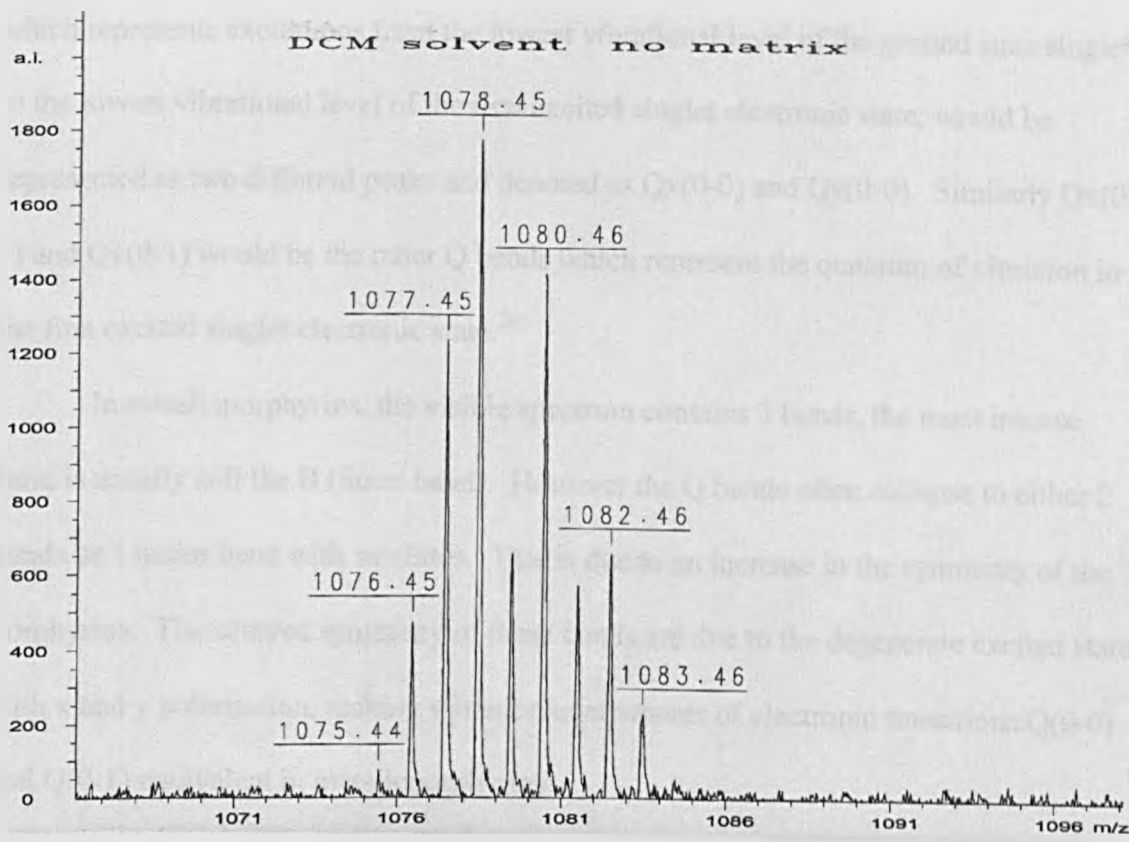


Fig 44: MS showing isotopic patterns due to Pd in Pd(II) 5,10,15,20-tetra(pentafluorophenyl)porphyrin [58]

UV spectroscopy

A typical porphyrin absorption spectrum includes five absorption bands in the UV visible spectrum. This includes an intense near UV band called the B or Soret band, typically at ~ 400 nm, and four less intense bands, the Q bands, often seen between $\lambda = 500-600$ nm. These absorptions arise from π (highest occupied molecular orbital, HOMO) to π^* (lowest unoccupied molecular orbital, LUMO) transitions associated with the delocalised conjugate system. The unsymmetrical nature of the free base due to the

proton axis, excitations along the x axis and y axis are not degenerate. Hence, $Q(0,0)$, which represents excitations from the lowest vibrational level of the ground state singlet to the lowest vibrational level of the first excited singlet electronic state, would be represented as two different peaks and denoted as $Q_x(0-0)$ and $Q_y(0-0)$. Similarly $Q_x(0-1)$ and $Q_y(0-1)$ would be the other Q bands which represent the quantum of vibration in the first excited singlet electronic state.²⁰⁵

In metalloporphyrins, the visible spectrum contains 3 bands, the most intense band is usually still the B (Soret band). However the Q bands often collapse to either 2 bands or 1 major band with satellites. This is due to an increase in the symmetry of the porphyrins. The squared symmetry of these bands are due to the degenerate excited states with x and y polarisation, making vibration components of electronic transitions $Q(0-0)$ and $Q(0-1)$ equivalent in metalloporphyrins.

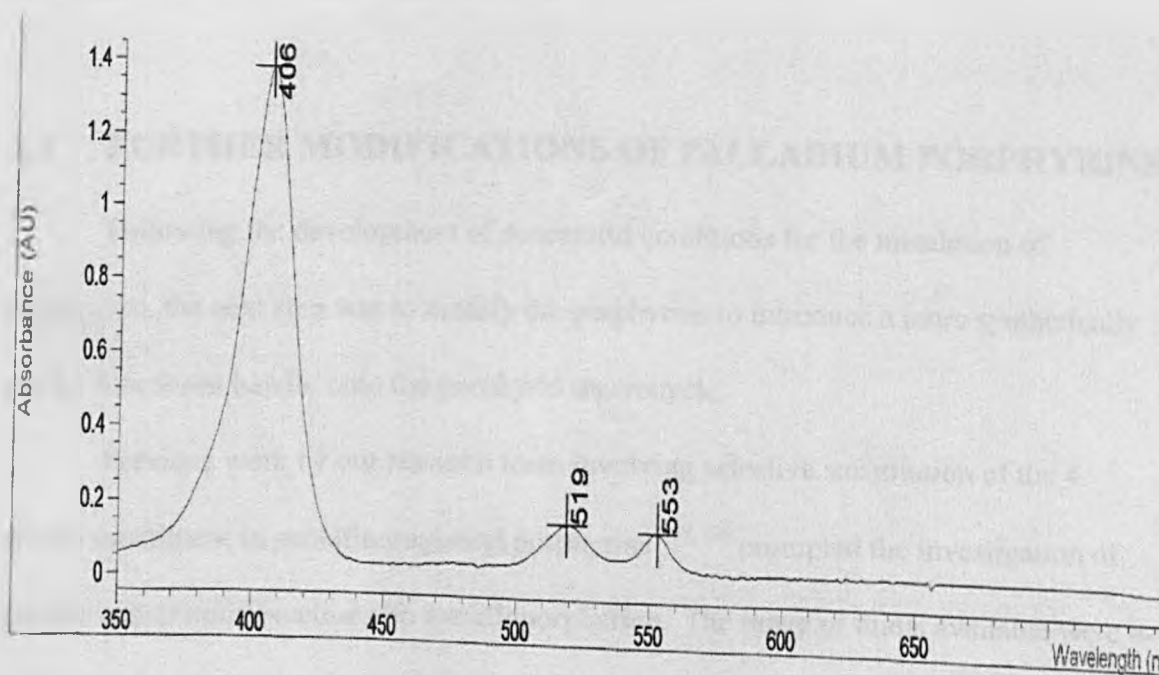


Fig 45: UV spectra for Pd(II) 5,10,15,20-tetra(pentafluorophenyl)porphyrin [58]

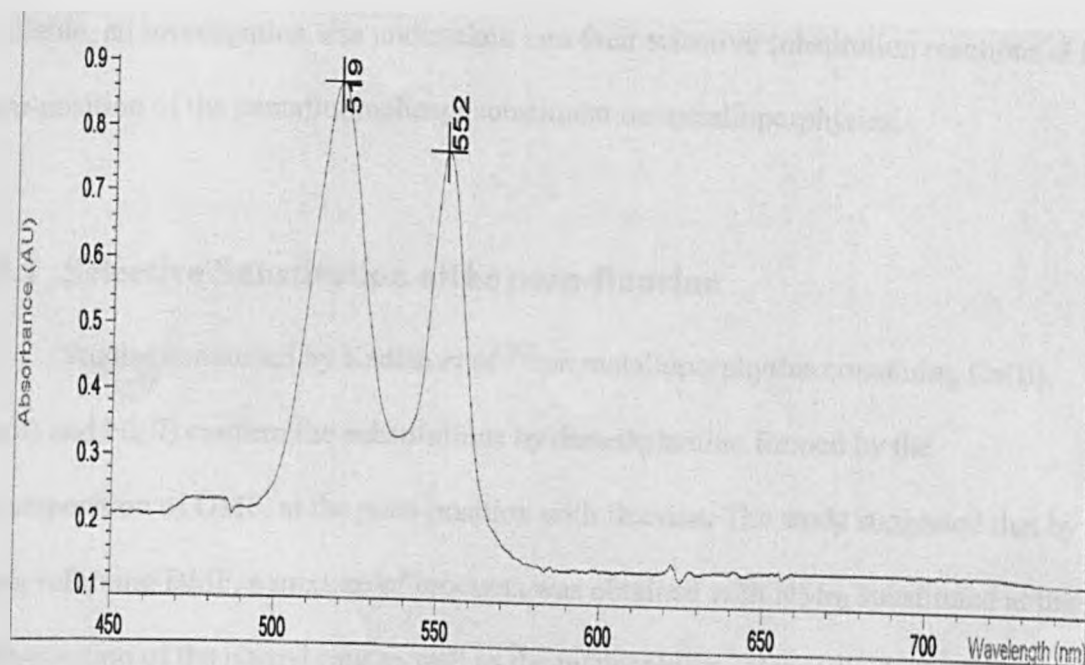


Fig 46: UV spectra showing collapsed Q bands for Pd(II) 5,10,15,20-tetra(pentafluorophenyl)porphyrin [58]

3.2 FURTHER MODIFICATIONS OF PALLADIUM PORPHYRINS

Following the development of successful conditions for the metalation of porphyrins, the next step was to modify the porphyrins to introduce a more synthetically useful functional handle onto the porphyrin macrocycle.

Previous work by our research team involving selective substitution of the 4-fluoro substituent in pentafluorophenyl porphyrins^{197, 198} prompted the investigation of similar substitution reactions on metalloporphyrins. The range of thiols available were 4-mercaptophenol, 2-mercaptoethanol, benzylmercaptan, benzenethiol, octadecanemercaptan and 4-aminobenzenethiol. With the different palladium porphyrins

available, an investigation was undertaken into their selective substitution reactions at the *para*-position of the pentafluorophenyl substituent on metalloporphyrins.

3.2.1 Selective Substitution of the *para*-fluorine

Studies conducted by Kadish *et al*²⁰² on metalloporphyrins containing Co(II), Cu(II) and Ni(II) confirm the substitutions by dimethylamino formed by the decomposition of DMF, at the *para*-position with fluorine. The study suggested that by using refluxing DMF, a mixture of products was obtained with NMe₂ substituted at the *para*-position of the phenyl ring as well as the nucleophiles. Hence products obtained were neither straight forward nor the expected porphyrin products.

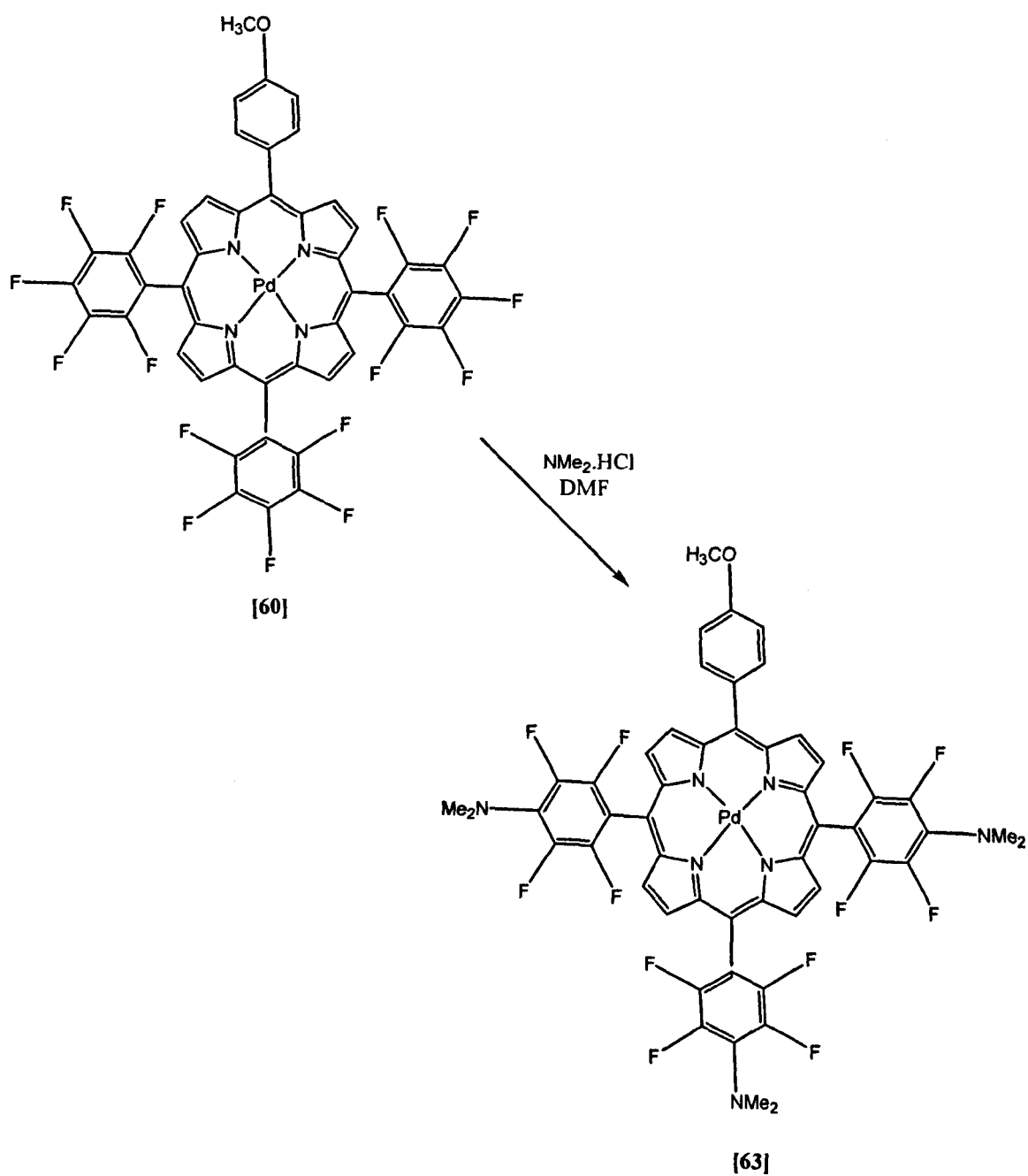
In 1991 Battioni *et al*²⁰⁶ confirmed the findings from Kadish *et al*²⁰², and suggested proper conditions for the preparation of functionalised polyhalogenated porphyrins in one step and with high yields, by selective substitution of the *para*-fluorine substituent on C₆F₅ groups of the metalloporphyrins by various nucleophiles. Battioni *et al*²⁰⁶ found that nucleophilic groups, such as amines, alcohols or thiols enabled selective substitution of fluorine at the *para*-position with high yields. Other nucleophiles, such as CN⁻, gave complex mixtures and low yields. Their work used the metalloporphyrin Zn(TF₅PP) and the nucleophiles used were NEt₂⁻, NHPr⁻, OEt⁻, OPh⁻ and SBU⁻. The procedure outlined in their work found DMF to be the best the solvent but reaction conditions to be at room temperature to avoid DMF degradation and competitive substitution.

3.2.2 Palladium Metalloporphyrin substitution of *para*-fluorine substituents in project.

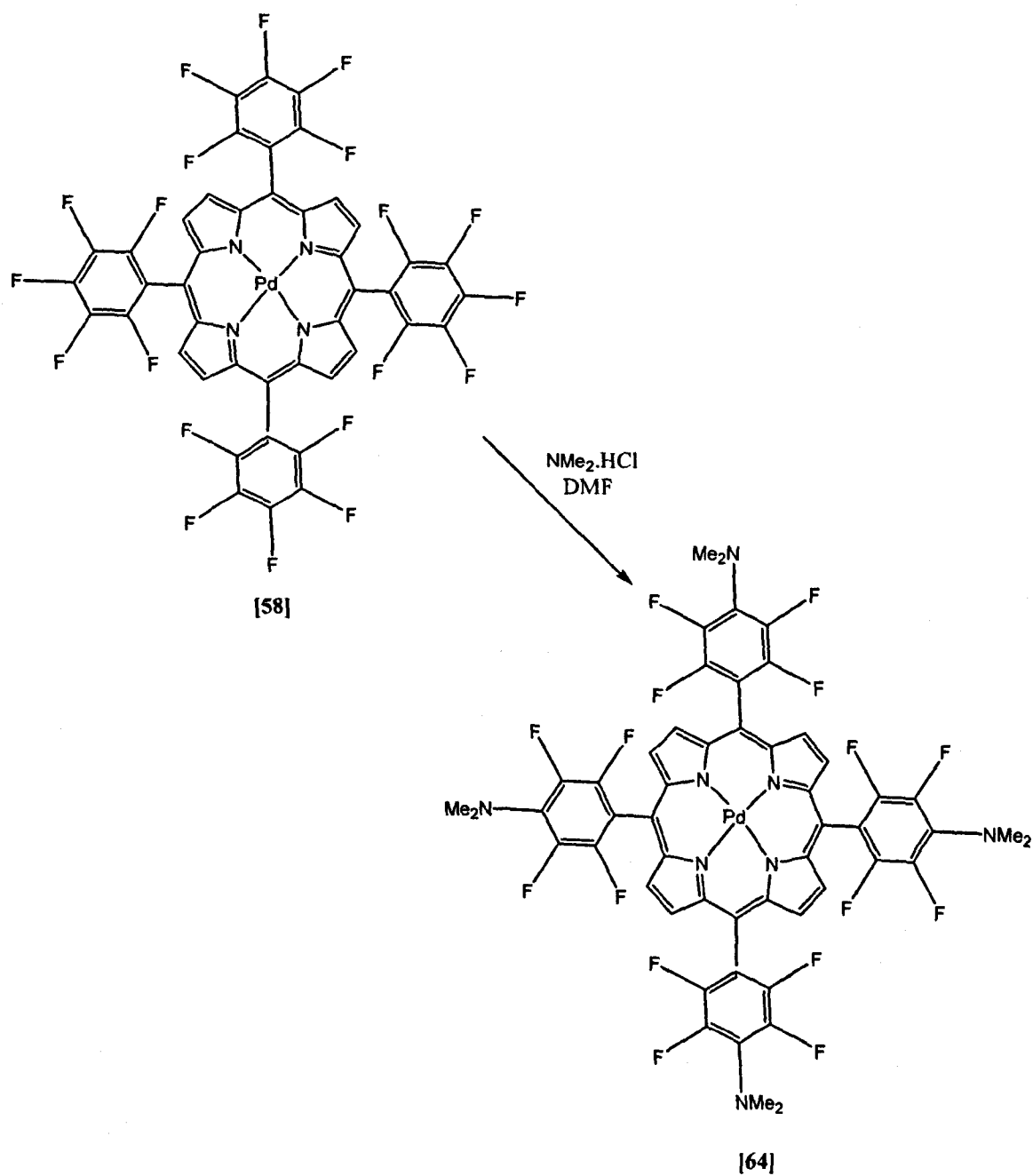
Unlike zinc porphyrins, palladium porphyrins were much harder to synthesise and as described earlier, required very harsh and inert conditions. Using reaction conditions outlined by Kadish *et al*²⁰² on metalloporphyrins and their substitution of the *para*-fluorine position on the pentafluorophenyl substituent with NMe₂ obtained by the breakdown of DMF, palladium porphyrins were reacted with (CH₃)₂NH.HCl in DMF. The reaction was driven to completion by using an excess of (CH₃)₂NH.HCl and both symmetrical and unsymmetrical tetraarylporphyrins were reacted.

Unsymmetrical Pd(II)-5-(4-methoxyphenyl)-10,15,20-tris(pentafluorophenyl) porphyrin [60] was reacted with (CH₃)₂NH.HCl in DMF. The scheme 47 below outlines the reactions involved. The product obtained, Pd(II)-5-(4-methoxyphenyl)-10,15,20-tris(2,3,5,6-tetrafluoro-N,N-dimethyl-4-aniliniumyl)porphyrin [63], indicated that all the *para*-fluorine position on the pentafluorophenyl substituent were substituted with NMe₂.

Similarly, symmetrical Pd(II)-5,10,15,20-tetra-(pentafluorophenyl)porphyrin [58] was reacted under the same conditions to give 5,10,15,20-tetrakis(2,3,5,6-tetrafluoro-N,N-dimethyl-4-aniliniumyl)porphyrin [64]. Again, the reaction indicated that all the *para*-fluorine position on the pentafluorophenyl substituent were substituted with NMe₂. The reaction was driven to completion and none of the mono, di- or tri-substituted products were isolated. Scheme 48 shows a summary of the reaction.



Scheme 47: Synthesis of Pd(II)-5-(4-methoxyphenyl)-10,15,20-tris(2,3,5,6-tetrafluoro-N,N-dimethyl-4-aniliniumyl)porphyrin [63]



Scheme 48: Synthesis of 5,10,15,20-tetrakis(2,3,5,6-tetrafluoro-N,N-dimethyl-4-aniiliniumyl)porphyrin [64].

Other than reactions with $(\text{CH}_3)_2\text{NH} \cdot \text{HCl}$, reaction conditions were sought which would allow thiol substitution reactions at *para*-fluorine positions selectively. The

method would also be required to be applicable to diarylporphyrins as well as symmetric and unsymmetric tetraarylporphyrins.

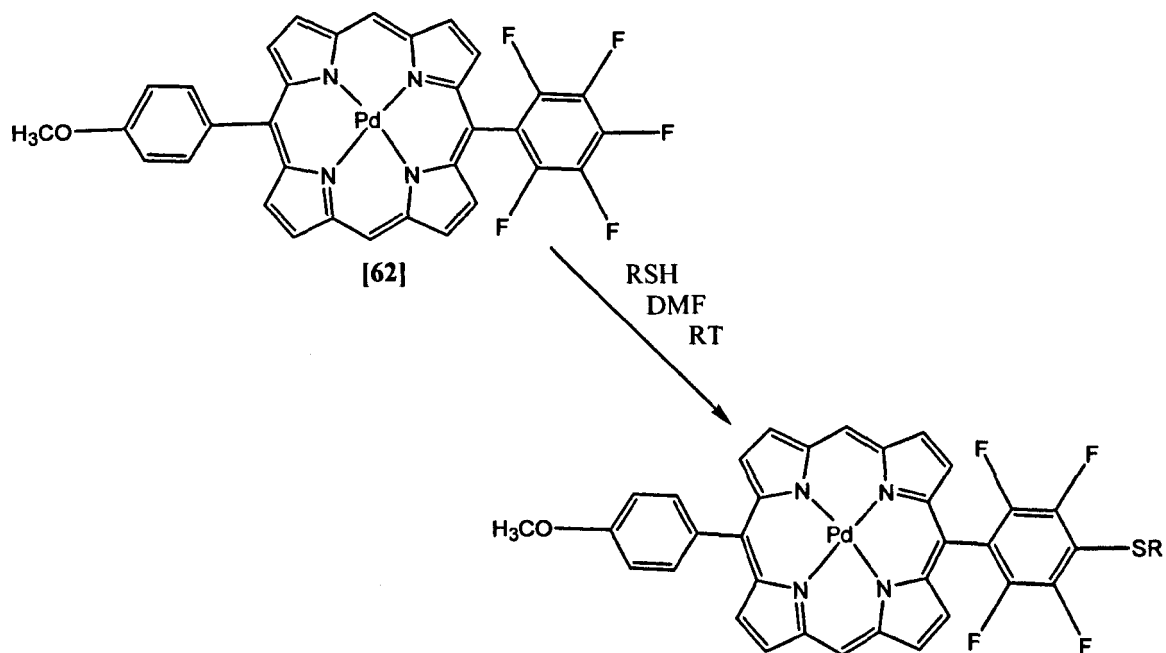
3.2.3 General Method for thiol substitution of *para*-fluorine substituents on Pd-Metalloporphyrin

Following the general method outlined in previous work by our research team involving selective substitution of the 4-fluoro substituent in pentafluorophenyl porphyrins,^{197, 198} reaction conditions were optimised for palladium porphyrins. Palladium porphyrin bearing pentafluorophenyl substituent was reacted with the thiol in a minimum amount of anhydrous DMF overnight, at room temperature and under argon and protected from light. The solvent was evaporated *in vacuo* and the solid re-dissolved into dichloromethane. The solution was then washed with saturated hydrogencarbonate, separated and concentrated to give the final product. The products were then analysed using TLC, UV, ¹H NMR and MS. Individual experiments are detailed in chapter four.

3.2.4 Synthetic achievements in thiol substitution of *para*-fluorines in project.

In instances where the diarylporphyrin Pd(II)-5-(4-methoxyphenyl)-15-(pentafluorophenyl)porphyrin was used, no extra purification of product was obtained as the thiol selectively substituted at the *para*-fluorine position on the pentafluorophenyl substituent. No further displacement of other fluorines was observed and the reactions always reached completion under the conditions used. The scheme below outlines the

reactions and products obtained.

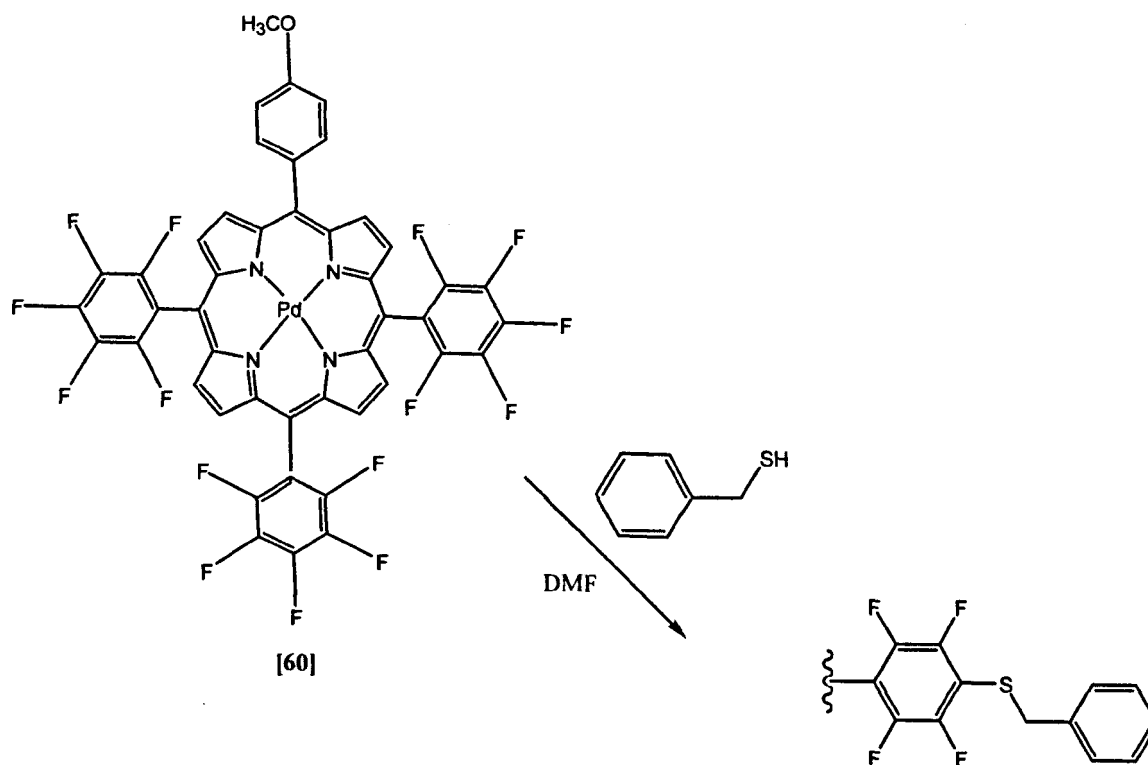


RSH	% yield
4-mercaptophenol [65]	78
Benzylmercapatan [66]	85
Benzenethiol [67]	40
2-Mercaptoethanol [68]	54
4-Aminobenzenethiol [69]	30
octadecanethiol [70]	40

Fig 49: Substitution reactions of Pd(II) 5-(pentafluorophenyl)-15-(4-methoxyphenyl)porphyrin using thiols.

For unsymmetrical Pd-tetraarylporphyrins with more than one pentafluorophenyl substituent, such as Pd(II)-5-(4-methoxyphenyl)-10,15,20-tris(pentafluorophenyl) porphyrin [60], fluorines at the *para*-positions of all three pentafluorophenyl substituents

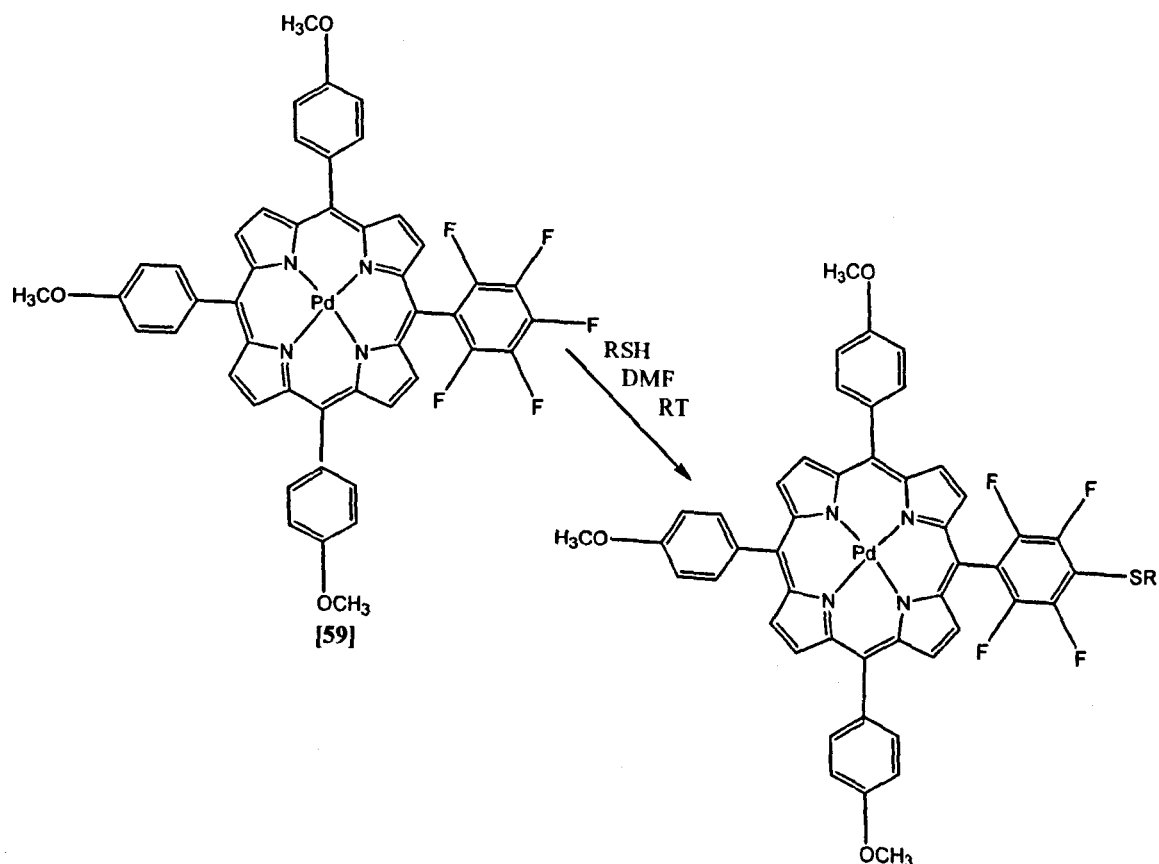
were replaced. In these cases, preparative TLC was used to separate the products. The mono-, di- and tri-substituted products were successfully purified as detailed in the experimental section [71-73] and characterised using TLC, UV, ¹H NMR and MS. The scheme below outlines the synthetic achievement.



Porphyrin	Yield (%)
Pd(II)-5-(4-benzylthio-2,3,5,6-tetrafluorophenyl)-10, 15-di-(pentafluorophenyl)-20-(4-methoxyphenyl)porphyrin [71]	8
Pd(II)-5, 10-di-(4-benzylthio-2,3,5,6-tetrafluorophenyl)-15-(pentafluorophenyl)-20-(4-methoxyphenyl)porphyrin [72]	9
Pd(II)-5, 10, 15-tris-(4-benzylthio-2,3,5,6-tetrafluorophenyl)-20-(4-methoxyphenyl)porphyrin [73]	2

Fig 50: Substitution reactions of Pd(II)-5-(4-methoxyphenyl)-10,15,20-tris(pentafluorophenyl) porphyrin using benzylmercaptan.

To avoid further multistep purifications, unsymmetrical Pd-porphyrins containing only one pentafluorophenyl substituent were synthesised. Pd(II)-5-(pentafluorophenyl)-10,15,20-tris(4-methoxyphenyl)porphyrin [59] was reacted further with different thiols. The table and scheme below outlines the reactions achieved.

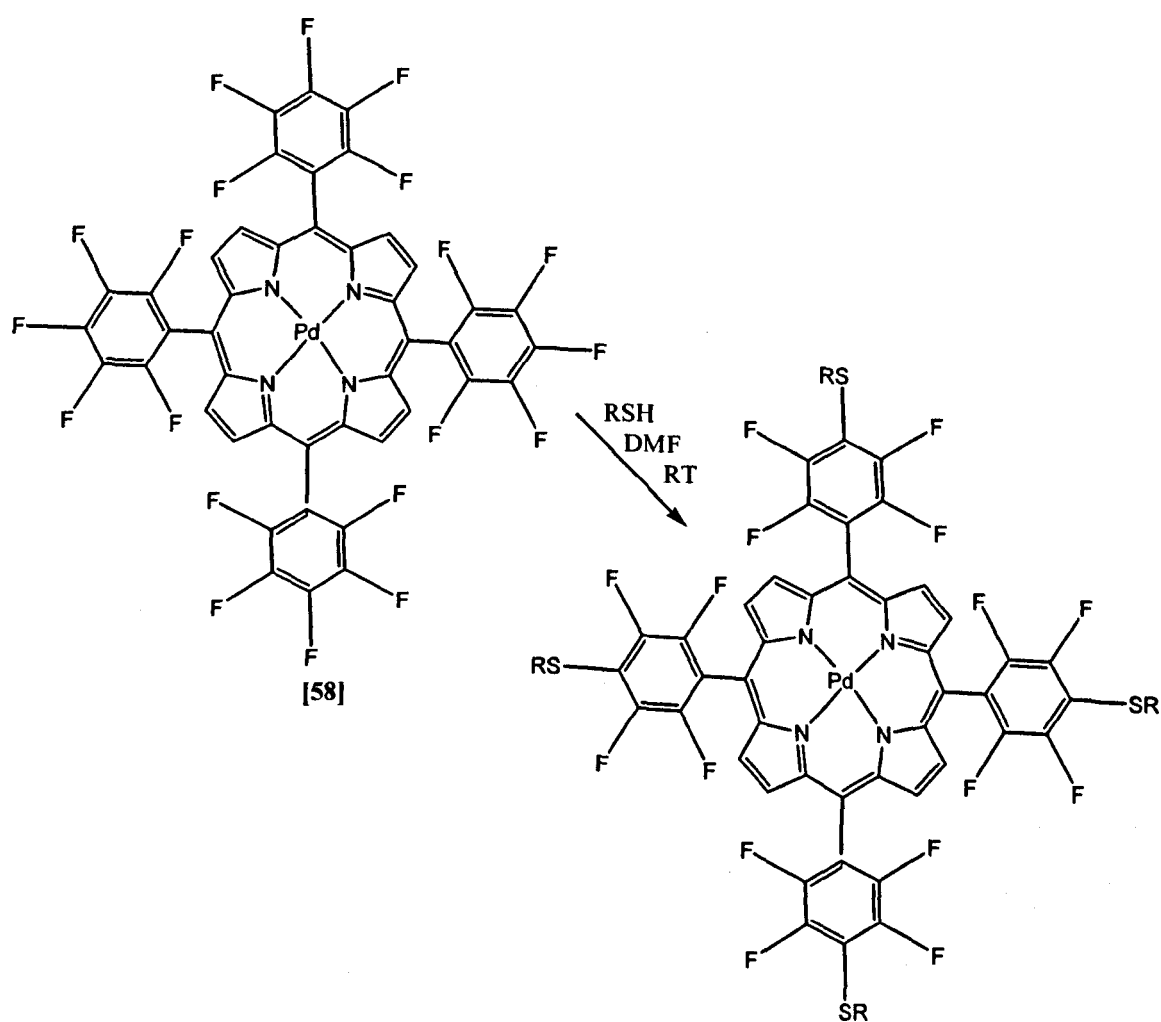


RSH	% Yield
4-mercaptophenol [74]	30
Benzenethiol [75]	40
2-Mercaptoethanol [76]	60
4-Aminobenzenethiol [77]	41
Octadecanethiol [78]	82

Fig 51: Thiol substitution reactions for Pd(II) 5-(pentafluorophenyl)-10,15,20-tris(4-methoxyphenyl)porphyrin

All the products obtained were analysed using TLC, UV, ^1H NMR and MS and were found to be single compounds.

Symmetrical tetraarylporphyrin, Pd(II)-5,10,15,20-tetra(pentafluorophenyl) porphyrin was used to react with different thiols. In certain cases, only the tetra-substituted product was obtained. These reactions are summarised in the scheme below.



RSH	% yield
4-mercaptophenol [79]	25
Benzenethiol [80]	9
2,3,5,6-tetra- <i>O</i> -acetyl- β -D-thioglucopyranose [81]	44
4-Aminobenzenethiol [82]	33

Fig 52: Thiol substitution reactions for Pd(II) 5,10,15,20-tetra-(pentafluorophenyl) porphyrin

However, in other cases, the mono-, di-, tri-, and tetra-substituted thiol metalloporphyrins were obtained. Again, only fluorines at the *para*-positions were displaced selectively. Using preparative TLC, the different products were separated and analysed. The separations were tedious and time consuming but gave a range of pure metalloporphyrins which had similar functionalities that could be used for further investigations. This was the case when the thiols:- benzylmercaptan, 2-mercaptoethanol and octadecanethiol were reacted with Pd(II) 5,10,15,20-tetra-(pentafluorophenyl) porphyrin [58]. The table below indicates which substituted products were obtained, represented with a tick and the porphyrin number associated. The full experimental details are found in chapter four.

RSH	mono-	di-	tri-	tetra-
benzylmercaptan	✓ [83]	✓ [84]	✓ [85]	✓ [86]
2-mercaptoethanol	✓ [87]	✓ [88]	✓ [89]	x
octadecanethiol	✓ [90]	✓ [91]	✓ [92]	✓ [93]

Fig 53: Thiol substitution reactions for Pd(II) 5,10,15,20-tetra-(pentafluorophenyl) where the mono-, di-, tri- and tetra-substituted products were obtained.

3.2.5 Conclusions.

The development of a synthetic procedure that would allow the palladium metal insertion into different porphyrins was achieved. Various Pd-metalloporphyrins were synthesised, purified and then analysed using some common analytical methods. TLC, UV, ¹H NMR and MS were used to identify and characterise these metalloporphyrins.

Pd porphyrins containing one, two, three or four pentafluorophenyl substituents were also synthesised. Once synthesised, the Pd-metalloporphyrins were reacted with different thiols for the selective substitution of *para*-fluorines on pentafluorophenyl substituents. The products obtained were purified and analysed to give a range of porphyrins that could be used for further work in future.

These Pd metalloporphyrins were initially synthesised to be used in studies as oxygen sensors. However, after the long and tedious effort to synthesise and functionalise the porphyrins, it was discovered that they were unsuitable for this purpose. This was due to the failure of cells incubated with the compounds to internalise the metalloporphyrins. The subject of the cells inability to uptake these metalloporphyrins is under investigation and may be developed further by future research into this area.

Further work suggestions include incorporating these metalloporphyrins into PEBBLEs (probes encapsulated by biologically localised embedding). Similar work has been done to use porphyrin PEBBLEs as oxygen sensors²⁰⁷ and also in particular platinum tetrakis(pentafluorophenyl)porphyrin immobilised in PEBBLEs²⁰⁸ has been used to measure oxygen concentrations in plants.

CHAPTER FOUR: EXPERIMENTAL

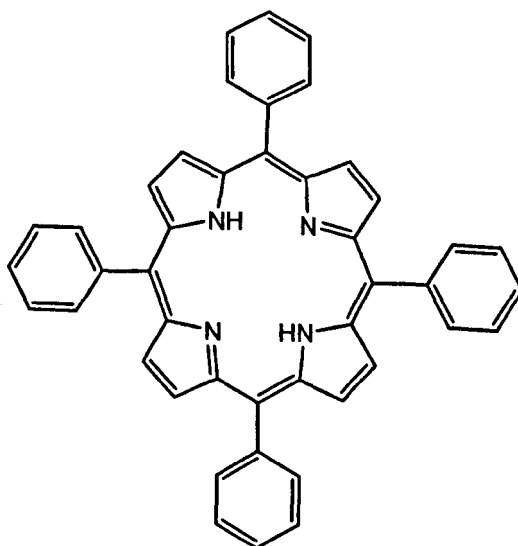
4.1 EQUIPMENT

- ^1H and ^{13}C NMR spectra were recorded on either a JEOL JNM-LA400 or JEOL JNM-GX270 NMR spectrometer. Chemical shifts (δ) are quoted in ppm relative to SiMe_4 , which was used as an internal standard. Coupling constants are given in Hertz.
- UV-visible spectra were measured on an Agilent 8453 diode array spectrometer.
- Mass spectra were recorded using either a Bruker Reflex IV matrix assisted laser desorption ionisation-time of flight (MALDI-TOF) mass spectrometer or a ThermoFinnigan LCQ Classic electrospray mass spectrometer. Samples analysed using MALDI-TOF were run in the absence of a matrix unless otherwise stated. Samples analysed by electrospray were directly loop injected through the inject/direct valve. Where present, the mass ion of the compound is indicated by M^+ and does not include counter ions.
- Melting points were recorded on a Gallenkemp or Philip Harris melting point instrument and are uncorrected. Melting points for porphyrins and metalloporphyrins were not obtained as they decompose at temperatures of $>350\text{ }^\circ\text{C}$.
- Thin-layer chromatography (TLC) was performed using Merck aluminium plates coated with silica gel 60 F₂₅₄ and visualised using either bromine vapour or under UV light. Gravity percolation chromatography was performed using Fluorochem Silica Gel 35-70 μm 60 \AA or ICN Silica Gel 32-63 μm 60 \AA .
- Solvents for TLC and chromatographic separation were purchased in house and used without further purification.

- Tetrahydrofuran was distilled over sodium wire under a nitrogen atmosphere with benzophenone as an indicator. All other reaction solvents and reagents were purchased from Aldrich, Avocado, Acros or Lancaster and used without further purification unless otherwise stated.
- Dryness of the products was assured by air drying the products as well as drying them under pressure. Dryness was confirmed by the lack of a ^1H NMR peak representing water protons in the product analysis.

4.2 METHODOLOGY

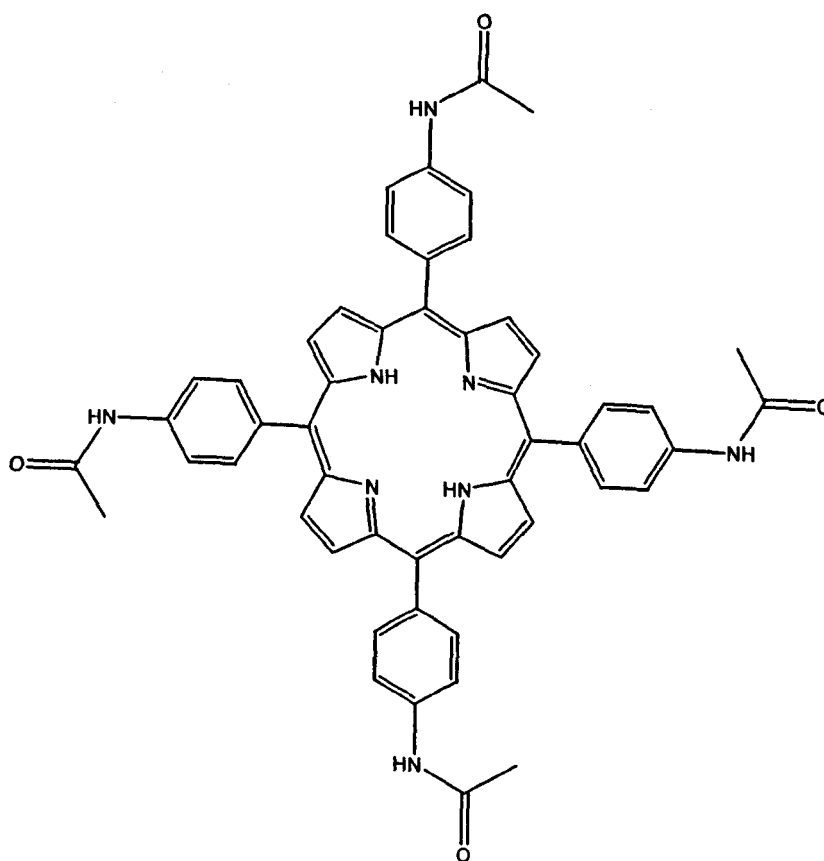
[18] 5,10,15,20-Tetraphenylporphyrin



To benzaldehyde (8.00 ml, 0.08 mol) dissolved in propionic acid (300 ml) was added

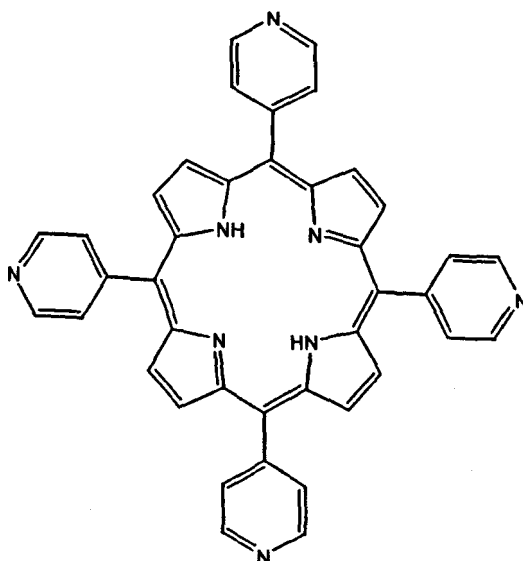
freshly distilled pyrrole (5.60 ml, 0.08 mol) and the solution stirred under reflux for 30 min. After cooling, the solution was filtered and the resulting solid was triturated thoroughly with methanol and then hot water. The purple crystals obtained were air dried and then finally dried under vacuum to remove any adsorbed acid (2.11 g, 17%); ^1H NMR [400MHz, CDCl_3] δ -2.77 (2H, br s, NH), 7.76 (12H, m, Ar-3, 4,5-H), 8.23 (8H, d, $J^* = 8\text{Hz}$, Ar-2, 6-H), 8.85 (8H, s, βH); ^{13}C NMR [67.50 MHz, CDCl_3] δ 120.19, 126.73, 127.75, 131.14 (overlap), 134.60, 142.22; MS (MALDI-TOF) m/z 614.70 [calc'd for $\text{C}_{44}\text{H}_{30}\text{N}_4$, M^+ 614.75].

[19] 5,10,15,20- Tetra-(4-acetamidophenyl)porphyrin



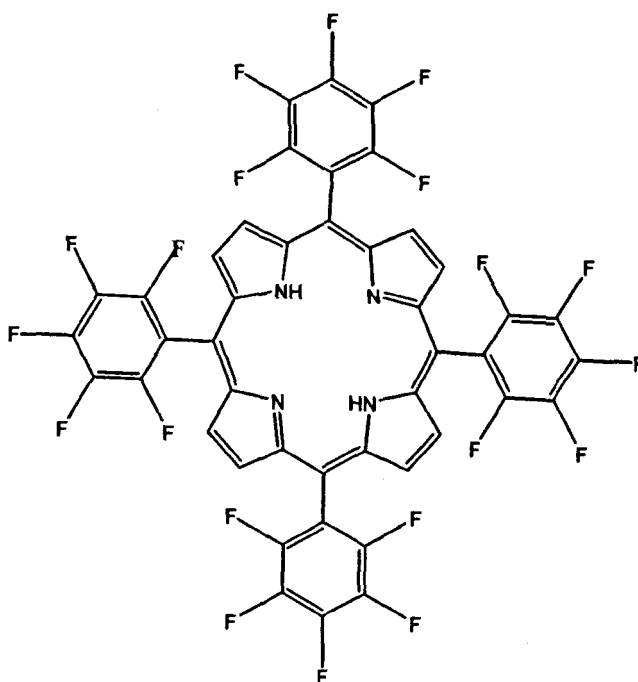
4-Acetamidobenzaldehyde (10 g, 0.06 mol) was dissolved in propionic acid (300 ml). Pyrrole (4.30 ml, 0.07 mol) was added and the mixture stirred under reflux for 30 min. After cooling, the solvent was removed *in vacuo* and the residual oil triturated thoroughly with methanol. The crude solid product was filtered and the mixture of porphyrin isomers purified by flash column chromatography (silica, eluent: CHCl₃/MeOH 19:1). Relevant fractions were combined and the solvent evaporated *in vacuo* to yield the product as a purple solid. (0.56 g, 5%); R_f = 0.8 (silica, CHCl₃/MeOH, 3:2); ¹H NMR [400 MHz, CDCl₃] δ -2.9(2H, br s, NH), 2.32 (12H, s, NHCOCH₃), 8.05 (8H, m, 10, 15, 20-Ar- 4, 6-H), 8.15 (8H, m, 5, 10, 15, 20-Ar-3, 5-H), 8.9 (8H, br s, βH), 10.4 (4H, br s, NHCOCH₃); UV-vis (CH₂Cl₂) λ_{max} 423, 456, 522, 556, 598,655 nm; MS (MALDI-TOF) m/z 843 [calc'd for C₅₂H₄₂O₄N₈, M⁺ 842.96].

[20] 5,10,15,20-Tetra-(4-pyridyl)porphyrin



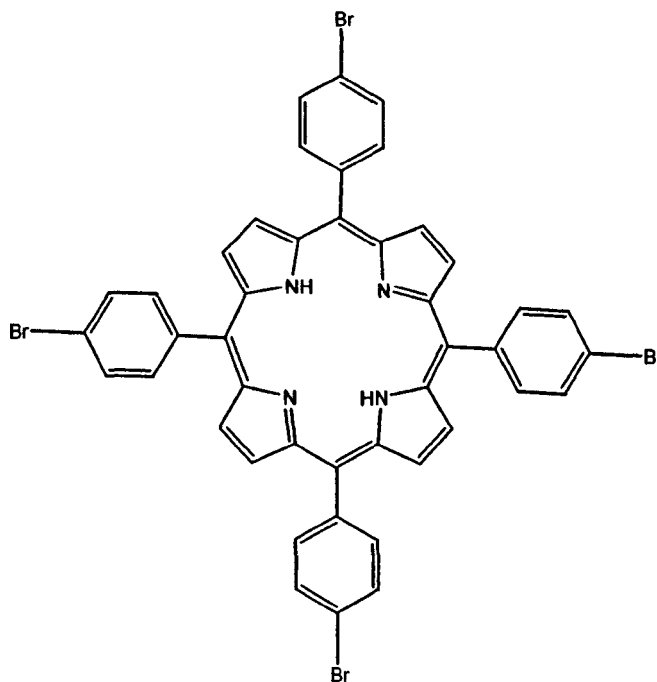
Pyridine-4-carboxyaldehyde (7.55 ml, 0.08 mol) was dissolved in propionic acid (300 ml) at 90 °C. Pyrrole (5.40 ml, 0.08 mol) was added and the mixture stirred under reflux for 30 min. Upon cooling the solvent was evaporated *in vacuo* and the residual oil was purified using flash column chromatography (silica, eluent: CHCl₃/ MeOH, 19:1). Relevant fractions were combined and the solvent evaporated *in vacuo* to yield the product as a purple solid. The product was recrystallised from (9:1) chloroform and methanol (0.60 g, 5%); R_f = 0.42 (silica, CHCl₃/ MeOH, 19:1); ¹H NMR [400 MHz, CDCl₃] δ -2.93 (2H, br s, NH), 8.17 (8H, m, Py-2, 6-H), 8.88 (8H, s, βH), 9.08 (8H, m, Py-3, 5-H); UV-vis (CH₂Cl₂) λ_{max} 416, 512, 545, 587, 642 nm; MS (MALDI-TOF) *m/z* 618 [calc'd for C₄₀H₂₆N₈, M⁺ 618.69].

[21] 5,10,15,20-Tetra-(pentafluorophenyl)porphyrin



Pentafluorobenzaldehyde (10 ml, 0.08 mol) was dissolved in propionic acid (300 ml). Pyrrole (5.60 ml, 0.08 mol) was added and the solution stirred under reflux for 30 min. After cooling, the solvent was removed *in vacuo* and the residual oil was triturated thoroughly with methanol. The resulting purple crystals were filtered, air dried and finally dried under vacuum to remove any adsorbed acid (0.70 g, 4%); R_f = 0.73 (silica, hexane); ¹H NMR [400 MHz, CDCl₃] δ -2.92 (2H, br s, NH), 8.92 (8H, s, βH); UV-vis (CH₂Cl₂) λ_{max} 412, 500, 583, 637, 656 nm; MS (MALDI-TOF) *m/z* 974.59 [calc'd for C₄₄H₁₀N₄F₂₀, M⁺ 974.56].

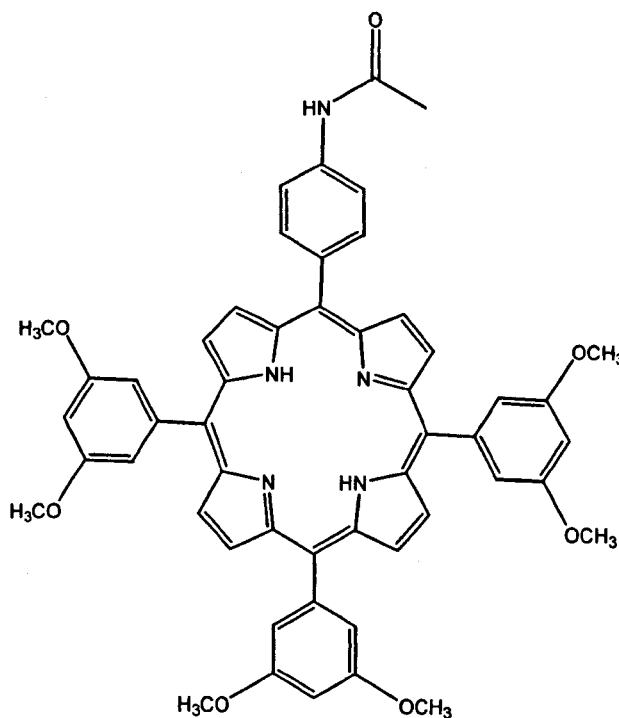
[22] 5,10,15,20-Tetra-(4-bromophenyl)porphyrin



4-Bromobenzaldehyde (16.96 g, 0.09 mol) was dissolved in propionic acid (300 ml). Pyrrole (6.40 ml, 0.09 mol) was added and the solution stirred under reflux for 30 min.

After cooling, the solution was filtered and the solid obtained was then triturated thoroughly with methanol. The resulting purple crystals were air dried and finally dried under vacuum to remove any adsorbed acid (4.44 g, 20%); $R_f = 0.88$ (silica, CHCl_3); ^1H NMR [400 MHz, CDCl_3] δ -2.88 (2H, br s, NH), 7.92 (8H, m, Ar-3, 5-H), 8.08 (8H, d, $J^* = 8\text{Hz}$, Ar-2, 6-H), 8.84 (8H, s, βH); ^{13}C NMR [67.5 MHz, CDCl_3] δ 77.52, 119.01, 122.67, 130.04, 131.32, 135.85, 140.84; MS (MALDI-TOF) m/z 930.42 [calc'd for $\text{C}_{44}\text{H}_{26}\text{N}_4\text{Br}_4$, M^+ 930.33].

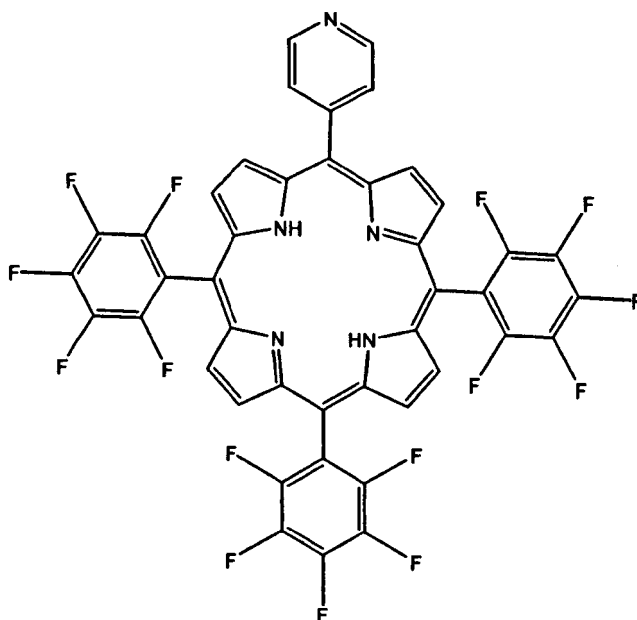
[23] 5-(4-Acetamidophenyl)-10,15,20-tris-(3,5-dimethoxyphenyl)porphyrin



4-Acetamidobenzaldehyde (5.04 g, 0.03 mol) and 3,5-dimethoxybenzaldehyde (15 ml, 0.09 mol) were stirred in propionic acid (450 ml) at 90 °C. Pyrrole (8.25 ml, 0.12 mol)

was then added and the mixture stirred under reflux for 30 min. Upon cooling the solvent was evaporated *in vacuo* to yield a dark purple solid. The crude mixture of porphyrin isomers was purified by flash column chromatography (silica, eluent: CH₂Cl₂/EtOAc, 4:1). Relevant fractions were combined and the solvent evaporated *in vacuo* to yield the product as a purple solid. (0.56g, 2%); R_f = 0.5 (silica, CH₂Cl₂/EtOAc, 4:1); ¹H NMR [400 MHz, CDCl₃] δ -2.80 (2H, br s, NH), 2.32 (3H, s, NHCOCH₃), 3.93 (18H, s, 3,5-OCH₃), 6.89 (3H, s, 10, 15, 20-Ar-4-H), 7.39 (6H, s, 10, 15, 20-Ar-2, 6-H), 7.85 (2H, d, *J** = 8 Hz, 5-Ar-3,5-H), 8.14 (2H, d, , *J** = 8 Hz, 5-Ar-2, 6-H), 8.84-8.94 (8H, m, βH), 9.17 (1H, br s, NHCOCH₃); MS (MALDI-TOF) *m/z* 852 [calc'd for C₅₂H₄₅O₇N₅, M⁺ 851.96].

[24] 5-(4-pyridyl)-10,15,20-tris-(pentafluorophenyl)porphyrin



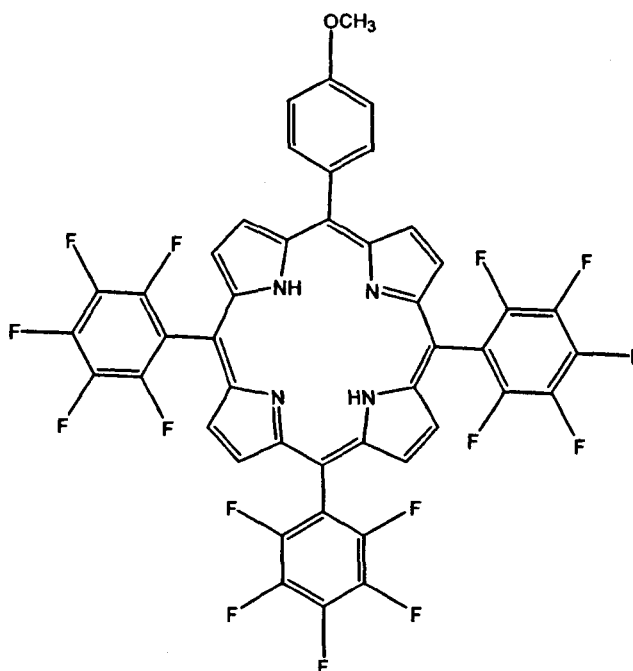
Pentafluorobenzaldehyde (3.70 ml, 0.03 mol) and pyridine-4-carboxyaldehyde (8.60 ml, 0.09 mol) were stirred in propionic acid (450 ml) at 90 °C. Pyrrole (8.25 ml, 0.12 mol) was then added and the mixture stirred under reflux for 30 min. Upon cooling the solvent was evaporated *in vacuo* and the crude product was dissolved in a minimal amount of dichloromethane. Silica (\approx 5 g) was added and the solvent evaporated *in vacuo* to yield the crude product adsorbed onto the silica. The mixture was purified using flash column chromatography (silica, eluent: CHCl₃/ MeOH, 19:1). The product was obtained as a purple solid which was recrystallised from (9:1) chloroform-methanol (0.60 g, 5%); R_f = 0.42 (silica, CH₂Cl₂); ¹H NMR [400 MHz, CDCl₃] δ -2.9 (2H, br s, NH), 8.25 (2H, m, Py-2, 6-H), 8.9 (8H, m, β H), 9.11 (2H, m, Py-3, 5-H); UV-vis (CH₂Cl₂) λ_{\max} 413, 508, 584, 638, 654 nm; MS (MALDI-TOF) *m/z* 885.70 calc'd for C₄₃H₁₄N₅F₁₅, M⁺ 885.5931]

[25] 5-(4-methoxyphenyl)-10,15,20-tris-(pentafluorophenyl)porphyrin and

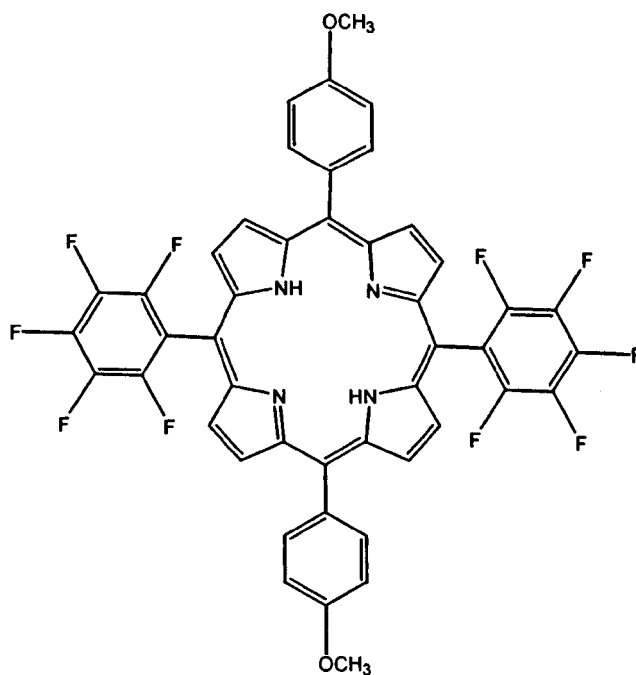
[26] 5, 15-di-(4-methoxyphenyl)-10,20-di-(pentafluorophenyl)porphyrin and

[27] 5-(pentafluorophenyl)-10,15,20-tris-(4-methoxyphenyl)porphyrin and

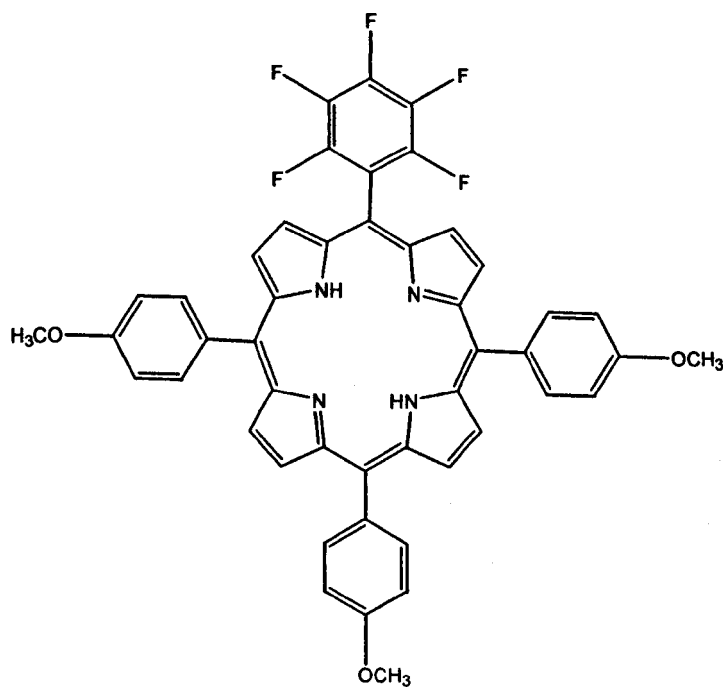
[28] 5,10,15,20-tetrakis-(4-methoxyphenyl)porphyrin



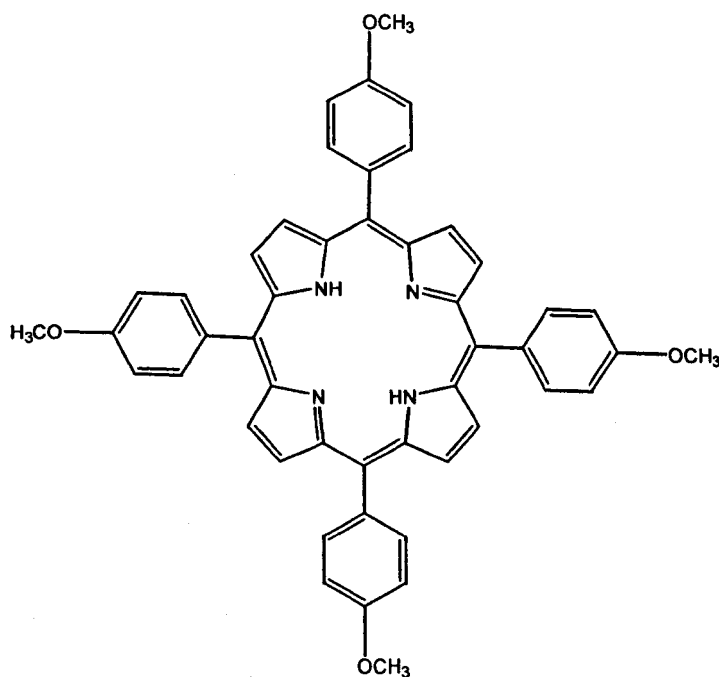
5-(4-methoxyphenyl)-10, 15, 20-tris-(pentafluorophenyl)porphyrin



5, 15-(4-methoxyphenyl)-10, 20-tris-(pentafluorophenyl)porphyrin



5-(pentafluorophenyl)-10, 15, 20-tris-(4-methoxyphenyl)porphyrin



5, 10, 15, 20-tetrakis-(4-methoxyphenyl)porphyrin

Pentafluorobenzaldehyde (6.20 ml, 0.05 mol) and 4-methoxybenzaldehyde (18.3 ml, 0.15 mol) were dissolved in propionic acid (250 ml) at 90 °C. Pyrrole (14 ml, 0.20 mol) was added and the solution stirred under reflux for 30 min. After cooling, the mixture was filtered and the purple crystals obtained were dried *in vacuo*. Following adsorption onto silica gel (5 g), purification by flash column chromatography was carried out (silica, eluent: CH₂Cl₂/ hexane, 1:1). Four fractions were obtained, the first being 5-(4-methoxyphenyl)-10, 15, 20-tris-(pentafluorophenyl)porphyrin which had R_f = 0.8. The next fraction was 5, 15-(4-methoxyphenyl)-10, 20-tris-(pentafluorophenyl)porphyrin, R_f = 0.6, followed by 5-(pentafluorophenyl)-10, 15, 20-tris-(4-methoxyphenyl)porphyrin, R_f = 0.4, and finally 5, 10, 15, 20-tetrakis-(4-methoxyphenyl)porphyrin R_f = 0.1. Concentration of the first fraction yielded a purple crystalline solid (0.03 g, 0.07%); ¹H

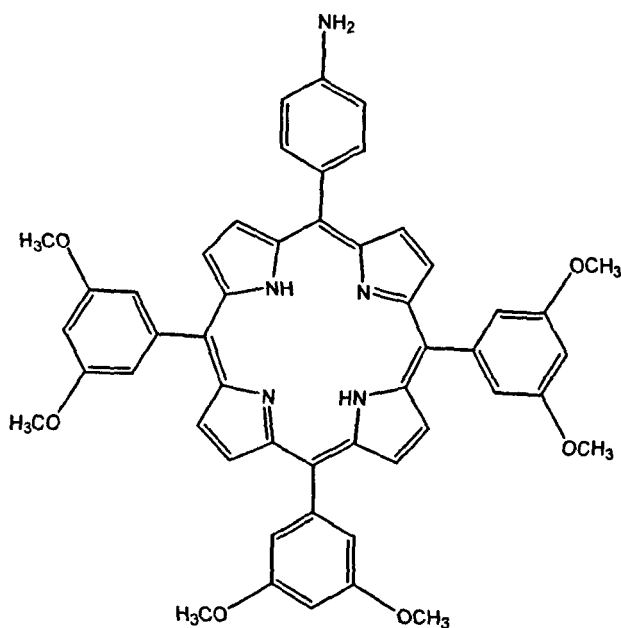
NMR [400 MHz, CDCl₃] δ -2.83 (2H, br s, NH), 4.12 (3H, s, CH₃), 7.34 (2H, d, $J^* = 9\text{Hz}$, 2, 6-Ar-H), 8.14 (2H, d, $J^* = 9\text{Hz}$, 3, 5-Ar-H), 8.81 (2H, m, βH), 8.9 (4H, m, βH), 9.01 (2H, m, βH); UV-vis (CH₂Cl₂) λ_{max} 412, 510, 542, 638, 654 nm; MS (MALDI-TOF) m/z 916.69 [calc'd for C₄₅H₁₇N₄F₁₅O, M⁺ 914.63].

Concentration of the second fraction yielded a purple crystalline solid (0.13 g, 0.30%); ¹H NMR [400 MHz, CDCl₃] δ -2.74 (2H, br s, NH), 4.11 (6H, s, CH₃), 7.32 (4H, d, $J^* = 9\text{Hz}$, 2, 6-Ar-H), 8.13 (4H, d, $J^* = 9\text{Hz}$, 3, 5-Ar-H), 8.76 (2H, m, βH), 8.84 (2H, s, βH), 8.89 (2H, s, βH), 8.98 (2H, m, βH); UV-vis (CH₂Cl₂) λ_{max} 420, 514, 548, 590, 650 nm; MS (MALDI-TOF) m/z 855.6 [calc'd for C₄₆H₂₄N₄F₁₀O₂, M⁺ 854.7052].

Concentration of the third fraction yielded a purple crystalline solid (0.51 g, 1.30%); ¹H NMR [400 MHz, CDCl₃] δ -2.73 (2H, br s, NH), 4.10 (9H, s, CH₃), 7.31 (6H, d, $J^* = 9\text{Hz}$, 2, 6-Ar-H), 8.13 (6H, d, $J^* = 9\text{Hz}$, 3, 5-Ar-H), 8.75 (2H, m, βH), 8.89 (4H, m, βH), 8.96 (2H, m, βH); UV-vis (CH₂Cl₂) λ_{max} 419, 516, 553, 591, 649 nm; MS (MALDI-TOF) m/z 795.6 [calc'd for C₄₇H₃₁N₄F₅O₃, M⁺ 794.7789].

Concentration of the final fraction yielded a purple crystalline solid (2.56 g, 7%); ¹H NMR [400 MHz, CDCl₃] δ -2.75 (2H, br s, NH), 4.09 (12H, s, CH₃), 7.30 (8H, d, $J^* = 9\text{Hz}$, 2, 6-Ar-H,), 8.11 (8H, d, $J^* = 9\text{Hz}$, 3, 5-Ar-H,), 8.86 (8H, m, βH); UV-vis (CH₂Cl₂) λ_{max} 422, 518, 554, 592, 650 nm; MS (MALDI-TOF) m/z 734 [calc'd for C₄₈H₃₈N₄O₄, M⁺ 914.6315].

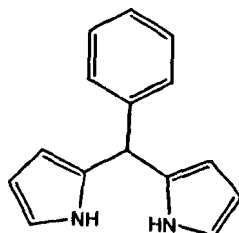
[29] 5-(4-Aminophenyl)-10,15,20-tris-(3,5-dimethoxyphenyl)porphyrin



5-(4-Acetamidophenyl)-10,15,20-tris-(3,5-dimethoxyphenyl)porphyrin (500 mg, 0.59 mmol) was dissolved in 18% HCl (100 ml) and the solution heated for two hours under reflux. Upon cooling the solvent was evaporated *in vacuo* to yield a green solid. The solid was redissolved in a 9:1 mixture of dichloromethane / triethylamine (200 ml) and stirred for 10 min at room temperature. The solution was then washed with water (3 × 200 ml) and brine (200 ml), the organic layer separated and dried (Na₂SO₄). The solvent was evaporated *in vacuo* and the crude purple solid purified by flash column chromatography (silica, eluent: CH₂Cl₂/EtOAc, 4:1). Relevant fractions were combined and the solvent evaporated *in vacuo* to yield the product as a purple solid. (0.48 g, 91%); R_f = 0.86 (silica, CH₂Cl₂/EtOAc, 4:1); ¹H NMR [400 MHz, CDCl₃] δ -2.20 (2H, br s, NH), 3.96 (18H, s, 3,5-OCH₃), 6.90 (3H, s, 10, 15, 20-Ar-4-H), 7.06 (2H, d, J* = 8 Hz, 5-

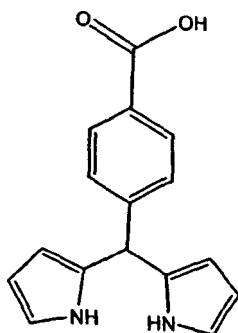
Ar-3, 5-H), 7.40 (6H, s, 10, 15, 20-Ar- 2, 6-H), 7.99 (2H, d, $J^* = 8$ Hz, 5-Ar-2, 6-H), 8.92 (8H, m, β H); UV-vis (CH_2Cl_2) λ_{max} 442, 517, 583, 593, 651 nm; MS (MALDI-TOF) m/z 809 [calc'd for $\text{C}_{50}\text{H}_{43}\text{O}_6\text{N}_5$, M^+ 809.92].

[30] 5-Phenyldipyrromethane



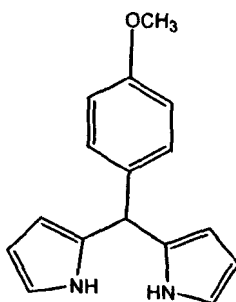
To freshly distilled pyrrole (150 ml, 2.16 mol) was added benzaldehyde (6 ml, 0.06 mol). The reaction mixture deoxygenated by bubbling argon through a stirred solution for 15 min. Trifluoroacetic acid (0.45 ml, 0.06 mol) was added and then the mixture stirred under argon for 15 min at ambient temperature. Excess pyrrole was removed *in vacuo* to yield dark tan oil. The oil was dissolved in a minimum amount of dichloromethane and purified by flash column chromatography (silica, eluent: hexane/ CH_2Cl_2 , 1:4). Relevant fractions (visualised by bromine vapour) were combined and the solvent removed *in vacuo* to yield the product as a grey solid (3.30 g, 25%); $R_f = 0.26$ (silica, eluent: hexane/ CH_2Cl_2 , 2:8); mp = 98-102 °C; ^1H NMR [400 MHz, CDCl_3] δ 5.42 (1H, s, 5-H), 5.89 (2H, m, 3-H), 6.15 (2H, m, 2-H), 6.64 (2H, m, 1-H), 7.18-7.32 (5H, m, Ar-H), 7.82 (2H, br s, NH); ^{13}C NMR [67.50 MHz, CDCl_3] δ 43.43, 107.37, 108.53, 117.81, 127.10, 128.53, 128.76, 132.44, 142.2; MS (MALDI-TOF) m/z 222.15 [calc'd for $\text{C}_{15}\text{H}_{14}\text{N}_2$, M^+ 222.12].

[31] 5-(4-Carboxyphenyl)dipyrromethane



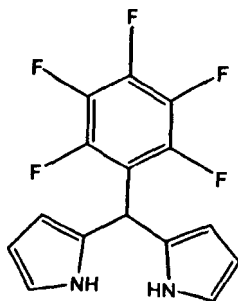
To freshly distilled pyrrole (100 ml, 1.44 mol) was added 4-carboxybenzaldehyde (5 g, 0.03 mol). The reaction mixture was deoxygenated by bubbling argon through the stirred solution for 15 min. Trifluoroacetic acid (0.23 ml, 0.03 mol) was added and the mixture stirred under argon for 15 min at ambient temperature. The solvent was removed *in vacuo* to yield pale brown oil which was dissolved into minimum amount of chloroform and 25% ethyl acetate and purified by flash column chromatography (silica, eluent: EtOAc/CH₃Cl, 1:3). Relevant fractions (visualised by bromine vapour) were concentrated *in vacuo* to yield the product as a beige solid (3.3 g, 38%); R_f = 0.05 (silica, eluent: EtOAc/CH₃Cl, 1:3); mp = 164-165 °C; ¹H NMR [400 MHz, CDCl₃] δ 5.52 (1H, s, 5-H), 5.81 (2H, m, 3-H), 6.05 (2H, m, 2-H), 6.68 (2H, m, 1-H), 7.27 (2H, d, *J** = 8.2 Hz, Ar-2, 6-H), 7.94 (2H, d, *J** = 8.2 Hz, Ar-3, 5-H), 9.17 (2H, br s, NH), 11.97 (1H, br s, COOH); MS (MALDI-TOF) *m/z* 266 [calc'd for C₁₆H₁₄O₂N₂, M⁺ 266.30].

[32] 5-(4-Methoxyphenyl)dipyrromethane



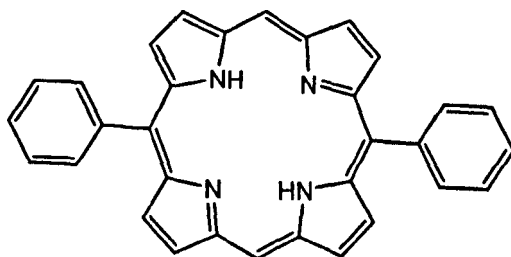
To freshly distilled pyrrole (150 ml, 2.16 mol) was added 4-methoxybenzaldehyde (9 g, 0.06 mol). The reaction mixture was deoxygenated by bubbling argon through the stirred solution for 15 min. Trifluoroacetic acid (0.45 ml, 0.06 mol) was then added and the mixture stirred under argon for a further 15 min at ambient temperature. The solvent was evaporated *in vacuo* to yield dark tan oil. The oil was purified by flash column chromatography (silica, eluent: hexane/CH₂Cl₂, 2:8). Relevant fractions (visualised by bromine vapour) were combined and concentrated *in vacuo* to yield the product as a grey solid (3.30 g, 25%); R_f = 0.26 (silica, eluent: CH₂Cl₂); mp > 138-140 °C ; ¹H NMR [400 MHz, CDCl₃] δ 3.80 (3H, s, OCH₃), 5.42 (1H, s, 5-H), 5.90 (2H, m, 3-H), 6.17 (2H, m, 2-H), 6.69 (2H, m, 1-H), 6.87 (2H, d, *J** = 8.6Hz, Ar-2, 6-H), 7.14 (2H, d, *J** = 8.6Hz, Ar-3, 5-H), 7.9 (2H, br s, NH); MS (MALDI-TOF) *m/z* 252 [calc'd for C₁₆H₁₆ON₂, M⁺ 252.32].

[33] 5-(Pentafluorophenyl)dipyrromethane



To freshly distilled pyrrole (150 ml, 2.16 mol) was added pentafluorobenzaldehyde (7.28 ml, 0.06 mol). The reaction mixture was stirred at room temperature and deoxygenated by bubbling nitrogen through the solution for 15 min. Trifluoroacetic acid (0.45 ml, 0.06 mol) was then added and the mixture stirred, under nitrogen for 15 min at ambient temperature. The solvent was evaporated *in vacuo* to yield dark brown oil. The oil was then purified using flash column chromatography (silica, eluent: CH₂Cl₂). The desired fractions (visualised by bromine vapour on TLC) were combined and concentrated *in vacuo* to yield the product as a pale beige solid (11.07 g, 60%); R_f = 0.68 (silica, CH₂Cl₂); mp 134 °C; ¹H NMR [400 MHz, CDCl₃] 5.77 (1H, s, 5-H), 5.79 (2H, m, 3-H), 5.94 (2H, m, 2-H), 6.65 (2H, m, 1-H), 10.7 (2H, br s, NH); MS (MALDI-TOF) *m/z* 312 [calc'd for C₁₅H₉N₂F₅, M⁺ 312.24].

[34] 5,15-Diphenylporphyrin

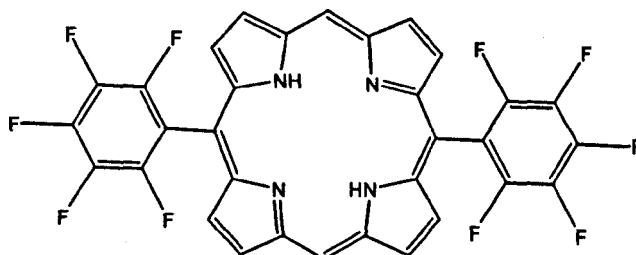


To a solution of 5-phenyldipyrromethane (0.50 g, 2.30 mmol) in dichloromethane (630 ml) was added trimethylorthoformate (18 ml, 0.17 mol). Trichloroacetic acid (8.83 g, 54 mmol) in dichloromethane (230 ml) was then added drop wise over a period of 15 min. After complete addition of the acid, the reaction was stirred under argon and protected from light for 4 hours at room temperature. The reaction was quenched by the addition of pyridine (15.60 ml) and the mixture stirred under argon and protected from light for a further 17 hours at room temperature. The solution was purged with compressed air for 10 min and then stirred open to air and light for 4 hours at room temperature. The solvent was removed *in vacuo* to yield a black solid which was purified using flash column chromatography (silica, eluent: hexane/CH₂Cl₂, 1:9). Relevant fractions were combined and the solvent evaporated *in vacuo* to yield the product as purple crystalline solid (0.06 g, 12%); ¹H NMR [400 MHz, CDCl₃] δ - 3.12 (2H, br s, NH), 7.81 (6H, m, Ar-3,4,5-H), 8.29 (4H, m, Ar-2,6-H), 9.10 (4H, d, *J** = 5 Hz, βH), 9.41 (4H, d, *J** = 5 Hz, βH), 10.33 (2H, s, 10, 20-H); ¹³C NMR [67.50 MHz, CDCl₃] δ 105.30, 119.10, 127.00, 127.80, 131.10, 131.70, 134.90, 141.40, 145.30, 147.20; MS (MALDI-TOF) *m/z* 462 [calc'd for C₃₂H₂₂N₄, M⁺ 462.18].

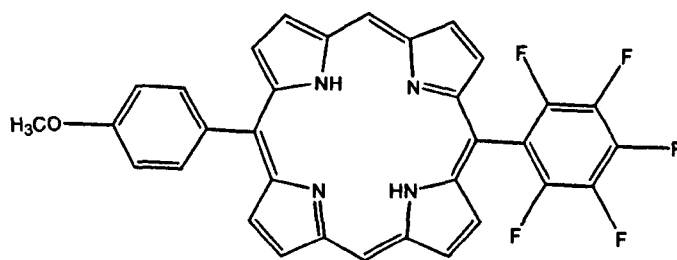
[35] 5,15- Di-(pentafluorophenyl)porphyrin and

[36] 5-pentafluorophenyl-15-(4-methoxyphenyl)porphyrin and

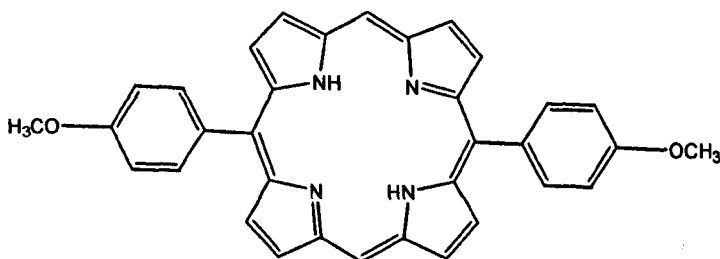
[37] 5,15-di-(4-methoxyphenyl)porphyrin



5, 15- di(pentafluorophenyl)porphyrin



5-pentafluorophenyl-15-(4-methoxyphenyl)porphyrin



5, 15-di-(4-methoxyphenyl)porphyrin

To a solution of 5-(4-methoxyphenyl)dipyrromethane (0.96 g, 3.8 mmol) and 5-(pentafluorophenyl)dipyrromethane (1.2g, 3.8 mmol) in dichloromethane (2000 ml) was

added trimethylorthoformate (57 ml, 527 mmol). Trichloroacetic acid (28 g, 171 mmol) in dichloromethane (700 ml) was then added drop wise over a period of 30 min. After complete addition of the acid, the reaction was stirred under argon and protected from light for 4 hours at room temperature. The reaction was quenched by the addition of pyridine (50 ml) and stirred under argon and protected from light for a further 17 hours at room temperature. The solution was purged with compressed air for 10 min and then stirred open to air and light for 4 hours at room temperature. The solvent was removed *in vacuo* to yield a black solid. The crude product was purified using flash column chromatography (silica, eluent: hexane/CH₂Cl₂, 1:2). Three different porphyrins were obtained and relevant fractions were combined and evaporated *in vacuo* to yield the products as purple crystalline solids.

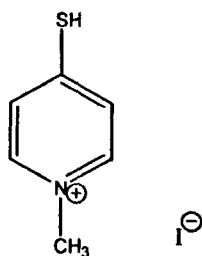
The first fraction was 5, 15- di(pentafluorophenyl)porphyrin Rf = 0.88 (silica, eluent: hexane/CH₂Cl₂, 1:2); (0.01 g, 0.5%); ¹H NMR [400 MHz, CDCl₃] δ -3.01 (2H, br s, NH), 9.02 (4H, m, βH), 9.50 (4H, m, βH), 10.40 (2H, br s, 10,20-H); MS (MALDI-TOF) *m/z* 642.43 [calc'd for C₃₂H₁₂N₄F₁₀, M⁺ 642.46].

The second fraction was 5-pentafluorophenyl-15-(4-methoxyphenyl)porphyrin Rf = 0.82 (silica, eluent: hexane/CH₂Cl₂, 1:2); (0.01 g, 0.6%); ¹H NMR [400 MHz, CDCl₃] δ -3.1 (2H, br s, NH), 4.14 (3H, br s, OCH₃), 7.38 (2H, m, Ar-3, 5-H), 8.2 (2H, m, Ar-2, 6-H), 9.02 (4H, m, βH), 9.49 (4H, m, βH), 10.34 (2H, br s, 10,20-H); MS (MALDI-TOF) *m/z* 582.46 [calc'd for C₃₃H₁₉N₄O F₅, M⁺ 582.53].

The final fraction was 5, 15-di-(4-methoxyphenyl)porphyrin Rf = 0.7 (silica, eluent:

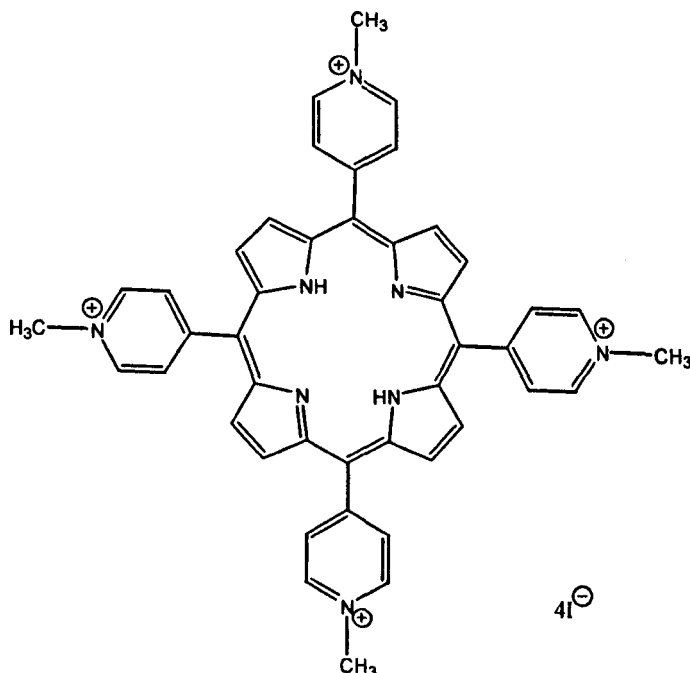
hexane/CH₂Cl₂, 1:2); (0.03 g, 1.6%); ¹H NMR [400 MHz, CDCl₃] δ -3.1 (2H, br s, NH), 4.13 (6H, br s, OCH₃), 7.37 (4H, m, Ar-3, 5-H), 8.2 (4H, m, Ar-2, 6-H), 9.12 (4H, m, βH), 9.40 (4H, m, βH), 10.31 (2H, br s, 10,20-H); MS (MALDI-TOF) *m/z* 522.52 [calc'd for C₃₄H₂₆N₄O₂, M⁺ 522.605].

[38] N-Methyl-4-mercaptopyridinium iodide



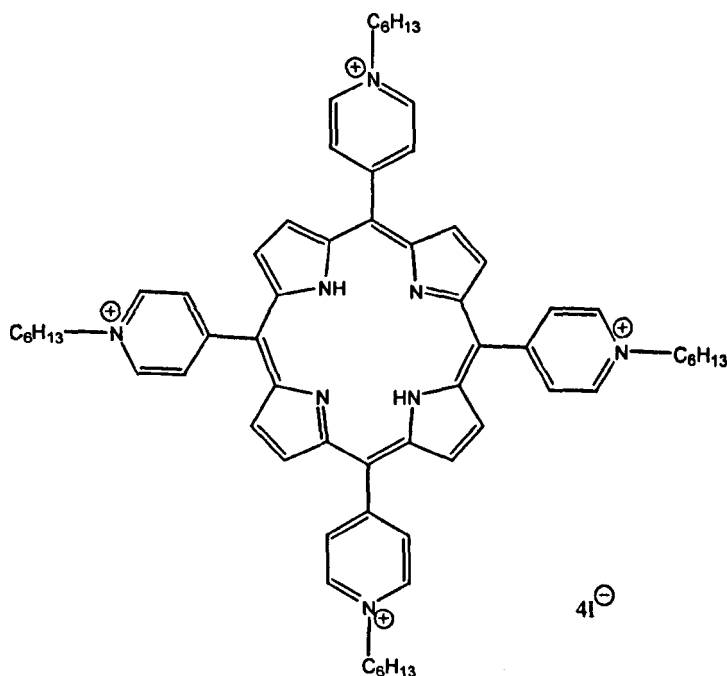
4-Mercaptopyridine (0.10 g, 9×10^{-4} mol) was added to anhydrous DMF (10 ml) and iodomethane (0.05 ml, 9×10^{-4} mol) was added. The mixture was stirred for 48 hours under argon and protected from light at ambient temperature. The solvent was evaporated *in vacuo* to yield the product as a beige solid (0.08 g, 35 %). R_f = 0.76 (silica, eluent: water/potassium nitrate/acetonitrile, 1:1:8); ¹H NMR [400 MHz, CDCl₃] δ 2.17 (1H, s, S-H), 4.4 (3H, s, CH₃), 7.76 (2H, d, *J** = 7 Hz, Ar- 2, 6-H), 8.47 (2H, d, *J** = 7 Hz, Ar- 3, 5-H); MS (MALDI-TOF) *m/z* 127 [calc'd for C₆H₈NS, M⁺ 126.20]

[39] 5,10,15,20-Tetra-(4-N-methylpyridiniumyl)porphyrin tetraiodide



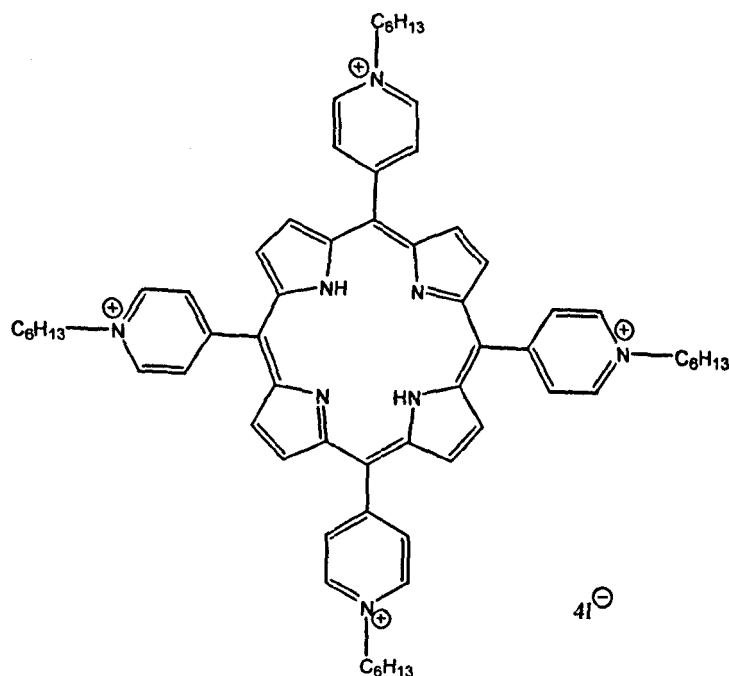
5,10,15,20-Tetra-(4-pyridyl)porphyrin (100 mg, 0.16 mmol) was dissolved in warm DMF (5 ml). Iodomethane (2 ml, 0.03 moles) was added and the mixture stirred under argon and protected from light for 24 hours at room temperature. The solvent was evaporated *in vacuo* to yield a purple solid (0.04 g, 20%); *R_f* = 0.13 (silica, eluent: water/potassium nitrate/acetonitrile, 1:1:8); ¹H NMR [400 MHz, CDCl₃] δ -3.10 (2H, br s, NH), 4.71 (12h, br s, N-CH₃), 8.99 (8H, m, Py-2, 6-H), 9.18 (8H, s, βH), 9.48 (8H, m, Py-3, 5-H); UV-vis (CH₂Cl₂) λ_{max} 416, 519, 550, 627, 660 nm; MS (MALDI-TOF) *m/z* 678 [calc'd for C₄₄H₃₈N₈, M⁺ 678.84].

[40] 5,10,15,20-Tetra-(4-N-hexylpyridiniumyl)porphyrin tetraiodide



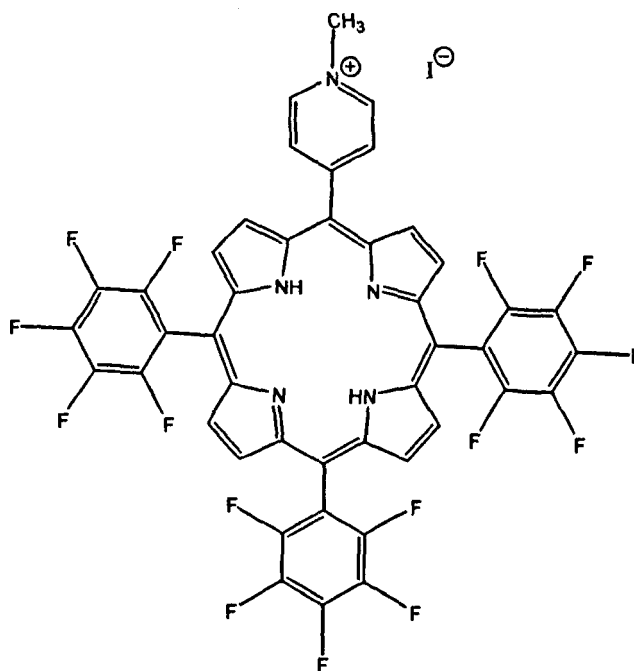
5,10,15,20-Tetra-(4-pyridyl)porphyrin (136 mg, 0.22 mmol) was dissolved in warm DMF (10 ml). Iodohexane (6.50 ml, 0.04 moles) was added and the mixture stirred under argon and protected from light for 24 hours at room temperature. The solvent was evaporated *in vacuo* to yield a purple solid (0.48 g, 150%); $R_f = 0.78$ (silica, eluent: water/potassium nitrate/acetonitrile, 1:1:8); $^1\text{H NMR}$ [400 MHz, CDCl_3] δ -3.09 (2H, br s, NH), 0.99 (3H, m, CH_3), 1.49 (4H, m, CH_2CH_2), 1.62 (2H, m, CH_2), 2.29 (2H, m, CH_2), 4.96 (2H, m, N- CH_2), 9.03 (8H, m, Py-2, 6-H), 9.23 (8H, s, βH), 9.58 (8H, m, Py-3, 5-H); UV-vis (CH_2Cl_2) λ_{max} 445, 528, 599, 653 nm; MS (MALDI-TOF) m/z 959.01 [calc'd for $\text{C}_{64}\text{H}_{78}\text{N}_8$, M^+ 959.39].

[41] 5,10,15,20-Tetra-(4-N-hexylpyridinium)porphyrin tetraiodide



5,10,15,20-Tetra-(4-pyridyl)porphyrin (136 mg, 0.22 mmol) was dissolved in warm DMF (10 ml). Iodohexane (6.50 ml, 0.04 moles) was added and the mixture stirred under argon and protected from light for 24 hours at room temperature. The solvent was evaporated *in vacuo* to yield a purple solid (0.48 g, 150%); $R_f = 0.78$ (silica, eluent: water/potassium nitrate/acetonitrile, 1:1:8); $^1\text{H NMR}$ [400 MHz, CDCl_3] δ -3.09 (2H, br s, NH), 0.99 (3H, m, CH_3), 1.49 (4H, m, CH_2CH_2), 1.62 (2H, m, CH_2), 2.29 (2H, m, CH_2), 4.96 (2H, m, N- CH_2), 9.03 (8H, m, Py-2, 6-H), 9.23 (8H, s, βH), 9.58 (8H, m, Py-3, 5-H); UV-vis (CH_2Cl_2) λ_{max} 445, 528, 599, 653 nm; MS (MALDI-TOF) m/z 959.01 [calc'd for $\text{C}_{64}\text{H}_{78}\text{N}_8$, M^+ 959.39].

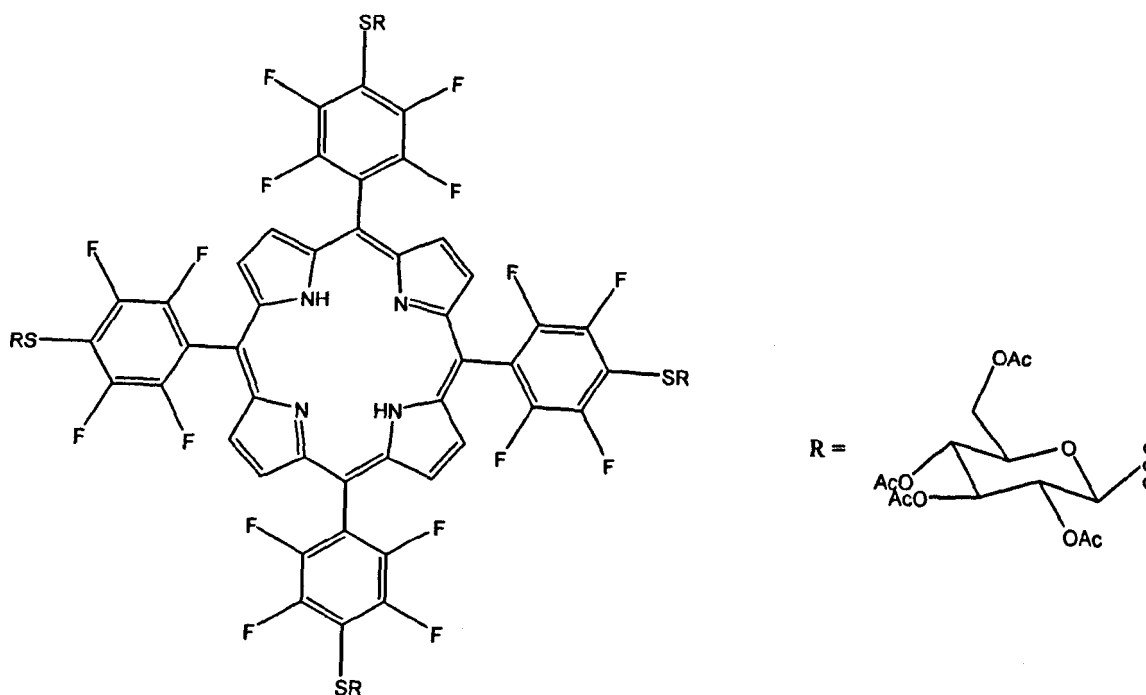
[42] 5-(4-N-Methylpyridiniumyl)-10,15,20-tris-(pentafluorophenyl)porphyrin iodide



5-(4-Pyridyl)10,15,20-tris-(pentafluorophenyl)porphyrin (20 mg, 2.3×10^{-5} mol) was dissolved in warm anhydrous DMF (5 ml). Iodomethane (0.5 ml, 0.01 moles) was added and the mixture stirred for 24 hours at room temperature, under argon and protected from light. The solvent was evaporated *in vacuo* to yield a purple solid (0.01 g, 38 %); Rf = 0.13 (silica, eluent: water/potassium nitrate/acetonitrile, 1:1:8); $^1\text{H NMR}$ [400 MHz, CDCl_3] δ -2.94 (2H, br s, NH), 4.69 (3H, br s, N-CH₃), 8.22 (8H, m, Py-2, 6-H), 8.30 (2H, m, Py-3, 5-H), 8.87 (2H, m, βH), 9.01 (2H, m, βH), 9.10 (2H, m, βH), 9.4 (2H, m, βH); UV-vis (CH_2Cl_2) λ_{max} 416, 520, 552, 625, 662 nm; MS (MALDI-TOF) m/z 900.67 [calc'd for $[\text{C}_{44}\text{H}_{17}\text{N}_5\text{F}_{15}]$, M^+ 900.63].

[43] 5,10,15,20-tetrakis[4-(2', 3', 4', 6'-tetra-*O*-acetyl- β -D-glucopyranosylthio)-2,3,

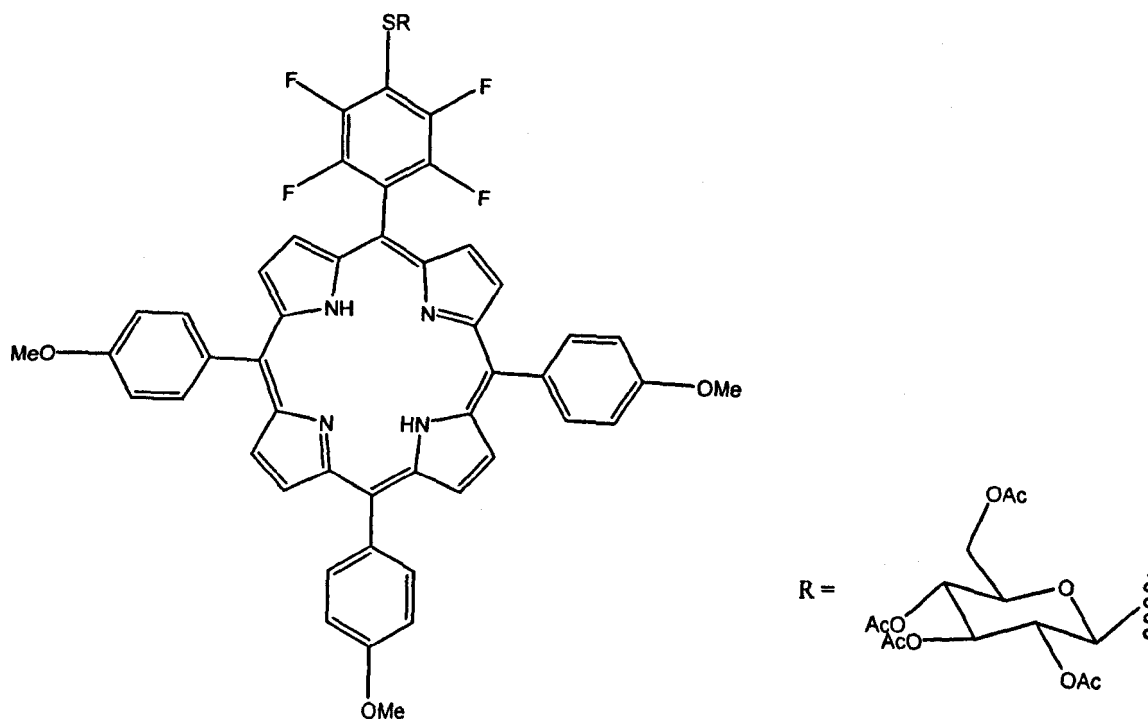
5,6-tetrafluorophenyl]porphyrin



5,10,15,20-Tetra(pentafluorophenyl)porphyrin (20 mg, 2.05×10^{-5} mol) was dissolved in anhydrous DMF (3 ml). 2,3,4,6-Tetra-*O*-acetyl- β -D-thioglucopyranose (6 eq, 44 mg, 1.23×10^{-4} mol) in DMF (3 ml) was added. The solution was stirred at room temperature and the reaction monitored by TLC. After 18 hours, the solvent was evaporated *in vacuo*, followed by separation using preparative TLC (silica eluent: toluene/acetone, 8:2) to yield the desired product as a purple brown solid (25 mg, 52 %); $R_f = 0.24$ (silica, eluent: toluene/acetone, 8:2); mp > 350 °C decomp; $^1\text{H NMR}$ [400 MHz, CDCl_3] δ -2.86 (2H, br s, NH), 2.08 (12H, s, OAc), 2.09 (12H, s, OAc), 2.10 (12H, s, OAc), 2.24 (12H, s, OAc), 3.92 (4H, m, H-5'ose), 4.32 (8H, d, $J^* = 3.1$ Hz, H-6_a' and H-6_b' ose), 5.20 (4H, t, $J^* =$

10.1 Hz, H-4'ose), 5.26 (8H, m, H-1', 2' ose), 5.38 (4H, t, $J^* = 9.3$ Hz, H-3'ose), 9.03 (8H, br s, β H); ^{13}C NMR [100.5 MHz, CDCl_3] δ 20.7, 61.9, 68.1, 70.7, 73.9, 76.5, 84.5, 104.3, 111.9, 122.1, 131.3, 145.1, 145.8, 147.6, 148.3, 169.4, 170.2, 170.7; UV-vis (CH_2Cl_2) λ_{max} 415, 508, 538, 584 and 658 nm; MS (MALDI-TOF) m/z 2353 [calc'd for $\text{C}_{100}\text{H}_{86}\text{N}_4\text{F}_{16}\text{S}_4\text{O}_{36}$, M^+ 2352]

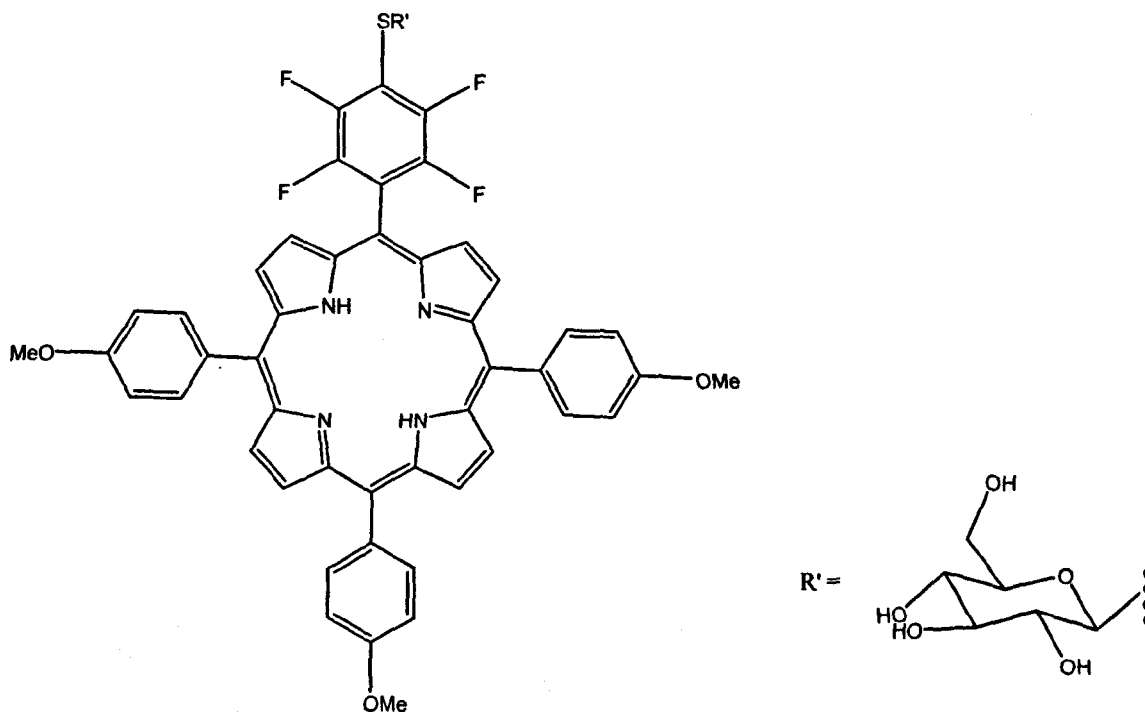
[44] 5-[4-(2', 3', 4', 6'-tetra-*O*-acetyl- β -D-glucopyranosylthio)-2,3,5,6-tetrafluorophenyl]-10,15,20-tris-(4-methoxyphenyl)porphyrin



5-(Pentafluorophenyl)-10,15,20-tris(4-methoxyphenyl)porphyrin (20 mg, 2.5×10^{-5} mol) was dissolved in anhydrous DMF (3 ml). 2,3,4,6-Tetra-*O*-acetyl- β -D-thioglucopyranose (1.5 eq, 13 mg, 3.77×10^{-5} mol) in DMF (3 ml) was added. The solution was stirred at room temperature and the reaction monitored by TLC. After 18 hours, the solvent was

evaporated in *vacuo*, followed by separation using preparative TLC (silica eluent: CH₂Cl₂) to yield the desired product as a purple brown solid (27 mg, 94 %); R_f = 0.61 (silica eluent: CH₂Cl₂); mp > 350 °C decomp; ¹H NMR [400 MHz, CDCl₃] δ -2.71 (2H, br s, NH), 2.07 (3H, s, OAc), 2.08 (3H, s, OAc), 2.09 (3H, s, OAc), 2.22 (3H, s, OAc), 3.89 (1H, m, H-5'ose), 4.07 (3H, s, O-CH₃), 4.30 (2H, m, H-6_a' and H-6_b' ose), 5.12 (1H, t, *J** = 9.8 Hz, H-4'ose), 5.23 (2H, m, H-1', 2' ose), 5.36 (1H, t, *J** = 9.2 Hz, H-3'ose), 7.28 (6H, dd, *J** = 8.4 and 4.0 Hz, H-2,6-methoxyphenyl), 8.11 (6H, dd, *J** = 8.7 and 3.9 Hz, H-3, 5-methoxyphenyl), 8.82 (2H, d, *J** = 4.8 Hz, βH), 8.85 (2H, d, *J** = 4.8 Hz, βH), 8.86 (2H, d, *J** = 4.8 Hz, βH), 8.96 (2H, d, *J** = 4.8 Hz, βH); ¹³C NMR [100.5 MHz, CDCl₃] δ 20.7, 29.7, 30.0, 30.2, 55.6, 112.3, 112.4, 122.1, 135.6, 159.6, 169.4, 161.7, 170.7; UV-vis (CH₂Cl₂) λ_{max} 422, 517, 553, 591 and 648 nm; MS (MALDI-TOF) *m/z* 1140 [calc'd for C₆₁H₅₀N₄F₄SO₁₂, M⁺ 1139.14].

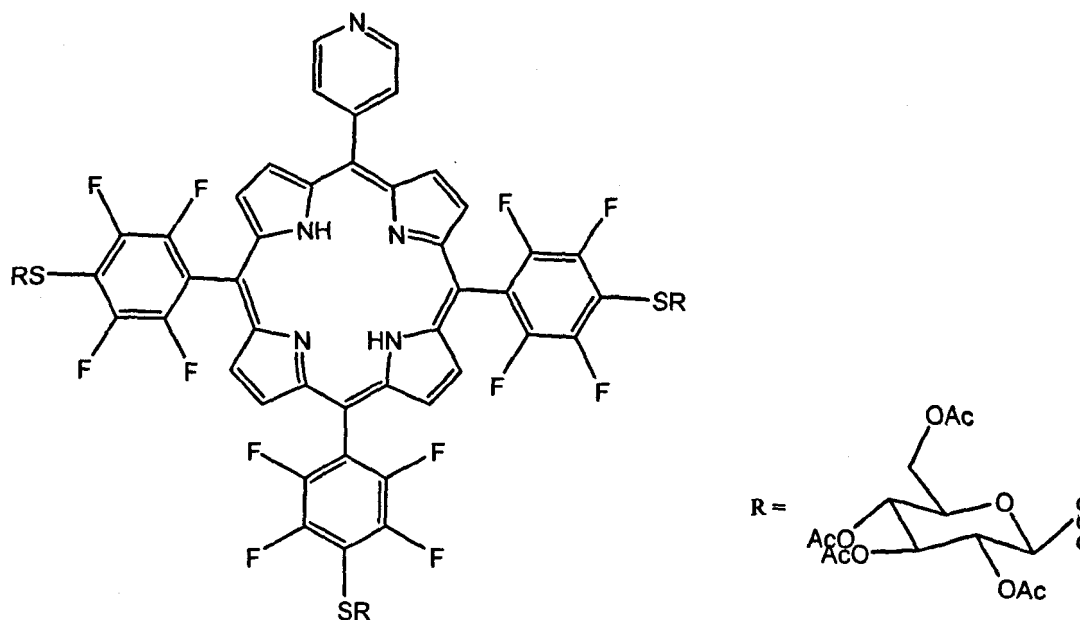
[45] 5-[4-(β-D-Glucopyranosylthio)-2,3,5,6-tetrafluorophenyl]-10,15,20-tris-(4-methoxyphenyl)porphyrin



5-[4-(2',3',4',6'-Tetra-*O*-acetyl-β-D-glucopyranosylthio)-2,3,5,6-tetrafluorophenyl]-10, 15,20-tris-(4-methoxyphenyl)porphyrin (30 mg, 2.6×10^{-5} mol) was dissolved in a mixture of [dichloromethane/methanol, 7:3] (3 ml) and sodium methoxide 0.5M solution in methanol (1.5 eq/OAc) was added. The mixture was stirred for an hour at 20 °C and the porphyrin was precipitated by the addition of hexane and filtered, giving a purple solid (23 mg, 92 %); $R_f = 0.32$ (silica eluent: methanol/ CH_2Cl_2 , 1:9); mp > 350 °C decomp; $^1\text{H NMR}$ [400 MHz, CDCl_3] δ -2.72 (2H, br s, NH), 3.51 (1H, m, H-ose), 3.81 (1H, m, H-ose), 4.04 (9H, s, O- CH_3), 4.73 (1H, br s, H-ose), 5.06 (1H, d, $J^* = 9.0$ Hz, H-ose), 5.19 (1H, br s, H-ose), 5.42 (1H, br s, H-ose), 5.84 (1H, br s, H-ose), 7.38 (6H, dd, $J^* = 8.7$ Hz and 3.9 Hz, H-2, 6-methoxyphenyl), 8.14 (6H, dd, $J^* = 8.7$ Hz and 3.9 Hz, 3.

5- methoxyphenyl), 8.87 (4H, br s, β H), 8.93 (2H, d, $J^* = 4.8$ Hz, β H), 9.09 (2H, d, $J^* = 4.8$ Hz, β H); ^{13}C NMR [100.5 MHz, CDCl_3] δ 28.9, 29.2, 55.4, 61.4, 70.4, 74.8, 78.1, 81.9, 84.6, 112.6, 120.4, 133, 135.4, 159.3; UV-vis (CH_2Cl_2) λ_{max} 420, 515, 551, 592 and 649 nm; MS (MALDI-TOF) m/z 971.89 [calc'd for $\text{C}_{53}\text{H}_{42}\text{N}_4\text{F}_4\text{SO}_8$, M^+ 970.99].

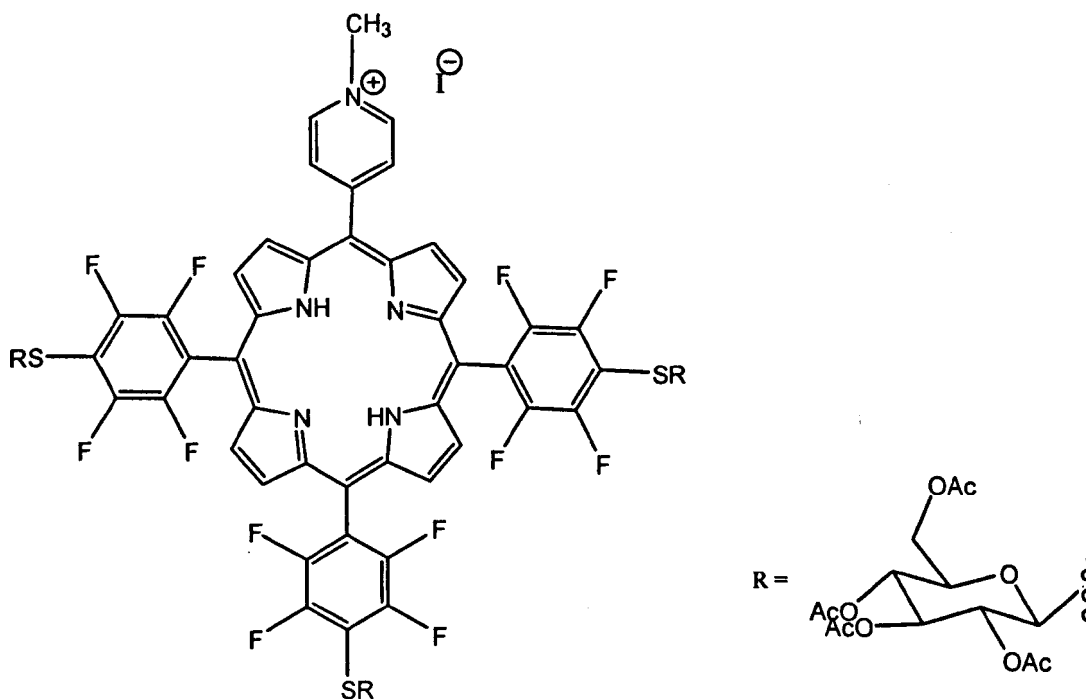
[46] 5-(4-pyridyl)-10,15,20-tris[4-(2', 3', 4', 6'-tetra-*O*-acetyl- β -D-glucopyranosylthio)-2,3,5,6-tetrafluorophenyl] porphyrin



5-(Pyridyl)-10,15,20-tris-(pentafluorophenyl)porphyrin (15 mg, 1.69×10^{-5} mol) was dissolved in dry anhydrous DMF (3 ml). 2,3,4,6- Tetra-*O*-acetyl- β -D-thioglucopyranose (4.5 eq, 27.7 mg, 7.61×10^{-5} mol) in DMF (4 ml) was added. The mixture was stirred at room temperature and the reaction monitored by TLC. After 16 hours, the solvent was evaporated *in vacuo*, followed by chromatographic purification (silica, eluent: toluene/

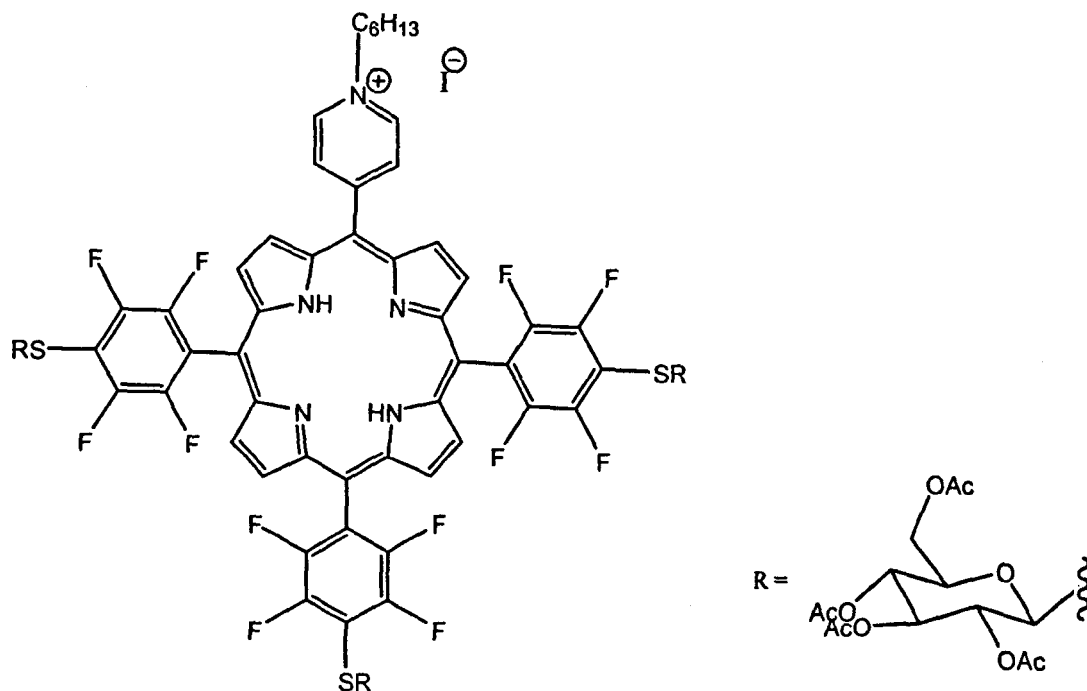
acetone, 7:3) yielding a purple solid (25 mg, 77 %); R_f = 0.23 (silica, eluent: toluene/acetone, 7:3); mp > 350 °C decomp; ¹H NMR [400 MHz, CDCl₃] δ - 2.85 (2H, br s, NH), 2.07 (9H, s, OAc), 2.09 (9H, s, OAc), 2.10 (9H, s, OAc), 2.23 (9H, s, OAc), 3.92 (3H, m, H-5'-ose), 4.33 (6H, d, J* = 3.4Hz, H-6a', 6b'ose), 5.24 (9H, m, H-1',2', 4'ose), 5.4 (3H, t, J* = 9.0Hz, H-3'-ose), 8.20 (2H, m, Py-2,6-H), 8.93 (2H, d, J* = 4.8Hz, β-H), 8.97 (2H, d, J* = 4.8Hz, β-H), 9.01 (4H, br s, β-H), 9.09 (2H, m, Py-3,5-H); UV-vis (CH₂Cl₂) λ_{max} 416, 510, 540, 585 and 624 nm; MS (MALDI-TOF) m/z 1920.3 [calc'd for C₈₅H₇₁N₅F₁₂S₃O₂₇, M⁺ 1918.67].

[47] 5-(N-Methyl-4-pyridyl)10,15,20-tris[4-(2', 3', 4', 6'-tetra-O-acetyl-β-D-glucopyranosylthio)-2,3,5,6-tetrafluorophenyl] porphyrin



5-(4-Pyridyl)-10,15,20-tris[4-(2', 3', 4', 6'-tetra-*O*-acetyl- β -D-glucopyranosylthio)-2,3,5,6-tetrafluorophenyl] porphyrin (0.01 g, 4.7×10^{-6} mol) was added to anhydrous DMF (5 ml). Methyl iodide (0.5 ml, 0.01 mol) was then added and the mixture stirred overnight at room temperature, under nitrogen and in the dark. The mixture was analysed using TLC (silica, eluent: water/potassium nitrate/acetonitrile, 1:1:8) and the solvent evaporated *in vacuo* to yield the product as a purple solid (0.03 g, 71 %); ^1H NMR [400MHz, CDCl_3] δ - 2.90 (2H, br s, NH), 2.07 (9H, s, OAc), 2.09 (9H, s, OAc), 2.10 (9H, s, OAc), 2.23 (9H, s, OAc), 3.95 (3H, m, H-5'-ose), 4.32 (6H, d, $J^* = 3.4\text{Hz}$, H-6a', 6b'ose), 4.99 (3H, br s, N-CH₃), 5.23 (9H, m, H-1',2', 4'ose) 5.39 (3H, t, $J^* = 9.0\text{Hz}$, H-3'-ose) 8.89 (2H, m, Py-2,6-H), 9.04(4H, m, β -H), 9.21(4H, m, β -H), 9.52 (2H, d, Py-3,5-H); UV-vis (CH_2Cl_2) λ_{max} 420, 513, 552, 588 and 643 nm; MS (MALDI-TOF) m/z 1933.16 [calc'd for $\text{C}_{86}\text{H}_{74}\text{N}_5\text{F}_{12}\text{S}_3\text{O}_{27}$, M^+ 1933.16].

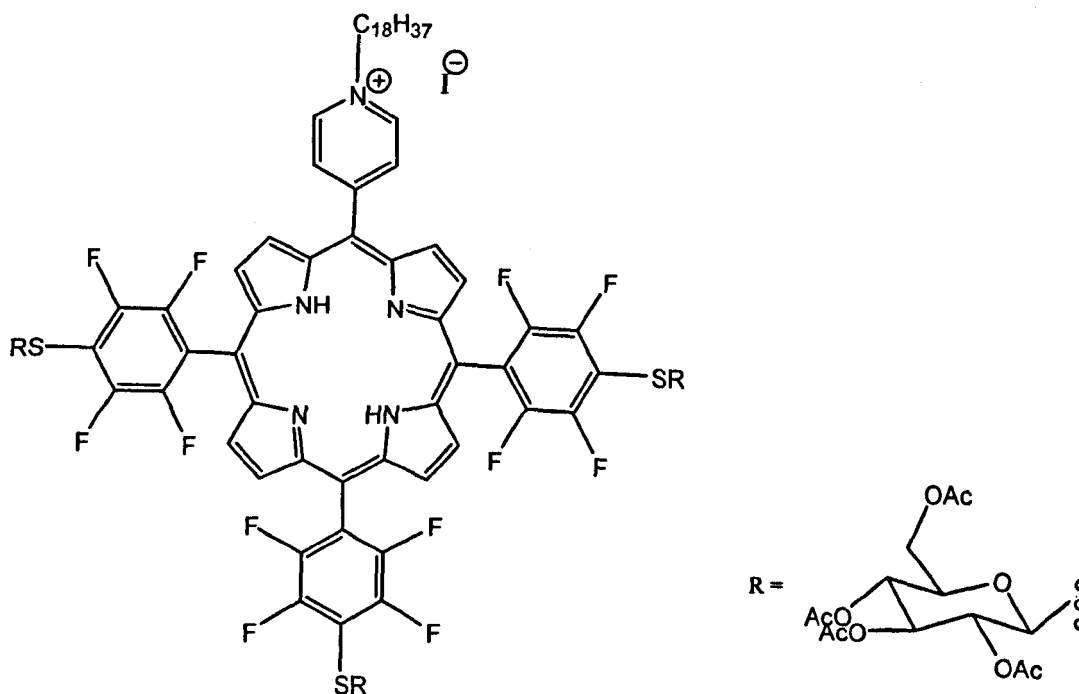
[48] 5-(N-Hexyl-4-pyridyl)10,15,20-tris-[4-(2', 3', 4', 6'-tetra-O-acetyl-β-D-glucopyranosylthio)-2,3,5,6-tetrafluorophenyl] porphyrin



5-(4-Pyridyl)-10,15,20-tris[4-(2',3',4',6'-tetra-O-acetyl-β-D-glucopyranosylthio)-2,3,5,6-tetrafluorophenyl] porphyrin (0.01 g, 4.7×10^{-6} mol) was added to anhydrous DMF (5 ml). Hexyliodide (0.5 ml, 3.47×10^{-3} mol) was added and the mixture stirred at room temperature overnight, under nitrogen and in the dark. The mixture was analysed using TLC (silica, eluent: water/potassium nitrate/acetonitrile, 1:1:8) and the solvent evaporated *in vacuo* to yield the product as a purple solid (0.03 g, 39 %); $^1\text{H NMR}$ [400MHz, CDCl_3] δ 2.89 (2H, br s, NH), 0.84 (3H, m, CH_3), 1.43 (4H, m, CH_2CH_2), 1.60 (2H, m, CH_2), 2.07 (9H, s, OAc), 2.09 (9H, s, OAc), 2.10 (9H, s, OAc), 2.23 (9H, s, OAc), 2.36 (2H, m, CH_2), 3.96 (3H, m, H-5'-ose), 4.32 (6H, d, $J^* = 3.4\text{Hz}$, H-6a', 6b'ose), 5.15 (2H, m, CH-N), 5.25 (9H, m, H-1',2',4'ose) 5.38 (3H, t, $J^* =$

9.0Hz, H-3'-ose), 8.89(2H, m, Py-2,6-H), 9.04(4H, m, β -H), 9.19(4H, m, β -H), 9.50 (2H, d, Py-3,5-H); UV-vis (CH_2Cl_2) λ_{max} 421, 513, 549, 589 and 660 nm; MS (MALDI-TOF) m/z 2004.6 [calc'd for $\text{C}_{91}\text{H}_{84}\text{N}_5\text{F}_{12}\text{S}_3\text{O}_{27}$, M^+ 2003.24].

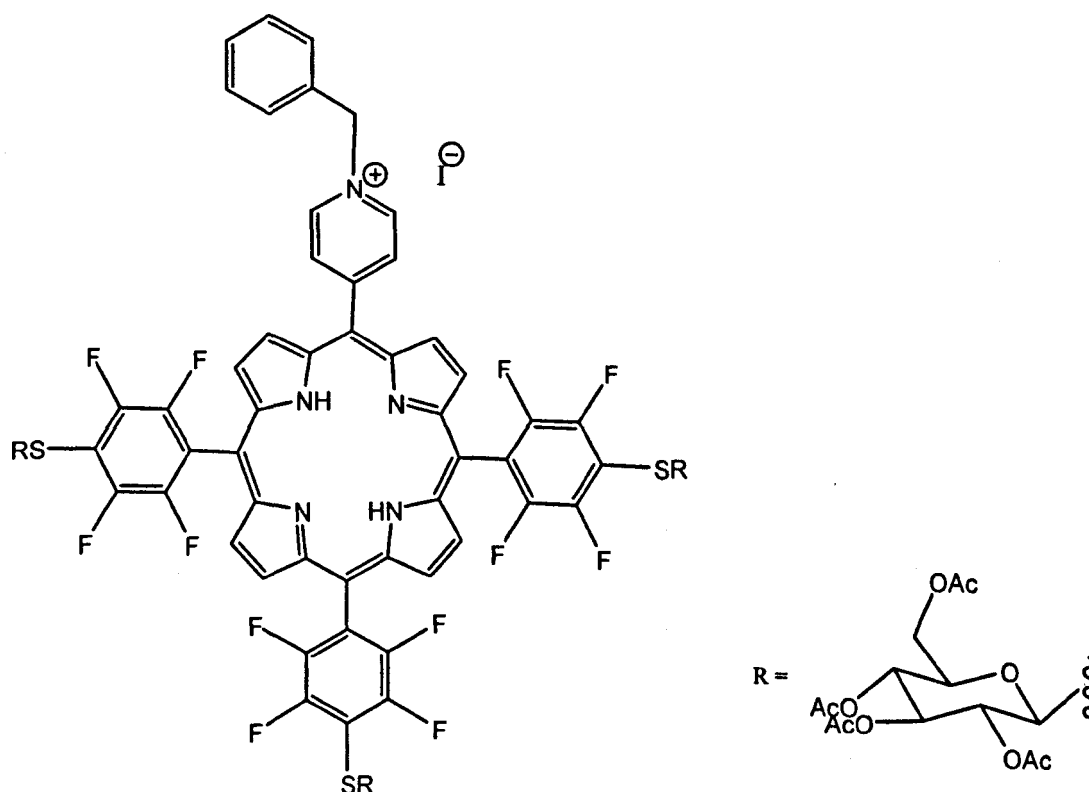
[49] 5-(N-Octadecyl-4-pyridyl)10,15,20-tris-[4-(2',3',4',6'-tetra-O-acetyl- β -D-glucopyranosylthio)-2,3,5,6-tetrafluorophenyl] porphyrin



5-(4-Pyridyl)-10,15,20-tris-[4-(2',3',4',6'-tetra-O-acetyl- β -D-glucopyranosylthio)-2,3,5,6-tetrafluorophenyl] porphyrin (0.01 g, 4.7×10^{-6} mol) was added to anhydrous DMF (5 ml). Octadecaneiodide (0.5 g, 1.31×10^{-3} mol) was added and the mixture stirred overnight at room temperature, under nitrogen and in the dark . The mixture was analysed using TLC (silica, eluent: water/potassium nitrate/acetonitrile, 1:1:8) and the

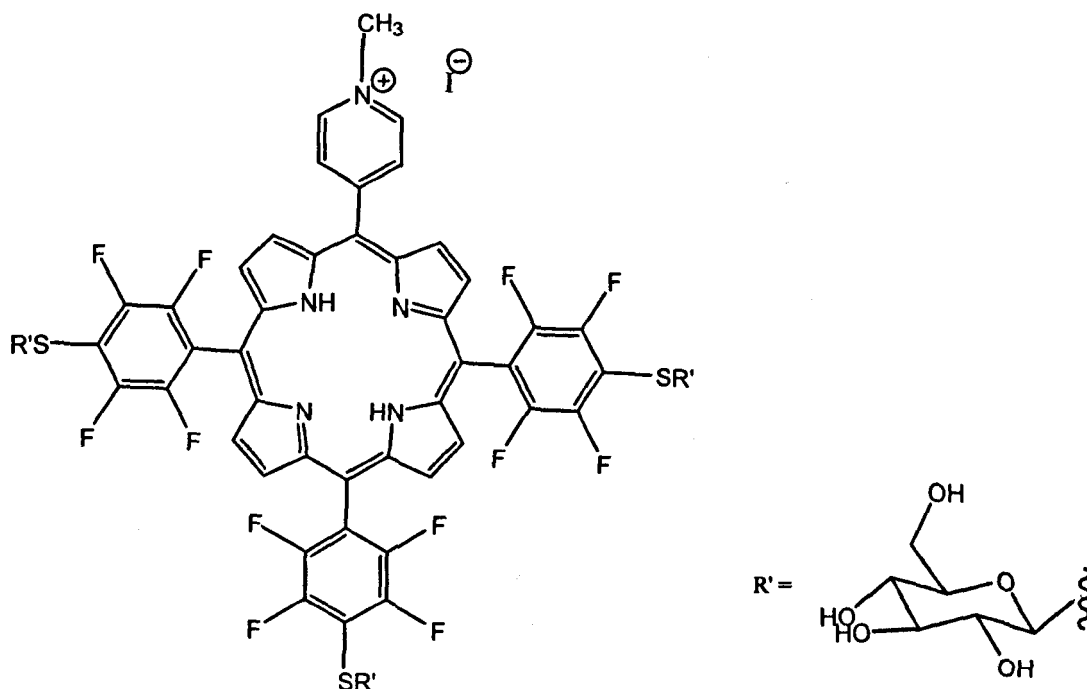
solvent evaporated *in vacuo* to yield the product as a purple solid (0.06 g, 62 %); δ - 2.87 (2H, br s, NH), 0.89 (3H, m, CH₃), 1.41 (30H, m, CH₂CH₂), 1.67 (2H, m, CH₂), 2.07 (9H, s, OAc), 2.09 (9H, s, OAc), 2.10 (9H, s, OAc), 2.23 (9H, s, OAc), 3.66 (2H, m, CH₂), 3.95 (3H, m, H-5'-ose), 4.32 (6H, d, $J^* = 3.4\text{Hz}$, H-6a', 6b'ose), 5.22 (9H, m, H-1',2', 4'ose), 5.40 (3H, t, $J = 9.0\text{Hz}$, H-3'-ose), 8.94 (2H, m, Py-2,6-H), 9.04 (4H, m, β -H), 9.15 (4H, m, β -H), 9.35 (2H, d, Py-3,5-H); UV-vis (CH₂Cl₂) λ_{max} 421, 514, 552, 590 and 660 nm; MS (MALDI-TOF) m/z 2172.3 [calc'd for C₁₀₃H₁₀₈N₅F₁₂S₃O₂₇, M⁺ 2172.20].

[50] 5-(N-Benzyl-4-pyridyl)10,15,20-tris-[4-(2', 3', 4', 6'-tetra-O-acetyl- β -D-glucopyranosylthio)-2,3,5,6-tetrafluorophenyl] porphyrin



5-(4-Pyridyl)-10,15,20-tris-[4-(2',3',4',6'-tetra-*O*-acetyl- β -D-glucopyranosylthio)-2,3,5,6-tetrafluorophenyl] porphyrin (0.01 g, 4.7×10^{-6} mol) was added to anhydrous DMF (5 ml). Octadecaneiodide (0.5 ml, 4.2×10^{-3} mol) was then added and the mixture stirred overnight at room temperature, under nitrogen and in the dark. The mixture was analysed using TLC (silica, eluent: water/potassium nitrate/acetonitrile, 1:1:8) and the solvent evaporated *in vacuo* to yield the product as a purple solid (0.04 g, 44 %); ^1H NMR [400MHz, CDCl_3] δ - 2.93 (2H, br s, NH), 2.07 (9H, s, OAc), 2.09 (9H, s, OAc), 2.10 (9H, s, OAc), 2.23 (9H, s, OAc), 3.89 (3H, m, H-5'-ose), 4.32 (6H, d, $J^* = 3.4\text{Hz}$, H-6a', 6b'ose), 4.71 (2H, m, CH_2Ar), 5.23 (9H, m, H-1',2', 4'ose), 5.38 (3H, t, $J^* = 9.0\text{Hz}$, H-3'-ose), 7.36 (4H, m, Ar-H), 8.77 (2H, m, Py-2,6-H), 9.04 (8H, m, β -H), 9.78 (2H, d, Py-3,5-H); UV-vis (CH_2Cl_2) λ_{max} 421, 513, 548, 587 and 660 nm; MS (MALDI-TOF) m/z 2010.2 [calc'd for $\text{C}_{92}\text{H}_{78}\text{N}_5\text{F}_{12}\text{S}_3\text{O}_{27}$, M^+ 2009.91].

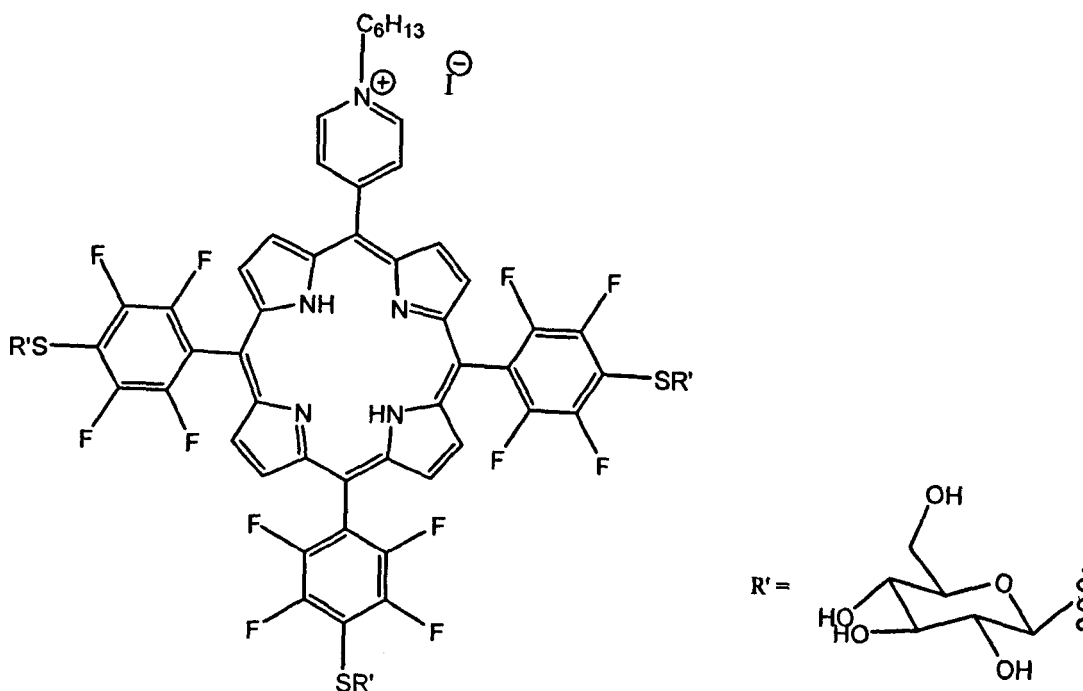
[51] 5-(N-methyl-4-pyridyl)10,15,20-tris[4-(β -D-glucopyranosylthio)-2,3,5,6-tetrafluorophenyl] porphyrin



5-(N-Methyl-4-pyridyl)-10,15,20-tris-[4-(2',3',4',6'-tetra-O-acetyl- β -D-glucopyranosylthio)-2,3,5,6-tetrafluorophenyl] porphyrin (17 mg, 8.8×10^{-6} mol) was dissolved in a mixture of [dichloromethane/methanol, 7:3] (3 ml) and sodium methoxide 0.5M solution in methanol (1.5 eq/OAc) added. The mixture was stirred for an hour at 20 °C and the porphyrin was precipitated by the addition of hexane and filtered, giving a purple solid (7 mg, 32 %); mp > 350 °C decomp¹H NMR [400MHz, DMSO] δ - 3.15 (2H, br s, NH), 3.50 (3H, m, H-ose), 3.83 (3H, m, H-ose), 4.70 (3H, br s, N-CH₃), 4.81 (3H, m, H-ose), 5.10 (3H, m, H-ose), 5.15 (3H, br s, H-ose), 5.32 (3H, br s, H-ose), 5.80 (3H, br s, H-ose), 9.09 (2H, m, Py-2,6-H), 9.32 (8H, m, β -H), 9.48 (2H, m, Py-3,5-H); UV-vis (CH₂Cl₂) λ_{\max} 414, 486, 512, 586 and 657 nm; MS (MALDI-TOF) m/z 1428.80

[calc'd for $C_{62}H_{50}N_5F_{12}S_3O_{15}$, M^+ 1429.63].

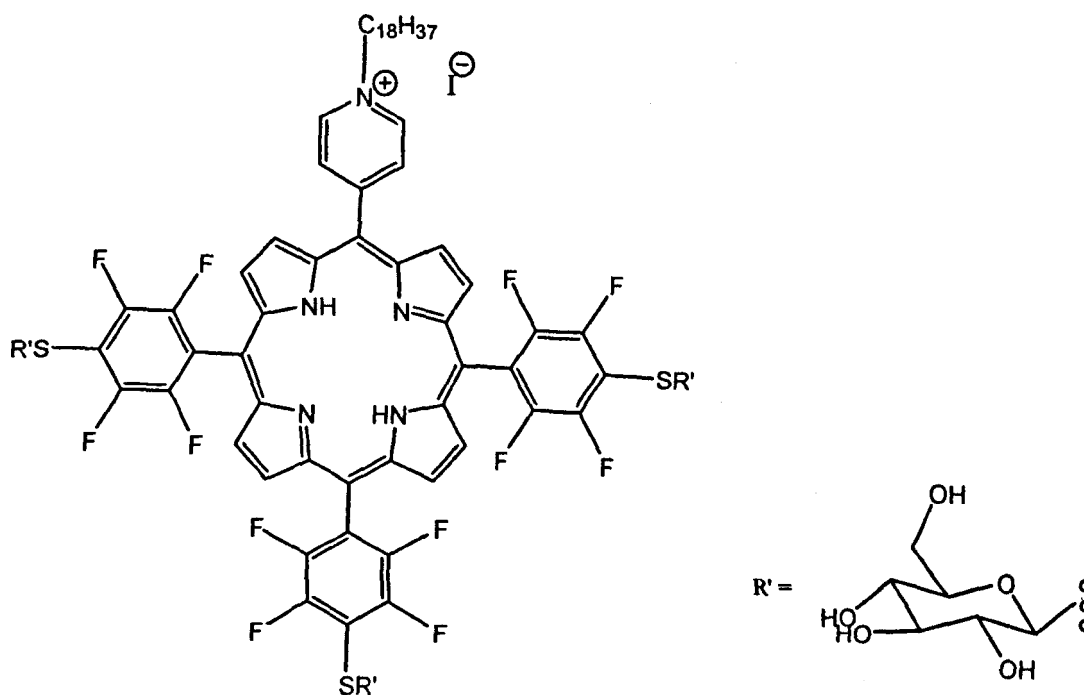
[52] 5-(N-Hexyl-4-pyridyl)10,15,20- tris-[4-(β -D-glucopyranosylthio)-2,3,5,6-tetrafluorophenyl] porphyrin



5-(N-Hexyl-4-pyridyl)-10,15,20-tris-[4-(2',3',4',6'-tetra-O-acetyl- β -D-glucopyranosylthio)-2,3,5,6-tetrafluorophenyl] porphyrin (12 mg, 5.99×10^{-6} mol) was dissolved in a mixture of [dichloromethane/methanol, 7:3] (3 ml) and sodium methoxide 0.5M solution in methanol (1.5 eq/OAc) added. The mixture was stirred for an hour at 20 °C and the porphyrin was precipitated by the addition of hexane and filtered, giving a purple solid (4 mg, 44 %); mp > 350 °C decomp; ¹H NMR [400MHz, DMSO] δ - 3.2 (2H, br s, NH), 0.8-2.5 (11H, m, CH₂), 3.50 (3H, m, H-ose), 3.83 (3H, m, H-ose), 4.73 (3H, br s, H-ose), 4.92 (3H, m, H-ose), 5.11 (3H, d, H-ose), 5.15 (2H, m, CH₂-N), 5.32

(3H, br s, H-ose), 5.90 (3H, br s, H-ose), 9.12 (2H, m, Py-2,6-H), 9.32 (8H, m, β -H), 9.57 (2H, m, Py-3,5-H); UV-vis (CH_2Cl_2) λ_{max} 418, 486, 511, 582 and 657nm; MS (MALDI-TOF) m/z 1499 [calc'd for $\text{C}_{67}\text{H}_{60}\text{N}_5\text{F}_{12}\text{S}_3\text{O}_{15}$, M^+ 1499.17].

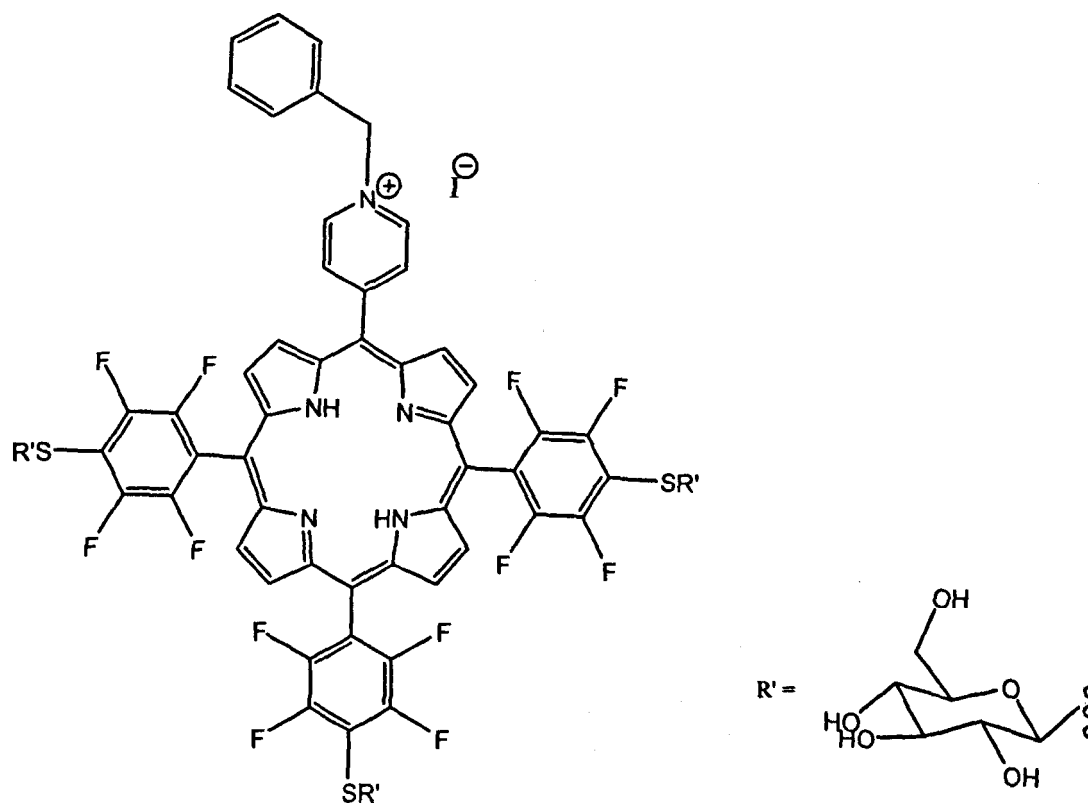
[53] 5-(N-Octadecyl-4-pyridyl)10,15,20-tris-[4-(β -D-glucopyranosylthio)-2,3,5,6-tetrafluorophenyl] porphyrin



5-(N-Octadecyl-4-pyridyl)-10,15,20-tris-[4-(2',3',4',6'-tetra-O-acetyl- β -D-glucopyranosylthio)-2,3,5,6-tetrafluorophenyl] porphyrin (28 mg, 1.29×10^{-5} mol) was dissolved in a mixture of [dichloromethane/methanol, 7:3] (3 ml) and sodium methoxide 0.5M solution in methanol (1.5 eq/OAc) added. The mixture was stirred for an hour at 20 °C and the porphyrin was precipitated by the addition of hexane and filtered, giving a purple solid (9 mg, 43 %); mp > 350 °C decomp; ¹H NMR [400MHz, DMSO] δ -3.2

(2H, br s, NH), 0.85 (3H, m, CH₃), 1.23 (30H, m, CH₂), 2.02 (2H, m, CH₂), 3.50 (3H, m, H-ose), 3.81 (3H, m, H-ose), 4.70 (3H, br s, H-ose), 4.90 (3H, m, H-ose), 5.09 (3H, br s, H-ose), 5.15 (2H, m, CH₂), 5.32 (3H, br s, H-ose), 5.90 (3H, br s, H-ose), 9.12 (2H, m, Py-2,6-H), 9.32 (8H, m, β-H), 9.57 (2H, m, Py-3,5-H); UV-vis (CH₂Cl₂) λ_{max} 417, 509, 541, 585 and 639 nm; MS (MALDI-TOF) *m/z* 1667.3 [calc'd for C₇₉H₈₄N₅F₁₂S₃O₁₅, M⁺ 1667.7]

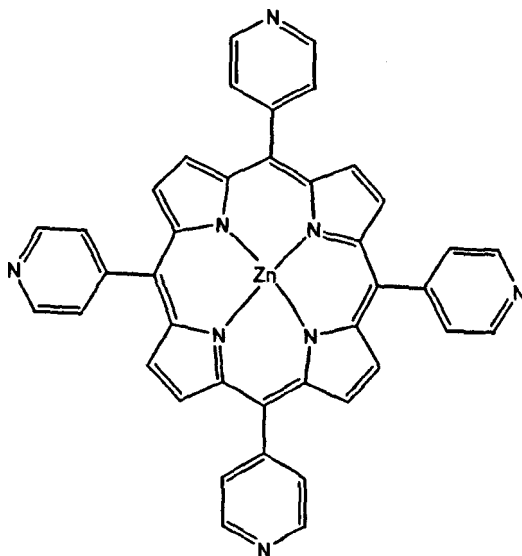
[54] 5-(*N*-Benzyl-4-pyridyl)10,15,20-tris-[4-(β-D-glucopyranosylthio)-2,3,5,6-tetrafluorophenyl] porphyrin



5-(*N*-Benzyl-4-pyridyl)-10,15,20-tris-[4-(2', 3', 4', 6'-tetra-*O*-acetyl-β-D-glucopyranosylthio)-2,3,5,6-tetrafluorophenyl] porphyrin (28 mg, 1.39 × 10⁻⁵ mol) was

dissolved in a mixture of [dichloromethane/methanol , 7:3] (3 ml) and sodium methoxide 0.5M solution in methanol (1.5 eq/OAc) added. The mixture was stirred for an hour at 20 °C and the porphyrin was precipitated by the addition of hexane and filtered, giving a purple solid (11 mg, 52 %); mp > 350 °C decomp; ¹H NMR [400MHz, DMSO] δ - 3.15 (2H, br s, NH), 3.50 (3H, m, H-ose), 3.70 (3H, m, H-ose), 4.70 (3H, br s, H-ose), 5.10 (3H, m, H-ose), 5.20 (2H, m, CH₂N), 5.31 (3H, br s, H-ose), 5.40 (3H, br s, H-ose), 5.80 (3H, br s, H-ose), 7.5 (2H, m, Ar-H), 7.7 (2H, m, Ar-H), 9.12 (2H, m, Py-2,6-H), 9.32 (8H, m, β-H), 9.57 (2H, m, Py-3,5-H); UV-vis (CH₂Cl₂) λ_{max} 418, 511, 585 and 641 nm; MS (MALDI-TOF) *m/z* 1504.5 [calc'd for C₆₈H₅₄N₅F₁₂S₃O₁₅, M⁺ 1505.36].

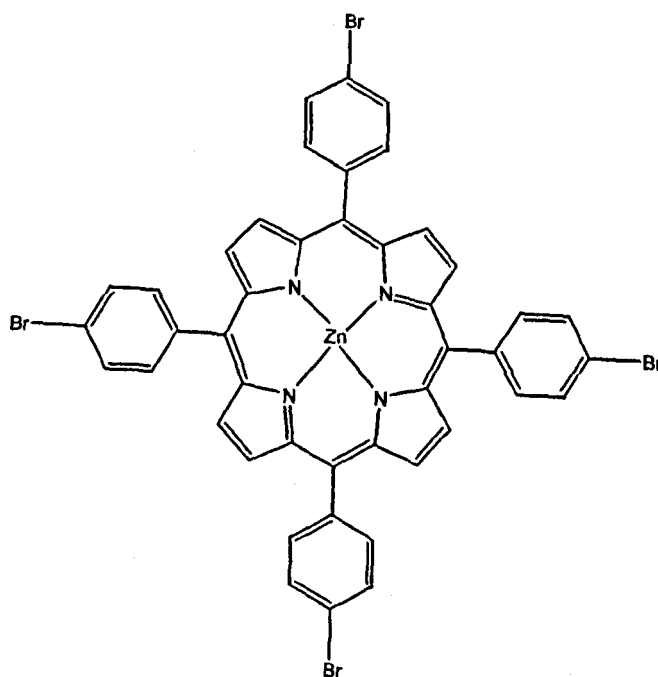
[55] Zn(II)-5,10,15,20-Tetra-(4-pyridyl)porphyrin



5,10,15,20-Tetra-(4-pyridyl)porphyrin (0.22 g, 0.162 mmol) was dissolved in chloroform (15 ml). The mixture was stirred at 140 °C under argon and protected from light for 30

min. A saturated solution of zinc acetate in methanol (1 ml) was added and the solution was heated for 30 min under reflux. After cooling, the solution was filtered and the solid obtained was then triturated thoroughly with methanol. The resulting purple crystals were air dried and finally dried under vacuum to yield the product as lustrous purple crystals (0.23 g, 93%); $R_f = 0.13$ (silica, CHCl_3); $^1\text{H NMR}$ [400 MHz, CDCl_3] δ 7.82 (8H, m, Py-2, 6-H), 8.09 (8H, m, Py-3, 5-H), 8.91 (8H, s, βH); UV-vis (CH_2Cl_2) λ_{max} 429, 567, 607 nm; MS (MALDI-TOF) m/z 682 [calc'd for $\text{ZnC}_{40}\text{H}_{24}\text{N}_8$, M^+ 682.06].

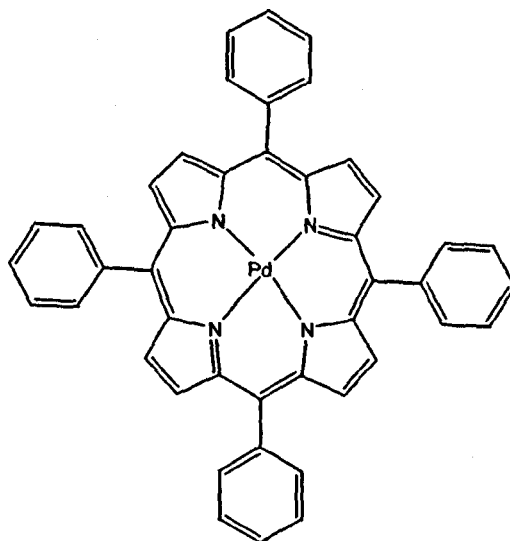
[56] Zn(II)-5,10,15,20-Tetra-(4-bromophenyl)porphyrin



5,10,15,20-Tetra-(4-bromophenyl) porphyrin (0.27 g, 0.29 mmol) was dissolved in hot chloroform (15 ml). The mixture was stirred at 140 °C under argon and protected from light for 30 min. A saturated solution of zinc acetate in methanol (1 ml) was added and

the solution was heated for 30 min under reflux. After cooling, the solution was filtered and the solid obtained was then triturated thoroughly with methanol. The resulting purple crystals were air dried and finally dried under vacuum to yield the product as lustrous purple crystals (0.18 g, 62%); $R_f = 0.84$ (silica, $\text{CHCl}_3/\text{MeOH}$, 19:1); $^1\text{H NMR}$ [400 MHz, CDCl_3] δ 7.89 (8H, m, 5, 10, 15, 20-Ar-3, 5-H), 8.08 (8H, d, $J^* = 8\text{Hz}$, 5, 10, 15, 20-Ar-2, 6-H), 8.95 (8H, s, βH); UV-vis (CH_2Cl_2) λ_{max} 417, 549, 589 nm; MS (MALDI-TOF) m/z 994.34 [calc'd for $\text{ZnC}_{44}\text{H}_{24}\text{N}_4\text{Br}_4$, M^+ 993.70].

[57] Pd(II)-5,10,15,20-Tetraphenylporphyrin

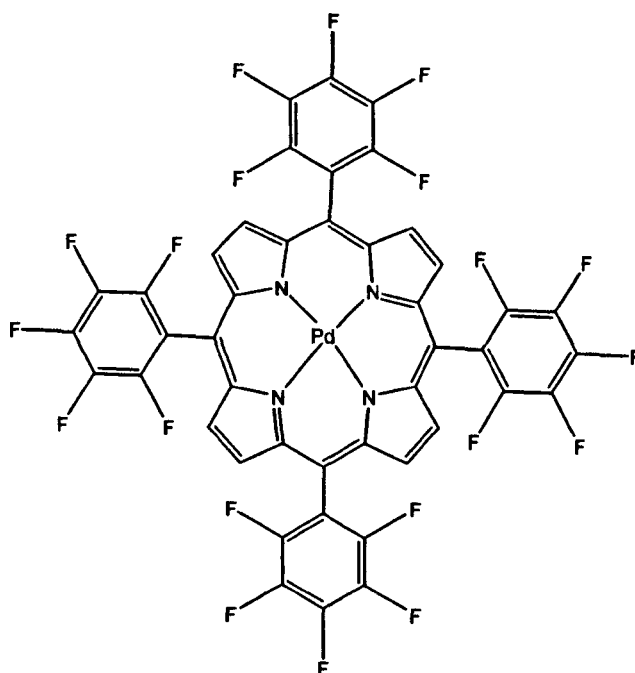


Palladium acetate (0.40 g, 1.78 mmol) was dissolved in anhydrous DMF (5 ml) and the mixture was stirred at 140 °C under argon and protected from light for 30 min.

5,10,15,20-Tetraphenylporphyrin (0.22g, 0.04 mmol) was then added and the solution stirred under reflux for a further seven hours. Upon cooling, the solvent was evaporated

in vacuo to yield the product as a purple solid (0.18g, 73%); $R_f = 0.44$ (silica, eluent: $\text{CH}_2\text{Cl}_2/\text{hexane}$ 1:1); $^1\text{H NMR}$ [400 MHz, CDCl_3] δ 7.72 (12H, m, Ar-3, 4,5-H), 8.10 (8H, d, $J^* = 8\text{Hz}$, Ar-2, 6-H), 8.74 (8H, s, βH); UV-vis (CH_2Cl_2) λ_{max} 417, 523, 552 nm; MS (MALDI-TOF) m/z 719 [calc'd for $\text{PdC}_{44}\text{H}_{28}\text{N}_4$, M^+ 719.15].

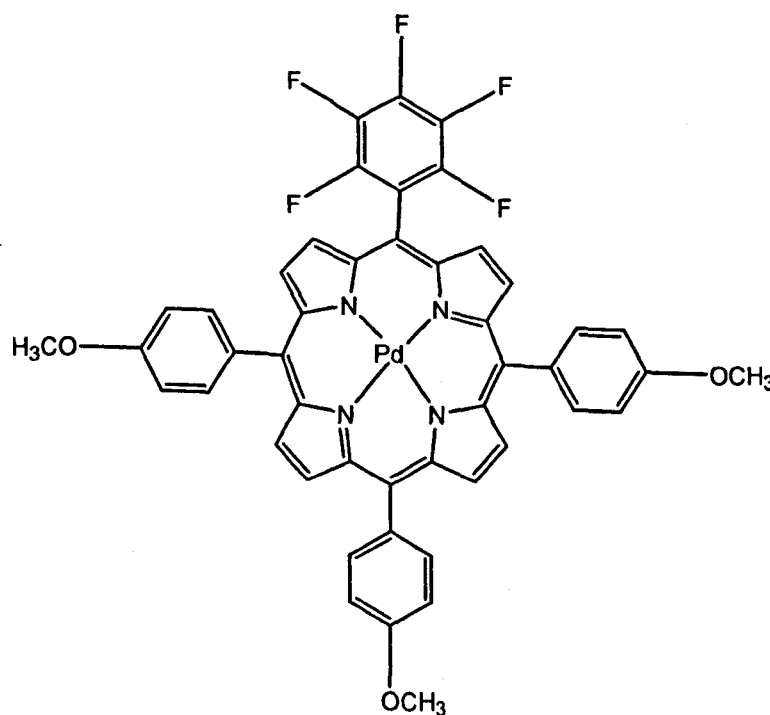
[58] Palladium 5,10,15,20-tetra-(pentafluorophenyl)porphyrin



Palladium acetate (0.29 g, 1.30 mmol) was dissolved in benzonitrile (40 ml). The mixture was heated under reflux at 240 °C, for 30 min under argon and protected from light. 5,10,15,20-Pentafluorophenylporphyrin (0.13 g, 0.13 mmol) was added and the mixture stirred under reflux for a further 72 hours. Upon cooling, the solvent was evaporated *in vacuo* and the crude product redissolved in a minimum amount of benzene. The solution was filtered through a neutral alumina column. The filtrate was collected

and the solvent removed *in vacuo* to obtain the product, which was recrystallised from chloroform to give the product (0.12 g, 85%); R_f = 0.4 (silica, ethyl acetate/ hexane, 1:4); ¹H NMR [400 MHz, CDCl₃] δ 8.92 (8H, s, βH); UV-vis (CH₂Cl₂) λ_{max} 406, 519, 552 nm; MS (MALDI-TOF) *m/z* 1078.5 [calc'd for PdC₄₄H₈N₄F₂₀, M⁺ 1078.96].

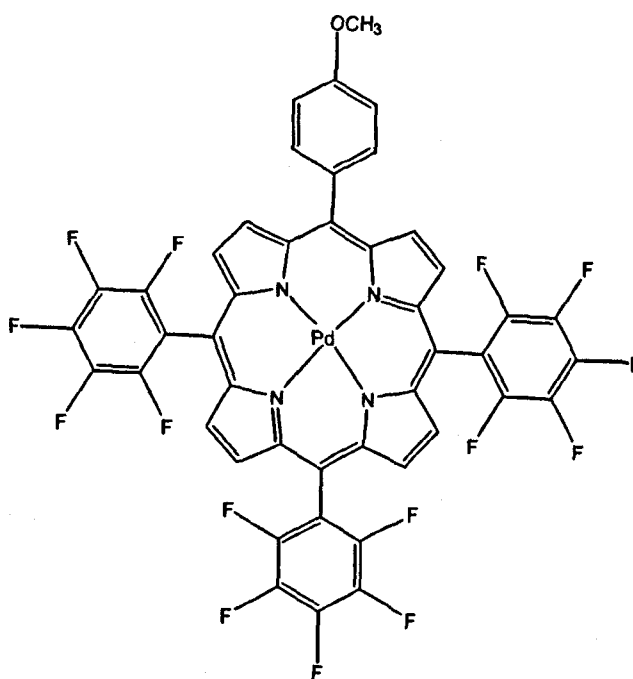
[59] Pd(II)-5-(Pentafluorophenyl)-10,15,20-tris-(4-methoxyphenyl)porphyrin



Palladium acetate (0.2 g, 8.9×10^{-4} mol) was dissolved in benzonitrile (10 ml). The mixture was heated under reflux at 240 °C, for 30 min under argon and protected from light. 5-(Pentafluorophenyl)-10,15,20-tris-(4-methoxyphenyl)porphyrin (0.07 g, 8.9×10^{-5} mol) was then added and the mixture stirred under reflux for a further 72 hours. Upon cooling, the solvent was evaporated *in vacuo* and the solid redissolved in a minimum

amount of benzene. The mixture was filtered through a neutral alumina column. The filtrate was collected and the solvent removed *in vacuo* to obtain the product, which was recrystallised from chloroform to give the product (0.03 g, 37 %); $R_f = 0.6$ (silica, eluent: CH_2Cl_2); $^1\text{H NMR}$ [400 MHz, CDCl_3] δ 4.10 (9H, s, CH_3), 7.42 (6H, m, Ar- 3, 5-H), 8.08 (6H, m, Ar-2, 6-H), 8.72 (2H, m, βH), 8.80 (4H, m, βH), 8.93 (2H, m, βH); UV-vis (CH_2Cl_2) λ_{max} 419, 525, 555 nm; MS (MALDI-TOF) m/z 898.40 [calc'd for $\text{PdC}_{47}\text{H}_{29}\text{O}_3\text{N}_4\text{F}_5$, M^+ 899.18]

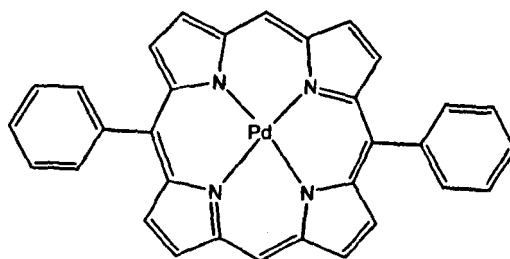
[60] Pd(II)-5-(4-methoxyphenyl)-10,15,20-tris-(pentafluorophenyl)porphyrin



Palladium acetate (0.06 g, 0.25 mmol) was dissolved in benzonitrile (5 ml). The mixture was heated under reflux at 240 °C, for 30 min under argon and protected from light. 5-(4-methoxyphenyl)-10,15,20-tris-(pentafluorophenyl)porphyrin (0.05g, 0.03 mmol) was

added and the mixture stirred under reflux for 72 hours. Upon cooling, the solvent was evaporated *in vacuo* and the solid redissolved in a minimum amount of benzene. The mixture was filtered through a neutral alumina column. The filtrate was collected and the solvent removed *in vacuo* to obtain the product, which was recrystallised from chloroform to give red crystalline solid (0.04 g, 69%); $R_f = 0.2$ (silica, eluent: CH_2Cl_2); $^1\text{H NMR}$ [400 MHz, CDCl_3] δ 4.11 (3H, s, CH_3), 7.92 (2H, m, Ar- 3, 5-H), 8.1 (2H, m, Ar-2, 6-H), 8.8 (2H, m, βH), 8.88 (4H, m, βH), 8.99 (2H, m, βH); UV-vis (CH_2Cl_2) λ_{max} 411, 521, 554 nm; MS (MALDI-TOF) m/z 1018.61 [calc'd for $\text{PdC}_{45}\text{H}_{15}\text{ON}_4\text{F}_{15}$, M^+ 1019.11].

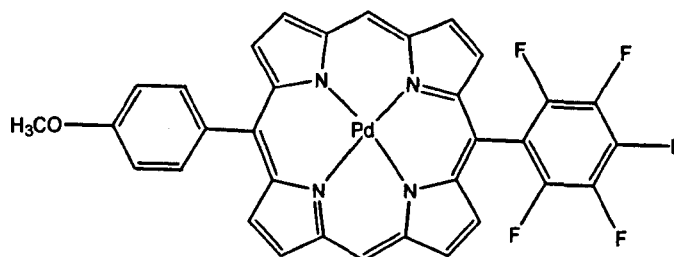
[61] Pd(II) 5,15-diphenylporphyrin



Palladium acetate (0.05 g, 2.2×10^{-4} mol) was dissolved in benzonitrile (5 ml). The mixture was heated under reflux at 240 °C, for 30 min under argon and protected from light. 5,15-Diphenylporphyrin (0.01 g, 2.2×10^{-5} mol) was added and the mixture stirred under reflux for a further 72 hours. Upon cooling, the solvent was evaporated *in vacuo* and the crude solid redissolved in a minimum amount of benzene. The solution was filtered through a neutral alumina column. The filtrate was collected and the solvent removed *in vacuo* to obtain the product, which was recrystallised from dichloromethane

to give the final product (0.01 g, 67%); Rf = 0.9 (silica, CH₂Cl₂); ¹H NMR [400 MHz, CDCl₃] δ 8.16 (6H, m, Ar-3, 4,5-H), 8.73 (4H,m, Ar-2, 6-H), 8.95 (4H, d, J* = 4.8Hz, βH), 9.42 (4H, d, J* = 4.8Hz, βH), 10.23 (2H, s, 10, 20-H); UV-vis (CH₂Cl₂) λ_{max} 403, 513, 545 nm; MS (MALDI-TOF) m/z 566.40 [calc'd for PdC₃₂H₂₀N₄, M⁺ 566.59].

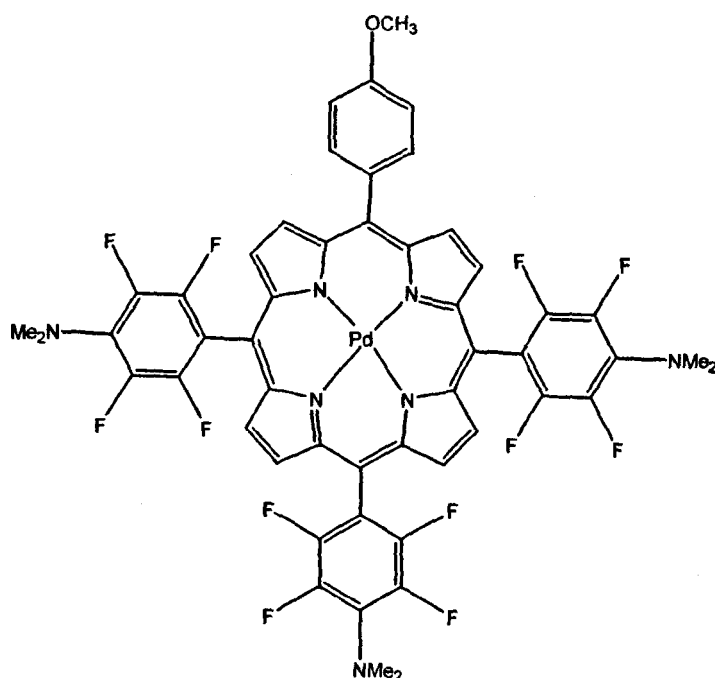
[62] Pd(II)-5-(pentafluorophenyl)-15-(4-methoxyphenyl)porphyrin



Palladium acetate (0.05 g, 2.2×10^{-4} mol) was dissolved in benzonitrile (5 ml). The mixture was heated under reflux at 240 °C, for 30 min under argon and protected from light. 5-(Pentafluorophenyl)-15-(4-methoxyphenyl)porphyrin (0.01 g, 2.2×10^{-5} mol) was added and the mixture was stirred under reflux for a further 72 hours. Upon cooling, the solvent was evaporated *in vacuo* and the solid redissolved into a minimum amount of benzene. The mixture was filtered through a neutral alumina column. The filtrate was collected and the solvent was removed *in vacuo* to obtain the solid, which was recrystallised from dichloromethane to give the product (0.01 g, 60%); Rf = 0.74 (silica, CH₂Cl₂); ¹H NMR [400 MHz, CDCl₃] δ 4.13 (3H, br s, CH₃), 7.38 (2H, m, Ar-3, 4,5-H), 8.13 (2H, m, Ar-2, 6-H), 9.07 (4H, m, J* = 4.8Hz, βH), 9.4 (4H, m, J* = 4.8Hz, βH), 10.34 (2H, s, 10, 20-H); UV-vis (CH₂Cl₂) λ_{max} 403, 513, 546 nm; MS (MALDI-TOF) m/z

686.4 [calc'd for PdC₃₃H₂₇N₄OF₅, M⁺ 686.94].

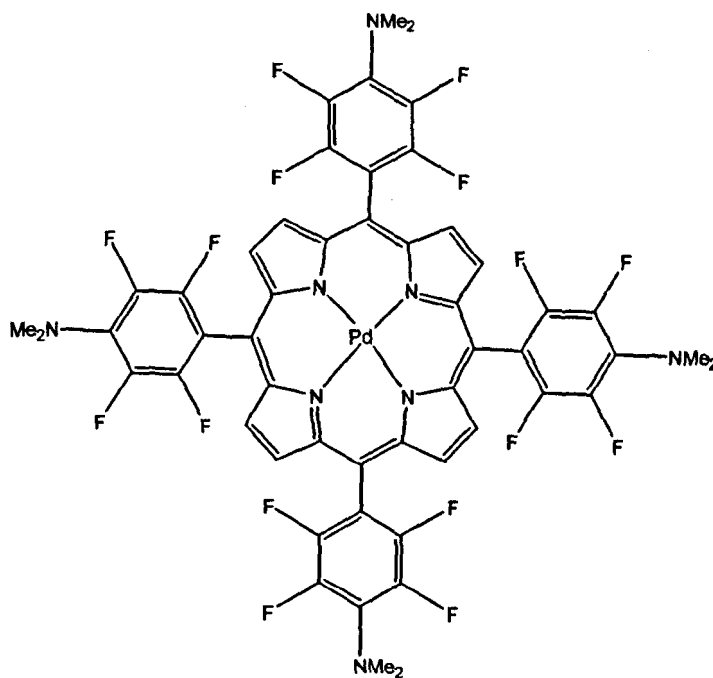
[63] Pd(II)-5-(4-methoxyphenyl)-10,15,20-tris-(2,3,5,6-tetrafluoro-N,N-dimethyl-4-aniliniumyl)porphyrin



5-(4-Methoxyphenyl)-10,15,20-tris(pentafluorophenyl)porphyrin (0.01 g, 5×10^{-6} mol) was added to anhydrous DMF (10 ml). The mixture was stirred under reflux at 140 °C, for 30 min under argon and protected from light. $(\text{CH}_3)_2\text{NH}\cdot\text{HCl}$ (1.6×10^{-3} g, 1.96×10^{-5} mol) was added and the mixture heated under reflux for a further 24 hours. The reaction was cooled to room temperature and the solvent evaporated *in vacuo* to yield the crude solid, which was further triturated with water to obtain the product as a red solid (0.01 g, 59 %); R_f = 0.64 (silica, CH₂Cl₂); ¹H NMR [400 MHz, CDCl₃] δ 3.3 (18H, s, NMe₂), 4.33 (3H, s, OCH₃), 7.9 (2H, m, Ar- 3, 5-H), 8.12 (2H, m, Ar-2, 6-H), 8.83 (2H, m, βH),

8.89 (4H, m, β H), 8.93 (2H, m, β H); UV-vis (CH_2Cl_2) λ_{max} 418, 523, 554, 607 nm; MS (MALDI-TOF) m/z 1093.9 [calc'd for $\text{C}_{51}\text{H}_{33}\text{N}_7\text{F}_{12}\text{OPd}$, M^+ 1094.34].

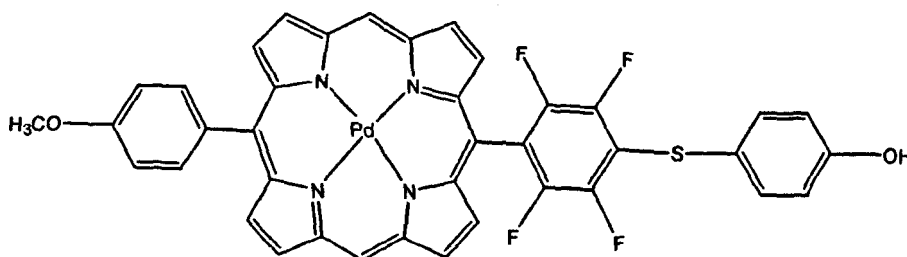
[64] Pd(II)Meso-tetrakis(2,3,5,6-tetrafluoro-*N,N*-dimethyl-4-aniliny)porphyrin



5,10,15,20-Pentafluorophenylporphyrin (0.13 g, 0.13 mmol), palladium acetate (0.29 g, 1.30 mmol) were added to anhydrous DMF (40 ml). The mixture was stirred under reflux at 140 °C, for 48 hours under argon and protected from light. $(\text{CH}_3)_2\text{NH}\cdot\text{HCl}$ (0.32 g, 3.9 mmol) was added and the mixture heated under reflux for a further 30 min. The reaction was cooled to room temperature and the solvent evaporated *in vacuo* to yield the crude product, which was purified further using flash column chromatography (silica, eluent: hexane/ethyl acetate, 8:2). Relevant fractions were combined, the solvent

removed *in vacuo* to yield the product. The product was recrystallised from chloroform to give purple crystals (0.02 g, 14%); Rf = 0.34 (silica, hexane/ethyl acetate, 8:2); ¹H NMR [400 MHz, CDCl₃] δ 3.29 (24H, s, NMe₂), 8.9 (8H, br s, βH); UV-vis (CH₂Cl₂) λ_{max} 418, 522, 554, 607 nm; MS (MALDI-TOF) *m/z* 1178.4 [calc'd for PdC₅₂H₃₂N₈F₁₆, M⁺ 1179.27].

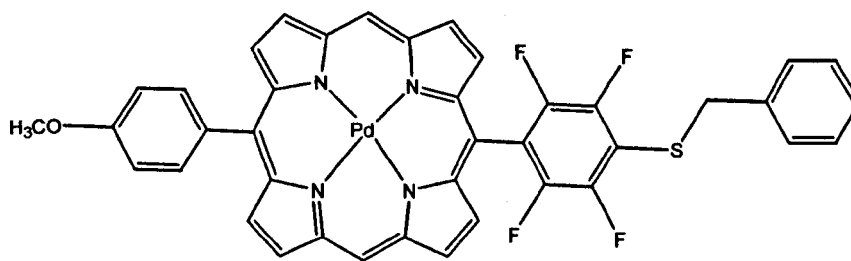
[65] Pd(II)-5-(4-thiophenol-2, 3, 5, 6-tetrafluorophenyl)-15-(4-methoxyphenyl)porphyrin



Pd (II)-5-(4-methoxyphenyl)-15-(pentafluorophenyl)porphyrin (9 mg, 1.3×10^{-5} mol) was dissolved in anhydrous DMF (5 ml) to which mercaptophenol (8.2×10^{-3} g, 6.5×10^{-5} mol) was added. The mixture was stirred at room temperature under argon and protected from light for 18 hours. The solvent was evaporated *in vacuo* and the solid redissolved in dichloromethane (10 ml). The mixture was washed with saturated sodium hydrogen carbonate (2×10 ml), separated and the organic layer dried *in vacuo*. The product was obtained as a reddish solid (0.08 g, 78%) Rf = 0.32 (silica, eluent: hexane/CH₂Cl₂, 1:1);

mp > 350 °C decomp; $^1\text{H NMR}$ [400 MHz, CDCl_3] δ 4.13 (3H, s, CH_3), 6.79 (2H, d, $J^* = 8.5$ Hz Ar-H), 7.37 (2H, m, 15-*m*-H), 7.74 (2H, d, $J^* = 8.5$ Hz, Ar-H), 8.14 (2H, m, 15-*o*-Ar-H), 8.80 (2H, m, βH), 8.94 (2H, m, βH), 9.07 (2H, m, βH), 9.37 (2H, m, βH), 10.3 (2H, s, 10, 20-H); UV-vis (CH_2Cl_2) λ_{max} 405, 514, 547 nm; MS (MALDI-TOF) m/z 792.5 [calc'd for $\text{PdC}_{39}\text{H}_{22}\text{O}_2\text{SN}_4\text{F}_4$, M^+ 793.10].

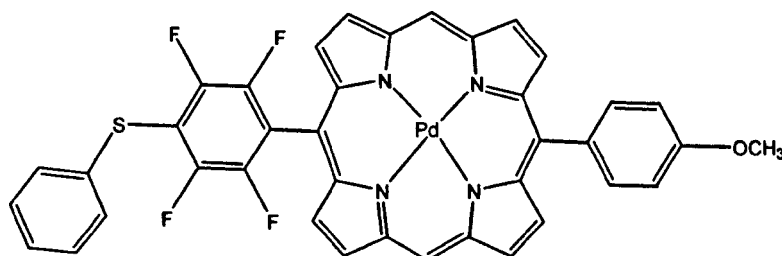
[66] Pd(II)-5-(4-benzylthio-2, 3, 5, 6-tetrafluorophenyl)-15-(4-methoxyphenyl)porphyrin



Pd(II)-5-(4-methoxyphenyl)-15-(pentafluorophenyl)porphyrin (9 mg, 1.3×10^{-5} mol) was dissolved in anhydrous DMF (5 ml) and benzylmercaptan (0.1 ml, 2×10^{-5} mol) was added. The mixture was allowed to stir at room temperature under argon and protected from light for 18 hours. The solvent was evaporated *in vacuo* and the solid redissolved in dichloromethane (10 ml). The solution was then washed with saturated sodium hydrogen carbonate (2×50 ml), separated and the organic layer concentrated *in vacuo*. The product was obtained as a red solid (8.5×10^{-5} g, 85%) $R_f = 0.4$ (silica, eluent: hexane/ CH_2Cl_2 , 1:1); $^1\text{H NMR}$ [400 MHz, CDCl_3] δ 4.1 (3H, s, CH_3), 4.5 (2H, m, CH_2Ph), 7.12 (2H, m, Ar- 3, 5-H), 7.23 (5H, m, Ph-H), 7.32 (2H, m, Ar-2, 6-H), 8.71

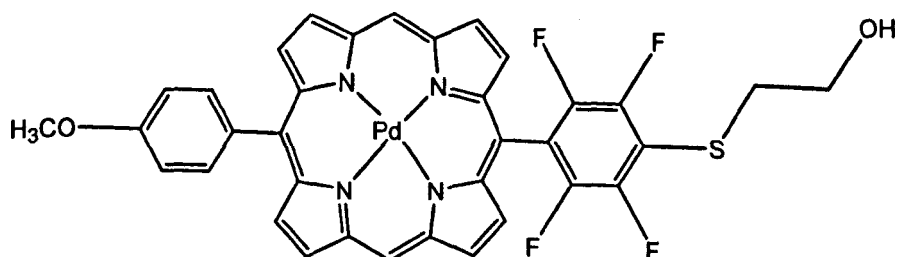
(2H, m, β H), 8.80 (4H, m, β H), 8.98 (2H, m, β H), 10.1 (2H, s, 10, 20-H); UV-vis (CH_2Cl_2) λ_{max} 407, 512, 546 nm; MS (MALDI-TOF) m/z 791.5 [calc'd for $\text{PdC}_{40}\text{H}_{24}\text{OSN}_4\text{F}_4$, M^+ 791.1294].

[67] **Pd(II)-5-(4-benzenethio-2,3,5,6-tetrafluorophenyl)-15-(4-methoxyphenyl)porphyrin**



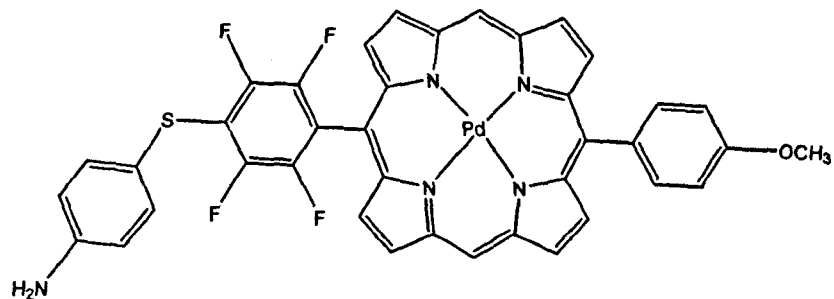
Palladium-5-(4-methoxyphenyl)-15-(pentafluorophenyl)porphyrin (0.03 g, 4.1×10^{-5} mol) was added in anhydrous DMF (5ml). Benzene thiol (5 μl , 4.9×10^{-5} mol) was then added and the mixture stirred for 72 hours at room temperature, under argon and protected from light. The solvent was evaporated *in vacuo* and the residue redissolved in dichloromethane (20 ml). The mixture was washed with saturated sodium hydrogen carbonate (2 \times 50 ml), separated and the organic layer concentrated *in vacuo*. The product was obtained as a red/brown solid (0.01 g, 40 %) $R_f = 0.48$ (silica, eluent: hexane/ CH_2Cl_2 , 1:1); $^1\text{H NMR}$ [400 MHz, CDCl_3] δ 4.12 (3H, m, OCH_3), 7.73 (5H, m, Ar-H), 8.16(2H, m, Ar- 3, 5-H), 8.8 (2H, m, Ar-2, 6-H), 9.00 (2H, s, β H), 9.10 (2H, s, β H), 9.38 (2H, s, β H), 9.44 (2H, s, β H), 10.38 (2H, s, meso-H); UV-vis (CH_2Cl_2) λ_{max} 405, 514, 547 nm; MS (MALDI-TOF) m/z 776.39 [calc'd for $\text{PdC}_{39}\text{H}_{22}\text{SON}_4\text{F}_4$, M^+

[68] Pd(II)-5-[4-(2-hydroxyethylthio)-2,3,5,6-(tetrafluorophenyl)]-15-(4-methoxyphenyl)porphyrin



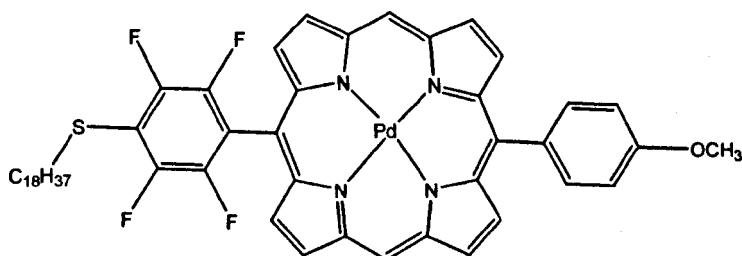
Pd(II)-5-(4-methoxyphenyl)-15-(pentafluorophenyl)porphyrin (6×10^{-3} g, 8.7×10^{-6} mol) was dissolved in anhydrous DMF (5 ml) and 2-mercaptoethanol (10 μ l, 0.1 mmol) was added. The mixture was stirred for 24 hours at room temperature, under argon and protected from light. The solvent was evaporated *in vacuo* and the residue redissolved in dichloromethane (20 ml). The mixture was washed with saturated sodium hydrogen carbonate (2 \times 50 ml), separated and the organic layer concentrated *in vacuo*. The product was analysed using TLC (silica, eluent: hexane/CH₂Cl₂, 1:1). The product was obtained as a reddish solid (3.5×10^{-3} g, 54 %) $R_f = 0.6$ (silica, eluent: hexane/CH₂Cl₂, 1:1); ¹H NMR [400 MHz, CDCl₃] δ 2.9 (2H, m, SCH₂), 3.94 (2H, m, CH₂OH), 4.13 (3H, br s, OCH₃), 7.83 (2H, m, Ar- 3, 5-H), 8.14 (2H, m, Ar-2, 6-H), 9.08 (4H, m, β H), 9.38 (4H, m, β H), 10.31 (2H, s, 10, 20-H); UV-vis (CH₂Cl₂) λ_{max} 406, 513, 547 nm; MS (MALDI-TOF) m/z 744.5 [calc'd for PdC₃₅H₂₂O₂SN₄F₄, M⁺ 745.05].

[69] Pd(II)-5-(4-aminobenzenethio-2,3,5,6-tetrafluorophenyl)-15-(4-methoxyphenyl)porphyrin



Palladium-5-(4-methoxyphenyl)-15-(pentafluorophenyl)porphyrin (0.03 g, 4.1×10^{-5} mol) was added in anhydrous DMF (5ml). 4-Aminobenzenethiol (6 mg, 4.9×10^{-5} mol) was then added and the mixture stirred at room temperature for 72 hours, under argon and protected from light. The solvent was evaporated *in vacuo* and the residue redissolved in dichloromethane (20 ml). The mixture was washed with saturated sodium hydrogen carbonate (2 \times 50 ml), separated and the organic layer concentrated *in vacuo*. The product was obtained as a red/brown solid (0.01 g, 30 %) $R_f = 0.56$ (silica, eluent: hexane/CH₂Cl₂, 1:1); ¹H NMR [400 MHz, CDCl₃] δ 4.02 (2H, s, NH₂), 4.12 (3H, m, OCH₃), 6.81 (2H, m, Ar-H), 7.36 (2H, m, Ar-H), 7.66 (2H, m, Ar- 3, 5-H), 8.98 (2H, m, Ar-2, 6-H), 8.98 (2H, s, β H), 9.09 (2H, s, β H), 9.36 (2H, s, β H), 9.42 (2H, s, β H), 10.36 (2H, s, meso-H); UV-vis (CH₂Cl₂) λ_{max} 406, 514, 547 nm; MS (MALDI-TOF) m/z 791.41 [calc'd for C₃₉H₂₃N₅F₄PdSO, M⁺ 792.12].

[70] Pd-5-(4-octadecylthio-2, 3, 5, 6-tetrafluorophenyl)-15-(4-methoxyphenyl)porphyrin

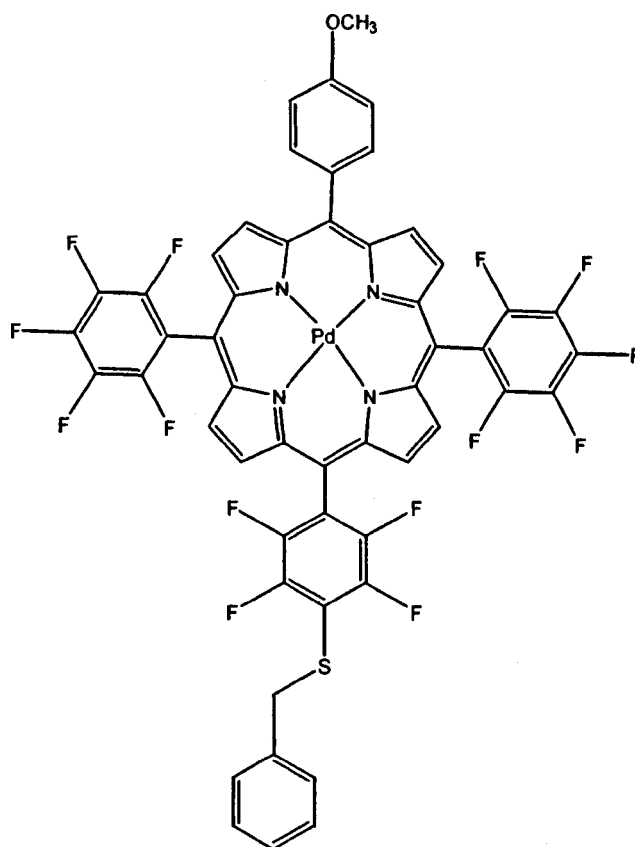


Palladium-5-(4-methoxyphenyl)-15-(pentafluorophenyl)porphyrin (7.81×10^{-3} g, 1.06×10^{-5} mol) was added in anhydrous DMF (5 ml). Octadecanethiol (4 mg, 1.3×10^{-5} mol) was then added and the mixture stirred for 72 hours at room temperature, under argon and protected from light. The solvent was evaporated *in vacuo* and the residue redissolved in dichloromethane (20 ml). The mixture was washed with saturated sodium hydrogen carbonate (2×50 ml), separated and the organic layer concentrated *in vacuo*. The solid was analysed using TLC (silica, eluent: hexane/ CH_2Cl_2 , 1:1) which indicated a mixture of two components. The solid was further purified using flash column chromatography (silica, eluent: hexane/ CH_2Cl_2 , 1:1) to obtain the product as fraction A. The product was obtained as a red solid (0.01 g, 40 %) $R_f = 0.36$ (silica, eluent: hexane/ CH_2Cl_2 , 1:1); ^1H NMR [400 MHz, CDCl_3] δ 0.84 (3H, m, CH_3), 1.23 (30H, m, CH_2), 1.86 (2H, m, $\text{CH}_2\text{CH}_2\text{SH}$), 3.28 (2H, m, CH_2SH), 4.12 (3H, m, OCH_3), 7.37(2H, m, Ar- 3, 5-H), 7.5 (2H, m, Ar-2, 6-H), 8.15 (2H, s, βH), 9.1 (2H, s, βH), 9.38 (2H, s, βH), 9.44 (2H, s, βH), 10.38 (2H, s, meso-H); UV-vis (CH_2Cl_2) λ_{max} 405, 513, 547 nm; MS (MALDI-TOF) m/z 952.75 [calc'd for $\text{C}_{51}\text{H}_{54}\text{N}_4\text{F}_4\text{PdSO}$, M^+ 953.50].

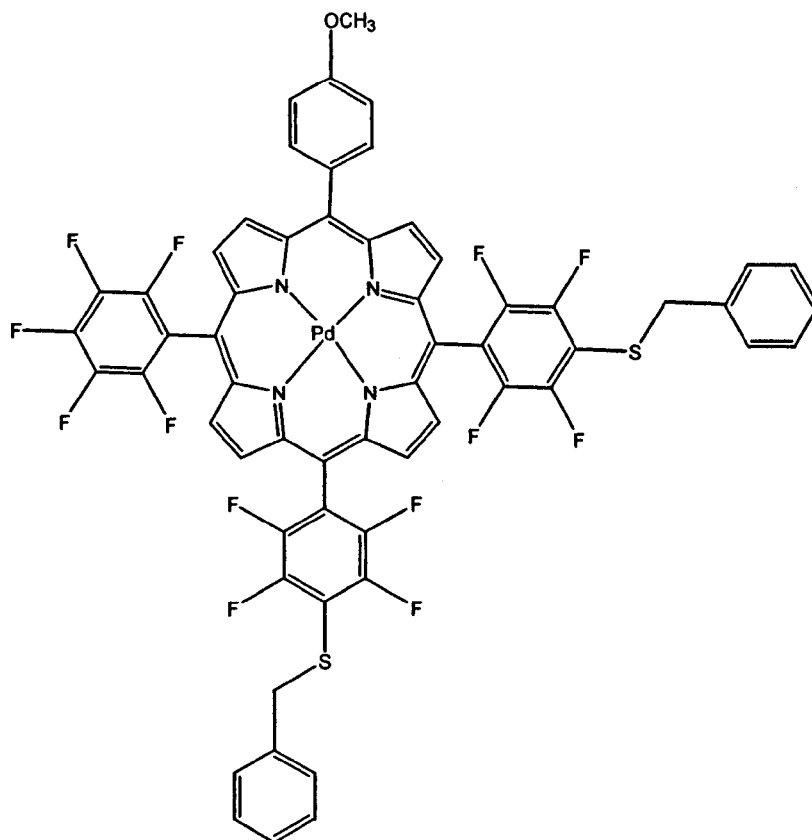
[71] Pd(II)-5-(4-benzylthio-2,3,5,6-tetrafluorophenyl)-10, 15-di-
(pentafluorophenyl)-20-(4-methoxyphenyl)porphyrin and

[72] Pd(II)-5, 10-di-(4-benzylthio-2,3,5,6-tetrafluorophenyl)-15-
(pentafluorophenyl)-20-(4-methoxyphenyl)porphyrin and

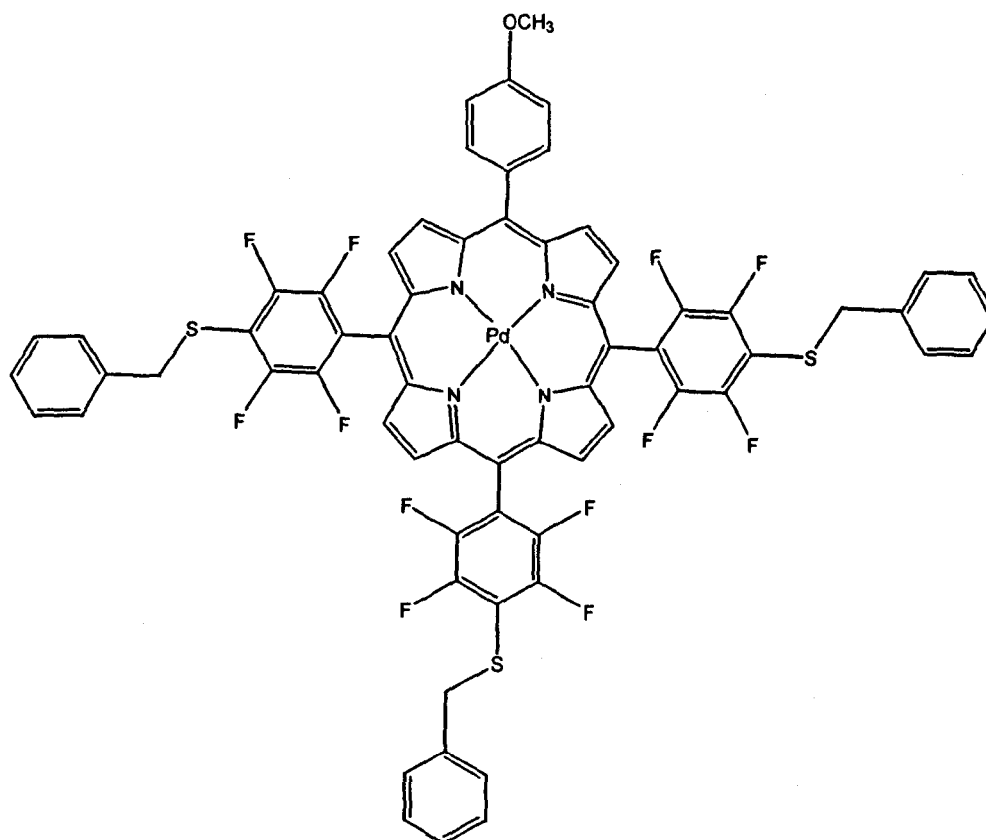
[73] Pd(II)-5, 10, 15-tris-(4-benzylthio-2,3,5,6-tetrafluorophenyl)-20-(4-
methoxyphenyl)porphyrin



Pd (II)-5-(4-benzylthio-2,3,5,6-tetrafluorophenyl)-10,15-(pentafluorophenyl)-20-(4-
methoxyphenyl)porphyrin



Pd (II)-5,10-(4-benzylthio-2,3,5,6-tetrafluorophenyl)-15-(pentafluorophenyl)-20-(4-methoxyphenyl)porphyrin



Pd(II)-5,10,15-(4-benzylthio-2,3,5,6-tetrafluorophenyl)-20-(4-methoxyphenyl)porphyrin

Pd(II)-5-(4-methoxyphenyl)-10, 15, 20-tris-(pentafluorophenyl)porphyrin (37 mg, 3.7×10^{-4} mol) was dissolved in anhydrous DMF (10 ml) to which benzylmercaptan (0.5 ml, 3.5×10^{-3} mol) was added. The mixture was stirred at room temperature under argon and protected from light for 24 hours. The solvent was evaporated *in vacuo* and the solid was redissolved in dichloromethane (10 ml). The mixture was washed with saturated sodium hydrogen carbonate (2 x 50 ml), separated and the organic layer concentrated *in vacuo*. The product was analysed using TLC (silica, eluent: hexane/CH₂Cl₂, 1:1). TLC analysis indicated a total of 6 products, which were further separated using preparative TLC. The

fractions were isolated, dissolved in dichloromethane and filtered through a silica column. Each fraction was then concentrated *in vacuo* to obtain the final products A-F.

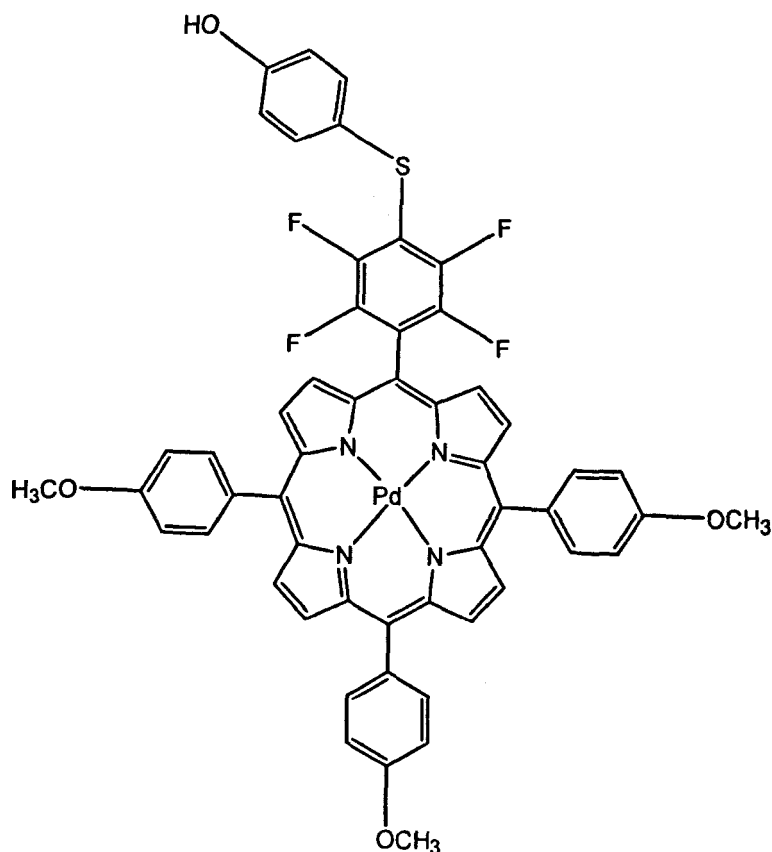
Fraction C was analysed to be the starting material and fraction D to be Pd (II)-5-(4-benzylthio-2,3,5,6-tetrafluorophenyl)-10,15-(pentafluorophenyl)-20-(4-methoxyphenyl)porphyrin. Fractions E and F were further analysed to be Pd (II)-5,10-(4-benzylthio-2,3,5,6-tetrafluorophenyl)-15-(pentafluorophenyl)-20-(4-methoxyphenyl)porphyrin and Pd(II)-5,10,15-(4-benzylthio-2,3,5,6-tetrafluorophenyl)-20-(4-methoxyphenyl)porphyrin respectively.

Fraction D (0.01 g, 8 %); Rf = 0.65 (silica, eluent: hexane/CH₂Cl₂, 1:1); ¹H NMR [400 MHz, CDCl₃] δ 4.11 (3H, s, CH₃), 4.42 (2H, m, CH₂Ph), 7.29 (2H, m, Ar- 3, 5-H), 7.49 (5H, m, Ph-H), 8.09 (2H, m, Ar-2, 6-H), 8.71 (2H, m, βH), 8.84 (4H, m, βH), 8.98 (2H, m, βH); UV-vis (CH₂Cl₂) λ_{max} 411, 521, 554 nm; MS (MALDI-TOF) *m/z* 1122.4 [calc'd for PdC₅₂H₂₂OSN₄F₁₄, M⁺ 1123.23].

Fraction E (0.01 g, 9 %); Rf = 0.6 (silica, eluent: hexane/CH₂Cl₂, 1:1); ¹H NMR [400 MHz, CDCl₃] δ 4.12 (3H, s, CH₃), 4.42 (4H, m, CH₂Ph), 7.29 (2H, m, Ar- 3, 5-H), 7.49 (10H, m, Ph-H), 8.09 (2H, m, Ar-2, 6-H), 8.64 (2H, m, βH), 8.82 (4H, m, βH), 8.96 (2H, m, βH); UV-vis (CH₂Cl₂) λ_{max} 411, 521, 554 nm; MS (MALDI-TOF) *m/z* 1226.5 [calc'd for PdC₅₉H₂₉OS₂N₄F₁₃, M⁺ 1227.43].

Fraction F (0.01 g, 2 %); Rf = 0.53 (silica, eluent: hexane/CH₂Cl₂, 1:1); ¹H NMR [400 MHz, CDCl₃] δ 4.12 (3H, s, CH₃), 4.43 (6H, m, CH₂Ph), 7.29 (2H, m, Ar- 3, 5-H), 7.56 (15H, m, Ph-H), 8.07 (2H, m, Ar-2, 6-H), 8.63 (2H, m, βH), 8.69 (4H, m, βH), 8.95 (2H, m, βH); UV-vis (CH₂Cl₂) λ_{max} 411, 521, 554 nm; MS (MALDI-TOF) *m/z* 1330.6 [calc'd for PdC₆₆H₃₆OS₃N₄F₁₂ M⁺ 1331.62].

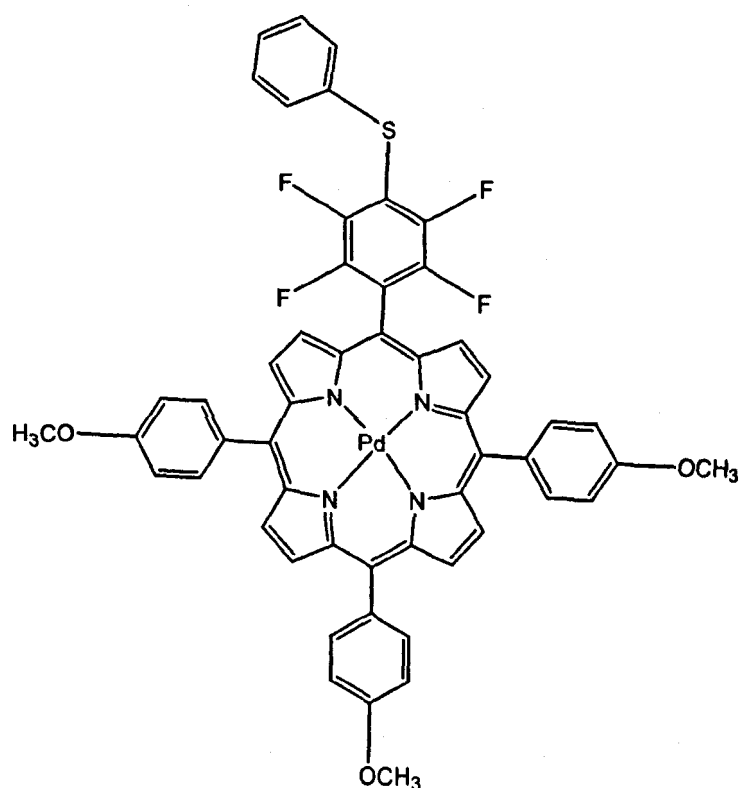
[74] Pd(II)-5-(4-thiophenol-2,3,5,6-tetrafluorophenyl)-10,15,20-tris-(4-methoxyphenyl)porphyrin



Palladium-5-(pentafluorophenyl)-10,15,20-(4-methoxyphenyl)porphyrin (0.01 g, 1.1×10^{-5} mol) was added in anhydrous DMF (5 ml). Thiophenol (1.7×10^{-3} g, 1.26×10^{-5} mol) was added and the mixture stirred for 72 hours at room temperature, under argon and protected from light. The solvent was evaporated *in vacuo* and the residue redissolved in dichloromethane (20 ml). The mixture was washed with saturated sodium hydrogen carbonate (2×50 ml) and the organic layer concentrated *in vacuo*. The product was obtained as a red solid (0.01 g, 30%) $R_f = 0.7$ (silica, eluent: hexane/ CH_2Cl_2 , 1:1); ^1H

NMR [400 MHz, CDCl₃] δ 4.09 (9H, m, OCH₃), 6.97 (2H, m, Ar-H), 7.31 (6H, m, Ar-3, 5-H), 7.6 (2H, m, Ar-H), 8.09 (6H, m, Ar-2, 6-H), 8.8 (2H, s, β H), 8.89 (4H, s, β H), 8.95 (2H, s, β H); UV-vis (CH₂Cl₂) λ_{\max} 420, 475, 525 nm; MS (MALDI-TOF) m/z 1004.69 [calc'd for C₅₃H₃₄N₄F₄PdSO₄, M⁺ 1005.35].

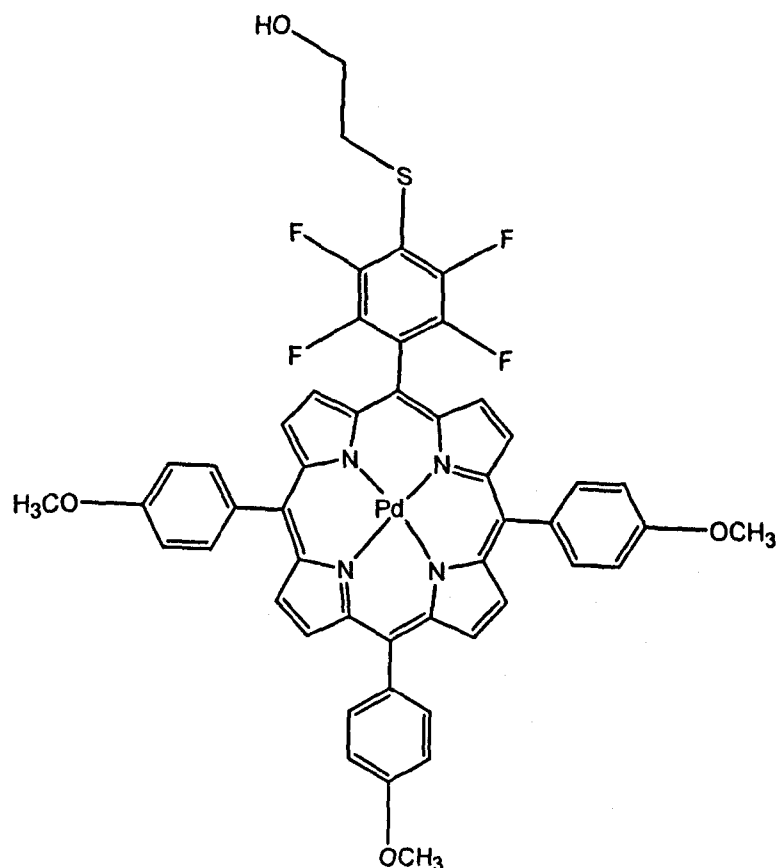
[75] Pd(II)-5-(4-thiobenzene-2,3,5,6-tetrafluorophenyl)-10,15,20-tris-(4-methoxyphenyl)porphyrin



Palladium-5-(pentafluorophenyl)-10,15,20-(4-methoxyphenyl)porphyrin (0.01 g, 1.1×10^{-5} mol) was added in anhydrous DMF (5 ml). Benzenethiol (1.37×10^{-3} ml, 1.33×10^{-5} mol) was added and the mixture stirred for 72 hours at room temperature, under argon

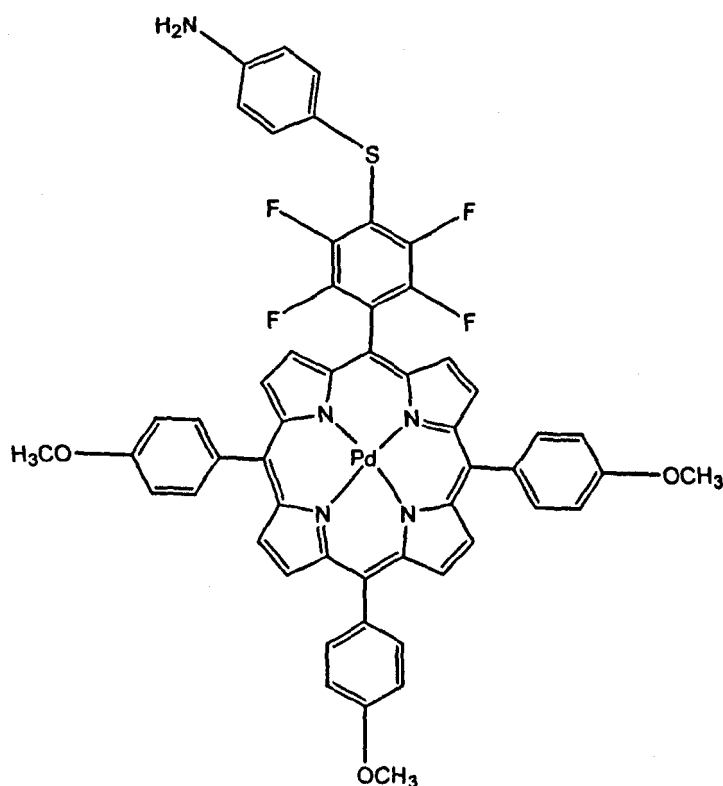
and protected from light . The solvent was evaporated *in vacuo* and the residue redissolved in dichloromethane (20 ml). The mixture was washed with saturated sodium hydrogen carbonate (2 × 50 ml), separated and the organic layer concentrated *in vacuo*. The product was obtained as a red solid (0.01 g, 40 %) $R_f = 0.63$ (silica, eluent: hexane/ CH_2Cl_2 , 1:1); $^1\text{H NMR}$ [400 MHz, CDCl_3] δ 4.09 (9H, m, OCH_3), 7.30 (6H, m, Ar- 3, 5-H), 7.34 (2H, m, Ar-H), 7.52 (2H, m, Ar-H), 8.1 (6H, m, Ar-2, 6-H), 9.0 (2H, s, βH), 9.1(4H, s, βH), 9.2 (2H, s, βH); UV-vis (CH_2Cl_2) λ_{max} 420, 475, 525 nm; MS (MALDI-TOF) m/z 988.7 [calc'd for $\text{C}_{53}\text{H}_{34}\text{N}_4\text{F}_4\text{PdSO}_3$, M^+ 989.35].

[76] Pd(II)-5-[4-(2 hydroxyethylthio)-2,3,5,6-tetrafluorophenyl]-10,15,20-tris-(4-methoxyphenyl)phenylporphyrin



Palladium-5-(pentafluorophenyl)-10,15,20-tris-(4-methoxyphenyl)porphyrin (0.01 g, 1.1×10^{-5} mol) was added in anhydrous DMF (5 ml). 2-Mercaptoethanol (9.4×10^{-4} ml, 1.34×10^{-5} mol) was added and the mixture stirred for 72 hours at room temperature, under argon and protected from light. The solvent was evaporated *in vacuo* and the residue redissolved in dichloromethane (20 ml). The mixture was washed with saturated sodium hydrogen carbonate (2×50 ml), separated and the organic layer concentrated *in vacuo*. The product was obtained as a red solid (0.01 g, 60 %) Rf = 0.72 (silica, eluent: hexane/CH₂Cl₂, 1:1); ¹H NMR [400 MHz, CDCl₃] δ 3.4 (2H, m, SCH₂), 4.0 (2H, m, CH₂OH), 4.09 (9H, m, OCH₃), 7.3 (6H, m, Ar- 3, 5-H), 8.09 (6H, m, Ar-2, 6-H), 8.78 (2H, s, βH), 8.88 (4H, s, βH), 8.96 (2H, s, βH); UV-vis (CH₂Cl₂) λ_{max} 420, 475, 525 nm; MS (MALDI-TOF) m/z 956.68 [calc'd for C₄₉H₃₄N₄F₄PdSO₄, M⁺ 957.31].

[77] Pd(II)-5-(4-aminobenzenethio-2,3,5,6-tetrafluorophenyl)-10,15,20-tris-(4-methoxyphenyl)porphyrin

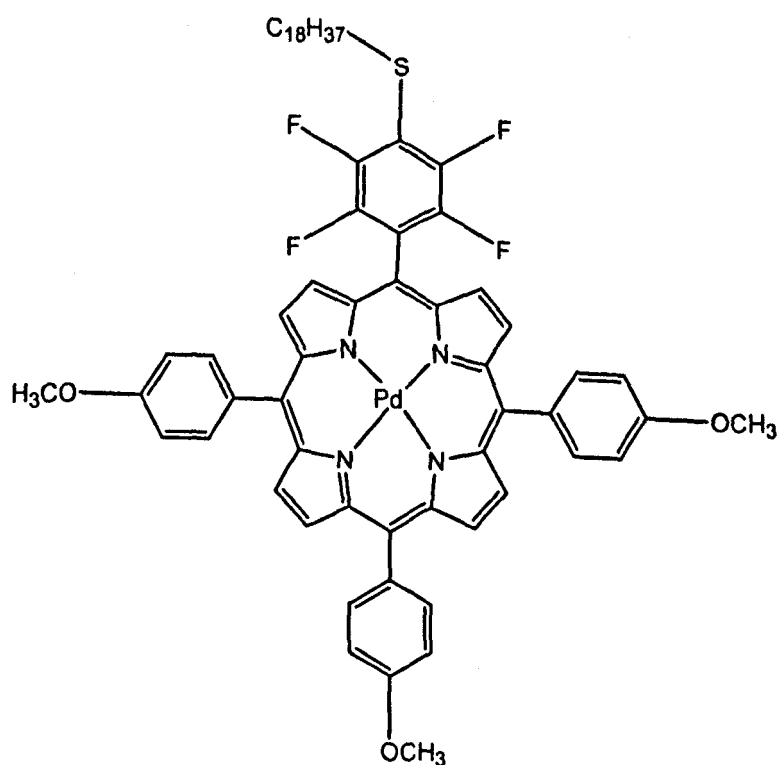


Pd(II)-5-(Pentafluorophenyl)-10,15,20-tris-(4_methoxyphenyl)porphyrin (0.02 g, 2.2×10^{-5} mol) was added in anhydrous DMF (5ml). 4-Aminobenzenethiol (3.34×10^{-3} g, 2.7×10^{-5} mol) was added and the mixture stirred at room temperature for 72 hours, under argon and protected from light . The solvent was evaporated *in vacuo* and the residue redissolved in dichloromethane (20 ml). The mixture was washed with saturated sodium hydrogen carbonate (2×50 ml), separated and the organic layer concentrated *in vacuo*. The product was analysed using TLC (silica, eluent: hexane/ CH_2Cl_2 , 1:1). TLC analysis indicated a mixture of products which were further purified using flash column chromatography (silica, eluent: hexane/ CH_2Cl_2 , 1:1) to yield the 6 fractions which were

collected, concentrated *in vacuo* and analysed. .

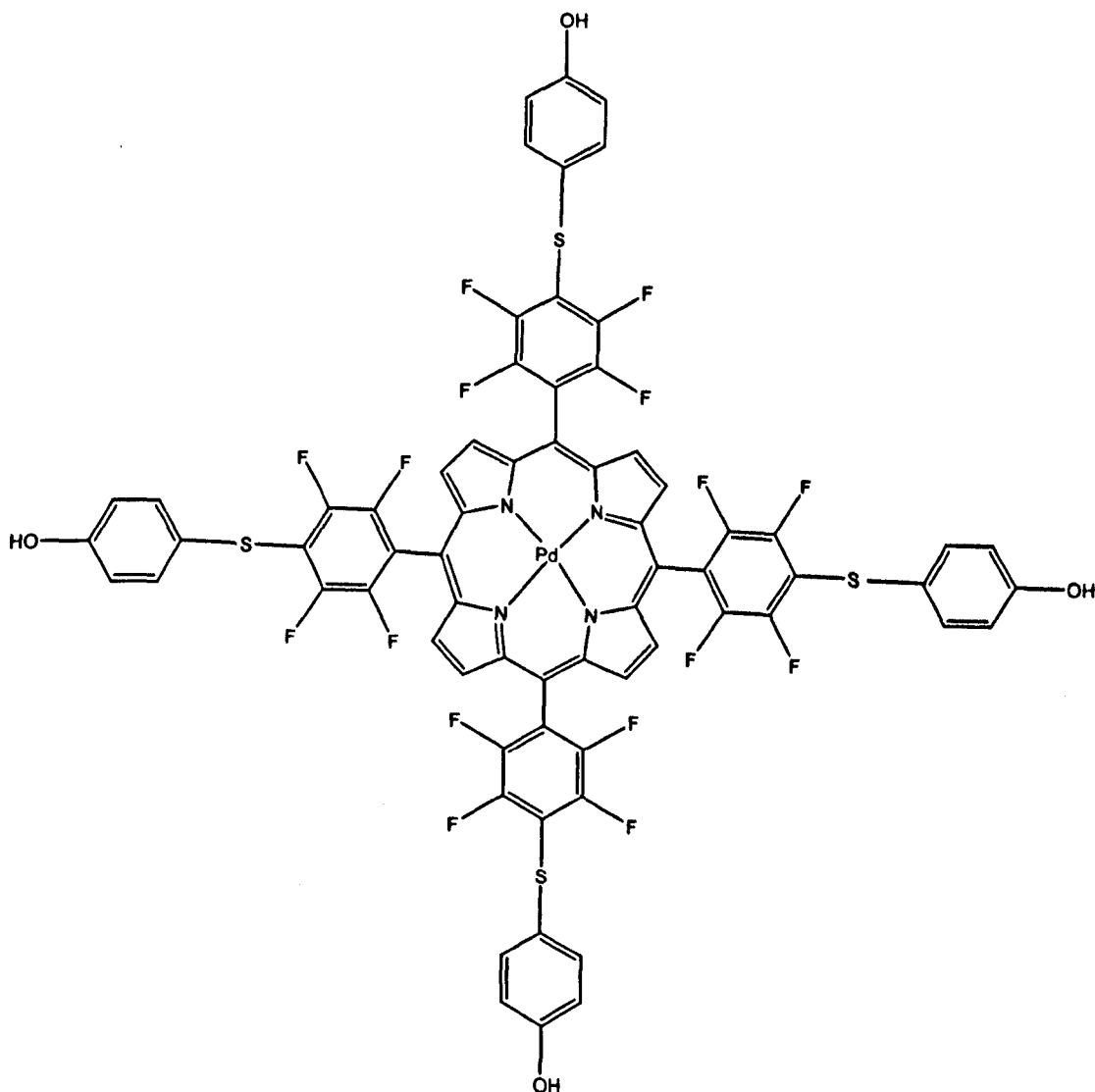
Fraction C was analysed as the desired product (0.01 g, 41 %) Rf = 0.8 (silica, eluent: hexane/CH₂Cl₂, 1:1); ¹H NMR [400 MHz, CDCl₃] δ 4.09 (2H, br s, NH₂), 4.10 (9H, br s, OCH₃), 7.22 (2H, m, Ar- 3, 5-H), 7.30 (6H, m, Ar-10, 15, 20-3,5-H), 7.68 (2H, m, Ar-2, 6-H), 8.09 (6H, m, Ar-10, 15, 20-2,6-H), 8.73 (2H, s, βH), 8.85 (4H, m, βH), 8.93 (2H, m, βH); UV-vis (CH₂Cl₂) λ_{max} 420, 525, 557 nm; MS (MALDI-TOF) m/z 1003.65 [calc'd for C₅₃H₃₅O₃N₅F₄SPd, M⁺ 1004.37].

[78] Pd(II)-5-(4-octadecylthio-2,3,5,6-tetrafluorophenyl)-tris-10,15,20-(4-methoxyphenyl)porphyrin



Palladium-5-(pentafluorophenyl)-10,15,20-tris-(4-methoxyphenyl)porphyrin (0.02 g, 2.2×10^{-5} mol) was added in anhydrous DMF (5 ml). Octadecanethiol (9 mg, 2.7×10^{-5} mol) was added and the mixture stirred for 72 hours at room temperature, under argon and protected from light. The solvent was evaporated *in vacuo* and the residue redissolved in dichloromethane (20 ml). The mixture was washed with saturated sodium hydrogen carbonate (2×50 ml), separated and the organic layer concentrated *in vacuo*. The solid was analysed using TLC (silica, eluent: hexane/ CH_2Cl_2 , 1:1) which indicated a mixture of three components. The solid was further purified using flash column chromatography (silica, eluent: hexane/ CH_2Cl_2 , 1:1) to obtain the product as the first eluting fraction. The product was obtained as a red solid (0.01 g, 35 %); $R_f = 0.82$ (silica, eluent: hexane/ CH_2Cl_2 , 1:1); $^1\text{H NMR}$ [400 MHz, CDCl_3] δ 0.84 (3H, m, CH_3), 1.23 (30H, m, CH_2), 1.88 (2H, m, $\text{CH}_2\text{CH}_2\text{SH}$), 3.27 (2H, m, CH_2SH), 4.08 (9H, m, OCH_3), 7.31 (6H, m, Ar-3, 5-H), 8.09 (6H, m, Ar-2, 6-H), 8.79 (2H, s, βH), 8.88 (4H, s, βH), 8.90 (2H, s, βH); UV-vis (CH_2Cl_2) λ_{max} 419, 476, 525 nm; MS (MALDI-TOF) m/z 1164.92 [calc'd for $\text{C}_{65}\text{H}_{66}\text{N}_4\text{F}_4\text{PdSO}_3$, M^+ 1165.74].

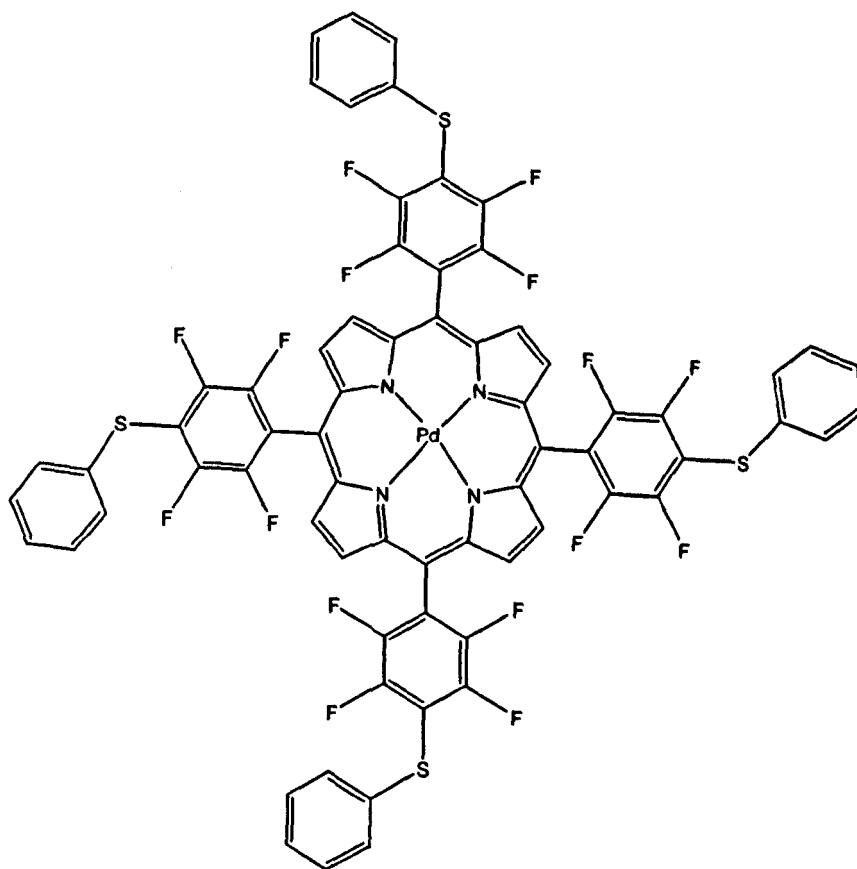
[79] Pd(II)-5,10,15,20-(4-thiophenol-2,3,5,6-tetrafluorophenyl)porphyrin



Pd(II)-5,10,15,20-tetra-(pentafluorophenyl)porphyrin (20 mg, 1.85×10^{-5} mol) was dissolved in anhydrous DMF (5 ml) to which mercaptophenol ($10 \mu\text{l}$, 9.3×10^{-5} mol) was added. The mixture was stirred at room temperature under argon and protected from light for 18 hours. The solvent was evaporated *in vacuo* and the solid redissolved into dichloromethane (10 ml). The mixture was washed with saturated sodium hydrogen

carbonate (2 X 50 ml), separated and the organic layer dried *in vacuo*. The product was analysed using TLC (silica, eluent: hexane/CH₂Cl₂, 1:1). TLC analysis indicated a single product (0.01 g, 25 %); R_f = 0.72 (silica, eluent: hexane/CH₂Cl₂, 1:1); ¹H NMR [400 MHz, CDCl₃] δ 6.79 (2H, d, *J** = 8.5 Hz Ar-H), 7.36 (2H, d, *J** = 8.5 Hz Ar-II), 8.87 (8H, m, βH); UV-vis (CH₂Cl₂) λ_{max} 411, 521, 554 nm; MS (MALDI-TOF) *m/z* 1502.8 [calc'd for PdC₆₈H₂₈S₄O₄N₄F₁₆, M⁺ 1503.63].

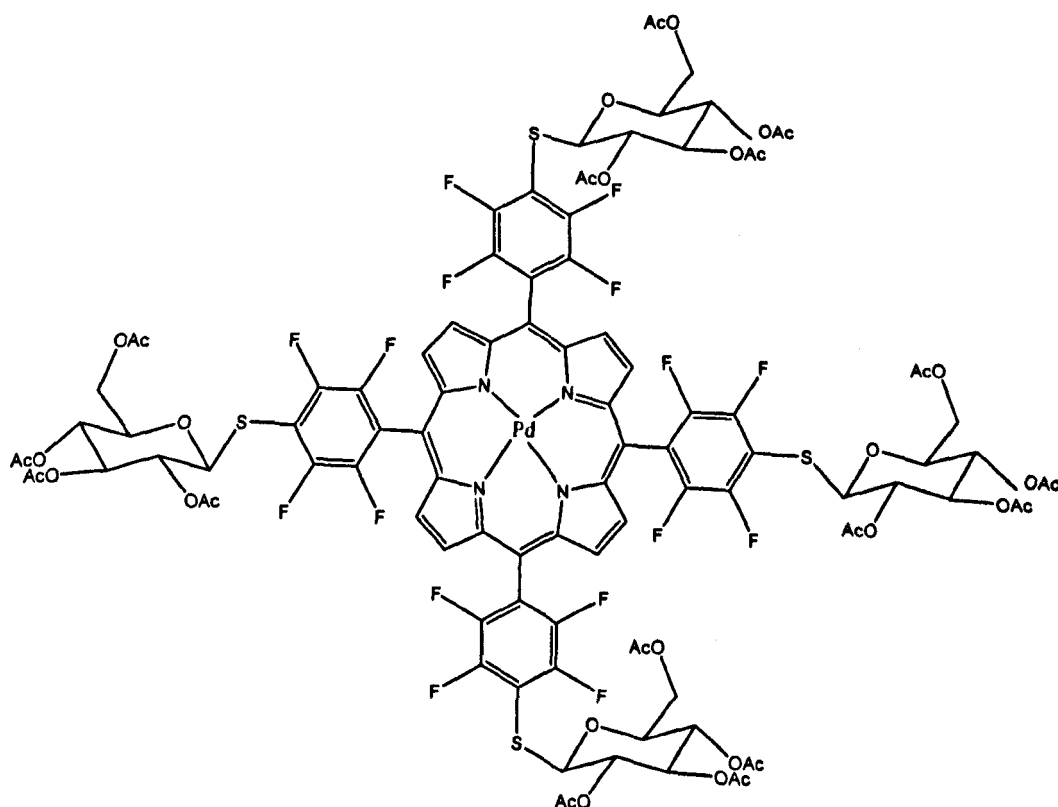
[80] Pd(II)-5,10,15,20-tetra-(4-benzenethio-2,3,5,6-tetrafluorophenyl)porphyrin



Palladium 5,10,15,20-(tetrapentafluorophenyl)porphyrin (0.14 g, 9.6 × 10⁻⁵ mol) was added in anhydrous DMF (10ml). Benzene thiol (0.64 ml, 4.8 × 10⁻⁴ mol) was added and

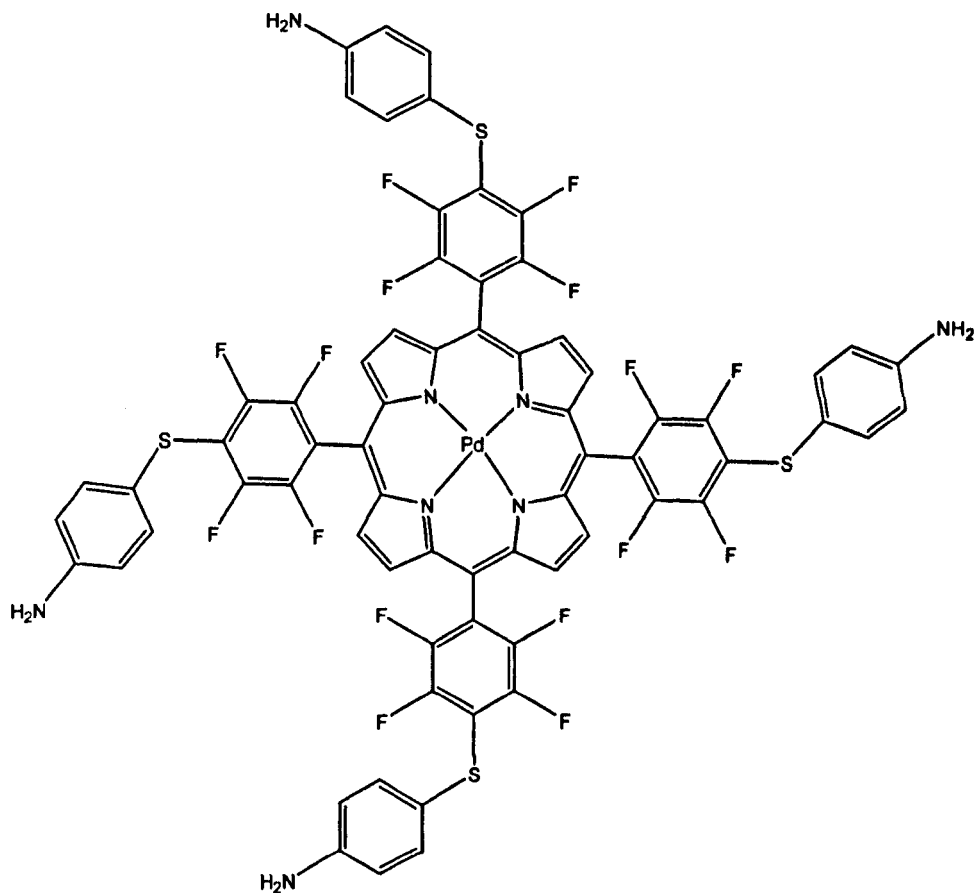
the mixture stirred for 72 hours at room temperature, under argon and protected from light. The solvent was evaporated *in vacuo* and the residue redissolved in dichloromethane (20 ml). The mixture was washed with saturated sodium hydrogen carbonate (2 × 50 ml), separated and the organic layer concentrated *in vacuo*. The product was analysed using TLC (silica, eluent: hexane/CH₂Cl₂, 1:1). The product was obtained as a reddish solid (0.01 g, 9 %) R_f = 0.8 (silica, eluent: hexane/CH₂Cl₂, 1:1); ¹H NMR [400 MHz, CDCl₃] δ 7.63 (8H, m, Ar- 3, 5-H), 7.71 (8H, m, Ar-2, 6-H), 8.89 (8H, s, βH); UV-vis (CH₂Cl₂) λ_{max} 411, 421, 554 nm; MS (MALDI-TOF) *m/z* 1439.63 [calc'd for PdC₆₈H₂₈S₄N₄F₁₆, M⁺ 1440.6].

[81] Pd(II)-5,10,15,20-tetrakis[4-(2', 3', 4', 6'-tetra-*O*-acetyl-β-D-glucopyranosylthio)-2,3,5,6-tetrafluorophenyl]porphyrin



Pd(II)-5,10,15,20-Tetra(pentafluorophenyl)porphyrin (20 mg, 1.86×10^{-4} mol) was dissolved in anhydrous DMF (3 ml). 2,3,4,6-Tetra-*O*-acetyl- β -D-thioglucopyranose (6 eq, 44 mg, 1.23×10^{-4} mol) in DMF (3 ml) was added. The solution was stirred at room temperature and the reaction monitored by TLC. After 18 hours, the solvent was evaporated in *vacuo*, followed by separation using preparative TLC (silica eluent: toluene/acetone, 8:2) to yield the desired product as a purple brown solid (20 mg, 44 %); $R_f = 0.20$ (silica, eluent: toluene/acetone, 8:2); mp > 350 °C decomp; $^1\text{H NMR}$ [400 MHz, CDCl_3] δ 2.04 (12H, s, OAc), 2.05 (12H, s, OAc), 2.06 (12H, s, OAc), 2.18 (12H, s, OAc), 4.1 (4H, m, H-5'ose), 4.3 (8H, m, H-6_a' and H-6_b' ose), 5.20 (4H, t, $J^* = 10.1$ Hz, H-4'ose), 5.26 (8H, m, H-1', 2' ose), 5.4 (4H, t, $J^* = 9.3$ Hz, H-3'ose), 9.2 (8H, br s, βH); MS (MALDI-TOF) m/z 2456.5 [calc'd for $\text{PdC}_{100}\text{H}_{84}\text{N}_4\text{F}_{16}\text{S}_4\text{O}_{36}$, M^+ 2456.40].

[82] Pd(II)-5,10,15,20-tetra-(4-aminobenzenethio-2,3,5,6-tetrafluorophenyl)porphyrin



Palladium 5,10,15,20-(tetrapentafluorophenyl)porphyrin (0.05 g, 4×10^{-5} mol) was added in anhydrous DMF (5 ml). 4-Aminobenzenethiol (0.03 g, 2.2×10^{-4} mol) was added and the mixture stirred for 72 hours at room temperature, under argon and protected from light. The solvent was evaporated *in vacuo* and the residue redissolved into dichloromethane (20 ml). The mixture was washed with saturated sodium hydrogen carbonate (2×50 ml) and the organic layer concentrated *in vacuo*. The solid was analysed using TLC (silica, eluent: hexane/ CH_2Cl_2 , 1:1) which indicated a mixture of five

components. The solid was further purified using flash column chromatography (silica, eluent: hexane/CH₂Cl₂, 1:1) to obtain the product as fraction E. The product was obtained as a reddish solid (0.02 g, 33 %) R_f = 0.82 (silica, eluent: hexane/CH₂Cl₂, 1:1); ¹H NMR [400 MHz, CDCl₃] δ 4.09 (8H, br s, NH₂), 6.77 (8H, m, Ar- 3, 5-H), 7.63 (8H, m, Ar-2, 6-H), 8.92 (8H, s, βH); UV-vis (CH₂Cl₂) λ_{max} 411, 521, 554 nm; MS (MALDI-TOF) *m/z* 1498.63 [calc'd for PdC₆₈H₃₂S₄N₈F₁₆, found.1499.69].

[83] Pd(II)-5-(4-benzylthio-2,3,5,6-tetrafluorophenyl)-10,15,20-

(pentafluorophenyl)porphyrin and

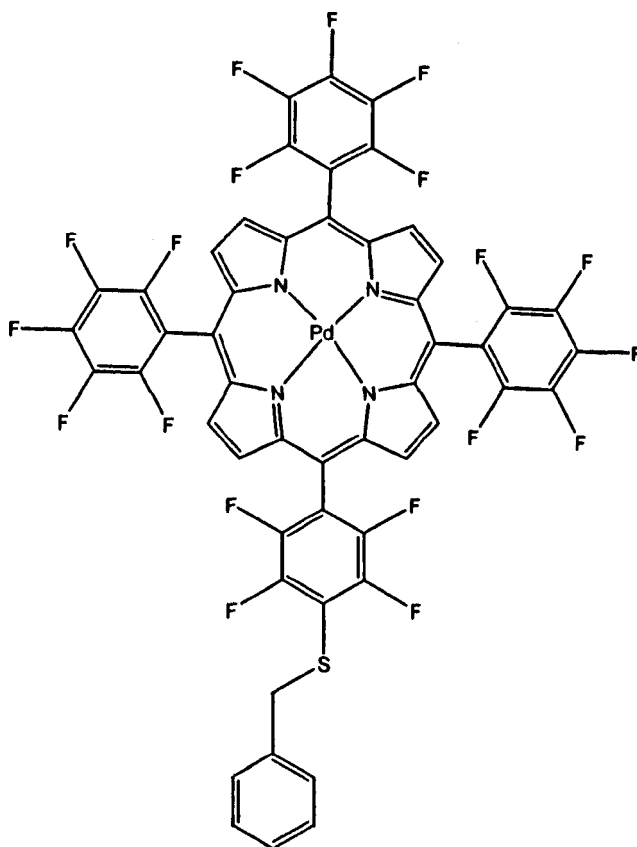
[84] Pd(II)-5,10-di-(4-benzylthio-2,3,5,6-tetrafluorophenyl)-15,20-di-

(pentafluorophenyl)porphyrin and

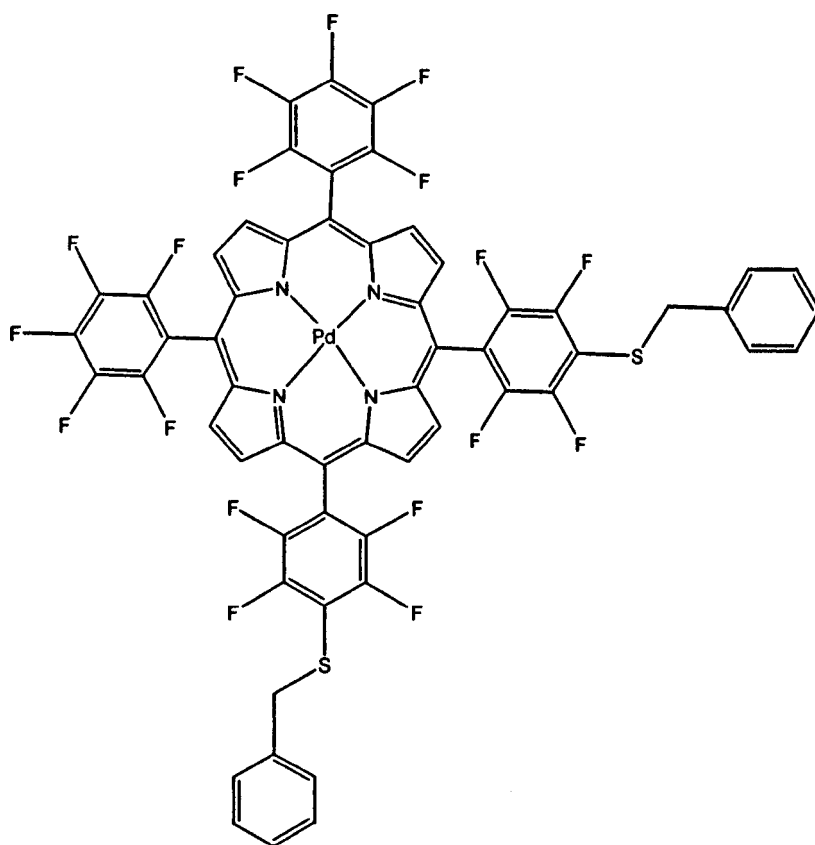
[85] Pd(II)-5,10,15-tris-(4-benzylthio-2,3,5,6-tetrafluorophenyl)-20-

(pentafluorophenyl)porphyrin and

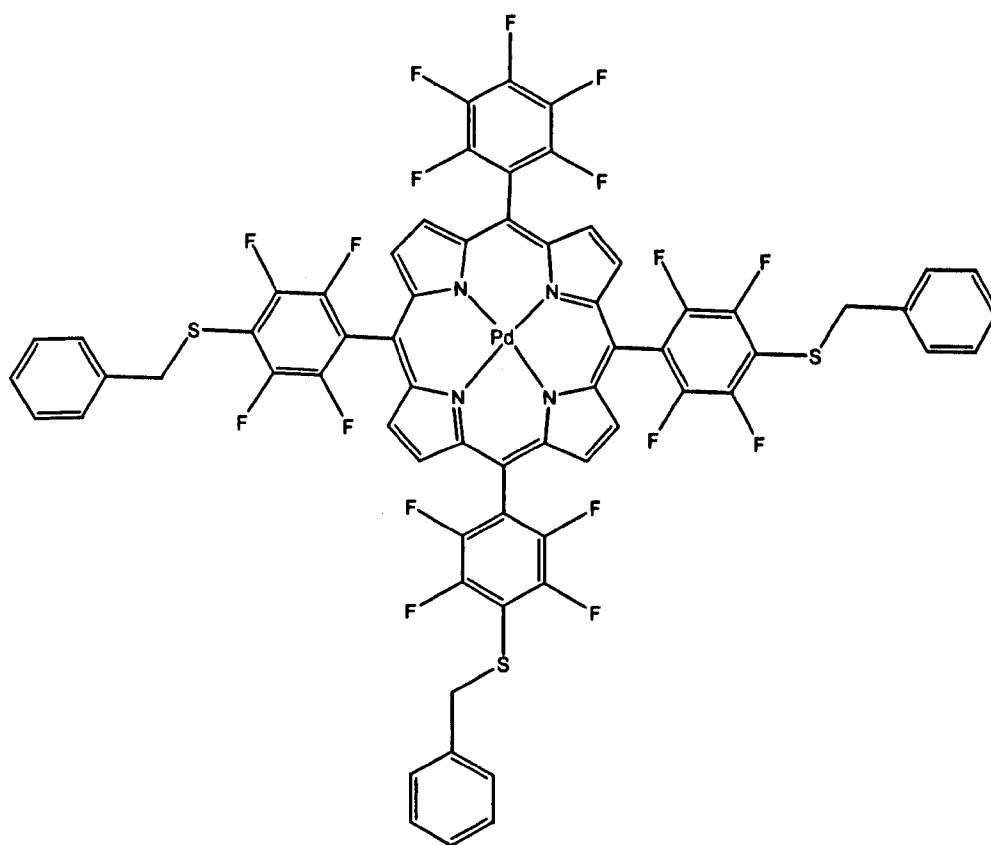
[86] Pd(II)-5,10,15,20-tetra-(4-benzylthio-2,3,5,6-tetrafluorophenyl)porphyrin



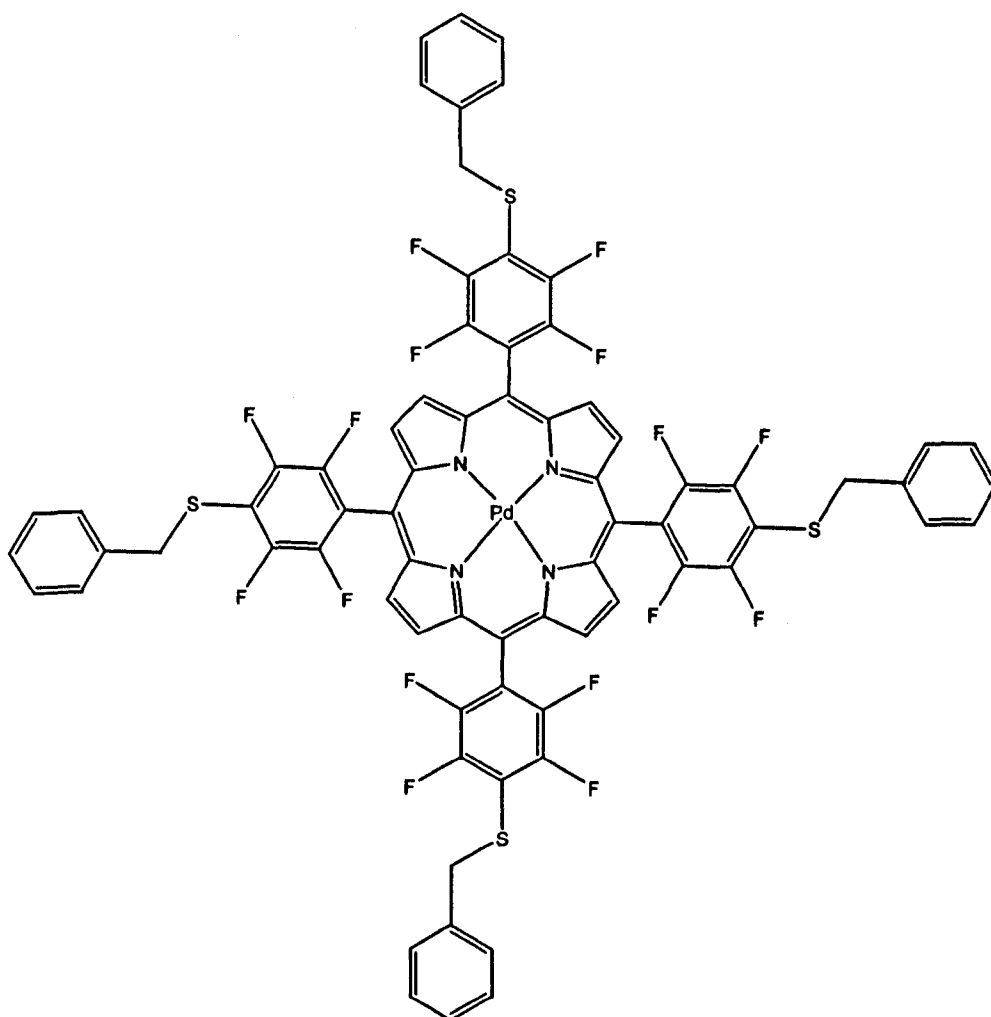
Pd(II)-5- (4-benzylthio-2,3,5,6-tetrafluorophenyl)-10,15,20-(pentafluorophenyl)porphyrin



Pd(II)-5,10-di-(4-benzylthio-2,3,5,6-tetrafluorophenyl)-15,20-di-(pentafluorophenyl)porphyrin



Pd(II)-5,10,15 -tris-(4-benzylthio-2,3,5,6-tetrafluorophenyl)-20-(pentafluorophenyl)porphyrin



Pd(II)-5,10,15,20-(4-benzylthio-2,3,5,6-tetrafluorophenyl)porphyrin

Pd(II)-5,10,15,20-tetra-(pentafluorophenyl)porphyrin (20 mg, 1.85×10^{-5} mol) was dissolved in anhydrous DMF (5 ml) to which benzylmercaptan (10 μ l, 9.3×10^{-5} mol) was added. The mixture was stirred at room temperature under argon and protected from light for 18 hours. The solvent was evaporated *in vacuo* and the solid was then redissolved in dichloromethane (10 ml). The mixture was washed with saturated sodium hydrogen carbonate (2 \times 50 ml), separated and the organic layer concentrated *in vacuo*. The solid was analysed using TLC (silica, eluent: hexane/CH₂Cl₂, 1:1) which indicated a

total of 5 products. The mixture was further separated using preparative TLC. The fractions were isolated, dissolved into dichloromethane and filtered through a silica column. Each fraction was then concentrated *in vacuo* to obtain the products A-E. Fraction A was analysed to be the starting material and as expected, the following fractions were mono-, di-, tri- and tetra- thiol substituted porphyrins respectively.

Fraction A, which eluted near the solvent line $R_f = 0.9$ as mentioned earlier was found to be the unreacted starting material.

Fraction B (0.01 g, 25 %); $R_f = 0.56$ (silica, eluent: hexane/ CH_2Cl_2 , 1:1); $^1\text{H NMR}$ [400 MHz, CDCl_3] δ 4.42 (2H, m, CH_2Ph), 7.50 (5H, m, Ph-H), 8.76 (2H, m, βH), 8.87 (6H, m, βH); UV-vis (CH_2Cl_2) λ_{max} 406, 519, 552 nm; MS (MALDI-TOF) m/z 1182.6 [calc'd for $\text{PdC}_{51}\text{H}_{15}\text{SN}_4\text{F}_{19}$, M^+ 1183.15].

Fraction C (0.01 g, 17 %); $R_f = 0.46$ (silica, eluent: hexane/ CH_2Cl_2 , 1:1); $^1\text{H NMR}$ [400 MHz, CDCl_3] δ 4.36 (4H, m, CH_2Ph), 7.43 (10H, m, Ph-H), 8.68 (4H, m, βH), 8.79 (4H, m, βH); UV-vis (CH_2Cl_2) λ_{max} 406, 519, 552 nm; MS (MALDI-TOF) m/z 1286.7 [calc'd for $\text{PdC}_{58}\text{H}_{22}\text{S}_2\text{N}_4\text{F}_{18}$, M^+ 1287.35].

Fraction D (0.01 g, 8 %); $R_f = 0.36$ (silica, eluent: hexane/ CH_2Cl_2 , 1:1); $^1\text{H NMR}$ [400 MHz, CDCl_3] δ 4.36 (6H, m, CH_2Ph), 7.42 (15H, m, Ph-H), 8.66 (6H, m, βH), 8.77 (2H, m, βH); UV-vis (CH_2Cl_2) λ_{max} 406, 519, 552 nm; MS (MALDI-TOF) m/z 1390.8 [calc'd for $\text{PdC}_{65}\text{H}_{29}\text{S}_3\text{N}_4\text{F}_{17}$, M^+ 1391.54].

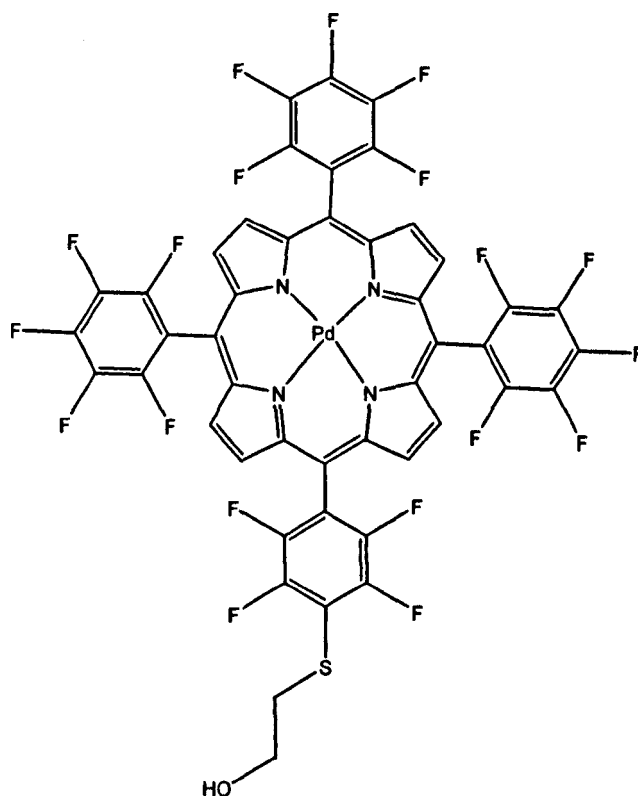
Fraction E (0.01 g, 36 %); $R_f = 0.28$ (silica, eluent: hexane/ CH_2Cl_2 , 1:1); $^1\text{H NMR}$ [400 MHz, CDCl_3] δ 4.38 (8H, m, CH_2Ph), 7.45 (20H, m, Ph-H), 8.66 (8H, br s, βH); UV-vis

(CH₂Cl₂) λ_{max} 406, 519, 552 nm; MS (MALDI-TOF) m/z 1496.8 [calc'd for PdC₇₂H₃₆S₄N₄F₁₆, M⁺ 1495.74].

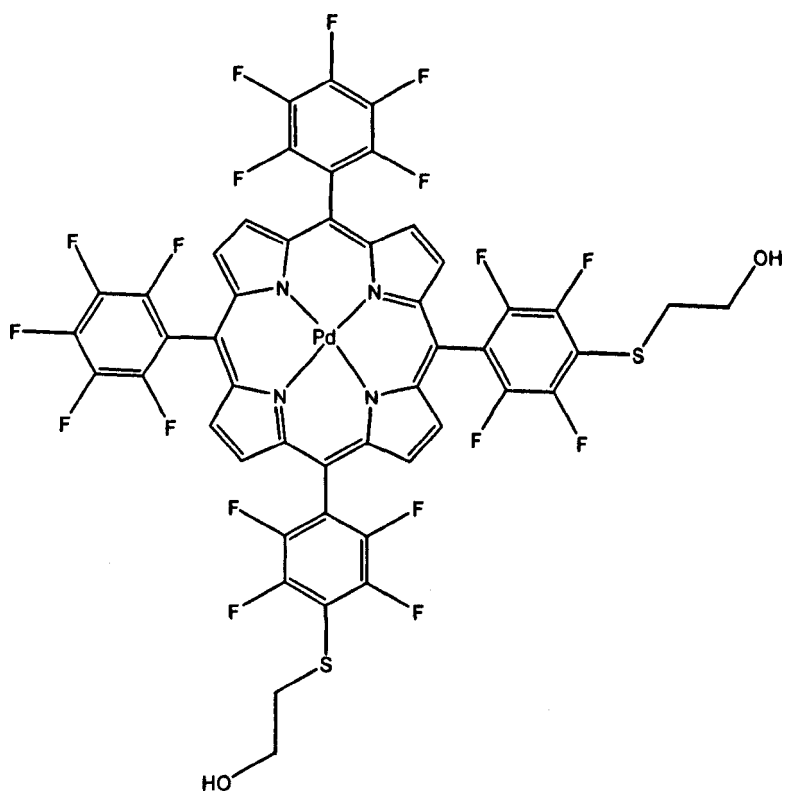
[87] Pd(II)-5-[4-(2-hydroxyethylthio)-2,3,5,6-tetrafluorophenyl]-10,15,20-tris-(pentafluorophenyl)porphyrin and

[88] Pd(II)-5,10-di-[4-(2-hydroxyethylthio)-2,3,5,6-tetrafluorophenyl]-15,20-di-(pentafluorophenyl)porphyrin and

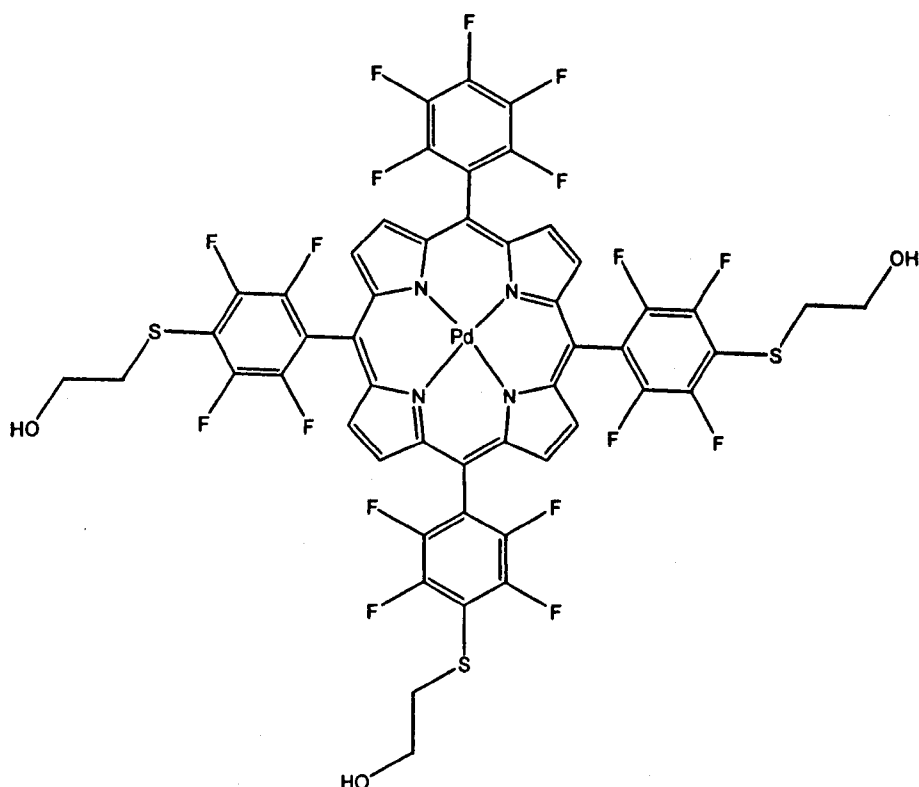
[89] Pd(II)-5,10,15-tris-[4-(2-hydroxyethylthio)-2,3,5,6-tetrafluorophenyl]-20-(pentafluorophenyl)porphyrin



Pd(II)-5-[4-(2-hydroxyethyl)thio-2,3,5,6-tetrafluorophenyl]-10,15,20-(pentafluorophenyl)porphyrin



Pd(II)-5,10-di-[4-(2-hydroxyethyl)thio-2,3,5,6-tetrafluorophenyl]-15,20-di-(pentafluorophenyl)porphyrin



Pd(II)-5,10,15 -tris-[4-(2-hydroxyethyl)thio-2,3,5,6-tetrafluorophenyl]-20-(pentafluorophenyl)porphyrin

Pd(II)-5,10,15,20-tetra-(pentafluorophenyl)porphyrin (20 mg, 1.85×10^{-5} mol) was dissolved in anhydrous DMF (5 ml) to which 2-mercaptoethanol (10 μ l, 0.1 mmol) was added. The mixture was stirred at room temperature under argon and protected from light for 18 hours. The solvent was evaporated *in vacuo* and the solid redissolved in dichloromethane (20 ml). The mixture was washed with saturated sodium hydrogen carbonate (2 \times 50 ml), separated and the organic layer dried *in vacuo*. The solid was analysed using TLC (silica, eluent: hexane/ CH_2Cl_2 , 1:1) which indicated a total of 4 products. The four products were further separated using preparative TLC. The fractions

were isolated, dissolved in dichloromethane and filtered through a silica column. Each fraction was then concentrated to obtain the products A-D. Fraction A was analysed to be the starting material and as expected, the following fractions were mono-, di-, and tri-thiol substituted porphyrins respectively. In this occasion, the tetra-thiol substituted product was not obtained.

Fraction A, which eluted near the solvent line $R_f = 0.9$ as mentioned earlier was found to be the unreacted starting material.

Fraction B (0.01 g, 33 %); $R_f = 0.56$ (silica, eluent: hexane/ CH_2Cl_2 , 1:1); $^1\text{H NMR}$ [400 MHz, CDCl_3] δ 3.46 (2H, t, $J^* = 5.5\text{Hz}$, SCH_2), 4.05 (2H, m, CH_2OH), 8.92 (8H, br s, βH); MS (MALDI-TOF) m/z 1136.5 [calc'd for $\text{PdC}_{46}\text{H}_{13}\text{SN}_4\text{F}_{19}$, M^+ 1137.08].

Fraction C (0.01 g, 41 %); $R_f = 0.67$ (silica, eluent: hexane/ CH_2Cl_2 , 1:1); $^1\text{H NMR}$ [400 MHz, CDCl_3] δ 3.46 (4H, t, $J^* = 5.5\text{Hz}$, SCH_2), 4.05 (4H, m, CH_2OH), 8.89 (8H, m, βH); MS (MALDI-TOF) m/z 1194.5 [calc'd for $\text{PdC}_{48}\text{H}_{18}\text{SN}_4\text{F}_{18}\text{O}_2$, M^+ 1195.21].

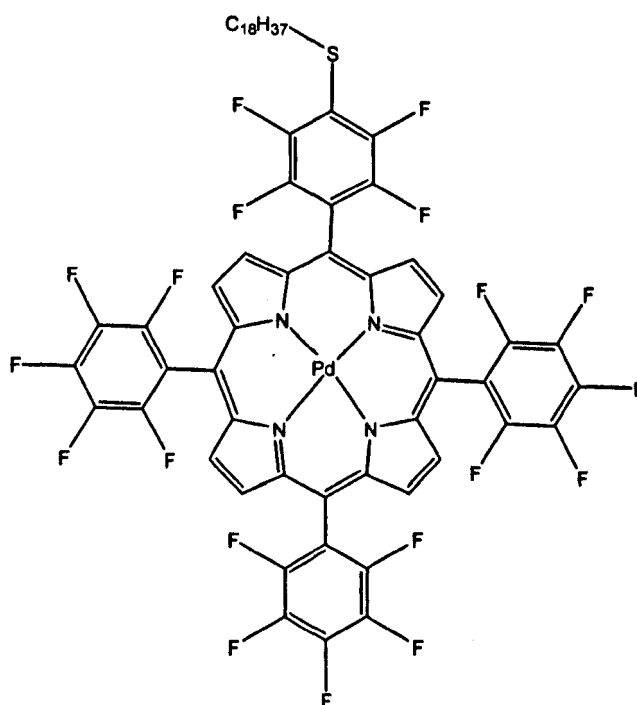
Fraction D (0.01 g, 22 %); $R_f = 0.31$ (silica, eluent: hexane/ CH_2Cl_2 , 1:1); $^1\text{H NMR}$ [400 MHz, CDCl_3] δ 3.46 (6H, t, $J^* = 5.5\text{Hz}$, SCH_2), 4.05 (6H, m, CH_2OH), 8.89 (8H, m, βH); MS (MALDI-TOF) m/z 1252.4 [calc'd for $\text{PdC}_{46}\text{H}_{13}\text{SN}_4\text{F}_{19}$, M^+ 1253.33].

[90] Pd(II)-5-(4-octadecylthio-2,3,5,6-tetrafluorophenyl)-10,15,20-
(pentafluorophenyl)]porphyrin and

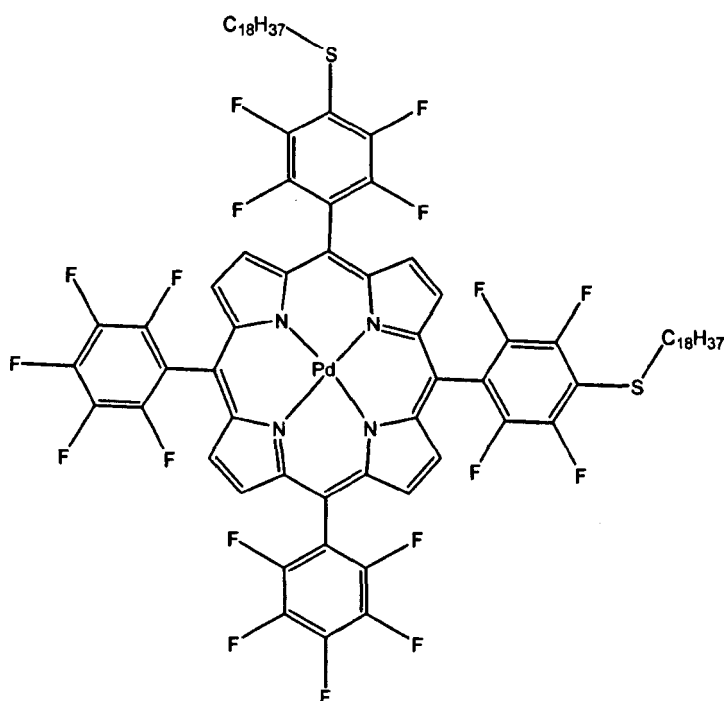
[91] Pd(II)-5,10-di-(4-octadecylthio-2,3,5,6-tetrafluorophenyl)-15,20-di-
(pentafluorophenyl)]porphyrin and

[92] Pd(II)-5,10,15-tris-(4-octadecylthio-2,3,5,6-tetrafluorophenyl)-20-
(pentafluorophenyl)]porphyrin and

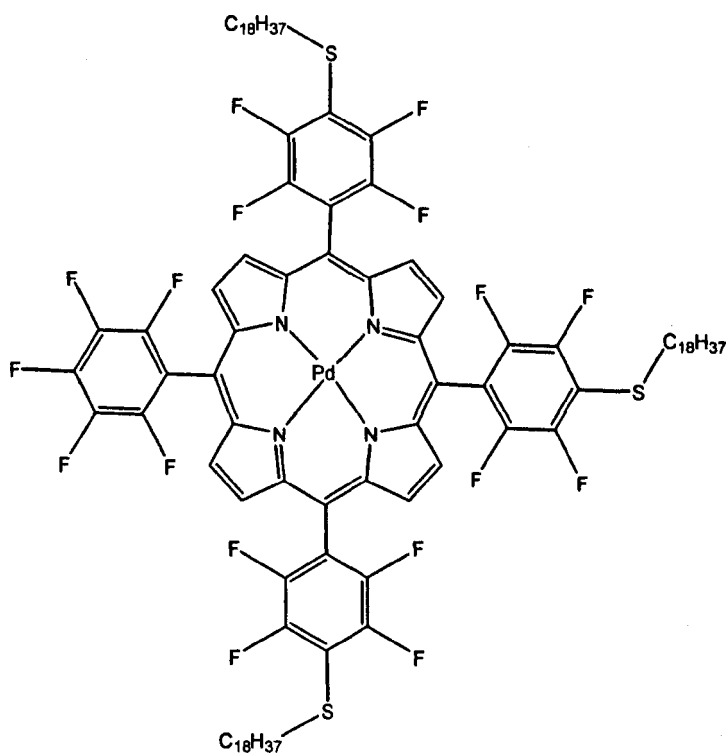
[93] Pd(II)-5,10,15,20-tetrakis(4-octadecylthio-2,3,5,6-tetrafluorophenyl)porphyrin



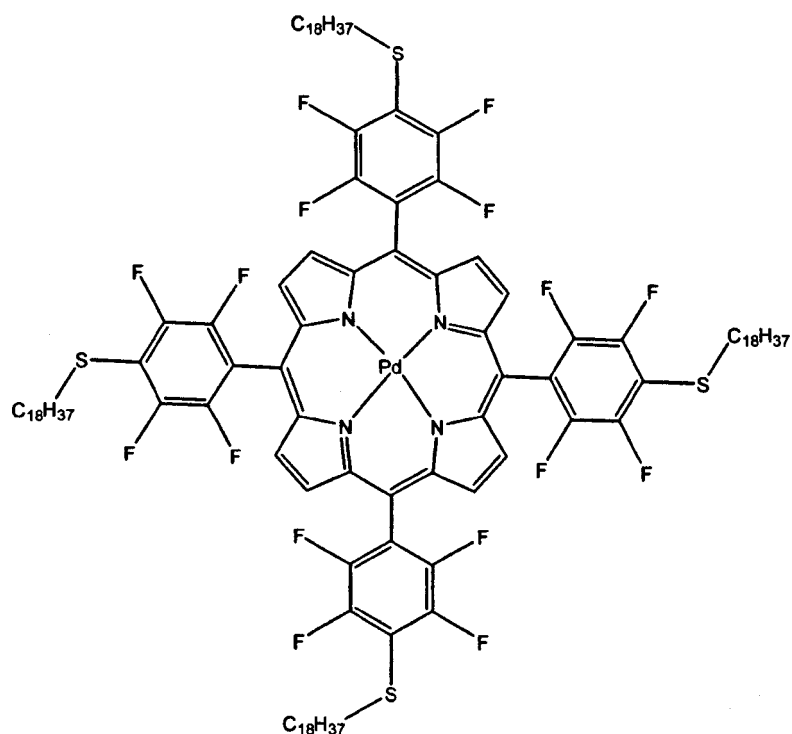
Pd(II)-5-[(4-octadecylthio)-2,3,5,6-(tetrafluorophenyl)-10,15,20-
(pentafluorophenyl)]porphyrin



Pd(II)-5,10-di-[(4-octadecylthio)-2,3,5,6-(tetrafluorophenyl)]-15,20-di-(pentafluorophenyl)porphyrin



Pd(II)-5,10,15-tris-[(4-octadecylthio)-2,3,5,6-(tetrafluorophenyl)]-20-(pentafluorophenyl)porphyrin



Pd(II)-5,10,15,20-tetrakis[(4-octadecylthio)-2,3,5,6-(tetrafluorophenyl)]porphyrin

Pd(II)-5,10,15,20-tetra-(pentafluorophenyl)porphyrin (0.05 g, 4.3×10^{-5} mol) was dissolved in anhydrous DMF (5 ml) and octadecanemercaptan (0.06 g, 2.2×10^{-4} mol) was added. The mixture was stirred for 18 hours at room temperature, under argon and protected from light. The solvent was evaporated *in vacuo* and the residue redissolved in dichloromethane (10 ml). The mixture was washed with saturated sodium hydrogen carbonate (2×50 ml), separated and the organic layer concentrated *in vacuo*. The solid was analysed using TLC (silica, eluent: hexane/ CH_2Cl_2 , 1:1) which indicated a total of 5 components. The mixture was attempted to be separated using preparative TLC. Fraction A was analysed to be the starting material and as expected, the

following fractions were mono-, di-, tri- and tetra- thiol substituted porphyrins respectively.

Fraction A, which eluted near the solvent line $R_f = 0.9$ as mentioned earlier was found to be the unreacted starting material. The later fractions $R_f = 0.7, 0.55, 0.46$ and 0.38 however were not separable using preparative TLC or flash column chromatography. Their presence was confirmed using; MS (MALDI-TOF).

Fraction B; $R_f = 0.7$ (silica, eluent: hexane/ CH_2Cl_2 , 1:1); MS (MALDI-TOF) m/z 1345 [calc'd for $\text{C}_{62}\text{H}_{45}\text{F}_{19}\text{N}_4\text{PdS}$, $M^+1345.5$].

Fraction C; $R_f = 0.55$ (silica, eluent: hexane/ CH_2Cl_2 , 1:1); MS (MALDI-TOF) m/z 1611 [calc'd for $\text{C}_{80}\text{H}_{82}\text{F}_{18}\text{N}_4\text{PdS}_2$, $M^+1612.06$].

Fraction D; $R_f = 0.46$ (silica, eluent: hexane/ CH_2Cl_2 , 1:1); MS (MALDI-TOF) m/z 1879 [calc'd for $\text{C}_{98}\text{H}_{119}\text{F}_{17}\text{N}_4\text{PdS}_3$, $M^+1878.61$].

Fraction E; $R_f = 0.38$ (silica, eluent: hexane/ CH_2Cl_2 , 1:1); MS (MALDI-TOF) m/z 2145 [calc'd for $\text{C}_{116}\text{H}_{156}\text{F}_{16}\text{N}_4\text{PdS}_4$, $M^+2145.17$].

REFERENCES

1. Vanderkooi, M.; Maniara, G.; Green, T. J.; Wilson, D. F. *J. Biol. Chem.* **1997**, *262*, 5476-5482.
2. Bonnett, R. *Rev. Contemp. Pharmacother* **1999**, *10*, 1-17.
3. Raab, O. *Z. Biol* **1900**, *39*.
4. Pandey, R.K.; Zheng, G. *Porphyrins as photosensitizers in photodynamic therapy*; **2000**.
5. Policard, A. *Compt. Rend. Soc. Biol.* **1924**, *91*, 1423-1424.
6. Figge, F.J.H. *The relationship of pyrrole compounds to carcinogenesis*; **1945**.
7. Figge, F.J.H. *Ann.Int.Med.* **1947**, *24*, 143-146.
8. Figge, F.J.H.; Wiland, G. S.; Manganiello, L.O.J. *Proc. Soc. Exp. Biol. Med.* **1948**, *68*, 143-146.
9. Ramussen-Taxdal, D. S.; Ward, D. E.; Figge, F.J.H. *Cancer* **1955**, *8*, 78-81.
10. Winkleman, J. *J. Natl. Cancer. Inst.* **1961**, *27*, 1369-1377.
11. Winkleman, J. *Cancer. Res.* **1962**, *22*, 589-596.
12. Winkleman, J. *Experimentia* **1967**, 949-950.
13. Gilbert, A.; Baggott, J. *Essentials of molecular photochemistry.* **1991**.
14. <http://www.chemicool.com>
15. Foote, C. S. *Photochem. Photobiol.* **1991**, *54*, 659.
16. Milgrom, L.; MacRobert, S. *Chem.Br.* **1998**, *34*, 45-50.
17. Bonnett, R.; Berenbaum, M.; *Ciba Found Symp.* **1989**, *146*, 40-59.
18. Dolphin, D.; *Can. J. Chem.* **1994**, 1005-1013.
19. Hirth, A.; Michelsen, U.; Wöhrle, D.; *Chem. Unserer Zeit.* **1999**, *33*, 84-94.

20. Sternberg, E.D.; Dolphin, D.; Brückner, C.; *Tetrahedron*. **1998**, *54*, 4151-4202.
21. Spikes, J.D.; Bommer, J.C.; *Chlorophylls*. **1991**, 1181-1204.
22. Oleinick, N.L.; Evans, H.H.; *Radiation Res.* **1998**, *150*, 5146-5156.
23. Dougherty, T.J.; Gomer, C.J.; Henderson, B.W.; Jori, G.; Kessel, D.; Karbelik, M.; Moan, J.; Peng, Q.; *J. Natl. Cancer. Inst.* **1998**, *90*, 889-905.
24. Hsi, R.A.; Rosenthal, D.I.; Glastein, E.; *Drugs*. **1999**, *57*, 725-734.
25. Ben-Hur, E.; Dubbelman, T.M.A.R.; *Photochem. Photobiol.* **1993**, *58*, 890-894.
26. Henderson, B.W.; Bellnier, D.A.; *Ciba Found Symp.* **1989**, *146*, 112-130.
27. Henderson, B.W.; Dougherty, T.J.; *Photochem. Photobiol.* **1992**, *55*, 145-157.
28. Moon, J.; Berg, K.; *Photochem. Photobiol.* **1992**, *55*, 931-948.
29. Webber, J.; Kessel, D.; Fromm, D.; *Yale J. Biol. Med.* **1997**, *70*, 127-137.
30. Jori, G.; *EPA Newslett.* **1997**, *60*, 12-18.
31. Mac Robert, A.J.; Bown, S.G; Phillips, D.; *Ciba Found Symp.* **1989**, *146*, 4-16.
32. Henderson, B.W.; Dougherty, T.J.; Schwartz, S.; *Photodynamic therapy: Basic principles and applications*, **1992**, 1-15.
33. Lipson, R.L.; Baldes, E.J.; Olsen, A.M.; *J. Natl. Cancer. Inst.* **1961**, *26*, 1-11.
34. Dougherty, T.J.; *J. Clin. Laser. Med. Surg.* **1996**, *14*, 219-221.
35. Dougherty, T.J.; *J. Natl. Cancer. Inst.* **1974**, *52*, 1333-1336.
36. Weishaupt, K.R.; Gomer, C.J.; Dougherty, T.J.; *Cancer. Res.* **1976**, *36*, 2326-2329.
37. Brown, S.; *Photodynamic News.* **1999**, *2(1)*, 1-4.
38. Dougherty, T.J.; *Photochem. Photobiol.* **1993**, *58*, 895-900.
39. Axcan Pharma Inc. <http://www.axcan.com>.
40. Bonnett, R.; Berenbaum, M.C.; *Porphyrin Photosensitization*, **1983**, 241-250.

41. Pandey, R.K.; Herman, C.K.; *Chem. Ind.* **1998**, 739-743.
42. Hamblin, M.R.; Hasan, T.; *Opt. Photonics News.* **1996**, 16-21.
43. Jori, G.; *Photochem. Photobiol.* **1992**, *62*, 371-378.
44. Bonnett, R.; *Tumour photochemotherapy.* **1989**, 8-10.
45. Ochsner, M.; *Arzneim-Forsch.* **1997**, *47*, 1185-1194.
46. Van Lier, J.E.; Spikes, J.D.; *Ciba Found Symp.* **1989**, *146*, 17-32.
47. Doiron, D.R.; Svaasand, A.E.; *Porphyrin Photosensitization*, **1983**, 63-76.
48. Doiron, D.R.; Gomer, C.J.; Fountain, S.W.; Razum, N.J.; *Porphyrins in Tumor phototherapy*, **1984**, 281-291.
49. Brown, S.B.; Truscott, T.G.; *Chem. Br.* **1993**, 955-958.
50. Kreimer-Birnbaum, M.; *Semin. Hematol.* **1989**, *26*, 157-173.
51. Wilson, B.C.; *Ciba Found Symp.* **1989**, *146*, 60-77.
52. Berg, K.; Moan, J.; *Photochem. Photobiol.* **1997**, *65*, 403-409.
53. Peng, Q.; Berg, K.; Moan, J.; Kongshaug, M.; Nesland, J.M.; *Photochem. Photobiol.* **1997**, *65*, 235-251.
54. Redmond, R.W.; Gamlin, J.N.; *Photochem. Photobiol.* **1999**, *70*, 391-475.
55. DUSA Pharmaceuticals Inc. <http://www.dusapharma.com>.
56. Nyman, E.S.; Hynninen, P.H.; *Photochem. Photobiol.* **2004**, *73*, 1-28.
57. Kessel, D.; *Biochem. Pharmacol.* **1984**, *33*, 1389-1393.
58. Gomer, C.J.; *Photochem. Photobiol.* **1991**, *54*, 1093-1107.
59. Sessler, J.L.; Miller, R.A.; *Biochem. Pharmacol.* **2000**, *59*, 733-739.
60. Labbe, R.F.; Nishida, G.; *Biophys. Acta.* **1957**, *26*, 437.
61. Falk, J.E.; *Porphyrins and metalloporphyrins.* **1964**.

62. Hynninen, P.H.; Ellfolk, N.; *Acta. Chem. Scand.* **1973**, *27*, 1795-1806.
63. Callot, H.J.; Johnson, A.W.; Sweeney, A.; *J. Chem. Soc. Perkin Trans I.* **1973**, 1324-1327.
64. Richter, A.M.; Kelly, B.; Chow, J.; Liu, J.D.; Towers, G.H.N.; Levy, J.; Dolphin, D.; *J. Natl. Cancer Inst.* **1987**, *79*, 1327-1332.
65. Yon-Hin, P.; Wijesekera, T.P.; Dolphin, D.; *Tetrahedron Lett.* **1991**, *32*, 2875-2878.
66. Pandey, R.K.; Shiau, F.Y.; Ramachandaran, K.; Dougherty, T.J.; Smith, K.M.; *J. Chem. Soc. Perkin. Trans I.* **1992**, 1377-1383.
67. Sternberg, E.; Dolphin, D.; *Curr. Med. Chem* **3**. **1996**, 239-272.
68. Monforts, F.P.; Gerlach, B.; Haake, G.; Höper, F.; Kusch, D.; Meler, A.; Scheuric, G.; Brauer, H. D.; Schiwon, K.; Schermann, G.; *Int. Soc. Opt. Eng.* **1994**, 29-39.
69. Monforts, F.P.; Kusch, D.; Höper, F.; Braun, S.; G.; Brauer, H. D.; Gerlach, B.; Schermann, G.; Moser, J.G.; *Int. Soc. Opt. Eng.* **1996**, 212-221.
70. Hynninen, P.H.; *Acta Chem. Scand.* **1977**, *31*, 829-835.
71. Strain, H. H.; Sherma, J.; *J. Chem. Edu.* **1969**, *46*, 476-483.
72. Hynninen, P.H.; *Chlorophylls.* **1991**, 145-209.
73. Hamblin, M.R.; Newman, E.L.; *Photochem. Photobiol.* **1994**, *26*, 45-56.
74. Hamblin, M.R.; Newman, E.L.; *Photochem. Photobiol.* **1994**, *26*, 147-157.
75. Brasseur, N.; Langlois, R.; La Madeline, C.; Oullet, R.; Van Lier, J.E.; *Photochem. Photobiol.* **1999**, *69*, 345-352.
76. Mew, D.; Wat, C.K.; Towers, G.H.; Levy, J.G.; *J. Immunol.* **1983**, *30*, 1473-1477.
77. Davis, N.; Liu, D.; Jain, A.K.; Jiang, S-Y.; Jiang, F.; Richter, A.; Levy, J.G.; *Photochem. Photobiol.* **1993**, *57*, 641-647.

78. Goff, B.A.; Blak, J.; Bamberg, M.P.; Hasan, T.; *Br. J. Cancer*. 1996, 74, 1194-1198.
79. Oseroff, A.R.; Ohuoha, D.; Hasa, T.; Bommer, J.C.; Yarmush, M.L.; *Pro. Natl. Acad. Sci.* 1986, 83, 8744-8749.
80. Vauenraets, M.B.; Visser, G.W.M.; Steward, F.A.; Stigter, M.; Oppelaar, H.; Postmus, P.E.; Snow, G.B.; Van Dongen, G.A.; *Cancer Research*. 1999, 59, 1505-1513.
81. Dilkes, M.G.; DeJode, M.L.; Rowntree-Taylor, A.; McGillian, J.A.; Kenyon, G.S.; Mc Kelvie, P.; *Lasers Med. Sci. II*. 1996, 23-29.
82. Brasseur, N.; Oullet, R.; Madeline, C.L.; Van Lier, J.E.; *Br. J. Cancer*. 1999, 80, 1533-1541.
83. Westermann, P.; Glanzmann, T.; Andrejevic, S.; Braichotte, D.R.; Farrer, M.; *Int.J. Cancer*. 1998, 76, 842-850.
84. Hamblin, M.R.; Miller, J.L.; Rizvi, I.; Maytin, E.V.; Hasan, T.; *Photochem. Photobiol.* 2000, 72, 533-540.
85. Kessel, D.; *Cancer Lett.* 1986, 33, 183.
86. Shulock, J.R.; Wade, M.H.; Lin, C.W.; *Photochem. Photobiol.* 1990, 51, 451.
87. Schell, C.; Hombrecher, H.K.; *Chem. Eur. J.* 1999, 5, 587.
88. Kieda, C.; Monsigny, M.; *Invasion Metastasis*. 1986, 6, 347.
89. Mansigny, M.; Roche, A.C.; Midox, P.; Kieda, C.; Mayer, R.; *Lectins and glycoconjugates in oncology*. 1988, 1.
90. Konstantinov, K.; Chuppa, S.; Sajan, E.; Tsai, Y.; Yoon, S.; Golini, F.; *Trends Biotechnol.* 1994, 12, 324-333.
91. Sol, V.; Blais, J.C.; Bolbach, G.; Carre, V.; Granet, R.; Guilloton, M.; Spiro, M.;

- Krausz, P.; *Tetrahedron Lett.* **1997**, *38*, 6391-6394.
92. Maillard, P.; Hery, C.; Momentau, M.; *Tetrahedron Lett.* **1997**, *38*, 3731-3734.
93. Oulmi, D.; Maillard, P.; Guerquin-Kern, J.L.; Huel, C.; Momentau, M.; *J. Org. Chem.* **1995**, *60*, 1654-1564.
94. Kohata, K.; Higashio, H.; Yamaguchi, Y.; Koketsu, M.; Odashima, T.; *Bull. Chem. Soc. Jpn.* **1994**, *67*, 668-679.
95. Maillard, P.; Guerquin-Kern, J.L.; Huel, C.; Momentau, M.; *J. Org. Chem.* **1993**, *58*, 2774-2780.
96. Driaf, K.; Krausz, P.; Verneuil, B.; Spiro, M.; Blais, J.C.; Bolbach, G.; *Tetrahedron Lett.* **1993**, *34*, 1027-1030.
97. Ono, N.; Bougauch, M.; Maruyama, K.; *Tetrahedron Lett.* **1992**, *33*, 1629-1632.
98. Czuchajowski, L.; Habdas, J.; Viedbala, H.; Vandrekar, V.; *Tetrahedron Lett.* **1991**, *32*, 7511-7512.
99. Sol, V.; Blais, J.C.; Bolbach, G.; Carre, V.; Granet, R.; Guilloton, M.; Spiro, M.; Krausz, P.; *J. Org. Chem.* **1999**, *64*, 4431-4444.
100. Lindsey, J.S.; Hsu, H.C.; Schreiman, I.C.; *Tetrahedron Lett.* **1986**, *27*, 4969-4970.
101. Mikata, Y.; Onchi, Y.; Tabata, K.; Ogura, S.; Okura, I.; Ono, H.; Yano, S.; *Tetrahedron Lett.* **1998**, *39*, 4505-4508.
102. Gandin, E.; Lion, Y.; Van de Vorst, A.; *Photochem. Photobiol.* **1983**, *37*, 271-278.
103. Laville, I.; Figueiredo, T.; Looock, B.; Pigaglio, S.; Maillard, P.; Grierson, D.; Carrez, D.; Croisy, A.; Blais, J.; *Bioorg. Med. Chem.* **2003**, *11*, 1643-1652.
104. Swartz, H.M.; *Biochem. Soc. Trans.* **2001**, *30*, 248-252.
105. Silver, I.A.; *Undersea. Med. Soc.* **1984**, *62*, 215-238.

106. Wolfbeis, O.S.; *Fiber Optics chemical sensors and biosensors*. CRC Press, 1991.
107. Li, X.M.; Ruan, F.C.; Wong, K.Y.; *Analyst*. 1993, 118, 289.
108. Sacksteder, L.A.; Demas, J.N.; DeGraff, B.A.; *Anal. Chem.* 1993, 65, 3480.
109. Gruber, W.R.; Klimant, I.; Wolfbeis, O.S.; *Proc.* 1993, 1885.
110. Hartmann, P.; Leiner, M.J.; *Anal. Chem.* 1995, 67, 88-93.
111. Mandal, K.; Pearson, T.D.L.; Demas, J.N.; *Inorg. Chem.* 1981, 20, 786.
112. McMurray, H.N.; Douglas, P.; Busa, C.; Garley, M.S.; *Photochem. Photobiol.* 1994, 80, 283.
113. Delpy, D.T.; Cape, M.; *Philos. Trans. R. Soc. London. Ser. B.* 1997, 352, 649-659.
114. Pogue, B.W.; Poplack, S.P.; McBride, T.O.; Wells, W.A.; Osterman, K.S.; Osterberg, U.L.; Paulsen, K.D.; *Radiology*. 2001, 286, 261-266.
115. Hunjan, S.; Zhao, D.; Constantinescu, A.; Hahn, E.W.; Antich, P.P.; Mason, R.P.; *Int. J. Radiat. Oncol. Bio. Phys.* 2001, 49, 1097-1108.
116. Hunjan, S.; Mason, R.P.; Constantinescu, A.; Pesche, P.; Hahn, E.W.; Antich, P.P.; *Int. J. Radiat. Oncol. Bio. Phys.* 1998, 41, 161-171.
117. Sotak, C.H.; Hees, P.S.; Huang, H.N.; Hung, M.H.; Krespan, C.G.; Reynolds, S.; *Magn. Reson. Med.* 1993. 29, 188-195.
118. Van der Sanden, B.P.; Heerschp, A.; Simonetti, A.W.; Rijken, P.F.; Peters, H.P.; Stuben, G.; Van der Kogel, A.J.; *Int. J. Radiat. Oncol. Biol. Phys.* 1999. 44, 649-658.
119. Mancini, D.M.; Wilson, J.R.; Bolingher, L.; Li, H.; Kendrick, K.; Chance, B.; Leigh, J.S.; *Circulation*. 1994, 90, 500-508.
120. Dunn, J.F.; Swartz, H.M.; *Adv. Exp. Biol. Med.* 1998, 428, 645-650.
121. Ogawa, S.; Lee, T.M.; Kay, A.R.; Tank, D.W.; *Proc. Natl. Acad. Sci.* 1990, 87, 9868-

9872.

122. Khalil, G.; Gouterman, M.; Ching, S.; Costin, C.; Coyle, L.; Gouin, S.; Green, E.; Sadilek, M.; Wan, R.; Yearyeen, J.; Zelelow, B.; *J. Porph. Phthal.* **2002**, *6*, 135-145.
123. Papkovsky, D.B.; Ponomarev, G.V.; Trebznack, W.; O' Leary, P.; *Anal. Chem.* **1995**, *67*, 4112-4117.
124. Papkovsky, D.B.; Olah, J.; Troyanvosky, I.V.; Sadovsky, N.A.; Rumayantseva, V.D.; Mironov, A.F.; Yaropolov, A.I.; Savitsky, A.P.; *Biosensors Bioelectronics.* **1992**, *7*, 199-206.
125. Zhang, H.; Sun, Y.; Ye, K.; Zhang, P.; Wang, Y.; *J. Mater. Chem.*, **2005**, *15*(31), 3181.
126. Lakowicz, J.R.; *Principles of fluorescence spectroscopy.* **1991**.
127. Vinogradov, S.A.; Fernandez, M.A.; Dupan, B.W.; Wilson, D.F.; *Comparative Chemistry and Physiology Part A.* **2002**, 147-152.
128. Wilson, D.F.; Vinogradov, S.A.; Dugan, B.W.; Biruski, D.; Waldron, L.; Evans, S.A.; *Comparative Chemistry and Physiology Part A.* **2002**, 153-159.
129. Wilson, D.F.; Rumsey, W.L.; Green, T.J.; Vanderkooi, J.M.; *J. Biol. Chem.* **1988**, *263*, 2712.
130. Rumsey, W.R.; Vanderkooi, J.M.; Wilson, D.F.; *Science.* **1989**, *241*, 1649-1651.
131. Dunphy, I.; Vinogradov, S.A.; Wilson, D.F.; *Anal. Biochem.* **2002**, *310*, 191-198.
132. Wilson, D.F.; Evans, S.M.; Jenkins, W.T.; Vinogradov, S.A.; Ong, E.; Dewhirst, M.W.; *Adv Exp Med Biol.* **1998**, *454*, 603-9.
133. Amao, Y.; Asai, K.; Okura, I.; *Anal. Commun.* **1999**, *36*, 179-180.
134. Lee, S.K.; Shin, Y.B.; Pyo, H.B.; Park, S.H.; Ogura, S.I.; Okura, I.; *Bull. Korean.*

- Chem. Soc.* **2001**, 22.
135. Nuzzo, R.G.; Fusco, F.A.; Allara, D.L.; *J. Am. Chem. Soc.* **1987**, 109, 235.
136. Kalyanasundaram, K.; *Photochemistry of polypyridine and porphyrin complexes.*
1992.
137. Vinogradov, S.A.; Wilson, D.F.; *Adv. Exp. Med. Biol.* **1997**, 428, 657-662.
138. Rietveid, I.B.; Kim, E.; Vinogradov, S.A.; *Tetrahedron.* **2003**, 59, 3821-3831.
139. Kimura, M.; Nakada, K.; Yamaguchi, Y.; Hanabusa, K.; Shirai, H.; Kobayashi, N.;
Chem. Commun. **1997**, 1215-1216.
140. Rozkhov, V.V.; Wilson, D.F.; Vinogradov, S.A.; *Polym. Master. Sci. Eng.* **2001**,
601-603.
141. Atkins, P.W.; *Physical Chemistry, 5th Ed.* **1994**, 598-599.
142. Hermanson, G.T.; *Bioconjugate Techniques.* **1996**, 297-364.
143. Frey, T.G.; Mannella, C.A.; *Trends Biochem. Sci.* **2000**, 25, 319.
144. Kessel, D.; Luo, Y.; *Photochem. Photobiol.* **1998**, 42, 89-95.
145. Cummings, M.C.; Winterford, C.M.; Walker, N.I.; *Am. J. Surg. Pathol.* **1997**, 21,
88.
146. Pal, P.; Zeng, H.; Durocher, G.; Girard, D.; Giasson, R.; Blanchard, L.; Gaboury, L.;
Villeneuve, L.; *Photochem. Photobiol.* **1996**, 98, 65-72.
147. Deckwerth, T.L.; Johnson Jr E.M.; *J. Cell. Biol.* **1993**, 123, 1207-1222.
148. Kaprelyants, A.S.; Kell, D.B.; *J. Appl. Bacteriol.* **1992**, 72, 410.
149. Bucana, C.D.; Giavazzi, R.; Nayar, R.; O'Brian, C.A.; Seid, C.; Earnest L.E.; Fan,
D.; *Exp. Cell. Res.* **1990**, 190, 69.
150. Lynch, R.M.; Fogarty, K.E.; Fay, F.S.; *J. Cell. Biol.* **1991**, 112, 385.

151. Castedo, M.; Hirsch, T.; Susin, S.A.; Zamzami, N.; Marchetti, P.; Macho, A.; Kroemer, G.; *J. Immunol.* **1996**, *157*, 512-521.
152. Macho, A.; Decaudin, D.; Castedo, M.; Hirsh, T.; Susin, S.A.; Zamzami, N.; Kroemer, G.; *Cytometry*. **1996**, *25*, 333-340.
153. Zamzami, N.; Marchetti, P.; Castedo, M.; Zanin, C.; Vayssiere, J.L.; Petit, P.X.; Kroemer, G.; *J. Exp. Med.* **1995**, *181*, 1661-1672.
154. Petit, P.X.; Le Coeur, H.; Zorn, E.; Dauget, C.; Mignotte, B.; Gougeon, M.L.; *J. Cell. Biol.* **1995**, *130*, 157-167.
155. Petit, J.M.; Maftah, A.; Ratinaud, M.H.; Julien, R.; *Eur. J. Biochem.* **1992**, *209*, 267-273.
156. Simpson, P.B.; Mehotra, S.; Lange, G.D.; Russell, J.T.; *J. Biol. Chem.* **1997**, *272*, 22654-22661.
157. Nieminen, A.L.; Byrne, A.M.; Herman, B.; Lemasters, J.I.; *Am. J. Physiol.* **1997**, *41*, C1286-C1294.
158. Metivier, D.; Dallaporta, B.; Zamzami, N.; Larochette, N.; Susin, S.A.; Marzo, I.; Kroemer, G.; *Immunol. Lett.* **1998**, *61*, 157-163.
159. Minamikawa, T.; Sriratana, A.; Williams, D.A.; Bowser, D.N.; Hill, J.S.; Nagley, P.; *J. Cell. Sci.* **1999**, *112*, 2419-2430.
160. Sandberg, S.; Glette, J.; Hopen, G.; Solberg, O.; Romslo, I.; *Photochem. Photobiol.* **1981**, *34*, 471-475.
161. Sandberg, S.; Romslo, I.; *Biochem. Biophys. Acta.* **1980**, *593*, 187-195.
162. Woodburn, K.W.; Vardaxis, N.J.; Hill, J.S.; Kaye, A.H.; Phillips, D.R.; *Photochem. Photobiol.* **1991**, *54*, 725-732.

163. Dummn, H.; Cerncy, T.; Zimmermann, H.W.; *Photochem. Photobiol.* **1997**, *37*, 219-229.
164. Agarwal, M.L.; Clay, M.E.; Harvey, E.J.; Evans, Antunez, A.R.; Oleinick, N.L.; *Cancer Res.* **1991**, *51*, 5993-5996.
165. Luo, Y.; Chang, C.K.; Kessel, D.; *Photochem. Photobiol.* **1996**, *63*, 528-534.
166. Kessel, D.; Luo, Y.; Deng, Y.; Chang, C.K.; *Photochem. Photobiol.* **1997**, *65*, 422-426.
167. Zamzami, N.; Susin, S.A.; Marchetti, P.; Hirsch, T.; Gomez-Monterrey, I.; Castedo, M.; Kroemer, G.; *J. Exp. Med.* **1996**, *183*, 1533-154.
168. Liu, X.; Kim, C.N.; Yang, J.; Jemmerson, R.; Wang, X.; *Cell*, **1996**, *86*, 147--157.
169. Kessel, D.; Luo, Y.; *Cell Death. Diff.* **1999**, *6*, 28.
170. Kessel, D.; Luo, Y.; *J. Porph. Phthal.* **2001**, *5*, 181-184.
171. Woodburn, K.W.; Fan, Q.; Miles, D.R.; Kessel, D.; Luo, Y.; Young, S.W.; *Photochem. Photobiol.* **1997**, *65*, 410.
172. Kessel, D.; Woodburn, K.; Henderson, B.W.; Chang, C.K.; *Photochem. Photobiol.* **1995**, *65*, 875.
173. Kessel, D.; Luo, Y.; Deng, Y.; *Photochem. Photobiol.* **1998**, *42*, 89.
174. Kessel, D.; Luo, Y.; Deng, Y.; *Photochem. Photobiol.* **1997**, *66*, 479.
175. Roberts, W.G.; Shian, F.Y.; Nelson, J.S.; Smith, K.M.; Berns, M.W.; *J. Natl. Cancer Inst.* **1998**, *80*, 33.
176. Kessel, D.; Woodburn, K.; Gomer, C.J.; Jagerovic, N.; Smith, K.M.; *Photochem. Photobiol.* **1995**, *28*, 13.
177. Nobel foundation. [http://nobelprize.org/Hans Fischer](http://nobelprize.org/Hans_Fischer)

178. Nobel foundation. [http://nobelprize.org/R.B Woodward](http://nobelprize.org/R.B%20Woodward)
179. Rothmund, P.; *J. Am. Chem. Soc.* **1936**, *58*, 625.
180. Adler, A.D.; Longo, F.R.; Finarelli, J.D.; Goldmacher, J.; Assour, J.; Korsakoff, L.J.; *J. Org. Chem.* **1967**, *32*, 476.
181. Lindsey, J.S.; Schreiman, I.C.; Hsu, H.C.; Kearney, P.C.; Marguerettaz, A.M.; *J. Org. Chem.* **1987**, *52*, 827.
182. Arsenault, G.P.; Bullock, E.; MacDonald, S.F.; *J. Am. Chem. Soc.* **1960**, *82*, 4384.
183. Honeybourne, C.L.; Jackson, J.T.; Simmonds, D.J.; Jones, O.T.G. *Tetrahedron* **1980**, *36*, 1833.
184. Kalyasundaram, K.; *Photochem. Photobiol.* **1988**, *42*, 87.
185. Pasternack, R.F.; Huber, P.R.; Boyd, P.; Engasser, G.; Francesconi, L.; Gibbs, E.; Fasella, P.; Cerio-Venturo, G.; de Hinds, L.; *J. Am. Chem. Soc.* **1972**, *94*, 4511-4517.
186. Pasternack, R.F.; Gibbs, E.J.; Gaudemer, A.; Antebi, S.; Bassner, S.; De Pay, L.; Turner, D.H.; Williams, A.; La Place, F.; Lansard, M.H.; Merienne, C.; Perree-Fauvet, M.; *J. Am. Chem. Soc.* **1985**, *107*, 8179-8186.
187. Kasturi, M.S.; Platz, M.S.; *Photochem. Photobiol.* **1992**, *56*, 427.
188. Marzilli, L.G.; *New J. Chem.* **1990**, *140*, 4090.
189. Calender, D.W.; Nussbaum, J.M.; *Biochemistry*, **1996**, *35*, 12061.
190. Nitzan, . Dror, R.; Ladan, H.; Malik, Z.; Kimel, S.; Gottfried, V.; *Photochem. Photobiol.* **1995**, *62*, 342.
191. Pasternack, R.F.; Gibbs, E.J.; Villafranca, J.J.; *Biochemistry*, **1983**, *22*, 5409-5417.
192. Georgiou, G.N.; Ahmet, M.T.; Houlton, A.; Silver, J.; Cherry, R.J.; *Photochem.*

- Photobiol.* **1994**, *59*, 419-422.
193. Mehta, G.; Sambariah, T.; Maiya, G.B.; Sirish, M.; Chaterjee, D.; *J. Chem. Soc. Perkin. Trans. 1.* **1993**, *22*, 2667-2669.
194. Brandley, B.K.; Schnaar, R.L.; *J Leukoc Bio.* **1986**, *40*, 97-111.
195. Momentau, M.; Oulmi, D.; Maillard, P.; Croisy, A.; *Photodynamic therapy of cancer* **11**. **1994**, *12*.
196. Pasetto, P.; Chen X.; Drain, C.M.; Franck, R.W.; *Chem. Commun.* **2001**, *81*.
197. Shaw, S.J.; Elgie, K.J.; Edwards, C.; Boyle, R.W.; *Tetrahedron Lett.* **1999**, *40*, 1595.
198. Elgie, K.J.; Scobie, M.; Boyle, R.W.; *Tetrahedron Lett.* **2000**, *41*, 2753.
199. Ahmed, S.; Davoust, E.; Savoie, H.; Boa, A.N.; Boyle, R.W.; *Tetrahedron Lett.* **2004**, *45*, 6045-6047.
200. Mossmann, T.J.; *J. Immunol. Methods.* **1983**, *65*, 55-63.
201. Hartnell, R.D.; Arnold, D.P.; *Eur. J. Inorg. Chem.* **2004**, *6*, 1262-1269.
202. Kadish, K.M.; Araullo-Mc Adams, C.; Han, B.C.; Franzen, M.M.; *J. Am. Chem. Soc.* **1990**, *112*, 8364-8368.
203. Tyulyaeva, E.Y.; Lamova, T.N.; Andrianova, L.G.; *Russ. J. Inorg. Chem.* **2001**, *26*, 371-375.
204. Soini, A.E.; Yashunsky, D.V.; Meltola, N.J.; Ponomarev, G.V.; *J. Porph. Phthal.* **2001**, *5*, 735-774.
205. Spellane, P.J.; Gouterman, M.; Antipas, A.; Kim, S.; Liu, Y.C.; *Inorg. Chem.* **1980**, *19*, 386-391.
206. Battioni, P.; Brigaud, O.; Desvaux, H.; Mansuy, D.; Traylor, T.G.; *Tetrahedron Lett.* **1991**, *32*, 2893-2896.

207. Wolfbeis, O.S.; *J. Mater. Chem.* **2005**, *15*(27-28), 2657 - 2669.

208. Schmälzlin, E.; Van Dongen, J.T.; Klimant, I.; Marmodée, B.; Steup, M.; Fisahn, J.; Geigenberger, P.; Löhmansröben, H.G.; *Biophysical Journal.* **2005**, *89*, 1339-1345.